

**Effects of elevated atmospheric carbon dioxide
concentration on growth and physiology of
Sitka spruce (*Picea sitchensis* (Bong.) Carr.)**

Craig V. M. Barton
BSc (Hons) Ecological Science
(University of Edinburgh)

A thesis submitted in fulfilment of the requirements
for the degree of Doctor of Philosophy
to the
University of Edinburgh
1997



Abstract

Burning of fossil fuels and land use change is causing in an increase in the global atmospheric CO₂ concentration, [CO₂], which is predicted to double by the end of the next century. CO₂ is the main substrate for photosynthesis in terrestrial plants and since the current atmospheric [CO₂] limits photosynthesis in C₃ plants there has been much research into the impact of rising [CO₂] on growth and physiology of vegetation. However there are still many unanswered questions especially regarding the effects of long-term exposure to elevated [CO₂] and the interactions between [CO₂] and other variables, such as nutrients and water. These questions are especially relevant to trees and forests, since trees live for tens to hundreds of years and forests are typically nutrient limited. Moreover, forests play an important role in the global carbon cycle and a change in the way forests absorb or release CO₂ has implications for atmospheric [CO₂].

The aim of this thesis is to investigate the effects of elevated atmospheric carbon dioxide concentrations on the growth and physiology of Sitka spruce. Two experimental approaches were used; firstly the long term effect on mature tissue using branch bags and secondly the interaction between [CO₂] and nutrient supply rate on the growth and physiology of seedling trees was studied.

Six branches on six 16 year-old Sitka spruce trees were continuously exposed to elevated [CO₂] (~700 μmol mol⁻¹) for four years. Branch growth, shoot numbers, needle size, stomatal density, nutrient and carbohydrate concentration, photosynthesis and stomatal conductance were measured through the experiment.

There was no effect of elevated [CO₂] on the growth of the branches or needles, or on the nutrient or carbohydrate concentrations of needles. Neither was there evidence for an acclimation of photosynthesis or stomatal conductance to growth in elevated [CO₂] in current year needles. However, there was some down-regulation of photosynthesis in one-year-old needles coincident with an increase in soluble carbohydrate concentration.

In a second experiment one-year-old seedlings were re-potted into sand and grown for eight months in open-top chambers in either ambient or ~700 μmol mol⁻¹ [CO₂]. They were supplied with nutrients at two rates: a high rate designed to permit maximum growth rate and a low rate 1/10 the high rate. Growth was measured each week and six harvests were made during the experiment. A purpose built whole-tree

gas exchange system was used to measure independently above and below ground CO₂ fluxes over 24 hours. Shoot photosynthetic response to [CO₂] and needle nutrient and carbohydrate concentrations were also measured.

Elevated [CO₂] enhanced growth and increased allocation to roots at both high and low nutrient supply rates but, growth enhancement was larger at the high nutrient supply rate. Carbohydrate concentrations were higher and nutrient concentrations lower in needles grown in elevated [CO₂]. The reduction in maximum carboxylation rate ($V_{c_{max}}$) found in low nutrient supply and elevated [CO₂] shoots was attributed to lower nitrogen concentration in the needles.

Measurements of whole tree carbon budgets showed that growth in elevated [CO₂] did not increase the flux of carbon through the tree to the soil but low nutrient supply rate did.

In summary, branch bags allowed the study of the effect of elevated [CO₂] on mature branches in the absence of sink limitation and indicated down-regulation of photosynthesis in one-year-old needles. Elevated [CO₂] stimulated growth in seedlings even at low nutrient supply rate. Thus young Sitka spruce trees are likely to grow more quickly even on poor sites but will probably have down-regulation of photosynthesis in needles older than one year regardless of sink strength.

To Ana
To my parents

Acknowledgements

I wish to thank:

- Prof. Paul Jarvis for his guidance, encouragement and enthusiasm whenever mine faltered, and for his help in the preparation of this thesis.
- Prof. John Grace for his encouragement, advice and thought provoking ideas.
- Jon Massheder for his assistance with computer problems and for lending an ear to my gripes and moans; one of the joys of sharing an office.
- Mark Rayment for philosophical discussions, worldly advice and general abuse.
- The boys from the workshop especially Dave Mackenzie and Alec Harrower who gave assistance, advice and good cheer whenever required.
- Diarmuid for his help with harvests and biochemical analysis.
- Andy Gray for nutrient analysis.
- Dr H. Lee for help with the early stages of the branch bag experiment.
- My family for support.
- And last, but certainly not least, Ana Rey for her love, patience and constant support, and whose encouragement has been so important for the completion of this thesis.

The branch bag study was funded by the European Community through the Environment R&D Programme (EPOCH and ECO-CRAFT, Contract No. EV5V-CT92-0127) and the seedling experiment by the Leverhulme Trust.

This work contributes to the Global Change and Terrestrial Ecosystems (GCTE) Core Project of the International Geosphere-Biosphere Programme (IGBP).

CONTENTS

Abstract.....	ii
Symbols and abbreviations	xii

Chapter 1 Introduction

1.1 Introduction	1
1.1.1 Rising CO ₂	1
1.1.2 Effects of increasing [CO ₂] on forests	3
1.1.3 Sitka spruce.....	4
1.2 The issues.....	4
1.3 Aims of the study	5
1.4 Outline of the thesis	5

Part I: Effect of Elevated CO₂ on Mature Sitka Spruce Branches

Chapter 2 Branch Bag Experiment

2.1 Introduction	8
2.2 Branch autonomy	9
2.3 The Experiment.....	20
2.3.1 Objectives	10
2.3.2 The stand.....	10
2.3.3 The experimental design.....	11
2.3.4 Statistical analysis.....	12
2.3 Design of bag	12
2.3.1 Branch bag construction	12
2.3.2 Air supply	13
2.3.3 CO ₂ control and monitoring hardware and software	16
2.3.4 Environmental monitoring.....	18
2.4 Performance	18
2.4.1 CO ₂ control	18
2.4.2 Temperature	20
2.4.3 Properties of the polythene film.....	21

Chapter 3 Growth of Branches and Needles

3.1 Branch growth.....	22
3.1.1 Apical shoot extension.....	22
3.1.2 Internode diameters.....	23
3.2 Harvest analysis of branches	23
3.2.1 Number of shoots.....	24

3.2.2 Individual needle mass, area and specific leaf area.....	25
3.2.3 Total branch needle mass and area by age class.....	25
3.2.4 Needle frequency.....	29
3.2.5 Mass of wood.....	29
3.2.6 Density of wood.....	30
3.2.7 Summary of harvest results.....	30
3.3 Stem cross-section and leaf area.....	31
3.4 Needle physical properties.....	32
3.5 Stomatal density.....	33
3.6 Needle composition:.....	34
3.6.1 Chlorophyll.....	34
3.6.2 Starch.....	36
3.6.3 Soluble carbohydrate.....	38
3.6.4 Nutrients.....	39
3.7 Discussion.....	42
3.8 Conclusions.....	45

Chapter 4 Photosynthesis of Mature Branches

4.1 Introduction.....	46
4.2 Photosynthesis of shoots using natural light (in 1991).....	46
4.2.1 Method.....	46
4.2.2 Results.....	47
4.3 Photosynthesis of shoots using an artificial light source (in 1993).....	49
4.3.1 Method.....	49
4.3.2 Results.....	49
4.4 Respiration.....	52
4.4.1 Method.....	52
4.4.2 Results.....	53
4.5 A/Q response functions (in 1994)......	54
4.5.1 Method.....	54
4.5.2 Results.....	54
4.6 A/Ci response functions.....	56
4.6.1 Method.....	56
4.6.2 Results.....	56
4.7 Relationship between stomatal conductance and assimilation rate.....	59
4.7.1 Method.....	60
4.7.2 Results.....	61
4.8 Discussion.....	64
4.8.1 Photosynthesis.....	64
4.8.2 Stomatal conductance.....	66
4.8.3 The stomatal response model.....	66
4.8.4 Respiration.....	67
4.8.5 Branch bag effect.....	67
4.9 Conclusions.....	68

Part II: CO₂ and Nutrient Interactions in Sitka Spruce Seedlings

Chapter 5 Description of Experiment

5.1 Introduction	69
5.2 Aim of the experiment	71
5.3 Open-top chambers in the glasshouse	71
5.3.1 Design of chambers	71
5.3.2 Environmental monitoring	73
5.4 Chamber performance	73
5.4.1 CO ₂ control	73
5.4.2 Temperature	74
5.5 Plant material	75
5.6 Treatments	75
5.6.1 Growing medium	75
5.6.2 Nutrient treatment	76
5.7 Experimental design	77
5.8 Data analysis	77
5.9 Design of whole tree CO ₂ flux measurement chamber	78
5.9.1 Design of the chamber	78
5.9.2 Environmental monitoring	80
5.9.3 Flux measurement system	80
5.10 Flux calculations and corrections	81
5.10.1 Leak correction	81
5.10.2 H ₂ O flux corrections	82
5.10.3 Determination of K _{abs} for the chamber	83
5.10.4 Calculation of CO ₂ and H ₂ O fluxes	84

Chapter 6 Growth and Allocation in Seedling Trees

6.1 Introduction	86
6.2 Height and diameter increase over time	89
6.2.1 Increase in tree height	90
6.2.2 Increase in diameter	92
6.3 Harvest data	93
6.3.1 Number of shoots	94
6.3.2 Dry mass of trees	97
6.4 Allocation patterns	99
6.4.1 Leaf mass fraction	100
6.4.2 Root mass fraction	100
6.4.3 Functional and structural mass	102
6.5 Bud set	103
6.6 Discussion	103
6.7 Conclusions	107

Chapter 7 Shoot Photosynthesis, Carbohydrate and Nutrient Content

7.1 Introduction	108
7.2 Plant material	109
7.2.1 Sampling strategy for nutrient and carbohydrates	109
7.2.2 Material preparation.....	110
7.3 Starch	110
7.3.1 Method.....	110
7.3.2 Starch content at harvests	110
7.3.3 Diurnal changes in starch content of needles.....	112
7.4 Soluble carbohydrates.	113
7.4.1 Method.....	113
7.4.2 Soluble carbohydrates at harvests.....	113
7.4.3 Diurnal variation in soluble carbohydrate concentrations in needles ..	114
7.5 Total non-structural carbohydrates.....	115
7.5.1 At harvests	115
7.6 Nutrient concentrations	117
7.6.1 Method.....	117
7.6.2 Results	117
7.6.3 Nitrogen content of the trees.....	120
7.6.4 Discussion.....	121
7.7 Organic material in the sand	122
7.7.1 Loss on ignition	122
7.7.2 Soluble carbohydrate in sand.....	124
7.7.3 Discussion.....	126
7.8 A/C_i responses of individual shoots	126
7.8.1 Methodology.....	126
7.8.2 Analysis of A/C_i response functions	127
7.8.3 Nutrient analysis of A/C_i shoots.....	129
7.8.4 Chlorophyll content of A/C_i shoots.....	130
7.9 Discussion	132
7.9.1 Plant carbohydrates.....	132
7.9.2 Effect of carbohydrates on photosynthesis	134
7.9.3 Effects of nitrogen on photosynthesis.....	136
7.10 Conclusions.....	141

Chapter 8 Whole-tree CO_2 and H_2O Fluxes

8.1 Measurements of CO_2 and H_2O exchange of whole trees.....	142
8.1.1 Measurement protocol	142
8.1.2 Determination of leaf area and plant mass.....	142
8.1.3 Environmental conditions.....	144
8.1.4 Typical data.....	145

8.2 CO ₂ budget of trees.....	148
8.2.1 Basis for comparisons.....	148
8.2.2 Data analysis.....	150
8.2.3 CO ₂ gain.....	150
8.2.4 CO ₂ loss.....	151
8.2.5 CO ₂ Budgets.....	152
8.3 Water loss from trees.....	157
8.3.1 Transpiration.....	157
8.3.2 Water use efficiency.....	158
8.4 Discussion.....	159
8.4.1 Differential response between tree and shoot.....	159
8.4.2 Respiration.....	161
8.4.3 CO ₂ budget.....	162
8.4.4 Does growth at elevated CO ₂ lead to an increase in the flow of carbon through the atmosphere-plant-soil system?.....	164
8.5 Conclusions.....	166

Chapter 9 Synthesis and conclusions

9.1 Summary of results.....	167
9.2 Growth.....	168
9.3 Allocation.....	169
9.4 Needle carbohydrates.....	170
9.5 Photosynthesis.....	170
9.6 Stomatal conductance.....	171
9.7 Advantages and limitations of Branch Bags.....	172
9.8 Flux of carbon through the plant to the soil.....	172
9.9 Future Research.....	173

Appendices

Appendix A: Calculations used with LCA-3 measurements.....	176
Appendix B: Design of light-source for ADC PLC (C) cuvette.....	178
Appendix C: Nutrient Solution.....	180
Appendix D: Calculation of nutrient addition rates.....	181
Appendix E: Corrections to H ₂ O fluxes.....	183
Appendix F: A simple model describing soluble carbohydrate production and export from spruce needles.....	185

References	187
-------------------------	-----

Symbols

Symbol	Description	Units
α	initial slope of A/Q response curve	$\text{mol CO}_2 \text{ mol}^{-1} \text{ quanta}$
Γ	CO_2 compensation concentration.	$\mu\text{mol mol}^{-1}$
Γ^*	CO_2 compensation concentration in absence of mitochondrial respiration	$\mu\text{mol mol}^{-1}$
θ	convexity of A/Q response curve	
a_1	empirical coefficient in L-BWB model	$\mu\text{mol mol}^{-1}$
A	Net photosynthetic rate	$\mu\text{mol m}^{-2} \text{ s}^{-1}$
A_{sat}	PPFD and CO_2 saturated rate of photosynthesis	$\mu\text{mol m}^{-2} \text{ s}^{-1}$
C	Carbon content of plant	$\text{g C g}^{-1} \text{ plant}$
C_a	CO_2 concentration within the cuvette	$\mu\text{mol mol}^{-1}$
C_i	Intercellular CO_2 concentration	$\mu\text{mol mol}^{-1}$
C_s	CO_2 concentration at the leaf surface	$\mu\text{mol mol}^{-1}$
D_o	Empirical coefficient in L-BWB model	kPa
D_s	Vapour pressure deficit at the leaf surface	kPa
E	Transpiration rate	$\text{mol m}^{-2} \text{ s}^{-1}$
e_a	Vapour pressure of the air	kPa
$e_s(T)$	Saturation vapour pressure at $T^\circ\text{C}$	kPa
F_s, F_r	Shoot fraction and root fraction, respectively.	.
G	Relative growth rate determined from harvest data	$\text{mol C g}^{-1} \text{ day}^{-1}$
g_s	Stomatal conductance to water vapour	$\text{mol m}^{-2} \text{ s}^{-1}$
g_0	Stomatal conductance as $A \rightarrow 0$ when PPFD $\rightarrow 0$	$\text{mol m}^{-2} \text{ s}^{-1}$
H	Relative humidity of the air	%
K_{abs}	Empirical correction	
k_c	Michaelis constant for carboxylation of Rubisco	$\mu\text{mol CO}_2 \text{ mol}^{-1}$
k_o	Michaelis constant for oxygenation of Rubisco	$\mu\text{mol O}_2 \text{ mol}^{-1}$
N	Nitrogen content of plant	$\text{g N g}^{-1} \text{ plant}$
P	Atmospheric pressure	kPa
P	Level of probability	.
P_{max}	PPFD-saturated rate of net photosynthesis	$\mu\text{mol m}^{-2} \text{ s}^{-1}$
Q	Incident PPFD	$\mu\text{mol m}^{-2} \text{ s}^{-1}$
R_A	Relative addition rate of nutrient	$\% \text{ day}^{-1}$
R_d	Dark respiration rate	$\mu\text{mol m}^{-2} \text{ s}^{-1}$
R_G	Relative growth rate of a plant	$\text{g g}^{-1} \text{ day}^{-1}$

R_{GC}	Relative growth rate of the plant in terms of carbon	$\text{g g}^{-1} \text{ day}^{-1}$
R_{GN}	Relative growth rate of the plant in terms of nitrogen	$\text{g g}^{-1} \text{ day}^{-1}$
S_C	Specific uptake of carbon by the shoot	$\text{g C g}^{-1} \text{ plant day}^{-1}$
S_N	Specific uptake of nitrogen by the root	$\text{g N g}^{-1} \text{ plant day}^{-1}$
t	Time	day
T_a	Air temperature	$^{\circ}\text{C}$
T_l	Leaf temperature	$^{\circ}\text{C}$
V_{cmax}	Maximum carboxylation rate of Rubisco	$\mu\text{mol m}^{-2} \text{ s}^{-1}$
w_a	Water vapour mole fraction of the air	mol mol^{-1}
W_s, W_r	Mass of shoot and root, respectively.	g

Abbreviations

Abbreviation	Description
A	Ambient CO ₂ treatment
<i>a/b</i>	Ratio between chlorophyll <i>a</i> and chlorophyll <i>b</i>
ATP	Adenosine triosphate
C	Control CO ₂ treatment for branch bags
C:N	Carbon:nitrogen ratio
Chl	Chlorophyll
current	Foliage from bud burst until bud burst the following year
C+1	Foliage between one and two years old
DMF	Dimethylformamide
E	Elevated CO ₂ treatment
FACE	Free air carbon dioxide enrichment
H	High nutrient supply rate treatment
IPCC	Intergovernmental Panel on Climate Change
IRGA	Infra-red gas analyser
L	Low nutrient supply rate treatment
LAI	Leaf area index
LAR	Leaf area ratio
L-BWB	Leunings modified Ball, Woodrow & Berry model
LMR	Leaf mass ratio
LSD	Fisher's least squared difference test
OTC	Open top chamber
P _i	Inorganic phosphate
PAR	Photosynthetically active radiation
PCR	Photosynthetic carbon reduction cycle
PGA	Phosphoglyceric acid
PPFD	Photosynthetically active photon flux density
PRT	Platinum resistance thermometer
R/S	Root to shoot ratio
RH	Relative humidity
Rubisco	Ribulose,1,5-bisphosphate carboxylase/oxygenase
RuBP	Ribulose-1,5-bisphosphate
SEM	One standard error of the mean
SLA	Specific leaf area
TNC	Total non-structural carbohydrates
TPU	Triose-phosphate utilization
VPD	Vapour pressure deficit
WUE	Water use efficiency

CHAPTER 1

Introduction

1.1 Introduction

1.1.1 Rising CO₂

There has been much interest and some concern over the past decade about the potential impact of rising atmospheric CO₂ concentrations and global climate change on the natural environment. The burning of fossil fuels, land-use change and deforestation, especially in the tropics, has resulted in the gradual rise of atmospheric CO₂ concentration (Neftel *et al.*, 1985; Keeling *et al.*, 1989; Tans *et al.*, 1990; Keeling *et al.*, 1995) from a pre-industrial value of *ca* 270 $\mu\text{mol mol}^{-1}$ to 365 $\mu\text{mol mol}^{-1}$ today (1997) (Neftel *et al.*, 1985; Barnola *et al.*, 1987). Continuing world-wide development and the IPCC 'business-as-usual scenario' leads to the prediction that the concentration will rise to 530 $\mu\text{mol mol}^{-1}$ by 2050 and could exceed 700 $\mu\text{mol mol}^{-1}$ by the end of the next century (Watson *et al.*, 1990).

CO₂ is a so called 'greenhouse' gas, so named because like the glass of a 'greenhouse' it allows short wave radiation from the sun to pass through but absorbs the long-wave radiation re-radiated from the ground, so trapping heat and leading to a rise in temperature. Thus the rising atmospheric CO₂ concentration is implicated with rising global temperatures, however there is uncertainty about the size of this warming. Historic records show a rise of *ca* 0.5 °C over the past century (Jones *et al.*, 1994) while General Circulation Models (GCM) predict that a doubling of atmospheric CO₂ will increase mean annual temperatures by 1.5 to 4.5 °C depending on latitude (Watson *et al.*, 1990). Concurrent with global warming there will be rising sea levels, changing rainfall amounts and altered weather patterns, all of which will have some effect on the biosphere. However, irrespective of any possible effects of global climate change on the biosphere the increase in atmospheric CO₂ concentration itself will have a direct effect on vegetation since CO₂ is the substrate for photosynthesis by all terrestrial higher plants.

Terrestrial higher plants exchange large amounts of CO₂ with the atmosphere each year; *ca* 15% of the atmospheric pool of carbon is assimilated in terrestrial-plant photosynthesis each year, with an approximately equal amount returned to the atmosphere as CO₂ in plant respiration and the decomposition of soil organic matter and plant litter (Amthor, 1995a). Thus a change in plant carbon metabolism can potentially affect the atmospheric CO₂ concentration.

Our current state of knowledge provides a good basis from which to understand the immediate response of photosynthesis to CO₂ in terms of its effects on the reactions catalysed by Rubisco (Stitt, 1991). Rising concentrations of CO₂ will i) increase the rate of carboxylation, and ii) decrease the rate of oxygenation and consequently, photorespiration. In conditions in which Rubisco is limiting, an increase of the CO₂ concentration from 350 μmol mol⁻¹ to 700 μmol mol⁻¹ may be expected to lead to an increase in photosynthesis of 78% (Stitt, 1993). A wealth of experimental data has shown that the initial increase in assimilation rate when plants are grown in elevated [CO₂] ranges from 10 to 100% with a doubling of [CO₂], depending on species and experimental conditions (see reviews by Cure & Acock, 1989; Eamus & Jarvis, 1989; Luxmoore *et al.*, 1993). However, after a period of growth in elevated [CO₂] a myriad of secondary and tertiary responses and interactions, including changes in tissue chemistry, carbon allocation and nutrient use may occur, all of which may interact to affect both photosynthetic rates and long-term growth (Chapter 7 gives more details of the mechanisms involved). These longer term responses to environmental changes are commonly termed 'acclimation' and involve an adjustment of amounts of enzymes required to balance physiological processes. Some workers have used the terms acclimation and down-regulation synonymously, however, this is incorrect since acclimation can be in either direction whereas down-regulation is a reduction. I use the term down-regulation to refer to a change in the photosynthetic system which leads to a reduction in photosynthesis when measured under identical conditions of PPFD, temperature, [CO₂] and humidity.

Even after acclimation and down-regulation, photosynthetic rates are generally higher in elevated [CO₂] and a small increase in photosynthetic rate over a long period of time may translate to a significant increase in growth. In short-term (< six months) studies of responses to elevated [CO₂] and varying resource availability, whole plant biomass was found to increase by 38% on average for conifers and by 63% for deciduous trees (see review by Ceulemans & Mousseau, 1994). There is considerable variation in the response to elevated [CO₂] amongst species and experiments and part of this has been attributed to experimental methodology. Down-

regulation of photosynthesis and lack of growth enhancement has been related to sink limitation in experiments where plants are grown in pots too small to permit free growth of roots (Arp, 1991; Thomas & Strain, 1991). Poor control of nutrient supply or limited nutrient capital within pots has also been implicated (McConnaughay *et al.*, 1993) and the need for adequate control of nutrients during elevated $[\text{CO}_2]$ studies is essential in order to separate the effects of $[\text{CO}_2]$ from the effects of nutrient limitation (see Linder & Rook, 1984; Linder & McDonald, 1994).

1.1.2 Effects of increasing $[\text{CO}_2]$ on forests

Forests range across some 30% of the Earth's land surface (Kramer, 1981), account for 65-70% of terrestrial net primary production (Woodwell *et al.*, 1978) and approximately 70% of terrestrial atmospheric carbon fixation (Waring & Schlesinger, 1985). Any increase in the global growth rate of forests would represent a large new sink for atmospheric CO_2 and it has been suggested that woody plants may be even more responsive to rising levels of atmospheric CO_2 than are herbaceous plants (Idso & Idso, 1994).

Increased forest growth in response to globally rising CO_2 concentrations could provide an additional sink for the additional carbon entering the atmosphere and may represent the 'missing sink' for carbon in the global carbon budget (Tans *et al.*, 1990). In trees a small increase in relative growth rate at an early stage can result in a large difference in size of individuals at the end of the first year of growth, or even after a number of years, because of the compound interest rule. Thus the differential effect of elevated CO_2 on seedling growth may ultimately determine forest community structure (Bazzaz & Miao, 1993). Even when growth enhancement is limited by environmental resources, elevated CO_2 concentrations may still result in increased resource use efficiency (Norby *et al.*, 1992).

From a commercial viewpoint there is interest in how elevated CO_2 will influence establishment, growth and timber quality (Conroy *et al.*, 1990). If CO_2 influences the time of bud burst or bud set (Murray *et al.*, 1994), then trees may become liable to frost damage and selection of provenances from different latitudes may be required for future crops.

From an ecological viewpoint forests represent complex ecosystems involving processes operating at widely different spatial and temporal scales. The hydrological, nutrient and carbon cycles all interact and a change to one may influence the others in far-reaching ways. As it is not easy to design experiments to explore the likely impact of rising $[\text{CO}_2]$ on these systems, because of spatial and temporal constraints, the

most promising approach is to use simulation models to explore the behaviour and make predictions. These large scale process models need to be based on accurate sub-models and so there is a need for knowledge of the underlying mechanisms or at the very least robust empirical relationships. Thus there is an urgent need for basic research using experiments on plants or model systems to improve our understanding and fill gaps in our knowledge.

1.1.3 Sitka spruce

Sitka spruce is native to western North America where it grows along the coast from Alaska to Northern California. It was introduced into Britain in 1831 and is now the most widely planted timber-producing species in upland forestry in Britain, accounting for over 50% of current planting (Rook, 1992) and yielding on average approximately $12 \text{ m}^3 \text{ ha}^{-1} \text{ year}^{-1}$. The low density and poor strength properties make it unsuitable for constructional timber and it is primarily used for the manufacture of particleboard and fibreboard and is ideal for pulp and the manufacture of paper (Rook, 1992).

Cannell (1987) attributed the high productivity of Sitka spruce to three things:

- needles persist for six to eight years, leading to deep canopies which can intercept almost all solar radiation;
- needles and shoots are structured to allow penetration of light deep into the canopy; and
- the photosynthetic apparatus has the ability to acclimate to low light and low temperature, so that there is net carbon gain throughout almost the whole year in the British climate.

1.2 The issues

Although much research has been done on Sitka spruce with respect to growth (Bradbury & Malcolm, 1978), shoot development (Baxter & Cannell, 1977; Ford *et al.*, 1987), needle growth (Chandler & Dale, 1990), root growth (Ford & Deans, 1977), photosynthesis (Ludlow & Jarvis, 1971; Leverenz & Jarvis, 1980), stomatal conductance (Leverenz *et al.*, 1982; Morison & Jarvis, 1983) and canopy structure and light interception (Norman & Jarvis, 1974; Wang & Jarvis, 1990), there have been only a few studies investigating the effects of elevated atmospheric CO_2 concentrations on the growth and physiology of Sitka spruce (Townend, 1993, 1995; Murray *et al.*, 1994, 1996) and none have been made on mature trees. Seedlings

differ in many ways from older trees, from obvious differences in size, structural complexity and phenology to less apparent differences in morphology and physiology (Eamus & Jarvis, 1989). As a result of these differences, it is uncertain whether the observed responses of seedlings to CO₂ are accurate indicators of the potential carbon gain of mature trees under elevated [CO₂] (Mousseau & Saugier, 1992) and, therefore, there is a need for research on the effects of elevated [CO₂] on mature trees.

Often the increase in assimilation rate associated with growth in elevated [CO₂] does not translate to an equivalent increase in growth rate, *i.e.* more carbon is fixed per unit leaf area but no more growth occurs per unit plant mass. This may be explained by a reduction in the leaf area ratio, an increase in respiration rate or by movement of carbon from the leaves to the roots and out into the soil or back to the atmosphere, *i.e.* an increase in the flux of carbon through the plant to the soil. An increase in the flux of carbon through vegetation to the soil may have important implications for carbon sequestration and nutrient cycling in forests. Therefore there is need for research to determine how the flux of carbon through the plant to the soil responds to elevated [CO₂] and if there is an interaction with nutrient availability.

1.3 Aims of the study

The goals of these investigations are as follows.

In part I

- To investigate the effects of elevated atmospheric [CO₂] on the growth and physiology of mature branches using a branch bag system.
- To determine if down-regulation of photosynthesis or acclimation of stomatal conductance occurs in shoots on mature branches grown in elevated [CO₂] even in the absence of sink limitation.

In Part II

- To investigate the interaction between elevated CO₂ concentration and nutrient supply rate on the growth and allocation patterns of seedling trees.
- To construct 24 hourly carbon budgets for trees grown at two different nutrient supply rates and two different atmospheric CO₂ concentrations in order to determine the fate of carbon fixed in photosynthesis.
- To test the hypothesis that the flux of carbon from the atmosphere through the tree to the soil is higher in elevated atmospheric CO₂ concentrations.

1.4 Outline of the thesis

The thesis is structured in two parts. Part I covers the effect of long term exposure to elevated atmospheric [CO₂] on the growth and physiology of branches of mature Sitka spruce trees using a branch bag system. While Part II investigates the effect of elevated [CO₂] and nutrient supply rate on the growth and physiology of seedlings during their second year. There are nine chapters with the following contents and purposes.

Chapter 1. Introduction

This chapter introduces the background and sets the context for the thesis.

Part I. Effect of elevated CO₂ on mature Sitka spruce branches

Chapter 2. Branch Bag Design

This chapter describes the need for studies on mature trees and gives a description of the branch bag system developed for the long term exposure of mature branches to elevated [CO₂]. It also describes the field site and experimental design used.

Chapter 3. Growth of Branches and Needles

This chapter focuses on the effects of elevated [CO₂] on the growth of the branches over four years. It presents the results of the final harvest with a detailed deconstruction of the branches into their component age classes and explores the effects of [CO₂] on needle mass, shoot numbers, wood mass, wood density, needle frequency and stomatal density. It also presents the non-structural carbohydrate, starch, chlorophyll and nutrient concentrations of needles from different age classes over the course of the experiment.

Chapter 4. Photosynthesis of Mature Branches

This chapter presents the effects of elevated [CO₂] on photosynthesis and stomatal conductance of the two youngest age-classes of shoots throughout the experiment. It describes the design of a light source used to measure light-saturated photosynthesis and the photosynthetic response functions to light and CO₂.

Part II. CO₂ and nutrient interactions in Sitka spruce seedlings

Chapter 5. Description of Experiment

This chapter describes an experiment to explore the effect of elevated [CO₂] and nutrient supply rate on Sitka spruce seedlings growing in potting-compost or sand. It describes the open top chambers used to grow and expose seedling trees to elevated atmospheric [CO₂], the experimental design and nutrient application protocol. It also describes the design and performance of a purpose-built chamber to measure the CO₂ and water vapour fluxes from the above and below ground parts of the trees.

Chapter 6. Growth and Allocation in Seedling Trees

This chapter presents the results of six harvests throughout the growing season and shows the effects of [CO₂] and nutrient supply rate on the growth, numbers of shoots and allocation. It presents a simple model using a functional balance approach and discusses the results in that context.

Chapter 7. Shoot Photosynthesis, Carbohydrate and Nutrient Content

This chapter shows the effect of elevated [CO₂] and nutrient supply rate on the non-structural carbohydrate and nutrient content of needles through the growing season. It also presents the effect of elevated [CO₂] and nutrient supply rate on the photosynthetic capacity of current year shoots and discusses the likely mechanisms for the observed effects.

Chapter 8. Whole-tree CO₂ and H₂O Fluxes

This chapter presents measurements made of CO₂ and H₂O fluxes from above and below ground components of the seedling trees using the whole-tree measurement chamber described in Chapter 5. It constructs a carbon budget based on the fluxes of CO₂ and changes in plant biomass and organic matter in the pot and discusses how nutrient availability and elevated [CO₂] influence the flux of carbon through the atmosphere-plant-soil system.

Chapter 9. Synthesis and Conclusions

This chapter brings together the results from the mature branch and seedling studies and discusses the differences in the responses to elevated [CO₂]. It also summarises the main conclusions drawn from the experiments.

PART I

Effect of Elevated CO₂ on Mature Sitka Spruce Branches

CHAPTER 2

Branch Bag Experiment

2.1 Introduction

The majority of experiments designed to investigate the response of trees to elevated CO₂ has been carried out on seedling and juvenile trees in controlled environment or open-top chambers. It is questionable to extrapolate observations on seedlings to mature trees since they behave differently, both physiologically and phenologically (Eamus & Jarvis, 1989; Jarvis, 1989). Therefore, to understand the likely impacts of increasing atmospheric CO₂ concentrations on forests, it is essential to evaluate the impact of enhanced CO₂ on mature trees under field conditions.

A number of methods are being used to study mature trees in field conditions. The most obvious solution is to expose whole stands to the desired elevated CO₂ concentration. The FACE (Free Air Carbon Enrichment) program at Duke Forest, North Carolina is an attempt to increase the local CO₂ concentration within a 30-m-diameter circular plot within a loblolly pine (*Pinus taeda*) forest (Lewin *et al.*, 1994; Ellsworth *et al.*, 1995). Although this technique offers the possibility of studying the effects of elevated CO₂ on the whole tree-undergrowth-soil system under natural conditions, there are a number of major drawbacks. The huge cost of construction and then the cost of CO₂ and technical support required to run the system, makes it impossible for many sites to adopt the technique, so limiting the scope for experimenting in areas with different species, climates and soil types. Furthermore, the cost of replication inhibits getting a large enough sample size for the results to be statistically persuasive.

An alternative approach is to enclose individual trees growing in a forest and expose them to the CO₂ treatment. Whole tree chambers enclosing trees up to 7 m tall growing within a forest stand are being installed at the Flakaliden research site in Sweden and also in Finland. These chambers have both CO₂ and temperature control and thus will permit the study of the effects and interactions of CO₂ and temperature

on mature trees. CO₂ consumption has been reduced by recirculating the air but at the cost of increasing the load on the temperature and humidity control system. Once again the drawback of this method is the cost, both in construction and running the chambers, especially when taking into account the number of replicates required to obtain statistically meaningful results.

Branch bags represent a far cheaper and more cost effectively replicated technique for studying the growth of mature tissue under elevated CO₂ conditions. Branch bags were first used in pollution studies where they permitted the manipulation of pollutant concentrations to which individual branches were exposed (Houpis & Surano, 1988; Houpis *et al.*, 1991; Teskey *et al.*, 1991). This experiment was the first to adopt the branch bag technique for the study of elevated CO₂, however, subsequently many groups around Europe and in the USA have successfully used branch bags with CO₂ enrichment (Dufrene *et al.*, 1993; Teskey 1995; Liu & Teskey 1995)

In essence a branch bag is simply an impermeable envelope placed around a branch with a fan forcing air, either ambient or modified in composition, through the bag. The aim is to modify the composition of the air surrounding the branch while maintaining temperature, light intensity and light quality as close to ambient as possible. There are many variations in the design of branch bags, utilising different materials and construction techniques. For example, some have been designed to operate both as a fumigation system but also enabling the measurement of whole branch photosynthesis and transpiration at regular intervals (Dufrene, *et al.*, 1993).

2.2 Branch autonomy

A criticism of the use of branch bags is that only individual branches are being exposed to the treatment conditions and that the response of those branches may have been different had the whole tree been exposed to the treatment. The validity of this criticism depends on the degree of autonomy of the branch. Sprugel *et al.* (1991) discussed the potential for branches of trees to be autonomous with respect to carbon, *i.e.* to be independent from other carbon sources. Using ¹⁴C labelling techniques branches have been shown to be almost completely autonomous with respect to carbon once they pass a certain stage of development (Sprugel *et al.*, 1991; Cregg *et al.*, 1993). Thus, a branch will not import carbon from the tree no matter how stressed it becomes. If it cannot meet its own carbon requirement then it will stop growing and eventually will die. Branch autonomy with respect to the import of carbon is an important issue when the experimental treatment induces stress or

damage, such as ozone or SO₂, which might be ameliorated at the branch level by the import of carbon to the damaged area from healthy, untreated, branches.

Elevated CO₂ treatments almost invariably lead to an increase in carbohydrate production (see reviews by Cure & Acock, 1989; Eamus & Jarvis, 1989; Luxmoore *et al.*, 1993) and it is export rather than import of carbon that may be important to the results; especially as source-sink relationships are believed to account, at least in part, for the observed changes in the photosynthetic capacity of plants exposed to elevated CO₂ (Arp, 1991; Stitt, 1991). A branch supplied with elevated CO₂ attached to a fast growing tree will experience a strong sink for its carbohydrate production, this may not be the case where the whole tree is exposed to elevated CO₂ and the enhanced sources may overwhelm the sinks, leading to potential changes in starch accumulation, sink initiation and down regulation of photosynthesis.

Even with this potential drawback to the technique I believe that it may be of value for comparative studies of the effects of long-term CO₂ enrichment on the physiology and developmental processes in trees. Especially those effects which occur at the leaf level, such as changes in stomatal conductance and also possible changes to rates of photosynthesis and respiration which may enable a branch to maintain a positive carbon balance lower in the canopy. Furthermore, branch bags allow us to investigate the effects of elevated CO₂ on non-sink limited branches which may give valuable insight into the mechanisms responsible for the observed effects of elevated CO₂.

2.3 The Experiment

2.3.1 Objectives

The objectives of the experiment were to determine the extent to which long term exposure (more than two years) to elevated atmospheric CO₂ concentrations affects the growth, phenology, carbohydrate status, photosynthesis and stomatal conductance of Sitka spruce branches in the absence of sink limitation.

2.3.2 The stand

Cuttings from a parent Sitka spruce [*Picea sitchensis* (Bong.) Carr.], taken in 1972 were grown in pots until 1984 they were then planted in a 12 X 12 block at 2.5 m spacing at Glencorse Mains near Penicuik, 17 km South of Edinburgh (55° 31' N, 3° 12' W). Soil at the site is of the 'Winton series of the Rowanhill' (Ragg & Futty, 1967), and more base rich than the acid forest soils typical of areas where Sitka spruce plantations are grown (Heaton & Crossley 1995).

2.3.3 The experimental design

In March 1991 a scaffolding platform with a walkway two metres above the ground was erected around a selected block of six trees. There were two trees between the experimental trees and the edge of the stand to the South, three to the West and seven to the North and East. Three branches of the third whorl on each of the six trees were chosen for treatment: one branch was left as an unbagged control (C), one bagged and supplied with ambient air (A) and one bagged and supplied with air enriched by the addition of CO₂ (E) to raise the concentration by 350 $\mu\text{mol mol}^{-1}$ above ambient (*i.e.* to *ca* 700 $\mu\text{mol mol}^{-1}$ depending on the ambient concentration). It was necessary to remove some branches on trees where there were more than four branches on the third whorl or where two branches were very close together. The treatments were allocated at random to the branches, however, in some cases where it was impossible to support a branch bag it was necessary to swap between a bagged and unbagged treatment. Figure 2.1 shows the orientation of the branches and the numbering system used to identify them. There were six replicates of each treatment. The bags were installed and running before bud burst, in 1991.

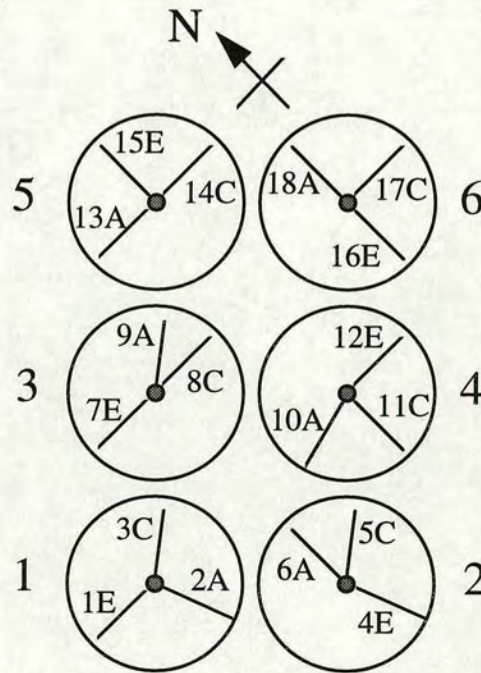


Figure 2.1 Plan of the block of trees indicating the tree number, branch number, orientation and treatment. A=ambient, E=elevated and C=control.

A description of the design of the branch bags has been published Barton, Lee & Jarvis (1993).

2.3.4 Statistical analysis

All data were visually inspected using scatter plots, box plots and distributions (SAS Insight) any spurious values or outliers were investigated for errors in measurement, calculation or transcription and corrected where possible or removed if a valid reason was apparent, e.g. a sensor malfunction.

Unless otherwise stated all results were analysed using a one way ANOVA and Tukey's studentized range test was used for comparison of means (Proc GLM, SAS institute, Cary, NC, USA). Comparison between the unbagged control (C) and the ambient bagged (A) treatments estimates the effect of the branch bags themselves while comparison of the (A) with the bagged elevated branches (E) estimates the effect of growth in elevated [CO₂].

2.4 Design of bag

2.4.1 Branch bag construction

The design of the bags was inspired by those of Teskey *et al.* (1991), and in essence, is similar: it is an open bottom design where the air stream enters from the apical end of the branch, passes through a diffusing screen then through the branch chamber and exits toward the basal end of the branch. However, the materials and construction are different. A low-cost light-weight, robust structure that moves with the branch was required. This differs from other designs where the bag and branch move independently, increasing the risk of branch abrasion (Houpis, *et al.*, 1991) or the tree is prevented from moving in the wind which may induce abnormal stresses.

A branch bag (Figure 2.1) consisted of a wire frame covered with a polyethylene sleeve. The frame was made of four hoops (0.57 m dia.) and four longitudinal struts of 5 mm diameter galvanised fencing wire spot-welded together. A collar of galvanised steel with an internal diameter of 10 cm allowed insertion of the air duct and sealing of the polyethylene sleeve. The hoops were spaced at 50 cm giving a bag volume of approximately 400 dm³. The longitudinal struts extend 80 cm beyond the last hoop to allow attachment to the tree trunk.

The sleeve was made from 1000 gauge (0.23 mm) polyethylene lay-flat tubing (Bailey Polythene Ltd, Ventnor, Isle of Wight) chosen for its transmission of longwave radiation and resistance to damage by Sitka spruce needles. A 1 m plastic zip (Coats, Glasgow, UK) sown into the sleeve allowed easy access to the branch. A diffuser of perforated polyethylene film with 1 cm diameter holes at 4 cm spacing

was stretched over the hoop nearest to the air inlet to distribute the air-flow evenly across the cross-section of the bag.

The branch bags were first built in 1991 then were replaced with a slightly modified design in May 1993 to facilitate the growth of the branches. The modified design used 20 mm diameter polyethylene water pipe bent into hoops (75 cm diameter) and 6 mm stainless steel rod for the longitudinal struts. The bags varied in length from 2 to 3 m depending on the size of the branch. Flat sheet polyethylene was attached to the frame and sealed with 100 mm wide polyethylene repair tape.

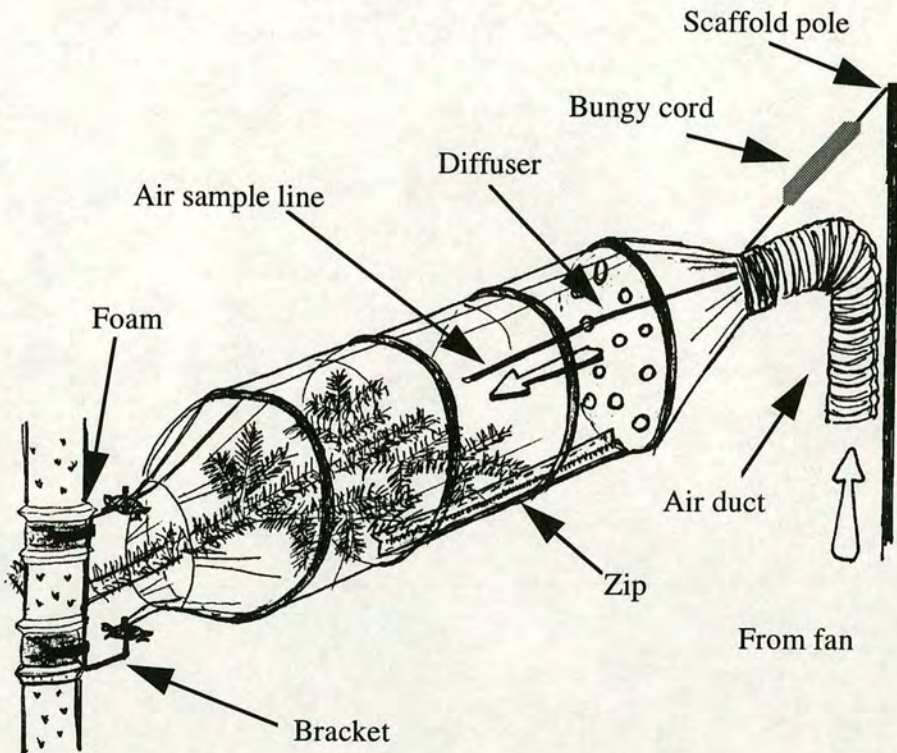


Figure 2.1 Diagram of a branch bag.

The bag was attached at the trunk by brackets made from 6 mm dia steel rod bent to shape and then brazed to two curved steel straps (Figure 2.1). To protect the tree, 3 cm thick foam rubber was wrapped around the trunk and the brackets were clamped onto the foam using large hose clips so that one arm of the bracket extended below the branch insertion point and one above it. The longitudinal struts of the bag were then connected to the bracket using retort stand clamps. The air inlet end of the bag was tied to the scaffold pole using nylon cord and rubber bungy cord. This gave a flexible connection to allow the tree movement in the wind.



Picture 1 Branch bags in 1991.



Picture 2 CO₂ monitoring and control system.

2.4.2 Air supply

The air was supplied to each bag by a fan blower (45 CTL, Airflow Developments Ltd, High Wycombe, UK: maximum air flow $5.4 \text{ m}^3 \text{ min}^{-1}$) which was mounted in a weather proof housing with 1 m long legs standing on the ground. Four fans were mounted in each of three housings, one fan per bag. An air duct made from unperforated plastic land drain with a diameter of 10 cm ran from the fan, passed through the bag collar and was taped in place with duct tape. The average length of ducting from the fan housing to a branch bag was 6 m. The end of the bag nearest the trunk was open but narrowed down to half the diameter of the bag in order to reduce incursions by wind.

A butterfly valve positioned in each duct close to the housing enabled manual setting of the air flow rate. The fans were capable of supplying up to ten air changes per minute but were usually run at three, a compromise between elevated temperature and conservation of CO_2 .

Air was originally drawn through the bottom of the housing but, because of high night-time CO_2 concentrations from soil respiration, which lead to abnormally high night-time CO_2 concentrations in the branch bags, the design was changed: the bottom of the housing was sealed and an extra length of duct was installed to draw air from branch height. A netting mesh was used to prevent insects being drawn into the air intake.

2.4.3 CO_2 control and monitoring hardware and software

The CO_2 monitoring and control system (Figure 2.2) consisted of sample and injection sub-units controlled by a personal computer *via* interface cards (AOP6 and ADC42, Blue Chip Technology, Clwyd, Wales, UK).

A diaphragm pump (B100SE, Charles Austen, Weybridge, UK) drew air continuously from all of the bags through 4 mm i.d. nylon sample lines. To allow for different flow resistances in the sample lines, each was fitted with a needle valve and flow meter to enable the flow rates through the lines to be balanced ($1 \text{ dm}^3 \text{ min}^{-1}$). Each sample line contained a 3-way solenoid valve which, when activated, diverted the airstream to the IRGA (infra-red gas analyser)(SBA-1 OEM, PP systems, Hitchin, UK), through which the air was drawn by the IRGA's internal pump. Thus, on switching, the IRGA rapidly stabilised (20 seconds) on a new sample line. The solenoids were controlled by the computer *via* a multiplexer and relays.

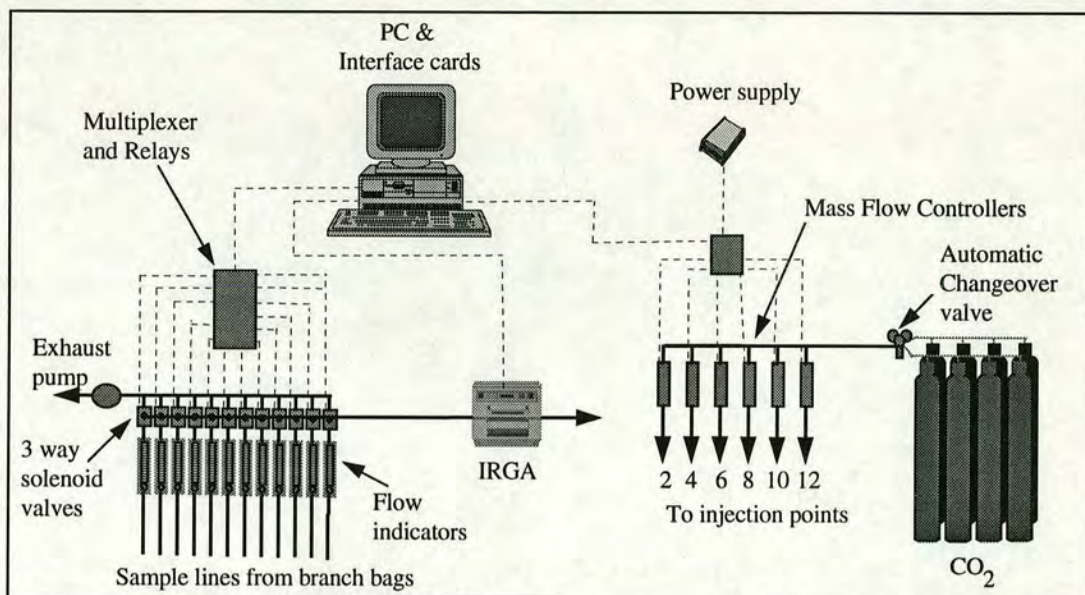


Figure 2.2 CO₂ control and monitoring system.

The software was written in Borland Turbo Pascal and has been used to monitor and control CO₂ concentrations in branch bags, open top chambers and growth rooms at a number of sites. It was designed to be flexible in order to be used in systems with different numbers of chambers (up to 24) and with mass flow controllers (software controlled) or needle valves (manual) metering the CO₂ injection.

Each elevated chamber can have an independent CO₂ setpoint which can be either a fixed value (i.e. 700 $\mu\text{mol mol}^{-1}$) or ambient plus a fixed increment (see below). Dynamic control of CO₂ concentration is achieved using mass flow controllers (FC260, Tylan General (UK) Ltd., Swindon, UK) driven by the PC interface card. The software uses a simple proportional feedback algorithm, with damping to reduce oscillations in the feedback loop which might arise because of fluctuations in the airflow through the chambers.

The control program cycles through the chambers. After selecting a chamber the IRGA is flushed without taking readings for a short period then readings are taken over a set time interval and the mean recorded. The flushing and sampling intervals are user defined to allow for IRGAs and pipework with different characteristics. After each cycle of measurements the readings are stored on the hard disc. The last 100 readings for each chamber are held in memory and used for graphical display.

The original aim was to maintain the CO₂ concentration in elevated bags at 700 $\mu\text{mol mol}^{-1}$, regardless of any variations in the background concentrations. The

bags were run using this system for the first six months with very tight control of the CO₂ concentration. However, since the ambient CO₂ concentration fluctuated both diurnally and with the weather systems the approach was changed to allow the elevated CO₂ bags to have a natural diurnal CO₂ cycle similar to that in the ambient bags. This was achieved by modifying the software, initially still using dynamic control with the mass flow controllers, so that the CO₂ concentration in the elevated bags was always 350 μmol mol⁻¹ above the ambient bags. However, analysis of the settings of the mass flow controllers over time demonstrated that the mass flow of air through the bags was reasonably constant and incursions of air into the open end of the bag were so slight that dynamic control was unnecessary. The mass flow controllers were, therefore, replaced by precision needle valves to give a constant fixed addition of CO₂ to the airstream. This allowed the mass flow controllers to be used with the newly installed whole-tree chambers which were more sensitive to wind and required dynamic adjustment of CO₂ injection.

CO₂ was initially supplied from gas-withdrawal cylinders, eight of which were manifolded together in two groups of four with an automatic changeover valve between the groups. In 1992 the site was extended to include 12 whole tree chambers containing birch. The increased demand for CO₂ necessitated supply being switched to palletted packs of 20 liquid-withdrawal cylinders (SK 450, Distillers MG Ltd., 680 Main Street, Bellshill, Lanarkshire, UK). Then in 1993 a six tonne bulk tank was installed thus reducing the frequency of delivery and labour required to maintain the CO₂ supply.

Liquid CO₂ passed from the palette/tank to a 2 kW vaporiser, through a pressure reducing valve set at 300 kPa and then through a fail-safe solenoid valve (in case of power failure). The flow was then split to supply each of the massflow controllers or needle valves for the branch bags and tree chambers. The CO₂ was injected into the air duct just after the butterfly valve and close to the fan housing, thus allowing mixing to occur as the air flowed through the duct. The six elevated CO₂ branch bags consumed approximately 14 kg of CO₂ per week.

2.4.4 Environmental monitoring

A data logger (CR7, Campbell Scientific, Shepshed, Leicestershire, UK) was used to log environmental data every half hour. Temperature in each bag was initially measured using a radiation shielded thermistor ventilated by the air sampling line. In 1993 the thermistors were replaced with fine wire differential thermocouples, one junction inside and the other outside each bag.

A quantum sensor (SD 1010, Macam Photometrics Ltd., Livingston, Scotland) was used to measure light above the canopy and two home-made ventilated psychrometers (Allen *et al.*, 1994) were used to measure ambient temperature and relative humidity within the canopy. In 1993 the psychrometers were replaced with temperature/humidity probes (HMP35A, Vaisala (UK) Ltd).

There was also a full weather station within 100 m of the site giving background environmental data.

2.5 Performance

The branch bags were run continuously from May 1991 to November 1994. The CO₂ enrichment regime was continuous apart from occasional power failures and equipment failure, amounting to less than 50 days in four years. There was also a two week period of downtime in November 1992 when the computer was stolen from the field site. The bags survived severe gales (>35 m s⁻¹ gusts) with no damage.

2.5.1 CO₂ control

Figure 2.3 shows a typical 48 hour course of CO₂ concentrations, recorded at 15 minute intervals, for an ambient and an elevated bag during two days in September 1992.

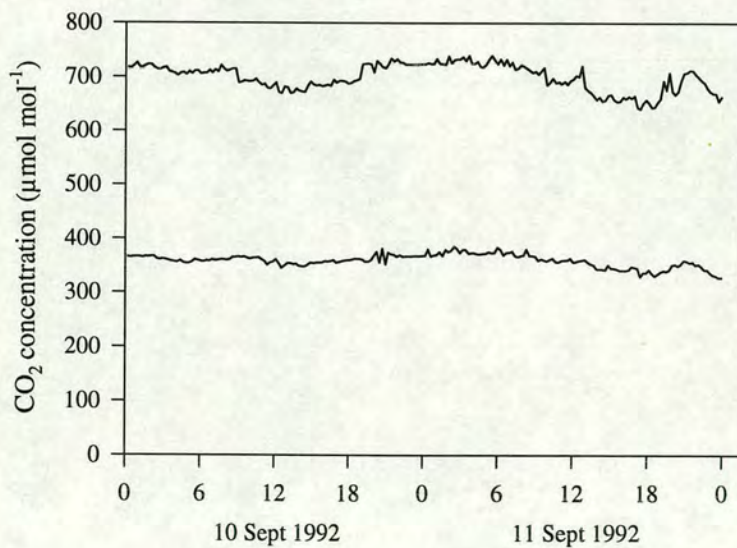


Figure 2.3 Typical 48 hourly course of CO₂ concentration within an ambient and elevated branch bag.

Figures 2.4A and 2.4B show frequency distributions of the deviations from the target CO₂ concentration for two 4 month periods. When dynamic control was in use CO₂ concentrations were within 10 $\mu\text{mol mol}^{-1}$ of the target concentration for 90 % of the time (Fig 2.4A). The CO₂ concentration was within 40 $\mu\text{mol mol}^{-1}$ of the target concentration for 90 % of the time when the mass flow controllers were exchanged for needle valves (Fig 2.4B). The needle valves required periodic manual adjustments to compensate for changes in pressure across the valve and slight changes in the mass air flow through the branch bags.

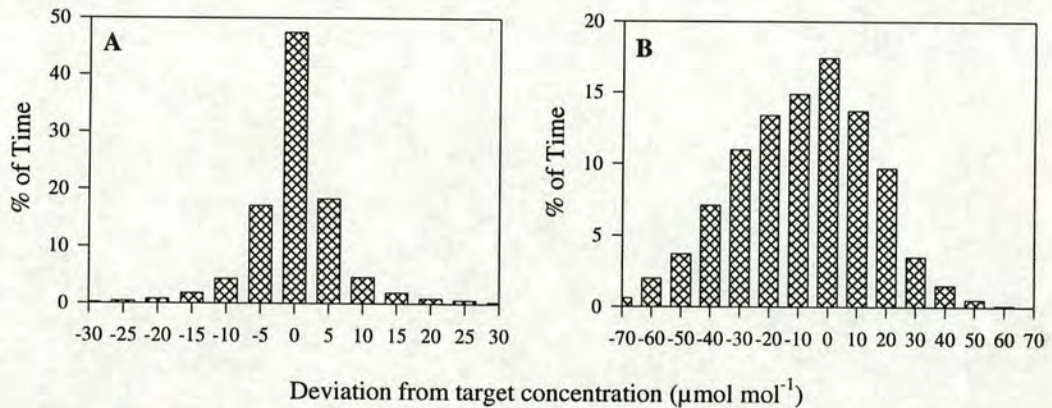


Figure 2.4 Frequency histogram of deviations from target CO₂ concentrations between June and September 1991 with active control of CO₂ using massflow controllers and a target [CO₂] of 700 $\mu\text{mol mol}^{-1}$ (A) and between June and September 1992 using needle valves controlling CO₂ and a target [CO₂] of ambient + 350 $\mu\text{mol mol}^{-1}$ (B).

2.5.2 Temperature

As with all field chamber systems (see Bonte & Mathy, 1988) which are not air conditioned, temperatures within the branch bags were slightly higher than ambient (Figure 2.5) but were less than 1.5 °C above ambient for 80% of the time, over the period June-September 1991 and April-September 1994 and less than 1.5 °C for 95% of the time during autumn and winter months.

Solar radiation is responsible for the bulk of the temperature increase (Figure 2.6) but there is also a constant heat input into the air stream from the fan motors which gives rise to an increase in temperature of approximately 0.5 °C. During periods of intense sunshine over-temperatures of 6 °C occasionally occurred (data not shown) but these were less frequent in the third and fourth years as the trees grew and shaded the bags.

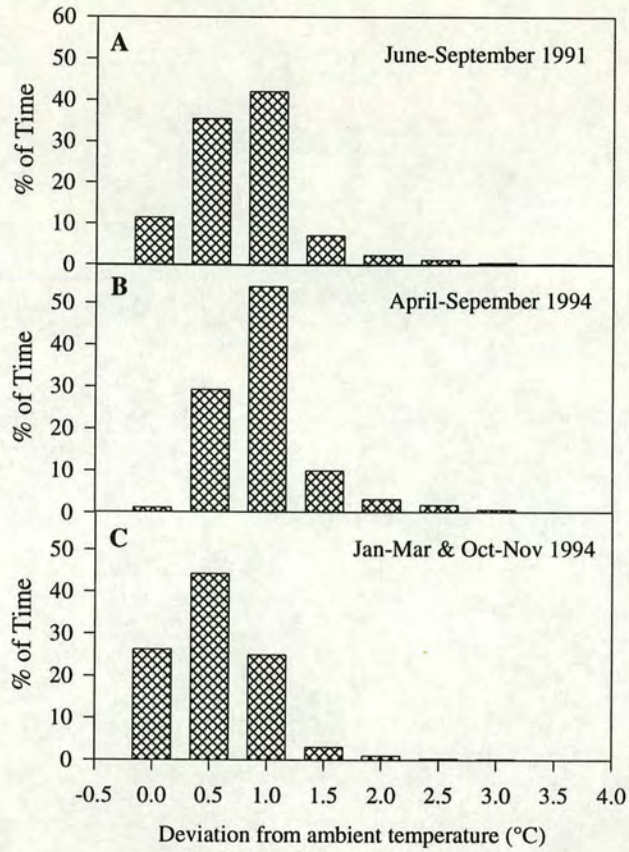


Figure 2.5 Frequency histogram of deviations in temperature from ambient within the branch bags.

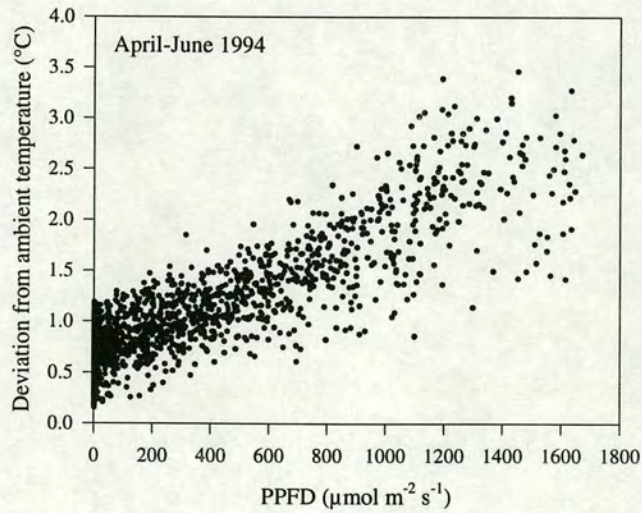


Figure 2.6 Relationship between the deviation from ambient temperature within the branch bags and photosynthetically active photon flux density during the period April-June 1994.

2.5.3 Properties of the polythene film

Light transmission of the polyethylene covering is shown in Figure 2.7 for new polyethylene film and film that has been part of a branch bag and weathered for one year. New film transmits 90% of the radiation between 350 and 850 nm, while transmission of film that has been weathered drops to 86%.

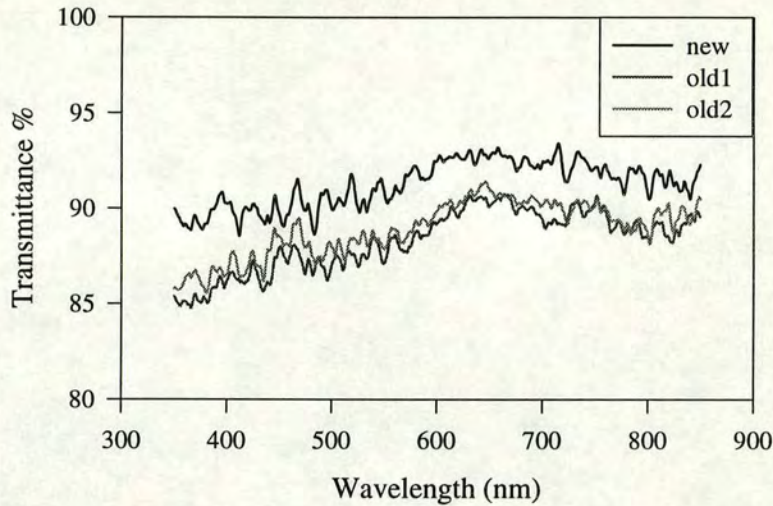


Figure 2.7 Light transmission of new and weathered polyethylene film.

The slight translucence of the film causes it to act as a diffuser scattering a proportion of the light. Under conditions of full sun or when the beam fraction is high this scattering of the incoming radiation may partially compensate for the attenuation, since light will be used more efficiently by the branch (Krueger & Ruth, 1969; Szawiawski & Wierzbieck, 1978)

The bags were washed periodically and the polyethylene sleeve was replaced each Spring to maintain maximum light transmission.

CHAPTER 3

Growth of Branches and Needles

3.1 Branch growth

3.1.1 Apical shoot extension

The length of the apical shoot of each branch was measured frequently during the growth period for each of the four years (Figure 3.1).

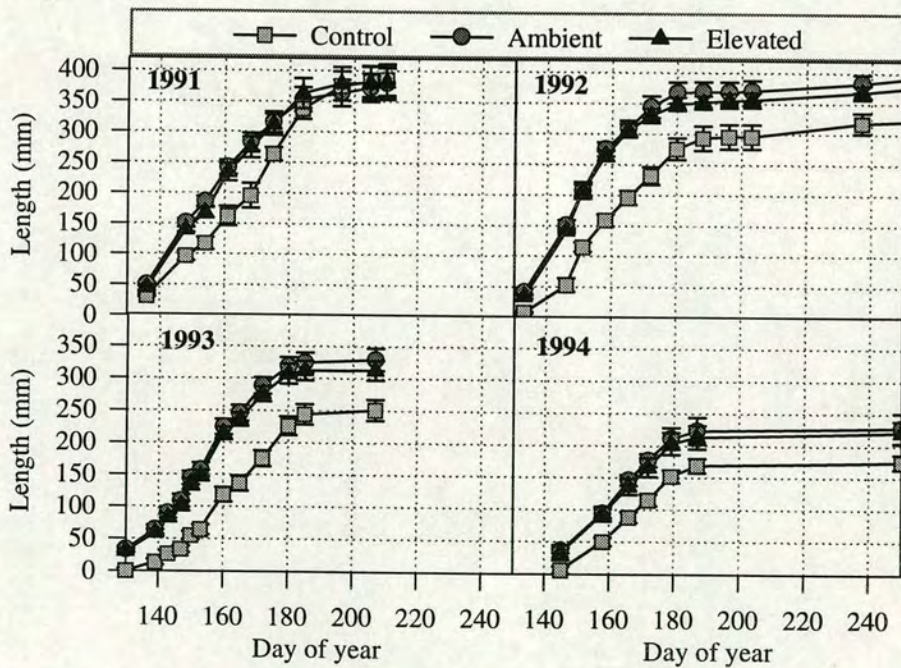


Figure 3.1 Apical shoot extensions for branches over four years. Mean \pm 1 SEM, n = 6.

There were no significant differences between CO₂ treatments in timing of bud burst or in the final length of shoots in any of the four years. In 1991 the bagged branches flushed a few days earlier than the control branches and extension finished earlier, nevertheless the final length was the same for all treatments. In following

years the **C** (unbagged, control) branches again flushed approximately ten days later but the shoots failed to attain the same final length as the **A** (ambient) and **E** (elevated) shoots. The bags were slightly ($< 1.5\text{ }^{\circ}\text{C}$) warmer than the unbagged controls and this almost certainly explains the earlier flushing.

3.1.2 Internode diameters

The diameters at the mid-point of each internode along each branch were measured at the end of each year in two orthogonal directions using a digital calliper (Figure 3.2). There were no significant differences in internode diameters between treatments in any of the four years.

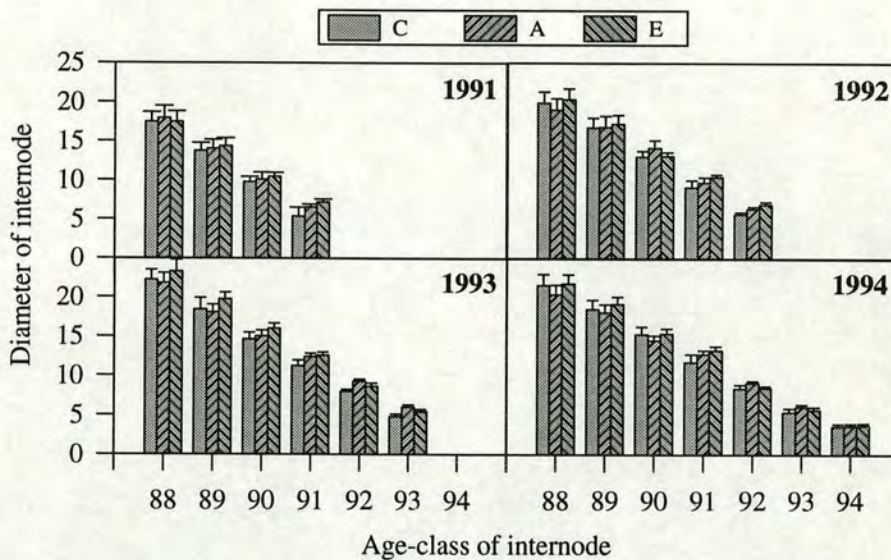


Figure 3.2 Diameters of each internode at the end of each year. Means ± 1 SEM, $n = 6$.

3.2 Harvest analysis of branches

The branches were harvested in November 1994. Each branch was dissected into age-classes of shoot whorl by whorl, along the length of the branch (see Figure 3.3). First, the lengths of first order laterals were measured and then they were removed and dissected into individual age-classes. The number of shoots in each age-class and fresh mass of each age-class were measured independently for each 'whorl' of first order laterals along each branch. The samples were dried at $70\text{ }^{\circ}\text{C}$ for 48 hours and then the needles were separated from the wood and dry mass for each component measured. Thus each branch was decomposed into 56 separate parts.

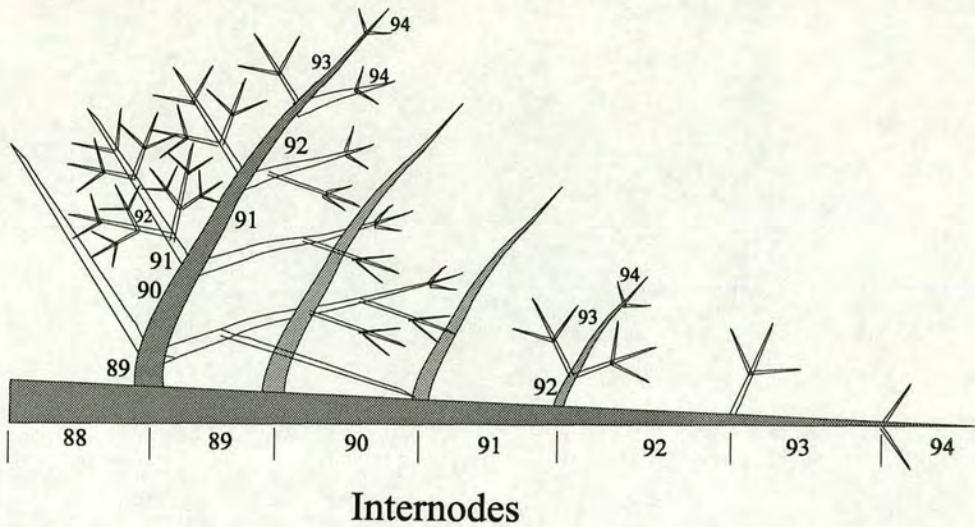


Figure 3.3 Branch structure and break-down into age-classes. Indicating branch internodes. First order branches are shaded with the 89 and 92 first order branches shown in detail.

3.2.1 Number of shoots

There were no significant differences in the number of shoots between treatments in any of the age-classes of shoot, although A did have fewer shoots than E and C in most of the age-classes. The numbers of shoots increased each year up to 1993 then declined in 1994. This pattern is typical of spruce where trifurcation occurs at most apices in young branches but as the branch becomes shaded the number of buds that flush each year declines.

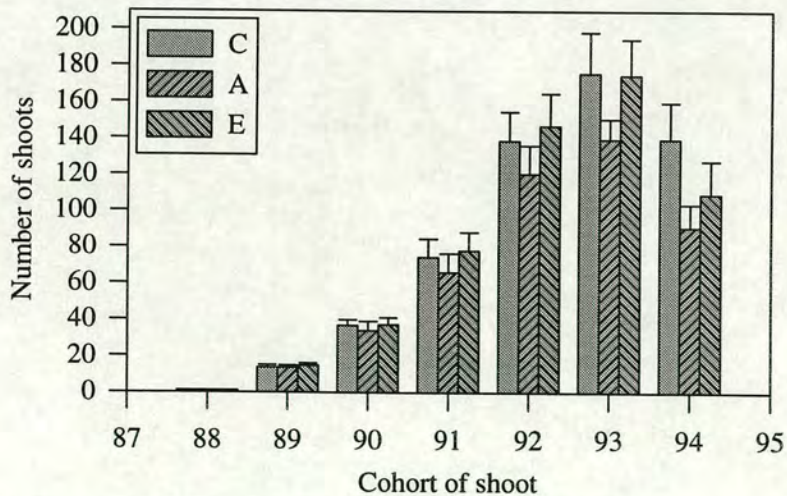


Figure 3.4 Number of shoots in each cohort when the branches were harvested (Nov. 94). Mean \pm 1 SEM, n = 6.

3.2.2 Individual needle mass, area and specific leaf area

Sub-samples of needles from each age class were taken from each branch to determine the specific leaf area (SLA). Fifteen needles from each branch and age-class were stuck on to a piece of paper using matt adhesive tape. An image analysis system comprising a high resolution video camera and image analysis software (Optimas) was used to measure the projected leaf area of the needles which were then oven dried at 70 °C for 24 hours and then weighed.

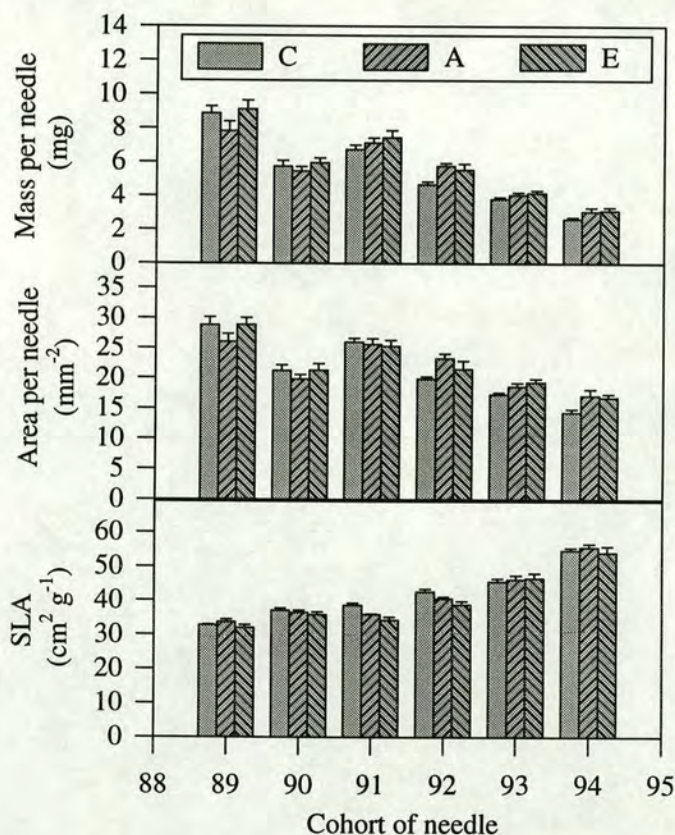


Figure 3.5 Mass, area and specific leaf area of needles for each cohort of needle at the harvest (Nov. 94). Mean \pm 1 SEM, $n = 6$.

The mass per needle decreased with age-class apart from the 1990 cohort which were lighter than might be expected. Projected needle area also decreased with age-class but not to the extent that the mass decreased and so the specific leaf area (SLA) increased with age-class (Figure 3.5). Spruce needles typically live for 5-15 years and once fully expanded, shortly after flushing, the length of a needle remains constant for the remainder of its lifetime however, the width, thickness and mass tend to increase as new phloem is produced each year (Ewers, 1982; Flower-Ellis, 1993).

The initial size of a needle and its cross sectional profile depend on its position in the canopy, current year needles are bigger at the top of the crown than at the bottom, where conditions are more shaded and branches are nearing their light compensation point (Leverenz & Jarvis, 1980; Niinemets & Kull, 1995). The observed differences in needle area and mass with age-class reflect these characteristic patterns of spruce needle growth.

There were no significant differences in mass, area or SLA between treatments, although C needles of the 92, 93 and 94 cohorts were slightly lighter and smaller, indicating a bag effect on needle growth but no CO₂ treatment effect.

3.2.3 Total branch needle mass and area by age class

The distribution of needle mass across age-classes at the time of the harvest showed the 1992 cohort to be the heaviest (Figure 3.6). As mentioned earlier needles produced at the top of the canopy are larger than those produced further down and needles tend to become heavier as they age, thus the distribution of needle mass at the time of harvest reflects the number produced in each year, the initial size and the increasing mass with age. Needles from the 89 and 90 cohorts showed no evidence of a response to the treatments but the 91, 92 and 93 cohorts were heavier both in response to the branch-bag and to the CO₂ treatment but, the differences were not statistically significant.

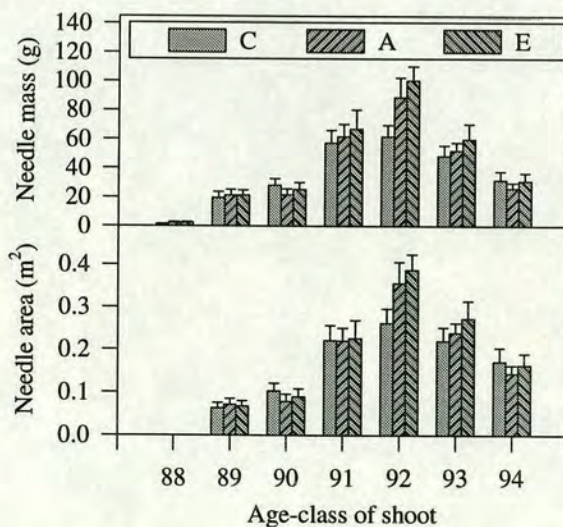


Figure 3.6 Needle mass and needle area for each branch broken down by age-class of shoot. Mean \pm 1 SEM, n = 6.

The projected area per needle probably increased slightly as the needles aged and as almost no needles were lost from the branch over the course of the experiment the total needle area per age-class on a branch at the time of harvest must have been the same or slightly larger than the area produced at the time the needles flushed. Thus the needle area in the current age-class rose each year from 1989 to 1992 then began to decline through 1993 and 1994 (Figure 3.6). This trend follows that of shoot numbers (Figure 3.4) except that the number of shoots in an age-class peaked in 1993, indicating a reduction in the needle area per shoot as shown in Figure 3.7. The unbagged branches had the same number of shoots but less leaf area per shoot ($P < 0.05$) than the bagged branches in 1992, 1993 and 1994, *i.e.* once the bags had been installed. However, there was no significant CO₂ effect.

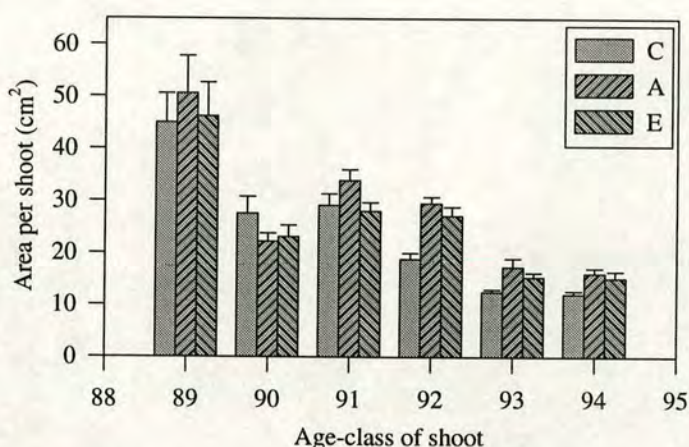


Figure 3.7 Mean projected needle area per shoot at the time of harvest. Calculated by dividing the summed needle area of each age-class by the number of shoots in that age-class for each branch. Means \pm 1 SEM, $n = 6$.

The proportion of leaf area in the current, the C+1 (*i.e.* one-year-old) and C > 2 (*i.e.* more than one-year-old) age classes, after needle expansion in each of the years 1991 to 1994, was calculated assuming the needle area just after needle expansion was the same as at the time of the harvest (this ignores any increases in needle area over time). In 1991 the current year needles accounted for more than 50% of the needle area on the branch but this gradually declined as the demography changed and by 1994 the current needles only accounted for ~15% of the total area (Figure 3.8). *N.B.* needles change from one age-class to the next when the new buds flush in May and not on 1st January, a convention that some researchers use.

Figure 3.8 shows the distribution of needle area by age-class on a branch as it ages and progressively becomes lower in the canopy. If we assume that all branches

follow the same demographic pattern and that the tree has six live whorls of branches then we can estimate the distribution of leaf area by age-class on the whole tree as follows:

$$C_n = \sum_{i=0}^{i=5-n} s_{(89+i)}$$

where

C_n = total needle area of age-class n , *i.e.* C_0 = current, $C_1 = C+1$, etc.

$s_{(89+i)}$ = needle area of $89+i$ cohort on the branch when it was harvested in November 1994 (see Figure 3.6).

The resulting distribution is shown in Figure 3.9 and shows that the current age-class accounts for the largest single fraction, ~33%, of all needle area, with the amounts in each age-class declining with age.

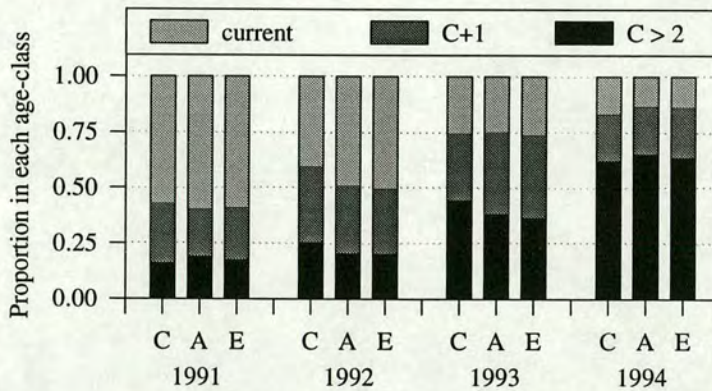


Figure 3.8 Proportion of total projected needle area in current, C+1 and C > 2 (needles older than one) age-classes at the end of each of the four years of the experiment. Estimated from the distribution of needle area obtained at the harvest in November 1994.

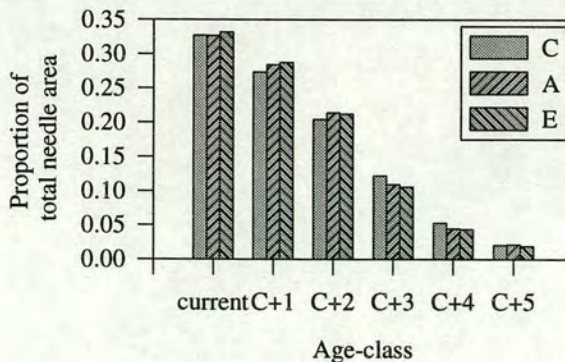


Figure 3.9 Estimated proportion of needle area of each age-class on a whole tree with six live whorls assuming the same demographic distribution found on the experimental branches when they were harvested.

3.2.4 Needle frequency.

After oven-drying the branches the needle frequency (number of needles per centimetre length of shoot) was determined by counting the needle pegs on a 3 cm length of each of the five internodes from each branch. As internodes age they increase in diameter but not in length and so the needle frequency is conserved, furthermore the needle pegs remain even if the needle has senesced and fallen off. An impression was made by rolling a length of each internode in plasticine and then counting the dents made by the needle pegs.

There were no differences in needle frequencies between treatments. Needle frequency increased with the age class of the internode while the length of the internode (or apical shoot) decreased with age class (Figure 3.1).

Table 3.1 Needle frequency (No. per cm length) measured on branch internodes for five age-classes of internode. Means with the same letter are not significantly different ($P < 0.05$), $n = 6$.

Age-class of internode	Needles cm^{-1} length
88	14.8 a
90	15.8 ab
92	17.2 bc
93	17.4 bc
94	18.1 c

3.2.5 Mass of wood

Wood mass declined with age-class despite the increase in the number of shoots. **E** wood from each age-class was heavier than **A** wood, although not significantly (Figure 3.10). **C** shoots of the 88, 89 and 90 cohorts were a similar mass to **E** but the 91, 92 and 93 were slightly lighter. The innermost growth rings of the 88, 89 and 90 shoots had formed prior to the start of the experiment and so might be expected to show proportionately less response to the treatments.

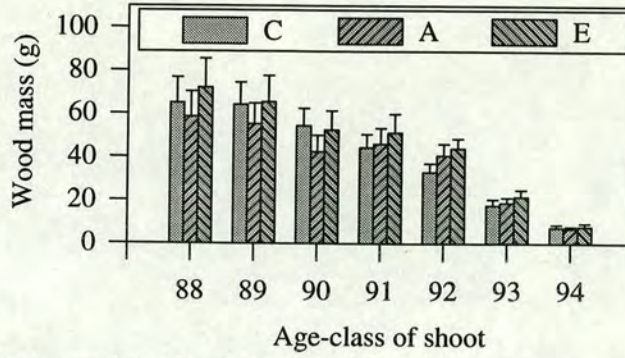


Figure 3.10 Dry mass of wood in each cohort of shoot at the harvest. Mean \pm 1 SEM, $n = 6$.

3.2.6 Density of wood

The density of each internode section was calculated by dividing the volume, determined from the midpoint diameter and length, by the dry mass of the section. Density increased with age-class but there were no significant differences between treatments. Part of the difference between age-classes may be attributed to the difference in density between wood and bark. Younger stems have proportionately thicker bark and so the calculated density will be more strongly influenced by the bark in younger stems.

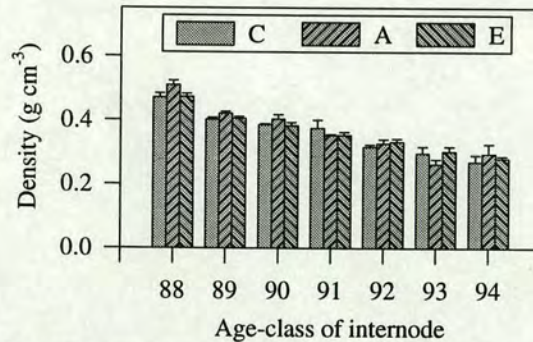


Figure 3.11 Density of wood in each internode age-class. Mean \pm 1 SEM, $n = 6$.

3.2.7 Summary of harvest results

There were no significant differences between the dry mass of needles or wood between the treatments at the harvest in November 1994 (Table 3.2). The total number of shoots was not effected by either the bag or the CO₂ treatment. The increase in the length of the control branches during the period of the experiment was significantly smaller than the bagged branches. The total projected needle area was not significantly different between treatments but the trend was for elevated branches to have larger area than ambient which was larger than the control.

Table 3.2 Dry mass of needles and wood of branches at harvest. Needle area was calculated from dry mass and the specific leaf area for each age-class. The length is the growth during the period of treatment (1991-1994). Means \pm 1 SEM, n = 6.

	Control	Ambient	Elevated
Length (cm)	102 \pm 6.8 **	129 \pm 4.3	124 \pm 1.9
Dry mass Needles (g)	286 \pm 43.2	269 \pm 41.7	314 \pm 49.6
Dry mass Wood (g)	248 \pm 35.4	273 \pm 35.8	307 \pm 44.8
Needle Area (m ²)	1.04 \pm 0.14	1.11 \pm 0.15	1.21 \pm 0.17

3.3 Stem cross-section and leaf area

According to the 'pipe model' theory there should be a relationship between the cross-sectional area of sapwood within a stem or shoot and the leaf area 'supported' by that stem or shoot (Shinozaki *et al.* 1964a, Shinozaki *et al.* 1964b). To investigate the strength of this relationship and to see whether the treatments had influenced it, the needle area supported by each internode (*i.e.* the cumulative area distal to the internode) was plotted against the cross-sectional area at the mid-point of the internode, calculated from the outside-bark diameter (Figure 3.12). A regression was calculated for each branch and the mean slope and intercept for each treatment determined. C had the lowest slope followed by E then A. The slope of C was significantly different from that of A but A and E were not different from one another ($P < 0.05$). The intercepts were not significantly different from one another. A steeper slope indicates more leaf area per unit cross-section of stem, *i.e.* per unit area of conducting tissue.

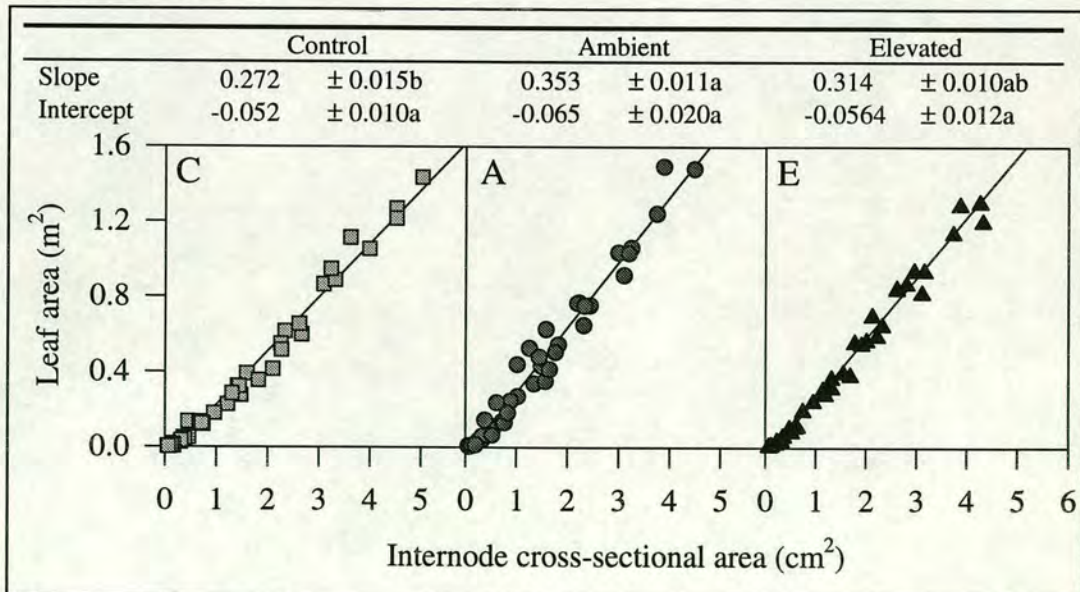


Figure 3.12 Relationship between internode cross-sectional area and the projected needle area 'supported' by the internode. Each graph shows six branches with six internodes. Lines are regressions with parameters given above (\pm 1 SE).

3.4 Needle physical properties

Needles were sampled from each age-class at regular intervals throughout the experiment to determine the effects of CO₂ concentration and branch bag on physical and biochemical properties of needles. Needles from the 91 cohort flushed under the treatment conditions but the buds were formed prior to installation of the branch bags. While needles from the 92, 93 and 94 cohorts were both initiated and expanded under treatment conditions and those from the 90 cohort were initiated and expanded outside branch bags, but secondary phloem development occurred under treatment conditions.

Length, midpoint width and thickness, fresh mass and dry mass were measured on five needles from each branch and age-class. The area was calculated as the length x width. Data for needles sampled in October 1993 are shown in Figure 3.13.

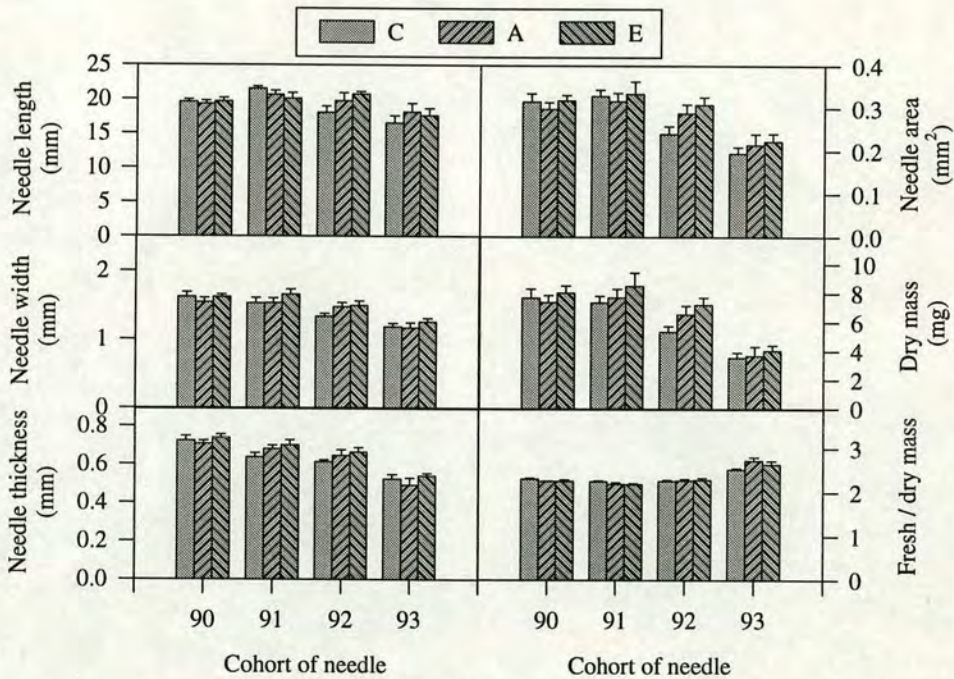


Figure 3.13 Needle properties of four cohorts of needle in October 1993. Mean \pm 1 SEM, $n = 6$.

There were no statistically significant differences in any of the physical properties of needles of the same age-class between treatments at any time during the experiment.

3.5 Stomatal density

The stomatal antechambers of Sitka spruce are filled with a matrix of wax tubules which show up as white dots on the needle surface. The stomata occur in a number of straight lines running along the length of the needle either side of the mid-vein and on both sides of the needle, however 70-80 % occur on the abaxial surface.

Stomatal density was determined on needles from the 1993 cohort in January 1994 using a stratified sampling strategy. One needle was collected from each of three shoots from three branches per treatment and carefully placed in a vial to prevent disturbance of the surface waxes. The needles were viewed with a binocular microscope fitted with a graticule at x40 magnification. Three 1 mm long 'fields' were viewed per needle. The width of the needle and width of the stomatal region were measured and the number of lines of stomata and number of stomata per line were counted. The stomatal density was calculated as the number of stomata in the field divided by the area of the field (see Figure 3.14).

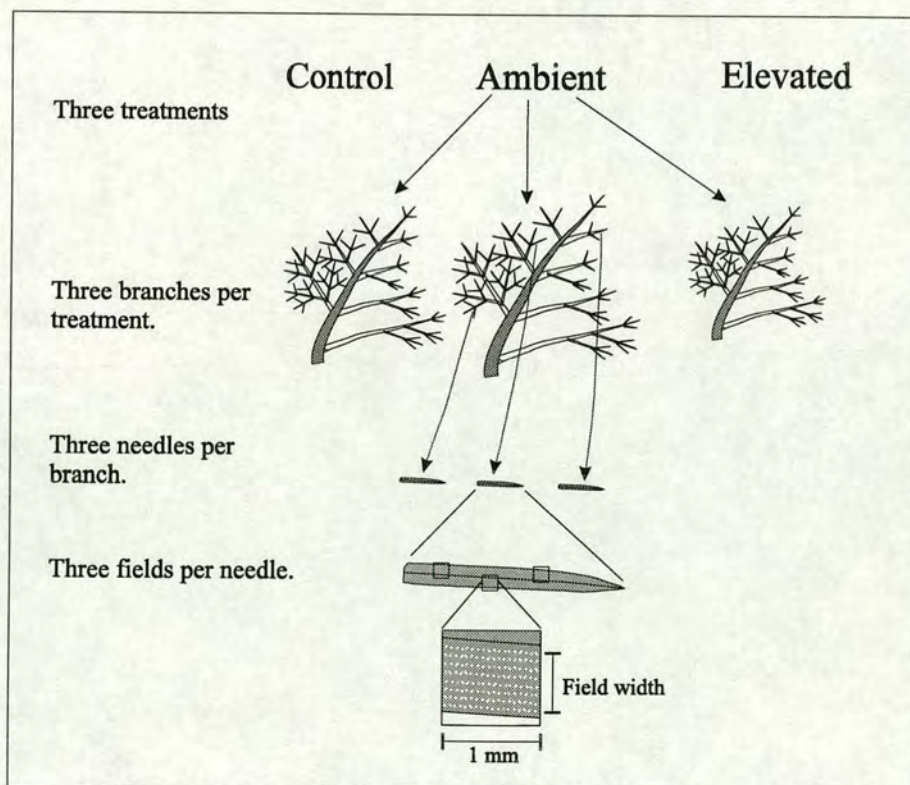


Figure 3.14 Diagram showing the sampling strategy used to determine stomatal density.

An analysis of variance using a nested design was used to test for any treatment differences (Proc Nested, SAS Institute, Cary, NC). There were no differences in the stomatal density between treatments (Table 3.3).

Table 3.3 Stomatal density of 1993 age-class of needles. Mean \pm 1 SEM, n = 3.

	Control	Ambient	Elevated
Stomatal density (mm ⁻²)	159.4 \pm 6.97	159.7 \pm 12.66	158.8 \pm 5.12

3.6 Needle composition

Needles were sampled periodically throughout the experiment from the three oldest age-classes of needle. These were analysed for chlorophyll, starch, soluble carbohydrate and nutrients. Needles were sampled between 11:00 and 13:00 to minimise any diurnal variation between samples. Samples to be used for starch, soluble carbohydrate and nutrient analyses were freeze dried, ground in a ball mill and stored in a desiccator until assayed. On some occasions it was necessary to pool samples from two branches of the same treatment and age-class as there was insufficient material for all of the assays.

3.6.1 Chlorophyll

Method

Chlorophyll *a*, chlorophyll *b* and total chlorophyll were determined on fresh needles according to the method described by Porra *et al.* (1989). Three needles from each age-class were placed in 3 cm³ of N,N-dimethylformamide (DMF) and kept in darkness for seven days. The absorbance of the resulting extract was then measured at 647, 664 and 750 nm with a spectrophotometer (CE 303, Cambridge Instruments, Cambridge, UK). Chlorophyll concentrations ($\mu\text{g cm}^{-3}$) were calculated based on the following equations (Porra *et al.*, 1989):

$$\text{Chl } a = 12.00 (A^{664} - A^{750}) - 3.11 (A^{647} - A^{750})$$

$$\text{Chl } b = 20.78 (A^{647} - A^{750}) - 4.88 (A^{664} - A^{750})$$

$$\text{Chl } (a+b) = 17.67 (A^{647} - A^{750}) + 7.12 (A^{664} - A^{750})$$

Results

There were no significant differences in chlorophyll content between treatments at any time during the experiment. The chlorophyll content per unit projected area of new needles was lower than that of older needles but gradually increased over the first year, while the chlorophyll content of one-year-old and older needles did not change over the course of the year (Figure 3.15).

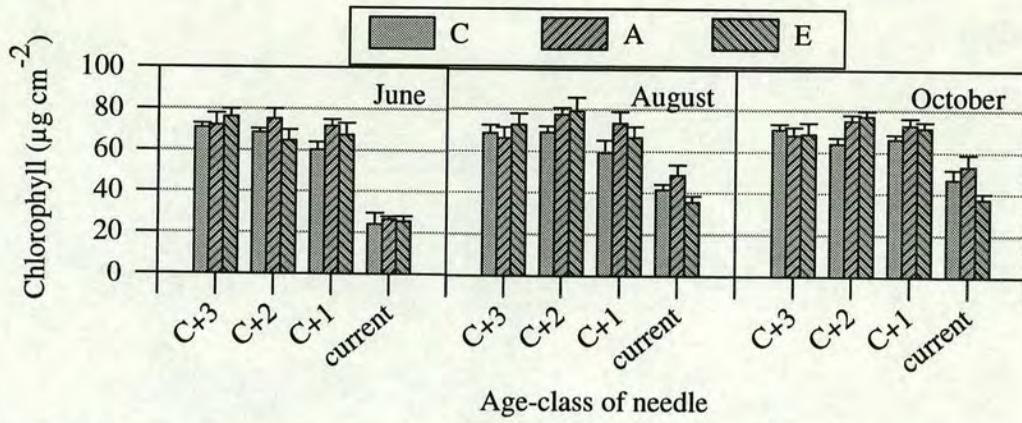


Figure 3.15 Total chlorophyll content of needles for four age-classes of needle at three times of year during 1993. Means \pm 1 SEM, $n = 6$.

When expressed on an area basis chlorophyll content increased with the age-class of needle as shown by data for August 1994 (Figure 3.16) ($P < 0.001$), but when expressed on a mass basis there were no significant differences between age classes. This suggests that chlorophyll content is more strongly correlated to needle mass than to needle area, a hypothesis that is supported by the regression of chlorophyll content against needle area and dry mass (Figure 3.17), where a higher r^2 for the chlorophyll versus dry mass is observed. The chl a / chl b ratio was not significantly affected by treatment or age-class of needle.

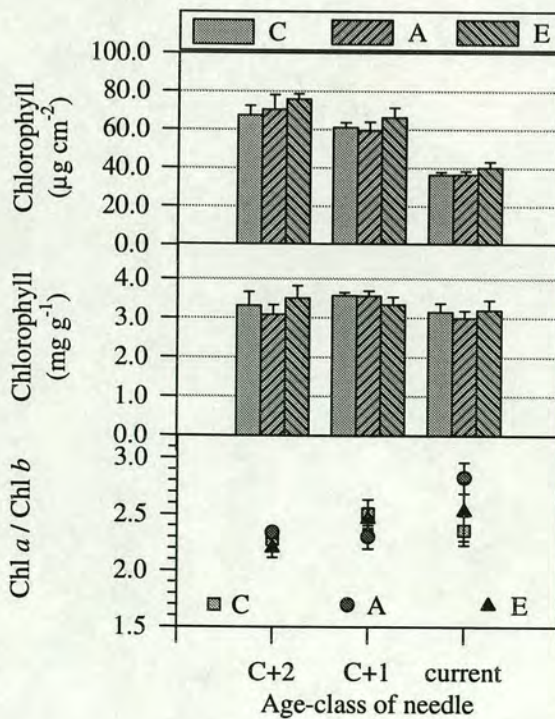


Figure 3.16 Chlorophyll content of three age-classes of needle in August 1994. Shown on an area and mass basis also the chl a / chl b ratio. Means \pm 1 SEM, $n = 6$.

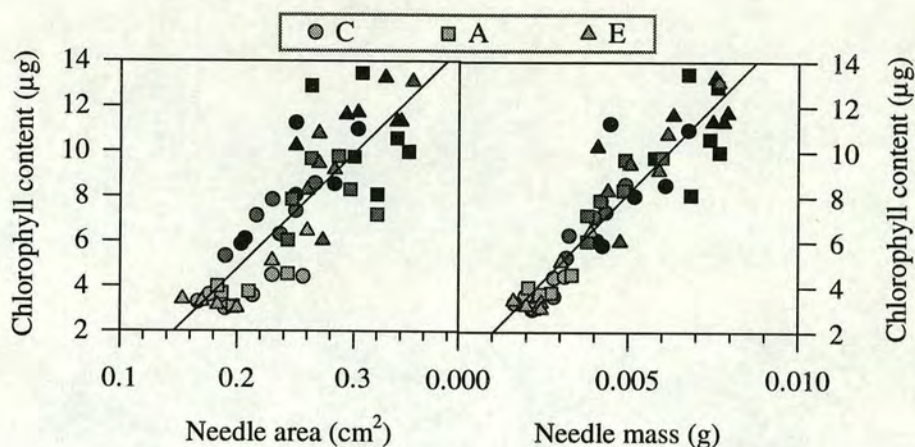


Figure 3.17 Relationships between chlorophyll content and projected area and dry mass of needles of three age classes sampled in August 1994. Light grey, dark grey and black indicate 94, 93 and 92 cohorts, respectively. Lines are regressions $\text{Chl} = -5.499 + 51.32 \cdot \text{area}$, $r^2 = 0.69$ and $\text{Chl} = 0.41 + 1553 \cdot \text{dry mass}$, $r^2 = 0.85$.

3.6.2 Starch

Method

Starch content was determined colorimetrically using the iodine method described by Allen (1989). Starch forms a blue complex with iodine that is measured spectroscopically. Starch was extracted from ~50 mg of finely ground material in test tubes with 5 cm³ of HClO₄ (32 % v/v) for 30 minutes at room temperature. The test tubes were then centrifuged at 4000 rpm for 15 minutes and 1 cm³ of the supernatant was made up to 25 cm³ with distilled water in a volumetric flask. After adding four drops of 0.1 N HCl and 250 µl 2 % iodine solution, absorbance was measured at 610 nm. Two standards, containing a known amount of starch, were run with each set of samples.

A calibration curve was made with pure starch as the standard and the percentage of starch on a dry mass basis was calculated as follows:

$$\% \text{ starch} = \frac{c \times V_{\text{sol}} \times V_{\text{HClO}_4}}{V_{\text{aliquot}} \times W_{\text{sample}}} \times 100$$

where:

c = concentration of starch (from calibration curve, mg cm⁻³).

V_{sol} = volume of the solution (25 cm³).

V_{HClO_4} = volume of perchloric acid (5 cm³).

V_{aliquot} = volume of the extracted sample (1 cm³).

W_{sample} = mass of freeze-dried sample (50 mg).

Results

The starch concentration in the needles varied through the year and between age-classes but there was no significant CO₂ treatment effect. Figure 3.18 shows starch concentration of three age-classes of needle during 1993. The pattern of starch accumulation in the needles showed an increase in starch concentration through the spring then a sudden drop to less than 0.5% for the remainder of the year. C+1 needles had the highest starch concentrations. Unfortunately the April 1993 samples were lost but Table 3.4 shows similar data for 1994. It is probable that the C+2 and C+1 age-classes in May 1993 accumulated similar amounts of starch as the C+1 needles in May 1994. The reserves of starch which build up in needles during spring are used to supply the demand for rapid growth when the buds flush in June. During the summer and autumn months photosynthetic production was exported from the needles and starch concentrations were almost zero, then during the winter and spring, reserves were again built up in the needles in preparation for bud burst.

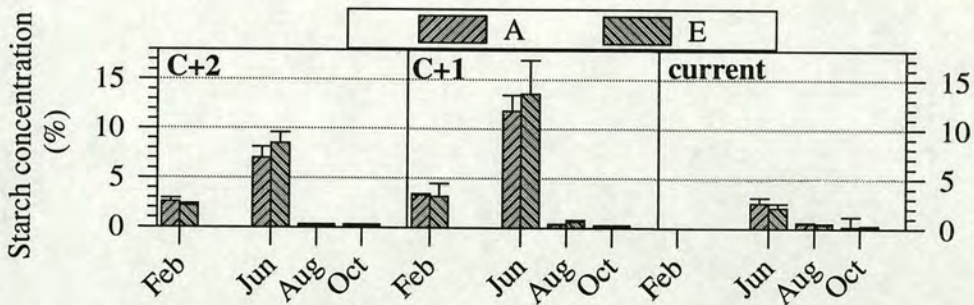


Figure 3.18 Starch concentration as a percentage of the dry mass for three age-classes of needle at four dates in 1993. Means \pm 1 SEM, $n = 6$.

Table 3.4 Starch concentration in needles during 1994 as a percentage of the dry mass. Means \pm 1 SEM, $n = 6$. * indicates significant difference at $P < 0.05$.

1994	Age-class	C	A	E
May	current	.	25.4 \pm 0.8*	30.1 \pm 2.0*
August	C+1	< 0.5	< 0.5	< 0.5
	current	< 0.5	< 0.5	< 0.5
November	C+3	< 0.5	< 0.5	< 0.5
	C+2	< 0.5	< 0.5	< 0.5
	C+1	< 0.5	< 0.5	< 0.5
	current	< 0.5	< 0.5	< 0.5

3.6.3 Soluble carbohydrate

Method

Soluble carbohydrates were measured by anion-exchange chromatography with pulsed amperometric detection. Soluble sugars and sugar alcohols were extracted from 50 mg of finely ground tissue in double-distilled water in a water bath at 30 °C for 15 minutes. After centrifuging, samples were filtered (0.2 µm pore), diluted (1/10) and analysed by ion chromatography [Ion Chromatography System HPLC, DX500, Carboapak PA carbohydrate column, Dionex Corporation, Sunnyvale, CA, USA]. A set of 10 pure polyol sugars (inositol, manitol, fucose, rhamnose, arabinose, galactose, glucose, xylose, fructose and sucrose) was run as a standard with each set of samples. For unknown peaks, a constant response factor (the average for the known peaks) was used to calculate the concentrations from the peak areas. However, all unknown peaks were very small.

Results

Figure 3.19 shows the concentration of soluble carbohydrate in four age-classes of needle at the harvest in November 1994 and for two age classes in August 1994 (white columns). There were higher concentrations of soluble carbohydrates in needles as they aged and concentrations were higher in August than in November, as would be expected. There were no significant differences in the concentrations between treatments but E needles did tend to have slightly higher concentrations than A needles.

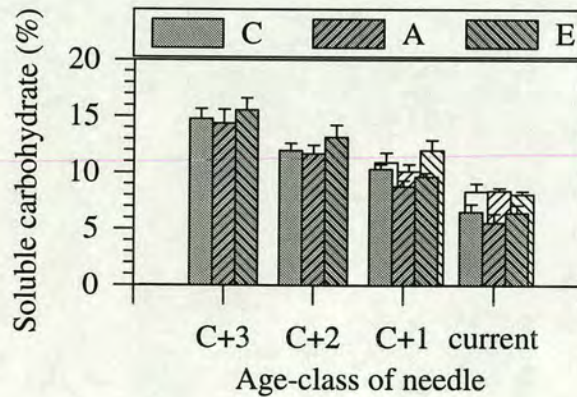


Figure 3.19 Soluble carbohydrate concentration of needles as a percentage of the dry mass from different age-classes of needle in August (white) and November (grey) 1994. Mean \pm 1 SEM, n = 6.

Concentrations of soluble carbohydrates in needles varied slightly over the year (Figure 3.20). There were no significant differences in concentrations between

treatments at any time of the year, but **E** needles sometimes had slightly more and never had less carbohydrate than **A** needles.

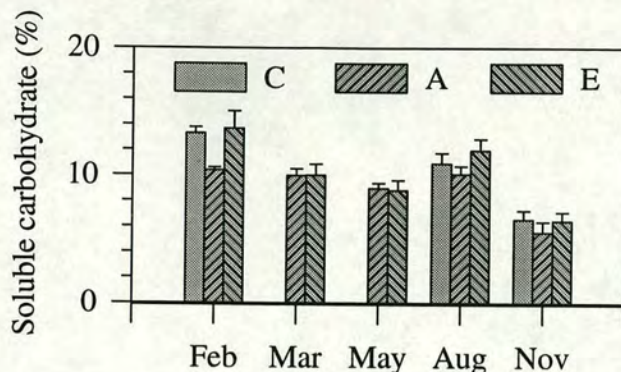


Figure 3.20 Soluble carbohydrate content of C+1 age-class needles during 1994 as a percentage of the dry mass of the needles. Mean \pm 1 SEM, n = 6.

Focusing on mid-summer, when one might expect any differences between **A** and **E** shoots to be apparent, still did not yield a statistically significant result, in either 1993 or 1994 (Figure 3.21). In both years current needles showed no response to CO₂ treatment while C+1 needles did have slightly higher concentrations when grown in elevated [CO₂].

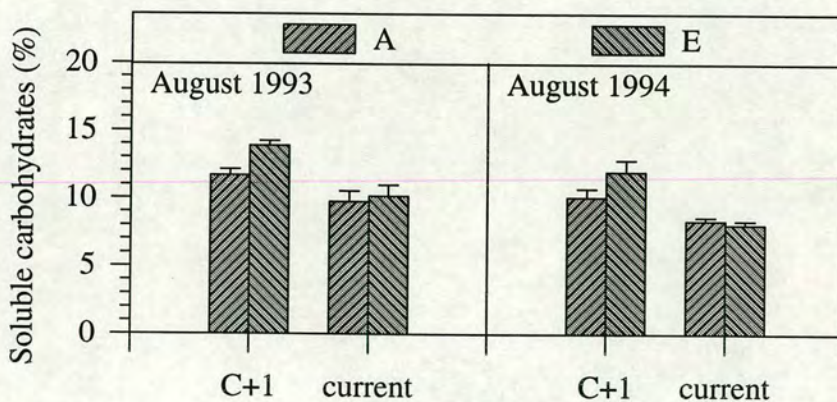


Figure 3.21 Concentration of soluble carbohydrate in current and C+1 needles in August 1993 and 1994. Means \pm 1 SEM.

3.6.4 Nutrients

Method

N, P, K, Ca and Mg concentrations were measured on finely ground sub-samples of the oven-dried needles of two age classes in February 1992, August 1993 and August 1994 and on the current age class in June 1992 using the method described by Allen (1989) with some modifications. On some occasions because of limited time or resources only the **A** and **E** treatments were analysed as this was the comparison of main interest.

Organic matter was oxidised using an acid oxidation process prior to analysis: 2 cm³ of concentrated H₂SO₄ were carefully added to 100 (± 10) mg of plant material in a test tube followed by H₂O₂ (2 x 75 cm³). Then, the sample tubes were heated at 320 °C for 6 h, cooled and made up to 100 cm³ with distilled water.

Nitrogen concentration was determined by a gas diffusion method using a flow injection analyser [Fiastar, Tecator Ltd., Wilsonville, Oregon, USA]. Total phosphorus was determined by a molybdenum blue method using the flow injection analyser as described in the application note ASN 60-04/83 [Perstorp Analytical Ltd., Maidenhead, Berkshire, UK]. Potassium, calcium and magnesium were determined by atomic absorption spectrometry [919 Atomic Absorption Spectrometer, UNICAM, Cambridge, UK].

Based on 100 mg of dried sample made up to a fixed volume of 100 cm³, the concentration of different macronutrients, *C*, was calculated as follows:

$$C = \frac{c \times V_{\text{sol}}}{W_{\text{sample}}}$$

where:

c = concentration of the solution (mg dm⁻³).

*V*_{sol} = volume of the solution (0.1dm³).

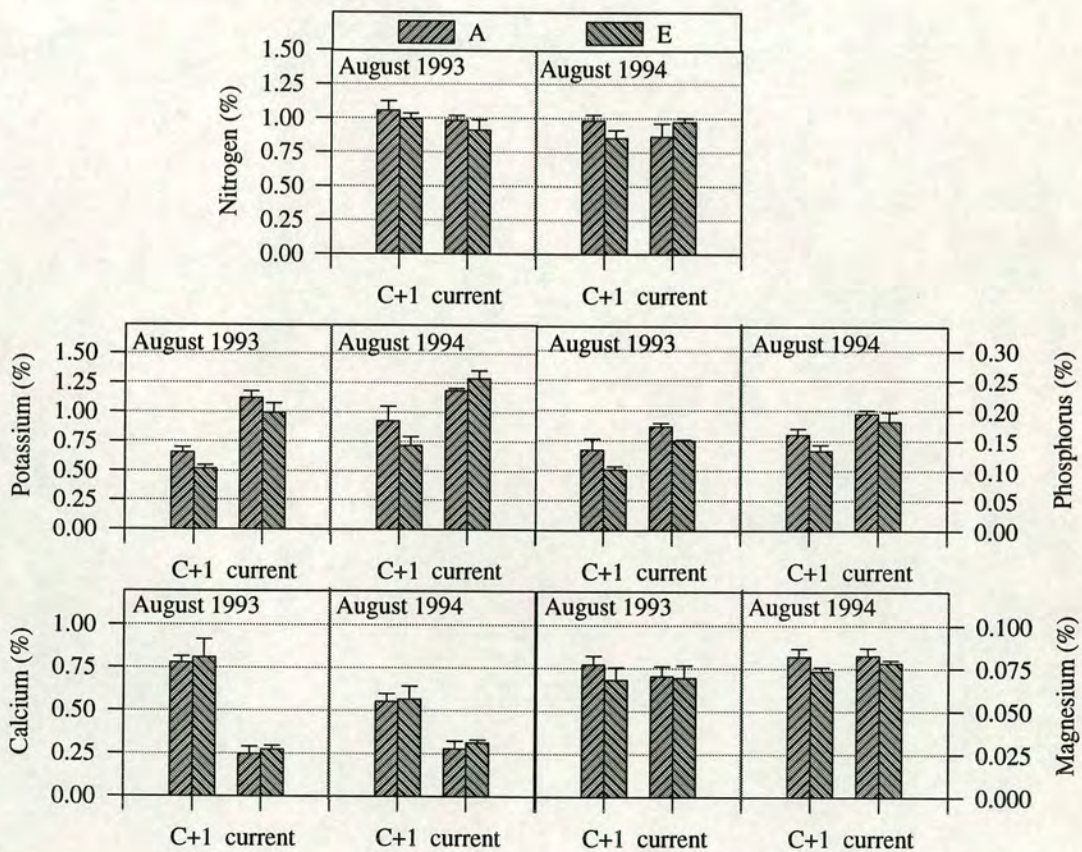
*W*_{sample} = original mass of the sample (0.1g).

Results

There were no significant differences in nutrient concentrations between treatments at any of the times they were sampled (Table 3.5).

Table 3.5 Nutrient concentrations in different age-classes of needle as a percentage of the dry mass on 5th February and 16th June 1992. Mean \pm 1 SEM, n = 3.

Nitrogen		C	A	E
05/02/92	C+1	1.15 \pm 0.08	1.14 \pm 0.23	1.16 \pm 0.13
05/02/92	current	1.15 \pm 0.14	1.60 \pm 0.31	1.25 \pm 0.31
16/06/92	current	1.39 \pm 0.06	1.29 \pm 0.04	1.16 \pm 0.10
Phosphorus		C	A	E
05/02/92	C+1	0.10 \pm 0.02	0.13 \pm 0.05	0.15 \pm 0.04
05/02/92	current	0.19 \pm 0.02	0.19 \pm 0.02	0.24 \pm 0.05
16/06/92	current	0.19 \pm 0.01	0.17 \pm 0.01	0.17 \pm 0.01
Potassium		C	A	E
05/02/92	C+1	0.53 \pm 0.17	0.57 \pm 0.19	0.73 \pm 0.15
05/02/92	current	0.72 \pm 0.04	0.69 \pm 0.11	0.70 \pm 0.10
16/06/92	current	0.70 \pm 0.1	0.63 \pm 0.1	0.61 \pm 0.3

**Figure 3.22** Nitrogen, potassium, phosphorus, calcium and magnesium concentrations in needles as a percentage of needle dry mass for current and C+1 age classes of needle in August 1993 and 1994. Mean \pm 1 SEM, n = 3.

3.7 Discussion

Growth of Sitka spruce is determinate and the buds are formed in late summer when the number of needle primordia are determined (Cannell & Willett, 1975; Baxter & Cannell, 1977). The buds that flushed in 1991 were formed in the late-summer of 1990, prior to the installation of the bags, thus the lack of difference in final lengths of bagged and unbagged shoots in 1991, in comparison to the differences in final length in subsequent years, is probably the result of differences in the size of the buds rather than in differences in expansion of the developing shoot.

The increase in shoot size seen in bagged branches has been attributed to the slightly higher temperatures found in the branch bags which led to buds containing more needle primordia; the increase in needle size may also result from increased cell division at higher temperatures. Ford *et al.*, (1987) studied the relationship between daily weather and shoot expansion in a 12-year-old stand of Sitka spruce and reported that shoot extension was five times more sensitive to temperature than to changes in solar radiation. However, the fact that the needle frequency was the same between bagged and unbagged branches suggests that the difference in shoot size was related to the number of primordia formed in late summer rather than to increased shoot expansion in the spring. There were no differences between the **A** and **E** branches in either internode length or needle frequency for any age-class of internode.

Internodes increase in diameter but not in length so the needle frequency is conserved as the internode ages. The needle frequency increased with the age-class of the internode (Table 3.1) while the length of the internode (or apical shoot) decreased with age-class (Figure 3.1). The decrease in length with age-class relative to the increase in needle frequency with age-class indicates that there was both a reduction in total needle number (during bud formation) and a reduction in the distance between needles during the expansion of the shoot from one years growth to the next. Growth in elevated CO₂ did not affect this developmental pattern of the branches.

Pipe-model theory suggests that a relationship exists between the cross-sectional area of sapwood and the area of foliage distal to the cross section, as there must be sufficient xylem vessels to permit transport of water to meet the transpiration demands of the leaf area (Shinozaki *et al.* 1964a, Shinozaki *et al.* 1964b), and this was shown to be applicable (Figure 3.12). Transpiration of a branch depends on the amount of leaf area, stomatal conductance, aerodynamic conductance, radiation absorbed and leaf surface VPD. Some plants show a decrease in stomatal conductance as [CO₂] increases (Morison, 1987; Eamus and Jarvis, 1989; Jarvis, 1989) and so assuming all else remains constant we would expect to see a decrease in

transpiration and thus possibly, if hydraulic conductance is limiting, an increase in the area of leaves per unit stem cross-section. The data do not support this hypothesis since **A** had most leaf area per unit stem cross-section followed by **E** then **C**. It may be that hydraulic conductance was not the limiting factor, and furthermore there is evidence to suggest that transpiration rates were not reduced in elevated CO_2 (see below). Also there are other constraints determining branch architecture such as the need for mechanical strength.

Growth of the branch in elevated CO_2 did not affect the needle area produced. Chapter 4 will show that more assimilation occurred in shoots of branches grown in elevated CO_2 but that this did not result in increases in the number of buds flushing, size of shoots, numbers of needles, needle area or the mass of the branch as a whole. Starch and soluble carbohydrate concentrations were slightly higher in **E** needles but not significantly so, and therefore one must assume that the extra assimilate was exported from the branch to the tree rather than being used locally for storage or growth. The fact that the increase in photosynthetic production within the branch did not stimulate growth is not particularly surprising, as mechanisms involving PPF, red/far red ratio and auxins related to apical dominance are more likely to control patterns of growth than a simple increase in carbohydrate production.

Enhanced growth in response to CO_2 was observed where whole trees were exposed to elevated CO_2 and an adequate nutrient supply was available (see Chapter 6).

Needle composition

Growth in elevated CO_2 had very little effect on the composition of needles of any age-class. Starch and soluble carbohydrate concentrations were slightly higher, especially in needles older than one year, but differences were not statistically significant. This lack of response to growth CO_2 concentration is probably a result of the strong sinks for carbohydrate within the tree. With only one branch exposed to elevated CO_2 concentrations it was very unlikely that sinks within the tree became saturated by over-production of carbohydrates and, provided the phloem could translocate the extra photosynthate away from the needles, a build up of photosynthate was unlikely.

Chlorophyll and nutrient concentrations were also unaffected by growth CO_2 concentration. The values for each nutrient were close to those below which the tree would be deemed nutrient deficient (Binns *et al.*, 1980). However those values are based on needles sampled from the uppermost whorl of branches and as the trees in

this experiment were growing on a former agricultural soil and were gaining approximately one metre in height each year it is very unlikely that they were suffering from nutrient deficiency. It is more likely that the low nutrient concentrations were a dilution effect caused by the rapid growth rate (Linder & Rook, 1984).

One commonly documented effect of elevated atmospheric CO₂ is a reduction in the nitrogen concentration of plant tissues (e.g. Wong, 1979; Norby *et al.*, 1986), this may be a result of dilution by increased carbohydrate storage or it may represent a re-allocation of nitrogen within the plant in response altered priorities between carbon fixation and nutrient acquisition. In young plants it may also reflect the normal ontogenetic process whereby larger plants have lower nitrogen concentrations (Coleman *et al.*, 1993). The lack of response of nitrogen concentration to elevated CO₂ in this experiment may be partly a result of the already low nitrogen concentrations in the needles (*cf.* seedling trees in Chapter 7).

There were some differences in nutrient concentrations between ages-classes of needles. Calcium concentrations were two to three times higher in C+1 needles than in current needles. Calcium is carried to the needle in the transpiration stream but unlike other nutrients is not re-translocated in the phloem and so concentrations tend to build up in the needle and are deposited as calcium oxalate crystals in the cell walls of the mesophyll (Marschner, 1995). Thus calcium concentrations tend to be correlated with cumulative transpiration (see Chapter 7, 7.6.2). Some studies have found that growth in elevated CO₂ leads to reduced stomatal conductances (DeLucia *et al.*, 1985; Norby & O'Neill, 1989; Sasek *et al.*, 1985) and if this translates to reduced transpiration then one might expect needles on branches grown in elevated CO₂ to have lower calcium concentrations than their counterparts grown at ambient CO₂. As this was not seen in either 1993 or 1994 (Figure 3.22), I conclude that cumulative transpiration was probably not influenced by growth at elevated CO₂ concentrations (see Chapter 4 for further discussion of stomatal conductance).

Potassium concentrations were higher in current needles and tended to be slightly lower in elevated grown needles. This result was also seen in the later experiment using seedling trees (see section 7.6.4).

3.8 Conclusions

Growth of branches and needles was not influenced by elevated CO₂ concentrations.

Stomatal density was not influenced by elevated CO₂ concentrations.

There was a branch bag effect on the timing of bud burst, the elongation of shoots and the mass and area of needles which has been attributed to slightly (1.5 °C) higher temperatures in the branch bags.

There was a very strong relationship between stem cross-sectional area and the leaf area distal to the cross section, which supports the pipe-model theory. However, there was no clear effect of CO₂ concentration on the amount of leaf area supported per unit stem area.

Lack of difference in foliar calcium concentrations in response to growth CO₂ concentration leads to the conclusion that transpiration rates were unaffected by growth CO₂ concentration.

The lack of response of individual branches to growth in elevated CO₂ indicates that an imbalance between source and sink for photosynthates is required for CO₂ to influence growth at the branch level. Increased production of photosynthate within a branch *per se* does not lead to changes in growth.

CHAPTER 4

Photosynthesis of Mature Branches

4.1 Introduction

The estimated distribution of needle area by age-class on a whole tree was calculated in the previous chapter and indicates that for a tree with six live whorls the current-year foliage accounts for 33% of all needle area and that 80% of the needle area is contained in the three youngest age-classes. As current-year needles tend to be the most physiologically active they are the most important single age-class in terms of both size and activity, and any sensitivity to elevated CO₂ concentration of this age-class would have a relatively large effect on the tree as a whole. For this reason I focused my study on the response of the current age-class to growth in elevated CO₂, while characterising the photosynthetic response of the one-year-old (C+1) shoots in less depth.

The method used to measure photosynthesis was modified from year to year in the light of experience. In 1991 and 1992 natural light was used but this proved to be variable, making it difficult to detect differences between treatments. An artificial light source was developed and used in 1993 and 1994 and this helped reduce variability. In 1994 emphasis was put on determining the response functions of assimilation to PPFD and intercellular [CO₂].

4.2 Photosynthesis of shoots using natural light (in 1991)

4.2.1 Method

Photosynthesis and stomatal conductance were measured on current and C+1 shoots using a portable gas exchange system (ADC LCA3, Analytical Development Company Ltd, Hoddesdon, Herts, UK). One shoot from the current and C+1 age classes per branch was prepared at the beginning of the season by removing needles

from either side of a central section to enable a gas-tight seal for the leaf cuvette (PLC(c), Analytical Development Company Ltd, Hoddesdon, Herts, UK). Because of the limited amount of tissue available within a branch bag, the same shoots were used repeatedly for gas exchange measurement throughout the season. The leaf area of each shoot was calculated non-destructively by measuring the projected area per needle of the needles that were removed in shoot preparation and multiplying this by the number of needles enclosed by the cuvette (~50). Preparation and measurements on current shoots could only be made after the shoot had fully hardened by the end of June.

Measurements were made using natural light at both 350 and 700 $\mu\text{mol mol}^{-1}$ $[\text{CO}_2]$, firstly at the growth concentration and then at the reciprocal concentration. The cuvette was placed on a shoot with the leaf thermistor in contact with the underside of a needle then, once the $[\text{CO}_2]$ and humidity differentials were stable (2-3 minutes), measurements were recorded. The $[\text{CO}_2]$ was then changed for the reciprocal $[\text{CO}_2]$ measurement, which took between two to five minutes to stabilise. Photosynthetic rate, transpiration rate and stomatal conductance were calculated from the $[\text{CO}_2]$ and humidity differentials using the equations from the ADC LCA3 manual (see Appendix A).

4.2.2 Results

In 1991 current shoots flushed and expanded in elevated $[\text{CO}_2]$ while C+1 shoots had flushed and expanded outside the treatment conditions during 1990. The buds of both age classes formed prior to installation of the branch bags.

Photosynthetic rates of C+1 shoots fell over the year (1991) while those of current shoots rose between June and July and then fell slightly in August (Figure 4.1) with the result that from August current shoots had higher rates than C+1 shoots. Control C+1 shoots had slightly (but not significantly) higher rates than A and E shoots. Photosynthetic rates measured at 700 $\mu\text{mol mol}^{-1}$ $[\text{CO}_2]$ were twice those measured at 350 $\mu\text{mol mol}^{-1}$ at the same time for all three growth treatments (C, A and E).

Stomatal conductances showed the same seasonal trend as photosynthesis (Figure 4.2). They fell over the season in C+1 shoots and rose then fell in current shoots, with current shoots having higher stomatal conductances than C+1 shoots. Measurement CO_2 concentrations had little effect on stomatal conductance, partly because the stomata were not given enough time to adjust to the new CO_2 concentration before the measurement was made (see 4.6.2 for stomatal response to $[\text{CO}_2]$). Thus E and A are best compared when E was measured at 700 $\mu\text{mol mol}^{-1}$ and A was measured at

$350 \mu\text{mol mol}^{-1}$ as this gives the best indication of the stomatal conductance before the cuvette was attached to the shoot and conditions were modified. There were no significant differences in stomatal conductance between **A** and **E** shoots of either age class.

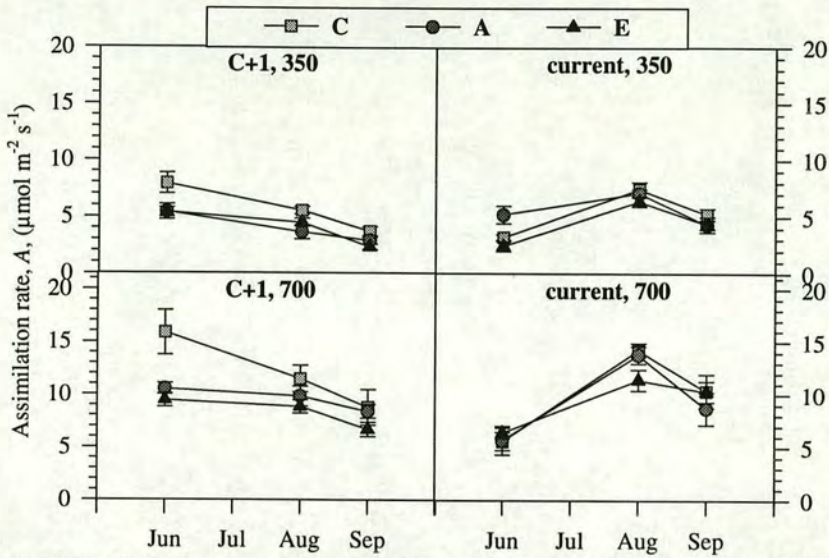


Figure 4.1 Net assimilation rates for current and C+1 shoots measured at 350 and $700 \mu\text{mol mol}^{-1}$ $[\text{CO}_2]$ at three times during 1991 for control **C**, ambient **A**, and elevated $[\text{CO}_2]$ **E** shoots. Data were collected using natural light with PPFD $> 300 \mu\text{mol m}^{-2} \text{s}^{-1}$, leaf temperature $20\text{--}32^\circ\text{C}$, VPD $0.8\text{--}2.4$ kPa. Means ± 1 SEM, $n = 6$.

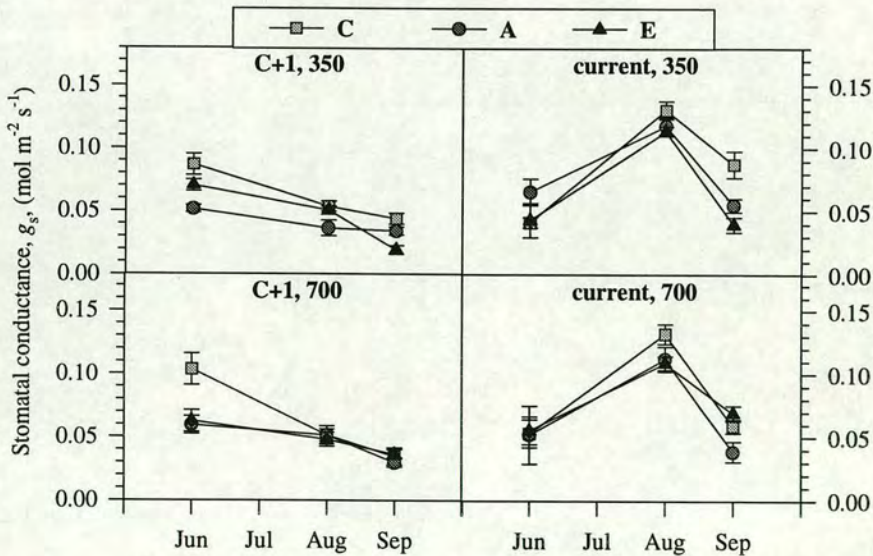


Figure 4.2 Stomatal conductance for current and C+1 shoots measured at 350 and $700 \mu\text{mol mol}^{-1}$ $[\text{CO}_2]$ at three times during 1991. Data were collected using natural light with PPFD $> 300 \mu\text{mol m}^{-2} \text{s}^{-1}$, leaf temperature $20\text{--}32^\circ\text{C}$, VPD $0.8\text{--}2.4$ kPa. Means ± 1 SEM, $n = 6$.

4.3 Photosynthesis of shoots using an artificial light source (in 1993)

4.3.1 Method

The preparation of shoots and the measurement protocol were the same as in 4.2.1, but instead of natural light an artificial light source was used since, making gas exchange measurements in the field in Scotland using natural light is very difficult for a number of reasons. On overcast days the PPFD within the leaf chamber rarely exceeds $200 \mu\text{mol m}^{-2} \text{s}^{-1}$, is often considerably less and is also variable. At sub-saturating PPFDs small changes in PPFD can result in significant changes in assimilation rate, thus increasing variation in the data and making comparisons between treatments difficult. Even on sunny days there are often clouds present which move across the solar disc giving rise to large variations in PPFD and this often coincides with the period a shoot is within the cuvette. Furthermore, when working within a forest canopy there is considerable spatial heterogeneity in PPFD from shoot to shoot and even along a shoot. For these reasons I designed and built a portable light source for use with the leaf chamber (see Appendix B). The light source reduced variation between measurements and allowed measurements to be made under cloudy and variable conditions. Measurements were made with a uniform, saturating PPFD of $800 \mu\text{mol m}^{-2} \text{s}^{-1}$ in the plane of the shoot.

4.3.2 Results.

Assimilation rates for current and C+1 shoots measured between July and September 1993 are shown in Figure 4.3. Assimilation rates of C+1 shoots did not show a seasonal pattern while assimilation rates of current shoots increased slightly in August then fell again in September. The two main observations are that current, unbagged C shoots had much higher assimilation rates than A and E shoots, which were not significantly different from one another. Current year A and E, and C+1, A shoots had similar assimilation rates but C+1, E shoots had lower rates at both 350 and $700 \mu\text{mol mol}^{-1}$, indicating possible downward acclimation of photosynthesis in E, C+1 needles. All shoots showed a doubling of assimilation rate when measured at $700 \mu\text{mol mol}^{-1} [\text{CO}_2]$ compared to $350 \mu\text{mol mol}^{-1}$.

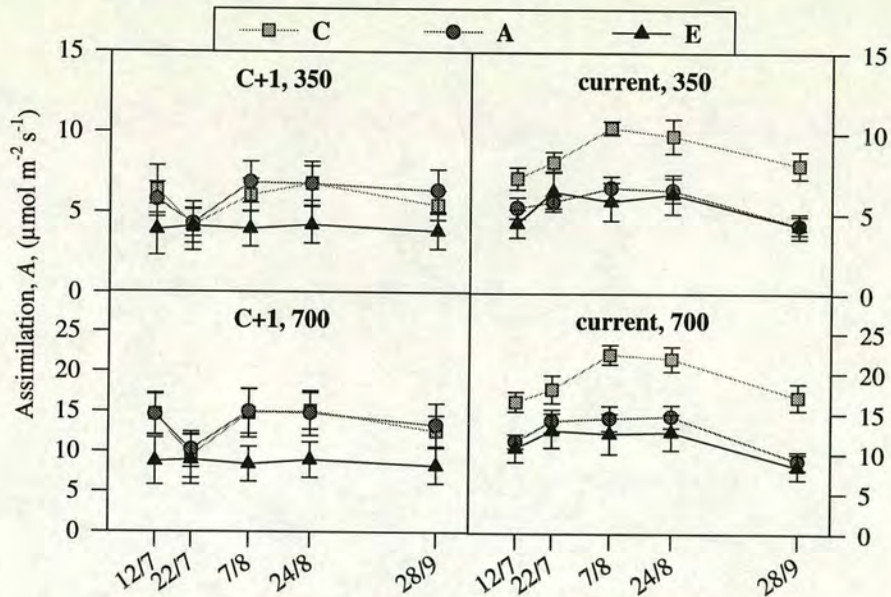


Figure 4.3 Net assimilation rate for current and C+1 shoots measured at 350 and 700 $\mu\text{mol mol}^{-1}$ $[\text{CO}_2]$ at five times during 1993. Data were collected using an artificial light source with $\text{PPFD} = 800 \mu\text{mol m}^{-2} \text{s}^{-1}$, leaf temperature 18-26 $^{\circ}\text{C}$, VPD 0.8-1.6 kPa. Means ± 1 SEM, $n = 6$.

The assimilation rates can be interpreted in greater detail by looking at the stomatal conductance (Figure 4.4), C_i (Figure 4.5) and C_i / C_a ratio (Figure 4.6) in conjunction with the assimilation rates.

Starting with the current age-class of needles, both assimilation rate and stomatal conductance were higher in C shoots but C_i and C_i / C_a ratio were the same for all treatments. Therefore the effect of the branch bag seems to have been to increase photosynthetic capacity and stomatal conductance in tandem. There were no differences in assimilation rate or stomatal conductance between current A and E shoots.

The C+1 shoots showed a different response. The effect of the branch bag was much smaller and E shoots had lower assimilation rates and stomatal conductances than A shoots. However, as the C_i of E shoots was higher than that of A shoots the reduction in assimilation rate was not a result of stomatal limitation (see 7.9.3) but a result of a decrease in photosynthetic capacity. This will be discussed more later.

The C_i / C_a ratio was remarkably conservative in the current needles regardless of treatment or measurement $[\text{CO}_2]$ (Figure 4.6) and this, combined with the lack of stomatal adjustment between measurement $[\text{CO}_2]$ (Figure 4.4), suggests that the A/C_i response is almost linear up to at least 500 $\mu\text{mol mol}^{-1}$ C_i . Since, if the slope of the A/C_i relationship was decreasing with C_i , the C_i/C_a would increase with C_a at constant

g_s . This agrees with A/C_i response curves measured on current shoots in 1994 (see Figure 4.9).

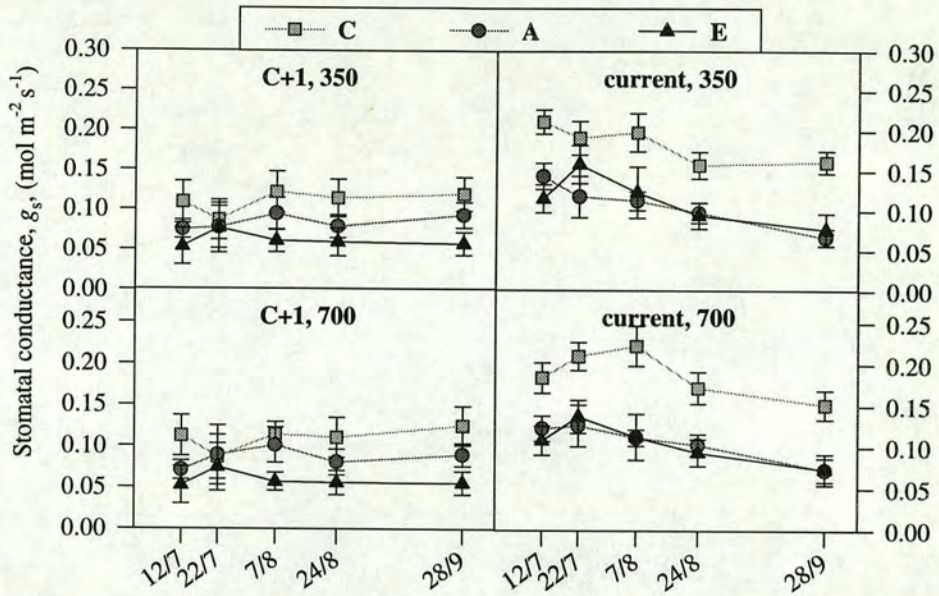


Figure 4.4 Stomatal conductance for current and C+1 shoots measured at 350 and 700 $\mu\text{mol mol}^{-1}$ $[\text{CO}_2]$ at five times during 1993. Data were collected using an artificial light source with $\text{PPFD} = 800 \mu\text{mol m}^{-2} \text{s}^{-1}$, leaf temperature 18-26 $^{\circ}\text{C}$, VPD 0.8-1.6 kPa. Means ± 1 SEM, $n = 6$.

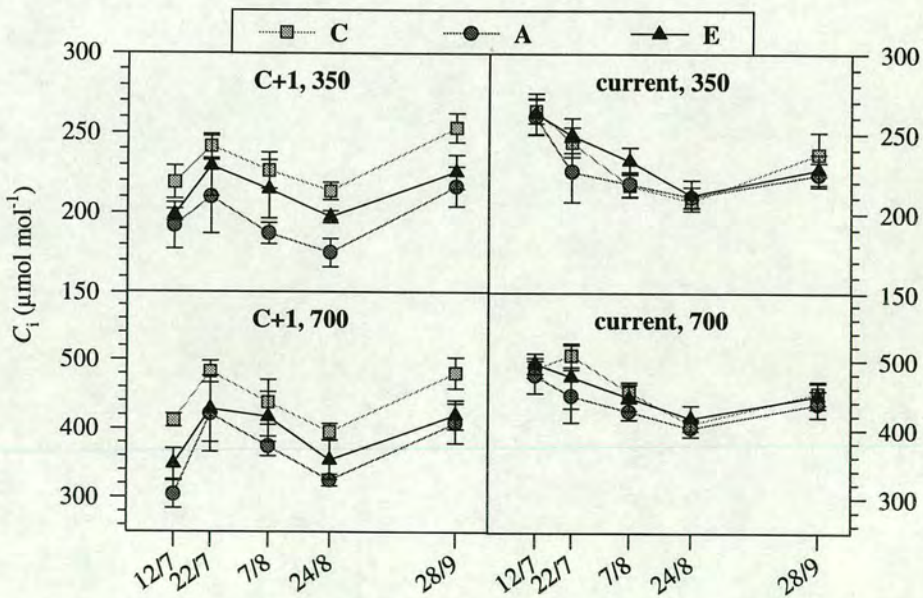


Figure 4.5 Internal CO_2 concentration for current and C+1 shoots measured at 350 and 700 $\mu\text{mol mol}^{-1}$ $[\text{CO}_2]$ at five times during 1993. Data were collected using an artificial light source with $\text{PPFD} = 800 \mu\text{mol m}^{-2} \text{s}^{-1}$, leaf temperature 18-26 $^{\circ}\text{C}$, VPD 0.8-1.6 kPa. Means ± 1 SEM, $n = 6$.



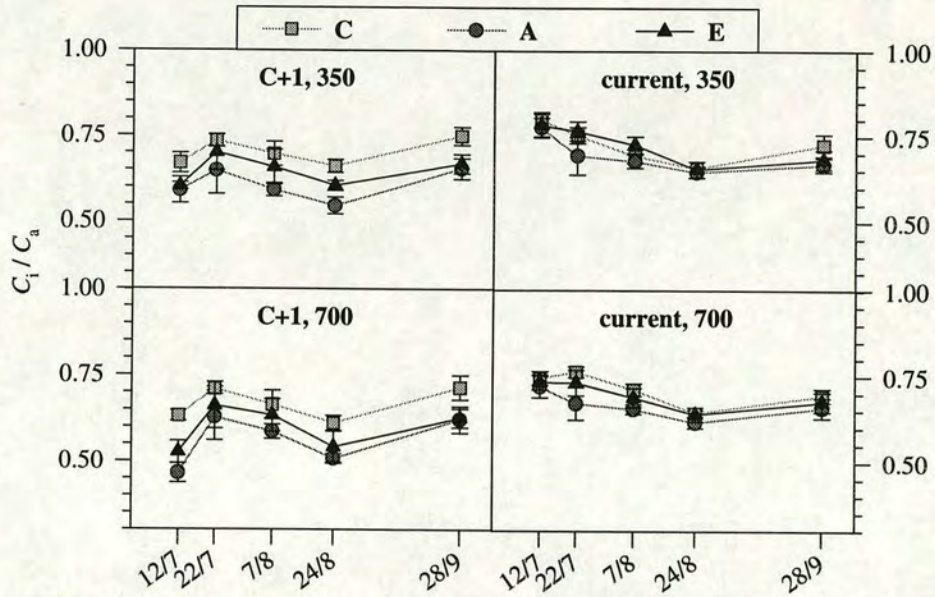


Figure 4.6 Ratio of intercellular $[CO_2]$ to chamber $[CO_2]$ for current and C+1 shoots measured at 350 and 700 $\mu mol\ mol^{-1}$ $[CO_2]$ at five times during 1993. Data were collected using an artificial light source with PPFD = 800 $\mu mol\ m^{-2}\ s^{-1}$, leaf temperature 18-26 $^{\circ}C$, VPD 0.8-1.6 kPa. Means \pm 1 SEM, $n = 6$.

The C_i/C_a for the C+1 shoots of similar size to that of the current shoots but was slightly more variable over the season reflecting the variation in C_i . The differences between treatments were larger in C+1 shoots but still small considering the differences in assimilation rates and stomatal conductances. It appears that stomatal conductance was adjusted to maintain a constant C_i/C_a despite a down-regulation of photosynthesis.

4.4 Respiration.

4.4.1 Method.

Dark respiration rates were measured during the day in August and September 1993 on pre-darkened shoots, using the same current year shoots as the photosynthesis measurements. Further measurements were made at night in September to determine if there was any significant difference between day and night-time respiration rates. The ADC LCA3 was not able accurately to measure the low differential CO_2 concentrations, which even at the lowest flow rate of 150 $cm^3\ min^{-1}$ were of the order of 2 to 3 $\mu mol\ mol^{-1}$. Therefore, I adapted the LCA3 conifer cuvette to be used with the Li-Cor 6200 as a closed system; the small volume of the conifer cuvette

combined with the high precision of the Li-Cor 6200 IRGA gave a much better system for measuring respiration rates.

Shoots were pre-darkened for at least one hour prior to measurement during daylight by covering them with a thick black cloth. The chamber was blacked out with metalised plastic film to ensure that no light reached the shoot during measurements. Daytime measurements were made between 12:00 and 17:00 while night-time measurements were made between 00:00 and 5:00. The chamber was clamped onto the shoot and then the rate of change of CO₂ concentration measured; from this and a knowledge of the volume of the system it was possible to calculate the CO₂ flux from the shoot.

Initially I attempted to measure respiration rates at the growth CO₂ concentrations but small diffusion leaks caused significant errors when measuring at 700 $\mu\text{mol mol}^{-1}$ and so in order to avoid any systematic errors between treatments I measured all shoots at 350 $\mu\text{mol mol}^{-1}$ [CO₂]. Where an E shoot was being measured the CO₂ to that branch bag was turned off to ensure that the CO₂ gradient across the chamber seals was minimised.

4.4.2 Results.

In August C shoots had significantly higher ($P < 0.05$) respiration rates than A and E shoots, which were not significantly different from each other. There were no significant differences between measurements made on pre-darkened shoots during the day and the same shoots measured at night (Figure 4.7). However, the night-time temperatures were ~ 8 °C cooler than those during daytime and, assuming a Q_{10} of 2, one would have expected night-time respiration rates to be almost half those of daytime rates. Thus either the true Q_{10} was close to 1 which is highly unlikely or, more probably, night-time respiration rates were higher than daytime rates (when corrected for temperature), *i.e.* the baseline rate of respiration was higher at night.

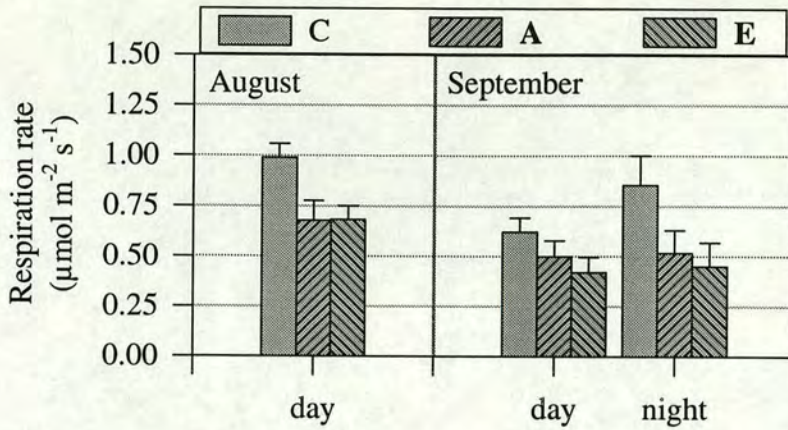


Figure 4.7 Dark respiration rates of current year shoots ($\mu\text{mol m}^{-2} \text{s}^{-1}$) during the day in August ($T_a = 26 \text{ }^\circ\text{C} \pm 0.1$) and during both day ($T_a = 24 \text{ }^\circ\text{C} \pm 0.8$) and night ($T_a = 16.6 \text{ }^\circ\text{C} \pm 0.8$) in September 1993, measured at $350 \mu\text{mol mol}^{-1} [\text{CO}_2]$. Mean ± 1 SEM, $n = 6$.

4.5 A/Q response functions (in 1994).

4.5.1 Method.

Net assimilation rate versus incident PPFD (A/Q) response functions were measured on current shoots during the 1994 growing season. Shoots were prepared as in 4.2.1 and a light source with neutral density filters (see Appendix B) was used to determine the relationship. The neutral density filters permitted variation of PPFD from 800 to $0 \mu\text{mol m}^{-2} \text{s}^{-1}$ in 11 steps. Shoots were measured at their growth $[\text{CO}_2]$ and E shoots were also measured at $350 \mu\text{mol mol}^{-1} [\text{CO}_2]$ to observe any acclimation effect. Shoots were first measured at $800 \mu\text{mol m}^{-2} \text{s}^{-1}$ PPFD then PPFD was reduced in steps to complete darkness. Measurements were made once the CO_2 differential had become stable, after at least five minutes.

4.5.2 Results.

To investigate the possible differences in the A/Q responses between treatments the data were fitted to a quadratic equation (Prioul & Chartier, 1977; Leverenz 1987) as follows:

$$A = \frac{\alpha \cdot Q + P_{\max} - \sqrt{(\alpha \cdot Q + P_{\max})^2 - 4 \cdot \alpha \cdot P_{\max} \cdot Q \cdot \theta}}{2 \cdot \theta} - R_d$$

where

$$A = \text{net assimilation rate, } \mu\text{mol m}^{-2} \text{s}^{-1},$$

- Q = incident PPFD, $\mu\text{mol m}^{-2} \text{s}^{-1}$,
 P_{max} = asymptotic or PPFD-saturated rate of net photosynthesis, $\mu\text{mol m}^{-2} \text{s}^{-1}$,
 α = initial slope of the response curve,
 θ = convexity of the response curve, and
 R_d = dark respiration rate, $\mu\text{mol m}^{-2} \text{s}^{-1}$.

Because of strong correlations between parameters and the large variability of R_d , R_d was fixed at 0.37, the mean value for all treatments. The remaining three parameters were then fitted using SAS, PROC NLIN. Table 4.1 shows the parameter values while the lines in Figure 4.8 show the fit of the function to the data. Correlations between parameters makes comparisons of individual parameters between treatments difficult and so an analysis of variance was used to determine if there were significant differences between the curves. This compares the variance when the model is fitted to each treatment separately, with the variance when the model is fitted to the combined data from two treatments (Ross, 1981). The A/Q response curves were all significantly different from each other ($P < 0.01$).

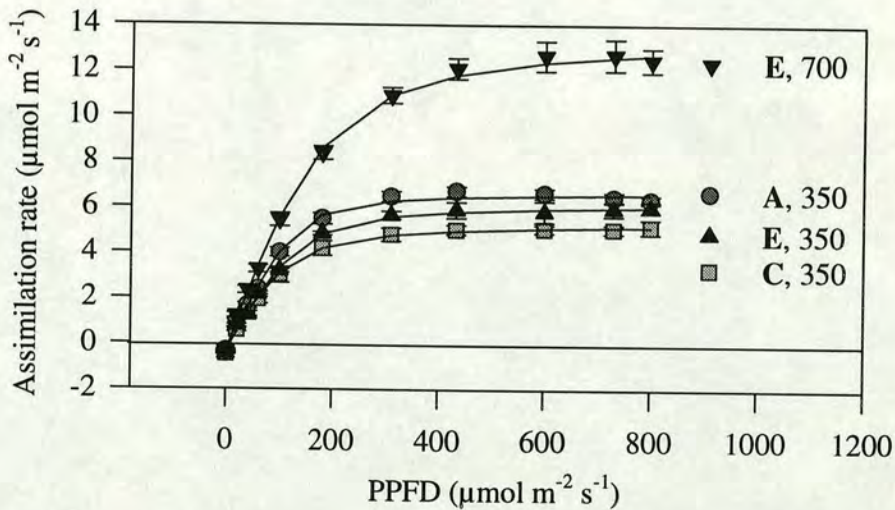


Figure 4.8 Relationship between assimilation rate and PPFD for current year shoots. All shoots were measured at $350 \mu\text{mol mol}^{-1} [\text{CO}_2]$ while E shoots were also measured at $700 \mu\text{mol mol}^{-1}$. Values are means ± 1 SEM, $n = 6$. Leaf temperature = $24 \pm 3 \text{ }^\circ\text{C}$, VPD = 0.6 ± 0.3 kPa. Lines are fitted model.

Table 4.1 Parameters obtained when fitting the model to A/Q response curves. Parameter values ± 1 S.E., $n = 6$.

	C_{350}	A_{350}	E_{350}	E_{700}
θ	0.80 ± 0.11	0.91 ± 0.04	0.86 ± 0.07	0.81 ± 0.37
α	0.045 ± 0.005	0.053 ± 0.003	0.043 ± 0.003	0.072 ± 0.005
P_{max}	5.72 ± 0.186	7.07 ± 0.133	6.58 ± 0.18	13.8 ± 1.49

4.6 A/C_i response functions

4.6.1 Method

The relationship between net assimilation rate and intercellular $[CO_2]$, A/C_i , was determined on current shoots in August 1994. The response functions were measured using the light source (Appendix B) with PPFD of $800 \mu\text{mol m}^{-2} \text{s}^{-1}$. The $[CO_2]$ entering the cuvette was adjusted upward in steps from the growth concentration of the shoot to the maximum measurable by the IRGA ($1700 \mu\text{mol mol}^{-1}$) then reduced back to the growth concentration and then in steps down to zero. To see the response of the stomata to changing $[CO_2]$ as well as that of the photosynthetic apparatus, it was necessary to allow between 20 and 40 minutes after a change in the $[CO_2]$ until the humidity and CO_2 differentials were stable before a reading was taken.

Preliminary measurements indicated a potential problem with a positive feedback loop: If the stomata begin to close for any reason, less water vapour enters the cuvette and the VPD increases, as a result of both lower water vapour pressure and higher air temperature because more energy is partitioned from latent heat to sensible heat, than before. The resulting increase in VPD could induce further stomatal closure leading to a runaway process and complete stomatal closure. To avoid this the air entering the cuvette was humidified to maintain the cuvette humidity at approximately 80% RH which at 23°C gives a VPD of 0.6 kPa.

Further measurements of assimilation at different CO_2 concentrations were made in September and October 1994 on both current and C+1 shoots. Because of limited time only four CO_2 concentrations were used 100, 355, 700 and $1400 \mu\text{mol mol}^{-1}$ and readings were taken more quickly after each $[CO_2]$ change, *i.e.* as soon as the CO_2 differential had stabilised (approximately 5-10 minutes), which did not give the stomata time to adjust fully.

4.6.2 Results

There were no differences between treatments in the A/C_i responses of the current shoots (Figure 4.9).

Stomata closed in response to increasing $[CO_2]$ but the relationship between stomatal conductance and C_i was the same for **A** and **E** shoots (Figure 4.10). The dashed lines indicate the predicted C_i and stomatal conductances under the growth $[CO_2]$ for the **A** and **E** shoots and demonstrate that **E** shoots may have 10% lower stomatal conductances than **A** shoots as a direct result of elevated $[CO_2]$. There was

no evidence of either up or downward acclimation in response to growth in elevated $[\text{CO}_2]$.

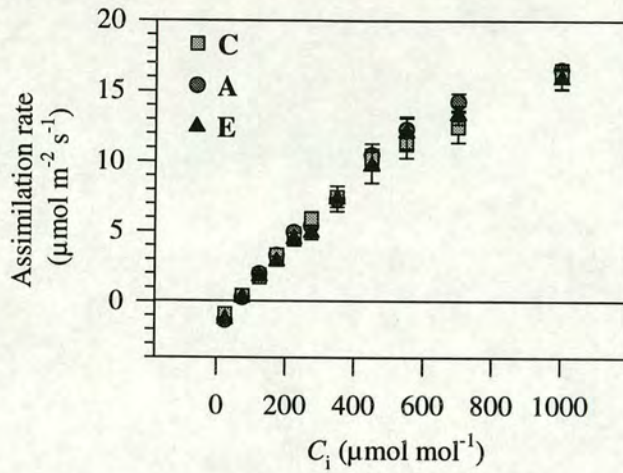


Figure 4.9 A/C_i functions for current year shoots measured in August 1994. Means \pm 1 SEM, $n = 6$. PPFD = $800 \mu\text{mol m}^{-2} \text{s}^{-1}$, leaf temperature $23 \text{ }^\circ\text{C} \pm 3$, VPD $0.6 \text{ kPa} \pm 0.3$.

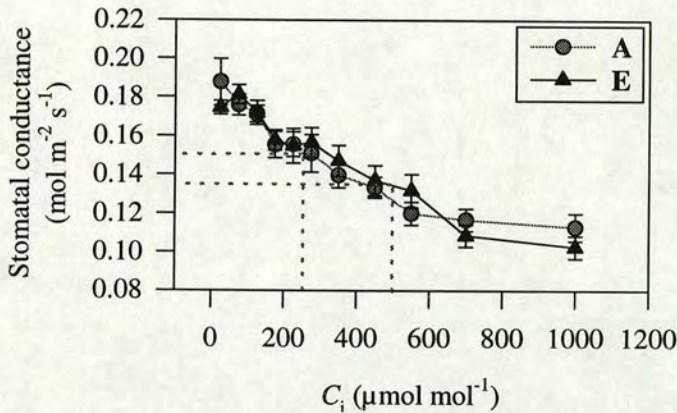


Figure 4.10 Relationship between stomatal conductance and internal CO_2 concentration for current year shoots measured in August 1994. Means \pm 1 SEM, $n = 6$. PPFD = $800 \mu\text{mol m}^{-2} \text{s}^{-1}$, leaf temperature $23 \text{ }^\circ\text{C} \pm 3$, VPD $0.6 \text{ kPa} \pm 0.3$. The broken lines indicate the values of C_i and g_s under growth CO_2 conditions.

In contrast to the current shoots (Figure 4.9), C+1 shoots did show signs of a downward acclimation of photosynthesis to growth in elevated $[\text{CO}_2]$, as seen in the concise A/C_i responses measured in September and October (Figure 4.11). Current, A and current, E shoots had very similar responses, while C+1, A had similar photosynthetic rates but a more flattened response, whereas C+1, E also had a flattened response but much lower photosynthetic rates. Thus there appears to be a change in the shape of the response curve with age and downward acclimation of

photosynthetic capacity in one-year old shoots in response to growth in elevated $[\text{CO}_2]$. Despite the strong down-regulation, **E** shoots would probably still have higher photosynthetic rates in the growth conditions as indicated by the broken lines on Figure 4.11.

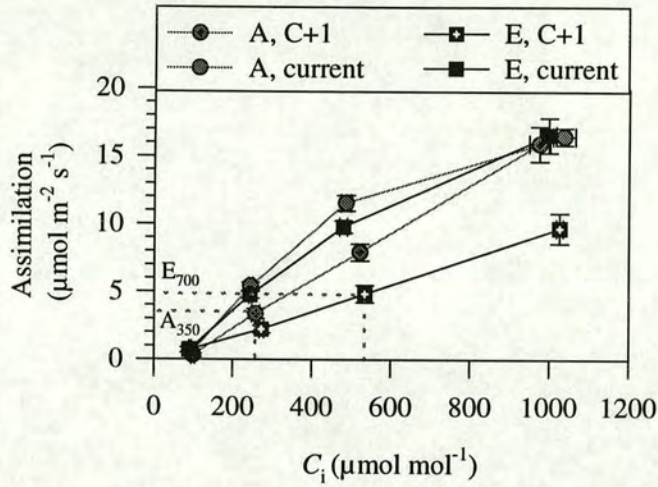


Figure 4.11 Concise A/C_i response functions for current and C+1 shoots measured in September and October 1994. Means ± 1 SEM, $n = 4-6$. PPFD = $800 \mu\text{mol m}^{-2} \text{s}^{-1}$, leaf temperature $23 \text{ }^\circ\text{C} \pm 3$, VPD $0.6 \text{ kPa} \pm 0.3$. Broken lines show A and C_i of C+1 shoots at their growth $[\text{CO}_2]$.

Stomatal conductances were lower in C+1 shoots than in current shoots and also lower in **E** than in **A** shoots (Figure 4.12). However, since measurements were made too quickly to allow the stomata to adjust to the changing CO_2 concentration the comparison between **E** and **A** probably reflects the state of the shoot under growth conditions.

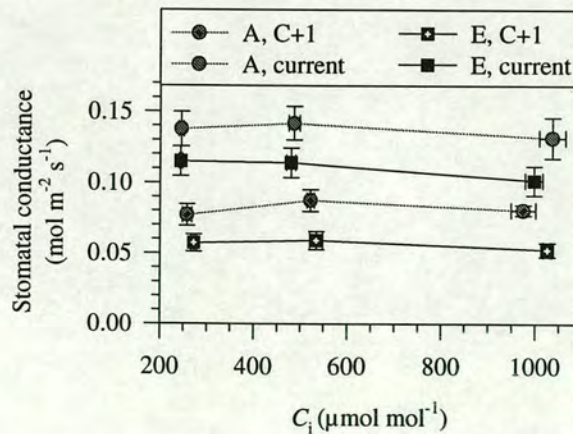


Figure 4.12 Relationship between stomatal conductance and internal CO_2 concentration for current and C+1 shoots measured in September and October 1994. PPFD = $800 \mu\text{mol m}^{-2} \text{s}^{-1}$, leaf temperature $23 \text{ }^\circ\text{C} \pm 3$, VPD $0.6 \text{ kPa} \pm 0.3$. Means ± 1 SEM, $n = 6$.

4.7 Relationship between stomatal conductance and assimilation rate

In order to predict the effects of increasing $[\text{CO}_2]$ on vegetation we need models which characterise the behaviour of plants preferably mechanistically but otherwise empirically. Although there is general consensus that the mechanistic model of photosynthesis first presented by Farquhar *et al* (1980) is robust and in good agreement with observations, there is no such consensus on a model for stomatal conductance, g_s . Various approaches have been used in the past to relate g_s to environmental variables (e.g. Jarvis, 1976) and one approach that has recently grown in popularity, because of its ease of application, is that of Ball *et al.* (1987) (BWB from here). It has long been noted that there is a correlation between g_s and A , and until recently it was assumed that g_s and A responded to environmental variables independently or that g_s 'controlled' A . However, the BWB model inverts the relationship such that g_s is a function of A . The original BWB model related g_s to A , $[\text{CO}_2]$, and relative humidity but further development of the model by other workers has led to the current version presented by Leuning (1995) (L-BWB from here) shown below.

$$g_s = g_0 + \frac{a_1 \cdot A}{[(C_s - \Gamma)(1 + D_s/D_o)]}$$

where

- g_s = stomatal conductance to CO_2 ($\text{mol m}^{-2} \text{s}^{-1}$),
- g_0 = the conductance as $A \rightarrow 0$ when PPF $\rightarrow 0$, ($\text{mol m}^{-2} \text{s}^{-1}$),
- D_s = vapour pressure deficit at the leaf surface, (kPa),
- C_s = $[\text{CO}_2]$ at the leaf surface, ($\mu\text{mol mol}^{-1}$),
- Γ = CO_2 compensation point, ($\mu\text{mol mol}^{-1}$), and
- D_o and a_1 are empirical coefficients (kPa and dimensionless, respectively).

The model has been shown to agree with a number of data sets (Leuning, 1990, 1995) but by no means all and there is some concern about its use as a component in larger models used to predict the effects of rising atmospheric $[\text{CO}_2]$ on vegetation at regional scales.

I have attempted to parameterise the L-BWB model using the data sets obtained in 1991, 1993 and the A/C_i data set of 1994 to assess if it can be used to predict stomatal conductances for Sitka spruce.

4.7.1 Method

Although the data collected both in natural light and with the light source showed a reasonable spread with respect to D_s , g_s and A there were only two $[CO_2]$ and so the data could not be used to determine Γ . Γ was obtained from the A/C_i responses measured in 1994 on current shoots by linear regression of the response at $C_i < 150 \mu\text{mol mol}^{-1}$ (i.e. from Figure 4.9) which gave a value of $64.6 \mu\text{mol mol}^{-1}$.

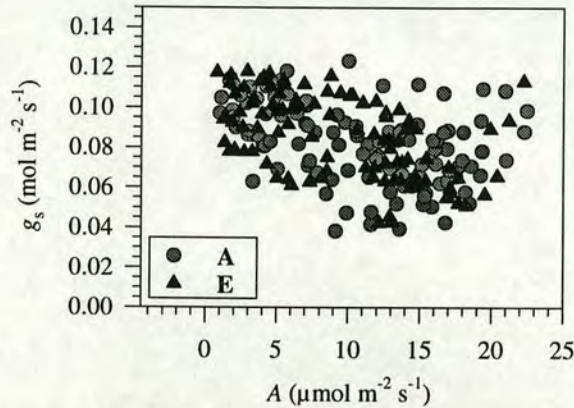


Figure 4.13 Stomatal conductance (CO_2) plotted against assimilation rate for the data in Figure 4.9 and Figure 4.10 on current shoots in 1994.

Data for **A** and **E** shoots from the A/C_i data-set (Figure 4.9 and Figure 4.10) showed the same response when g_s was plotted against A (Figure 4.13) and so were pooled for the model parameterisation. Only data with $C_i > 100$ were used as the relationship between g_s and A is known to breakdown at low C_i . The model was optimised for the predicted C_i rather than predicted g_s as this tends to give a better fit (Ball personal communication). The model is notoriously difficult to fit because of strong correlations between parameters, especially a_1 and D_o . Also since measurements were made at high PPFD it was not possible to obtain a good estimate of g_o and so it was fixed at $0.004 \text{ mol m}^{-2} \text{ s}^{-1}$ and then a_1 and D_o were obtained by fitting the model to the data-sets using non-linear curve fitting (proc NLIN, SAS).

4.7.2 Results

Figure 4.14 shows the values of g_s predicted by the L-BWB model plotted against the measured g_s for the 1994 A/C_i data-set. The model gave a reasonable fit in so far as the slope of the regression between predicted and actual g_s was very close to one however there was considerable unexplained variation. Plots of the residuals against the driving variables (Figure 4.15) are fairly well distributed indicating there was no systematic error in the model.

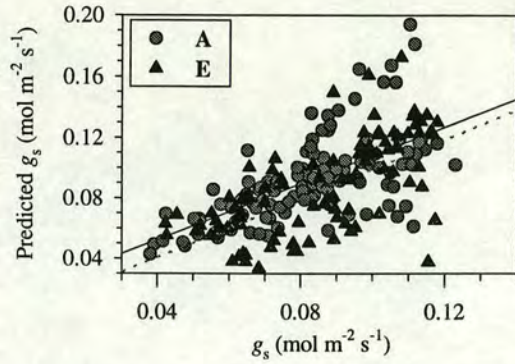


Figure 4.14 Stomatal conductance predicted by L-BWB model plotted against measured stomatal conductances from data obtained during determination of A/C_i responses on current shoots in 1994. $D_o = 0.44$, $g_o = 0.004$, $a_1 = 10.7$ and $\Gamma = 64.6$. The line shows the regression; predicted $g_s = 0.94g_s + 0.01$, $r^2 = 0.39$. Broken line shows one to one.

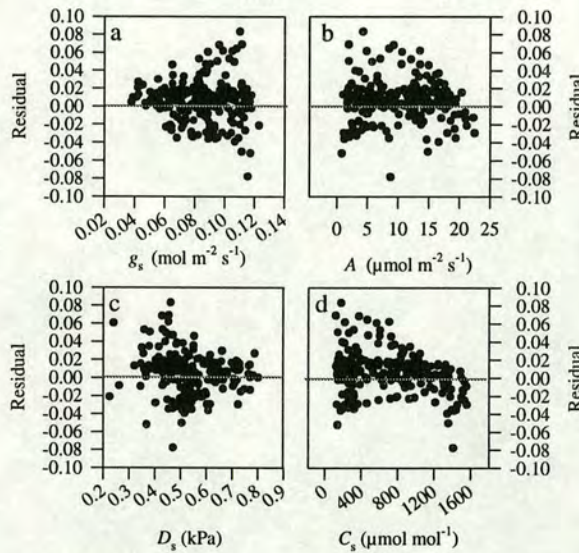


Figure 4.15 Plots of residuals (measured - predicted) against g_s , A , D_s and C_s for the L-BWB fit shown in Figure 4.14.

The L-BWB model was also fitted to the data-sets measured at two $[\text{CO}_2]$ under natural (1991) or artificial light (1993) (see 4.2 and 4.3). Only data measured at the growth $[\text{CO}_2]$ were used since not enough time was allowed for stomatal adjustment when measurements were made at the reciprocal concentration. Once again the model was reasonably good at predicting g_s especially for the 1991 data collected under natural light (Figure 4.16). As the **A** and **E** responses appeared to be slightly different the model was also fitted to the same data but with **A** and **E** fitted separately (Figure 4.17) this improved the r^2 from 0.74 to 0.81, however it is uncertain whether the change in parameterisation is a response to growth or measurement $[\text{CO}_2]$. To test this stomata from both treatments would need to be allowed enough time to adjust to the new conditions.

Figure 4.18 shows the results for the current shoots in 1993 measured with artificial light. The model was less good at predicting g_s in this case which was not surprising since the best fit of the model should be with the measurements made in natural light at growth $[CO_2]$ because the conditions within the cuvette were most similar to those the shoot had just experienced and so the stomata should have been closer to equilibrium (Figure 4.16a).

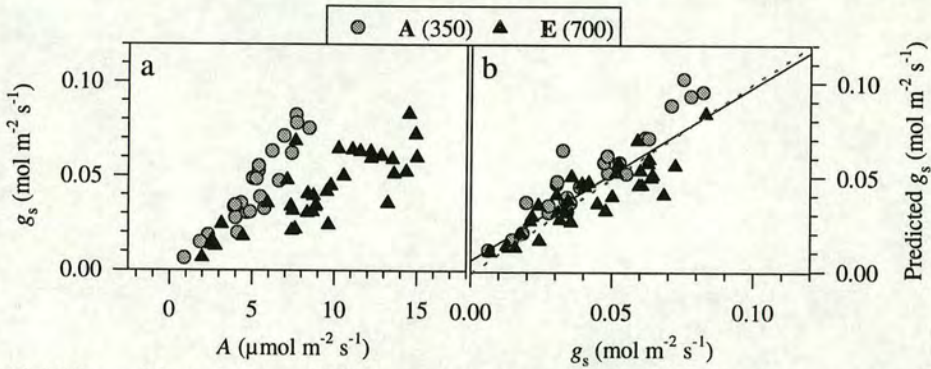


Figure 4.16 Stomatal conductance (CO_2) v assimilation rate (a) and predicted g_s v measured g_s (b) for data collected on current-year shoots in 1991 measured at growth $[CO_2]$ with natural light. $D_o = 4.07$, $g_o = 0.004$, $a_1 = 7.54$ and $\Gamma = 64.6$. Line is the regression predicted $g_s = g_s \cdot 0.82 + 0.017$, $r^2 = 0.75$.

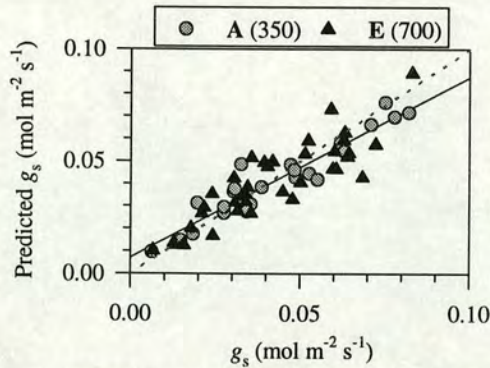


Figure 4.17 Predicted g_s v measured g_s for data collected on current-year shoots in 1991 with natural light for the same data as in Figure 4.16 but the **L-BWB** model was fitted to data measured for **A** and **E** separately. For **A** $D_o = 3.02$, $g_o = 0.004$, $a_1 = 2.54$ and $\Gamma = 64.6$ and for **E** $D_o = 1.29$, $g_o = 0.004$, $a_1 = 4.83$ and $\Gamma = 64.6$. Regression predicted $g_s = g_s \cdot 0.80g_s + 0.007$, $r^2 = 0.81$.

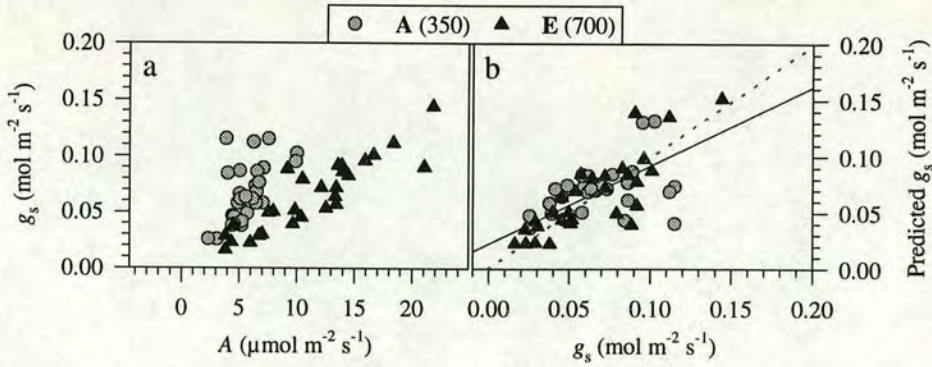


Figure 4.18 Stomatal conductance v assimilation rate (a) and predicted g_s v measured g_s (b) for data collected on current-year shoots in 1993 measured at growth $[CO_2]$ with an artificial light source. $D_o = 1$, $g_o = 0.004$, $a_1 = 6.22$ and $\Gamma = 64.6$. Regression predicted $g_s = 0.70g_s + 0.022$, $r^2 = 0.46$.

It was difficult to fit the model to the data because of strong correlations between parameters and high sensitivity to initial parameter values. It was necessary to fix D_o at 1 for the 1993 data set in order to obtain a fit. Parameter values obtained for the three data sets are shown in (Table 4.2).

Table 4.2 Parameter values for the L-BWB model fitted to three data-sets; 1991 current shoots in natural light, 1993 current shoots in artificial saturating PPFD and A/C_i response data in saturating PPFD. Γ was obtained from the A/C_i response curve the remaining parameters were obtained by non-linear regression. † indicates parameter fixed.

	Γ	g_o	D_o	a_1
1991 (combined)	64.6†	0.004†	4.07	7.54
1991 (E)	64.6†	0.004†	1.29	4.83
1991 (A)	64.6†	0.004†	3.02	2.54
1993	64.6†	0.004†	1†	6.22
1994 A/C_i	64.6†	0.004†	0.44	10.7

4.8 Discussion

4.8.1 Photosynthesis

Current-year-shoots did not show any down-regulation of photosynthetic capacity in response to growth in elevated $[CO_2]$ in any of the years of the experiment and so current, E shoots would have assimilated twice as much CO_2 as current, A shoots at their respective growth $[CO_2]$. One-year-old shoots, on the other hand, did show down-regulation, but nonetheless C+1, E shoots measured at $700 \mu\text{mol mol}^{-1} [CO_2]$ still had slightly higher photosynthetic rates than C+1, A shoots measured at $350 \mu\text{mol mol}^{-1}$, so the down-regulation did not completely remove the enhancement to photosynthesis in elevated $[CO_2]$ (see Figure 4.3 and Figure 4.11). The down-regulation observed in C+1 needles did not occur in 1991. Thus it seems that down-

regulation was an effect of long-term exposure rather than a higher sensitivity of C+1 needles to elevated $[\text{CO}_2]$, since needles were unaffected in their first year of exposure to elevated $[\text{CO}_2]$ but by the second year they had acclimated.

A number of mechanisms have been proposed to explain down-regulation of photosynthesis observed in plants grown in elevated $[\text{CO}_2]$. Most involve a feedback mechanism in which a build up of starch or soluble carbohydrates within the leaf occurs as a result of an imbalance between production and utilisation of carbohydrates. It is supposed that this build up of carbohydrates leads to a reduction of photosynthesis as a result of physical disruption of the chloroplasts by starch grains (Cave *et al.*, 1981; Wulff & Strain, 1981), or a limitation of the Calvin cycle when inorganic phosphate becomes limiting (Herold, 1980; Sharkey, 1985; Harley & Sharkey, 1991; Harley *et al.*, 1992), or by moderating expression of genes for proteins involved in photosynthesis (Stitt, 1993). Further mechanisms proposed to explain down-regulation are that the nitrogen concentration in leaves falls in response to elevated $[\text{CO}_2]$ or that nitrogen is re-partitioned between proteins involved with carboxylation, i.e. rubisco, those involved with light harvesting and electron transport, and those involved with starch and sucrose synthesis, in such a way as to optimise nitrogen distribution within the leaf (Sage *et al.*, 1988; Sharkey *et al.*, 1988; Stitt, 1991; Tissue *et al.*, 1993; Sage, 1994) (see Chapter 7 for a more detailed discussion of these mechanisms).

In this experiment foliar nitrogen concentrations and chlorophyll concentrations were not significantly different between treatments (see Chapter 3) and so reduction or re-partitioning of nitrogen is unlikely to be responsible for the observed down-regulation. Furthermore, starch concentrations in needles were negligible and can be ruled out. However, C+1, E needles did have slightly higher, although not statistically significantly, soluble carbohydrate concentrations than C+1, A needles (see Chapter 3) and it is possible that this was responsible for the down-regulation. The question arises as to why there was a build up of soluble carbohydrates in C+1 needles but not in current needles on the same branch and a possible explanation is given below.

One criticism of using a branch bag approach to investigate the effects of elevated CO_2 is that it is very unlikely that feedback inhibition will occur, since the tree is likely to be a strong sink for assimilates and only one branch exposed to elevated $[\text{CO}_2]$ would not significantly influence the carbon balance. However, if there is an influence of CO_2 at the needle or shoot scale the branch bag technique should detect it. The fact that current needles did not show down-regulation while C+1 shoots did

rules out feedback inhibition at the scale of the tree since if, for some reason, the sink strength was reduced such that there was an over production of assimilate then both current and C+1 shoots would be affected. Liu & Teskey (1995) used the same branch bag technique on loblolly pine and concluded after two years of exposure that loblolly pine trees did not show a downward acclimation of leaf-scale photosynthesis in response to long term exposure to elevated CO₂. However, they only measured current year needles.

A possible explanation for the down-regulation observed in C+1 shoots in this experiment is that the transport of assimilates out of the needles became limiting. Each year as a needle ages a proportion of the phloem dies and is replaced (Ewers, 1982): possibly the export from E needles of additional photosynthate may have reduced the longevity of phloem cells resulting in a gradual decline in transport capacity thus leading to a build up of soluble carbohydrates in the needle and consequent down-regulation of photosynthesis through feedback-inhibition. Thus the amount of new phloem produced each year maybe fixed or inadequately coupled to actual transport requirements. Further research is required into the poorly understood topic of secondary phloem development in conifer needles.

More CO₂ was fixed by both current and C+1 shoots and consequently by branches growing in elevated [CO₂], yet no extra growth, storage of carbohydrates or respiration occurred in those branches. This leads to the conclusion that all of the extra assimilate must have been exported from these branches to supply carbohydrate for growth and metabolic processes elsewhere in the tree. Where in the tree that growth occurs is largely influenced by apical dominance, light quality and PPFD, variables that control the initiation and sink strength of meristems.

4.8.2 Stomatal conductance

The typical short term response of stomata to CO₂ concentration is that they close as the CO₂ concentration rises (Morison, 1987; Eamus & Jarvis, 1989; Eamus *et al.*, 1993; Thomas *et al.*, 1994) and this was seen in the response of stomatal conductance (g_s) to C_i of current shoots measured in 1994. Furthermore, the E and A shoots showed the same response, indicating that there was no acclimation of stomatal response to growth in elevated [CO₂], at least in current year shoots. If all shoots followed this response then shoots growing in elevated [CO₂] would have consistently lower g_s than those in ambient [CO₂], whereas gas exchange measurements made throughout the experiment showed variable responses of g_s to elevated [CO₂]. In the first year there were no differences in g_s between treatments of

either age-class. In 1993 current shoots showed no differences, whereas C+1, E shoots had lower g_s , while in 1994 both E, current and E, C+1 shoots had lower stomatal conductances than their A counterparts. At the present time there is little consistency among studies on trees in elevated $[\text{CO}_2]$ concerning stomatal conductance in elevated CO_2 . There are reports of increased g_s (Norby & O'Neill, 1991), decreased g_s (DeLucia *et al.*, 1985), and no change (Bunce, 1992). The control of stomatal conductance is not fully understood: there are possibly some confounding interactions between light, humidity and CO_2 in these measurements.

4.8.3 The stomatal response model

The L-BWB stomatal conductance model gave good predictions of stomatal conductance when fitted to the data where conditions in the cuvette were close to those prior to attachment of the cuvette but did not do so well under changing conditions. The poor performance of the L-BWB model in predicting g_s for the data-sets collected when $[\text{CO}_2]$, humidity and PPFD were rapidly changed could be attributed to the fact that the stomata were not given adequate time to adjust and so the presumed relationship between g_s and A had been disturbed. However, the Leuning modification takes care of the variation in $[\text{CO}_2]$ and the variation in PPFD and D_s is exactly that which occurs naturally.

The A/C_i , g_s/C_i (1994) response data-set was obtained at ~ 23 °C and the 20-40 minute period left after changing the $[\text{CO}_2]$ allowed g_s and A time to reach a new steady state. The other variables were kept reasonably constant and this is a near ideal data-set on which to test the model. However, there was a considerable amount of variation between measured and predicted g_s and the model could not accurately predict g_s from A , D_s , and C_s therefore it would appear that there are other factors unaccounted for by the model which influence g_s .

Thus, it seems that the L-BWB model may be adequate to model the stomatal response of Sitka spruce in some circumstances but not in others and more data-sets covering a wider range of environmental conditions should be tested to discover under which conditions the model can be used. There is an urgent need for experiments specifically designed to discover the underlying mechanisms of stomatal action and how g_s is controlled.

As has often been reported, lower transpiration rates combined with increased assimilation rates lead to an increase in the instantaneous water use efficiency. However, some caution is required when relating stomatal conductance to transpiration, as under some conditions stomata have little control over transpiration

(Jarvis & McNaughton, 1986), although this is less of a problem with trees than small, sheltered plants, since trees tend to be well coupled to the atmosphere.

4.8.4 Respiration

Respiration in current shoots during August and September can be attributed to maintenance of the needles, translocation of assimilates and possibly to a small amount of growth as new phloem is developed. Respiration rates were the same for both A and E shoots but slightly higher in C shoots, indicating no response to growth in elevated $[\text{CO}_2]$ but a branch bag effect. Rates measured at night were the same as those measured on pre-darkened shoots during the day. However, lower temperatures at night would be expected to reduce respiration rates so that the lack of a reduction suggests that there was an increase in the baseline rate, i.e. the enzyme systems were more active at night.

The effect of elevated $[\text{CO}_2]$ on foliar respiration rates is currently in debate as increases, decreases and no change have all been reported in the literature. There is also some evidence for an instantaneous, reversible response to $[\text{CO}_2]$ (Bunce, 1990; El Koen *et al.*, 1991)(see Chapter 8, 8.4.1 for a more detailed discussion). All measurements in this study were made at $350 \mu\text{mol mol}^{-1} [\text{CO}_2]$ and so it is not possible to determine if there was an instantaneous response to $[\text{CO}_2]$. Extreme care is needed when attempting to observe differences in CO_2 fluxes as $[\text{CO}_2]$ changes, because even small leaks or non-linearity in an IRGA can lead to artefacts.

4.8.5 Branch bag effect

The effect of the branch bag was often more pronounced than that of elevated $[\text{CO}_2]$ this was especially true of the current year shoots in 1993 when photosynthetic rate, stomatal conductance and respiration rate were all significantly lower on shoots of bagged branches. The summer of 1993 was hot and dry and the higher temperatures inside branch bags may have stressed the shoots either directly or by increasing the transpiration rates which could lead to reduced water potentials. The slight reduction in PPFD may have played a part, but if this were the case I would have expected the same response in 1994. The presence of a bag effect does indicate that the bagged branches were not growing under ambient conditions and this has to be taken into consideration when interpreting the results as there is the possibility that the bag effect modified the response to elevated $[\text{CO}_2]$.

4.9 Conclusions

Current year shoots did not show any acclimation of photosynthesis to elevated CO_2 but one-year-old shoots did show some down-regulation after branches had been exposed for two years. As there were no differences in foliar nitrogen, chlorophyll or starch concentrations the small increase in soluble carbohydrate concentration may have been responsible for this down-regulation. The higher soluble carbohydrate concentrations in **E**, C+1 needles may have resulted from a reduction in the capacity to transport carbohydrates induced by the extra load placed on the phloem transport system by higher photosynthetic rates.

The respiration rate of current year shoots was not affected by growth in elevated $[\text{CO}_2]$ but was higher in unbagged shoots than in bagged shoots and higher at night than in the daytime.

Stomatal conductance did not show acclimation to long term exposure to elevated $[\text{CO}_2]$ but did show a short term response to $[\text{CO}_2]$ which translated to lower stomatal conductances in **E** shoots in their growth conditions.

The L-BWB model of stomatal conductance failed to predict accurately stomatal conductance and does not seem appropriate for Sitka spruce.

Branch bags allowed the study of the effect of elevated $[\text{CO}_2]$ on mature branches in the absence of sink limitation and thus enabled observation of the direct effects of elevated $[\text{CO}_2]$ on shoots and needles.

PART II

CO₂ and Nutrient Interactions in Sitka Spruce Seedlings

CHAPTER 5

Description of Experiment

5.1 Introduction

Rising atmospheric CO₂ concentrations have prompted considerable interest in the responses of C₃ plants to CO₂ enrichment. A wealth of experimental data has shown that the rate of net CO₂ assimilation is enhanced when plants are exposed to elevated CO₂, with assimilation increasing initially by 20-200% for a doubling of CO₂ concentration, depending on the species and experimental conditions (see reviews by Eamus & Jarvis, 1989; Idso & Idso, 1994; Ceulemans & Mousseau, 1994). This short-term increase in the photosynthetic rate with increased CO₂ concentration, as characterised during the measurement of A/Ci response curves, is relatively well understood (von Caemmerer & Farquhar, 1981; Sharkey, 1985). However, many studies have shown that the initial increases in CO₂ fixation are not sustained and a downward acclimation of assimilation rate to elevated CO₂ occurs. The mechanisms for this acclimation are not entirely certain but a number of hypotheses have been proposed; for example, photosynthate production may exceed sink demand to such a degree that non-structural carbohydrates accumulate in source leaves, leading to a feedback inhibition of photosynthesis. Accumulation of carbohydrates in leaves has been seen in almost all studies of plant growth in elevated CO₂ and may occur as starch accumulation in chloroplasts (Sasek *et al.*, 1985) or as an accumulation of soluble sugars, depending on the normal storage strategy of the species. An alternative hypothesis is that plants maximise resource-use efficiency by allocating resources, principally N, to maintain a balance between all components of the photosynthetic apparatus and between photosynthetic and non-photosynthetic processes (Bloom *et al.*, 1985; Stitt, 1991). Thus, down-regulation of photosynthesis may reflect either a relocation of N away from Rubisco and into light harvesting, electron transport and RuBP and P_i regeneration processes or reallocation of N away from photosynthesis altogether and into non-photosynthetic processes.

Nutrient availability has been strongly implicated in the response of photosynthesis and allocation of assimilates to elevated CO₂. In experiments where plants received ample nutrients, plants exhibited little or no photosynthetic down regulation (Idso,

Kimball & Allen 1991; Drake 1992). In contrast in cases where nutrient supply was limited down-regulation of photosynthesis rapidly occurred (Tissue & Oechel 1987). A possible explanation for these findings is that new growth requires both nutrients and assimilates and, if an imbalance between nutrient uptake and photosynthate production arises, photosynthate concentrations increase leading to feedback inhibition. In such nutrient limiting conditions, allocation of resources may be moved from production of new shoots to the root system, either to supply increased root activity per unit mass of root (Clement *et al.*, 1978; Rufty *et al.*, 1989) or for production of new roots, giving rise to an increase in the root to shoot ratio of plants grown in elevated CO₂ (see review by Ceulemans & Mousseau, 1994).

Even when downward acclimation of photosynthetic rates occurs, plants growing in elevated CO₂ concentrations almost always continue to have higher rates of photosynthesis than those in ambient CO₂. In a review of 28 controlled exposure studies, covering 30 boreal, temperate and tropical species it was observed that photosynthesis was increased by 46% for an approximate doubling of atmospheric CO₂ concentration. For a few species these enhanced photosynthetic rates exceeded twice that of the ambient grown controls (Luxmoore *et al.*, 1993).

Enhanced photosynthesis in plants grown under elevated CO₂ will result in extra assimilates which:

- 1) may be incorporated into new growth and become apparent as an increased relative growth rate;

- 2) may be incorporated into secondary metabolites or storage compounds; however, the size of the pools of these compounds are finite and once the storage pools are full the extra assimilate must go elsewhere.

- 3) may be 'burnt off' through increased rates of respiration; however, there is little evidence for increased respiration rates and even some for decreased respiration rates in plants exposed to elevated CO₂ (El Kohen *et al.*, 1991; Amthor *et al.*, 1992); nevertheless, increased growth rates incur a respiratory cost and assuming that the carbon use efficiency (g CO₂ evolved per g DM increase) remains constant, the respiration rate per unit mass should be proportional to the relative growth rate;

- 4) may be allocated to fine roots, with an increase in fine root turnover and enhanced exploration of the rooting volume rather than an increase in root biomass; the annual fine root production can constitute 60-80% of the total net primary production of a forest (Reichle *et al.*, 1973) so a relatively small increase could account for a significant amount of assimilates;

5) finally, assimilates may be exuded from roots to supply mycorrhizas and soil microbes in exchange for increased nutrient uptake; the uptake of nutrients requires metabolic energy (Pitman 1977); the enhanced availability of carbohydrates in the root system will thus enable increased nutrient uptake; in addition rhizosphere organisms secrete a number of organic acids that may hasten the chemical weathering of various soil minerals (Boyle & Voigt, 1973; Boyle *et al.*, 1974) and they are especially adept at making phosphorus available to plants (Molla *et al.*, 1984).

Increases in root activity, fine root turnover and root exudates would result in increased below ground respiration, as soil micro-organisms utilise the substrate, and this should be apparent as an increase in the rate of soil CO₂ efflux.

5.2 Aim of the experiment

The objectives of this study were: (1) to determine the effects of elevated CO₂ on biomass accumulation, carbon allocation patterns and carbohydrate content in juvenile Sitka spruce trees grown at two rates of nutrient supply; and (2) to study the fluxes of carbon in both above and below ground plant parts to determine if growth in elevated CO₂ increases the flux of carbon through the atmosphere-plant-soil system.

5.3 Open-top chambers in the Glasshouse

5.3.1 Design of chambers

The CO₂ exposure facilities used for this experiment were six small open-top chambers situated in a large, unheated glasshouse at The King's Buildings, Edinburgh. Each chamber was cylindrical 1.3 m in diameter and 1.7 m tall, constructed from sheets of corrugated acrylic plastic bolted to two aluminium hoops, one at the top and one at the bottom. Two doors on opposite sides of the chamber facilitated access. A heavy-duty, wire-mesh floor supported the pots 20 cm above the ground, leaving a space for a perforated polythene bag, which when inflated distributed the airflow evenly across the cross section of the chamber (Figure 5.1).

One fan blower per chamber (52 BTXL, Airflow Developments Ltd., High Wycombe, UK) mounted in a box attached to the glasshouse wall drew air through a filter from outside the glasshouse. A 15 cm plastic duct carried the air the distance of 2 m from the fan box to the perforated bag in the base of the chamber. Air was drawn from outside the glasshouse to maintain the temperature within the chambers as close to ambient as possible and to prevent air enriched in CO₂ from the elevated chambers

re-entering the system. A butterfly valve mounted in the duct close to the housing was used to regulate the airflow to approximately two air changes per minute. Pure CO₂ was introduced into the airstream just beyond the butterfly valve for the three elevated CO₂ chambers.

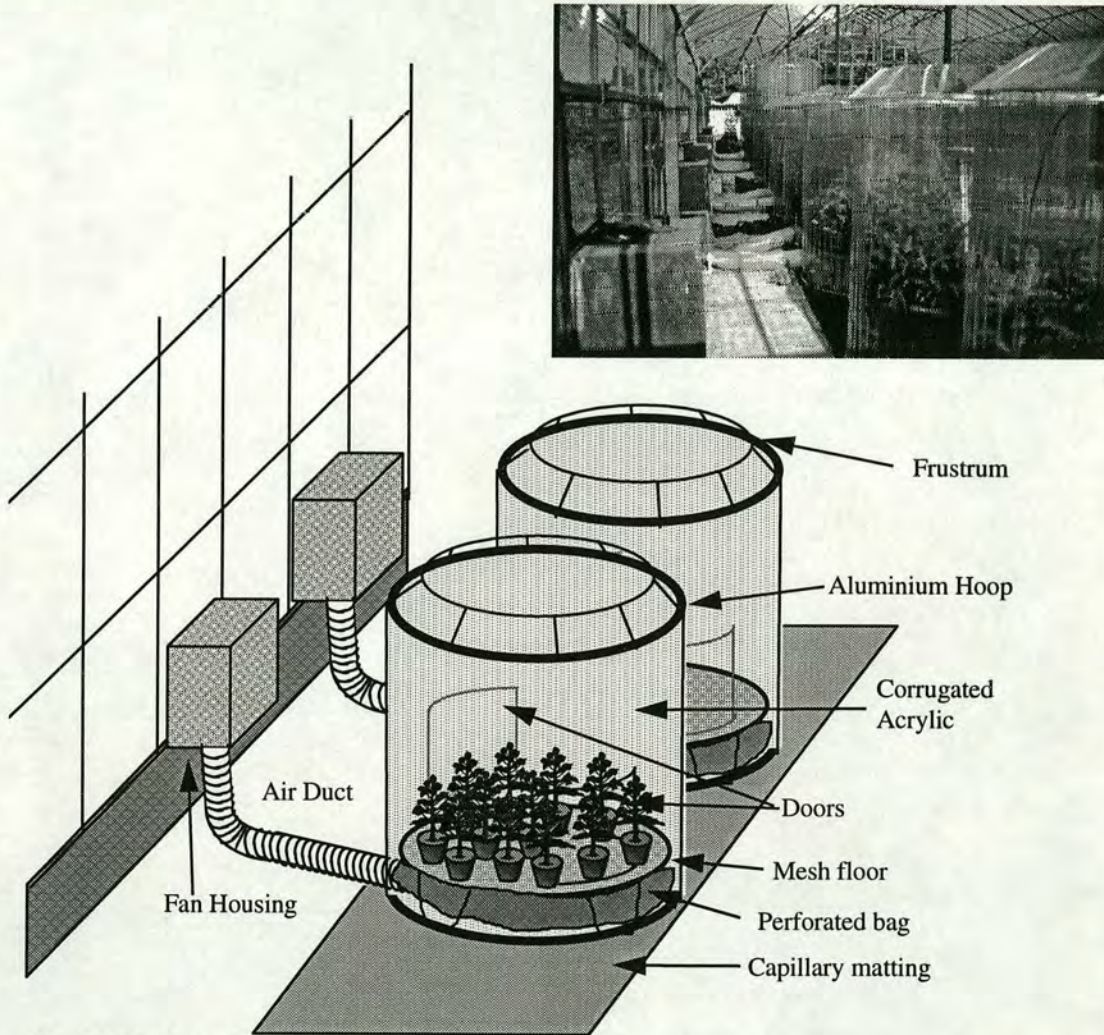


Figure 5.1 Open-top chambers in glasshouse.

The CO₂ monitoring and control system was the same as that used for the branch bags (see Chapter 2, 2.3.3) but using larger mass flow controllers ($0 - 2 \text{ dm}^{-3} \text{ min}^{-1}$, FC280 Tylan General Corp., Torrance, CA). CO₂ was supplied from eight gas-withdrawal cylinders linked together in two groups of four, with an automatic change-over valve between. CO₂ consumption was approximately 4 kg per chamber per day.

5.3.2 Environmental monitoring.

Air temperature in the chambers was measured using fine wire thermocouples, the reference junctions of which were all mounted in a common aluminium block with a platinum resistance thermometer. Background temperature and humidity within the glasshouse was measured with a combined temperature and humidity probe (HMP 35A, Vaisala (UK) Ltd., Cambridge, UK). Photosynthetically active photon flux density was measured close to each chamber using PAR sensors (Macam Photometrics Ltd., Livingston, UK). All sensors were calibrated at the beginning of the season. A datalogger (CR7, Campbell Scientific Ltd., Shepshed, UK) sampled every minute and stored half hourly averages.

5.4 Chamber Performance.

5.4.1 CO₂ control.

Despite being in the glasshouse, the open-top chambers were subject to incursions caused by downdrafts from the glasshouse roof vents when it was moderately windy. The vents were always open for ventilation apart from when very high wind speeds triggered the automatic system to close them. The active control of CO₂ injection allowed the system to compensate for changes in the mass flow of air passing through the chambers, caused by wind and clogging of the filters, so that the CO₂ concentrations within the elevated CO₂ chambers were maintained close to the target concentration. The CO₂ concentrations in the elevated CO₂ chambers were within 20 $\mu\text{mol mol}^{-1}$ of the target (ambient + 350 $\mu\text{mol mol}^{-1}$) for 70 % of the time during the period March to September. Figure 5.2 shows the deviations from the target concentration for all three chambers. There were no differences in mean daily CO₂ concentration between the three elevated CO₂ chambers.

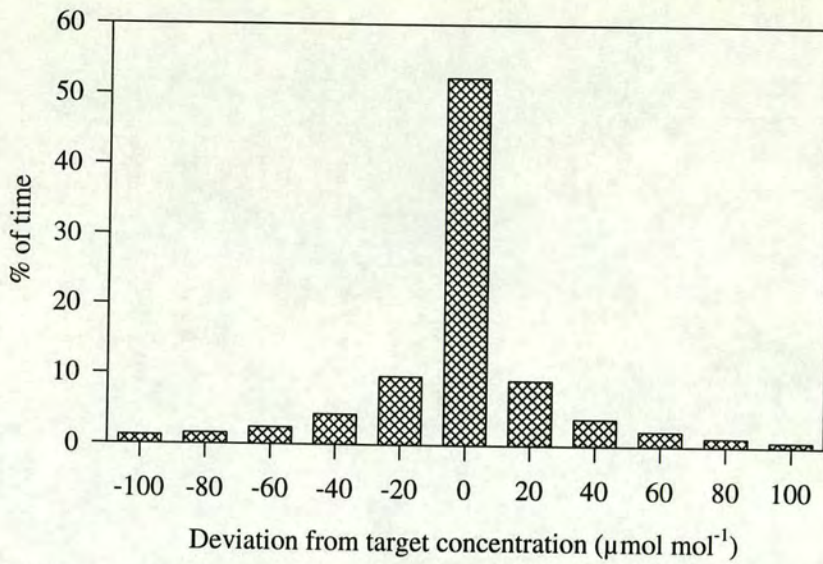


Figure 5.2 Histogram showing deviations from target CO₂ concentrations for glasshouse open-top chambers for March-September.

5.4.2 Temperature

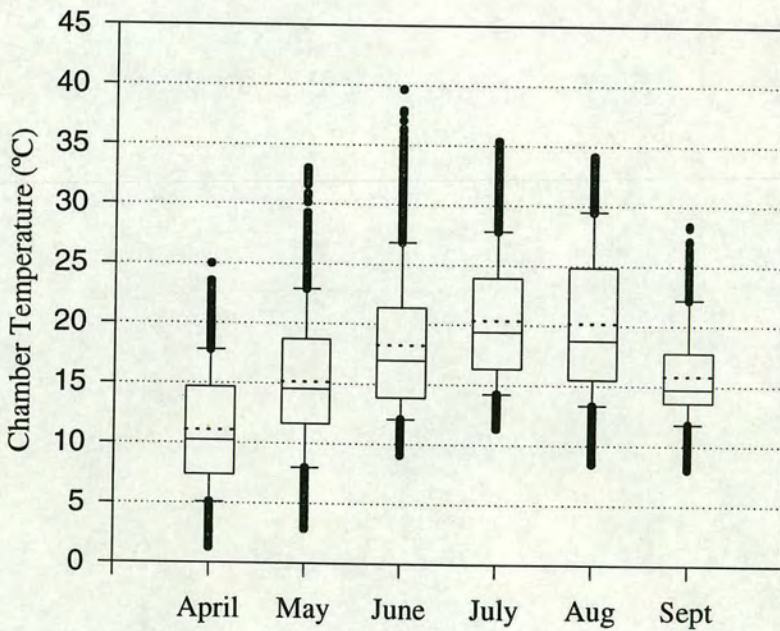


Figure 5.3 Monthly box plots of half hourly temperatures in the chambers. Boxes span 25th to 75th percentiles with 50th percentile (solid line) and mean (broken line). Whiskers span 10th to 90th percentiles. Dots show points outside the 10 and 90 percentiles.

The summer of 1995 was the hottest on record. Tukey box plots of half hourly temperatures averaged over the chambers indicate that chamber temperatures

occasionally exceeded 35 °C on very hot, sunny days (Figure 5.3). Mean daily temperatures were not statistically different amongst the chambers.

5.5 Plant material

In Spring 1994 Sitka spruce seeds (Queen Charlotte Island, provenance 83, seed lot 2015F) were sown in potting compost in individual 1 dm³ pots and grown in four polyethylene covered chambers, two at ambient CO₂ and two at approximately 700 μmol mol⁻¹ CO₂ concentration, in a glasshouse at the Institute of Terrestrial Ecology, 10 km South of Edinburgh. The compost contained a balanced fertiliser and the seedlings were watered regularly. In early April 1995, 140 healthy, uniform seedlings (approximately 30 cm tall) were selected for this experiment.

5.6 Treatments

5.6.1 Growing medium.

As one of the aims of the experiment was to determine CO₂ efflux from the root system it was desirable to grow the plants in sand, since this would avoid confounding effects of CO₂ released by oxidation of soil organic matter. Furthermore, growth in sand would enable nutrient supply to be more easily controlled. However, because root growth had just started there was concern that plants re-potted into sand may not have taken, so half were repotted into potting compost. As well as ensuring that at least some of the plants would grow successfully, this also enabled determination of any differences between plants grown in compost and sand, and this would help interpretation and extrapolation of information derived from plants grown in sand in the future.

The plants were re-potted into 5 dm³ pots which were assumed to be large enough to minimise root restriction that might influence the experiment (Arp 1991). For those re-potted into sand the original compost was gently teased and shaken from the roots, which were then dunked in a bucket of water to remove as much as possible of the remaining compost. A mound of sand was made inside the pot and the roots spread evenly around it and then the pot was filled with sand and a layer of gravel spread on the surface to discourage the growth of algae. The plants potted into 'soil' (a fertiliser-free potting compost of 70% peat, 20% sand and 10% gravel by volume) were simply transferred into the larger pots with the minimum of disturbance to the roots.

5.6.2 Nutrient treatment.

A quasi-Ingstad (*cf.* Ingstad 1982) approach was adopted to supply nutrients to the plants at an exponentially increasing rate designed to match the growth rate of the plants. The aim was to feed nutrients to the plants at two different supply rates: a high rate (H) which was calculated to be slightly more than that required for maximum growth rate of Sitka spruce of this age, and a low rate (L) which was 1/10 the high rate. An estimate of the maximum growth rate was determined from growth and harvest data from previous experiments at this Institute and from the results of Ingstad and Kähr (1985). Past experiments with Sitka spruce at Edinburgh gave relative growth rates (R_G) of between 0.5% and 1% day⁻¹, while Ingstad and Kähr found maximum rates to be 6% day⁻¹ for a number of conifer species grown under optimal conditions. The high temperature and low light conditions combined with slightly older plants were probably responsible for the lower R_G found at Edinburgh and, as conditions of light and temperature were expected to be similar during this study, a R_G of 2% day⁻¹ was chosen to avoid the risk of overfeeding the trees.

The nutrient solution was like that used by Murray *et al.* (1996) (see Appendix C) and was applied to each pot by pipette once a week just prior to watering. Table 5.1 shows the amounts applied each week for the H treatment (see Appendix D). The L treatment received 1/10 the H amount. The concentration of the feed solution was adjusted to ensure that at least 5 cm³ was applied to each pot; this enabled accurate pipetting and aided the even distribution of solution around the pot. Nutrient solution was only applied during the first 115 days which corresponded to the expected period of growth based on previous experiments with Sitka spruce seedlings at Edinburgh.

Date	Day	Nitrogen (mg)	Date	Day	Nitrogen (mg)
08/04/95	1	33	07/06/95	61	110
14/04/95	7	37	13/06/95	67	124
20/04/95	13	42	19/06/95	73	140
26/04/95	19	47	25/06/95	79	157
02/05/95	25	53	01/07/95	85	177
08/05/95	31	60	07/07/95	91	200
14/05/95	37	68	13/07/95	97	225
20/05/95	43	77	19/07/95	103	254
26/05/95	49	86	25/07/95	109	287
01/06/95	55	97	31/07/95	115	323

Table 5.1 Amounts of nitrogen applied to each H treatment pot (other nutrients applied relative to N see Appendix D).

5.7 Experimental design

An initial harvest of 10 ambient and 10 elevated trees was made in early April when the trees were moved from the Institute of Terrestrial Ecology to the University, at which time the experimental plants were re-potted. This harvest gave the baseline data for the first year of growth at two CO₂ concentrations.

The experimental design was a split plot consisting of three treatments:

- two levels of CO₂: ambient (**A**) and elevated (**E**) (ambient + 350 μmol mol⁻¹)
- two levels of nutrition: a low (**L**) and a high (**H**) supply rate.
- two kinds of growth medium: sand and 'soil' (a peat based compost).

The six open-top chambers were sequentially allocated ambient or elevated CO₂ treatments, the main plot factor. A replication (block) consists of two open-top chambers, each chamber being considered as a main plot. Five replicates of each of the four nutrient \times medium treatments were randomly placed in each chamber (Figure 5.4).

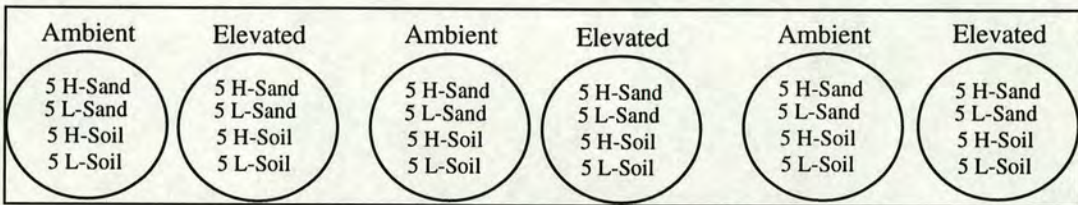


Figure 5.4 Experimental design of the glasshouse seedling Sitka spruce experiment.

5.8 Data analysis

All data were visually inspected using scatter plots, box plots and distributions (SAS Insight) any spurious values or outliers were investigated for errors in measurement, calculation or transcription and corrected where possible or removed if a valid reason was apparent, e.g. a sensor malfunction.

A split-plot ANOVA (Proc GLM, SAS) was used to determine the effects of the treatments on the dependant variables in the following chapters. Where interactions between treatments were significant a separate analysis was performed on each treatment.

5.9 Design of whole tree CO₂ flux measurement chamber

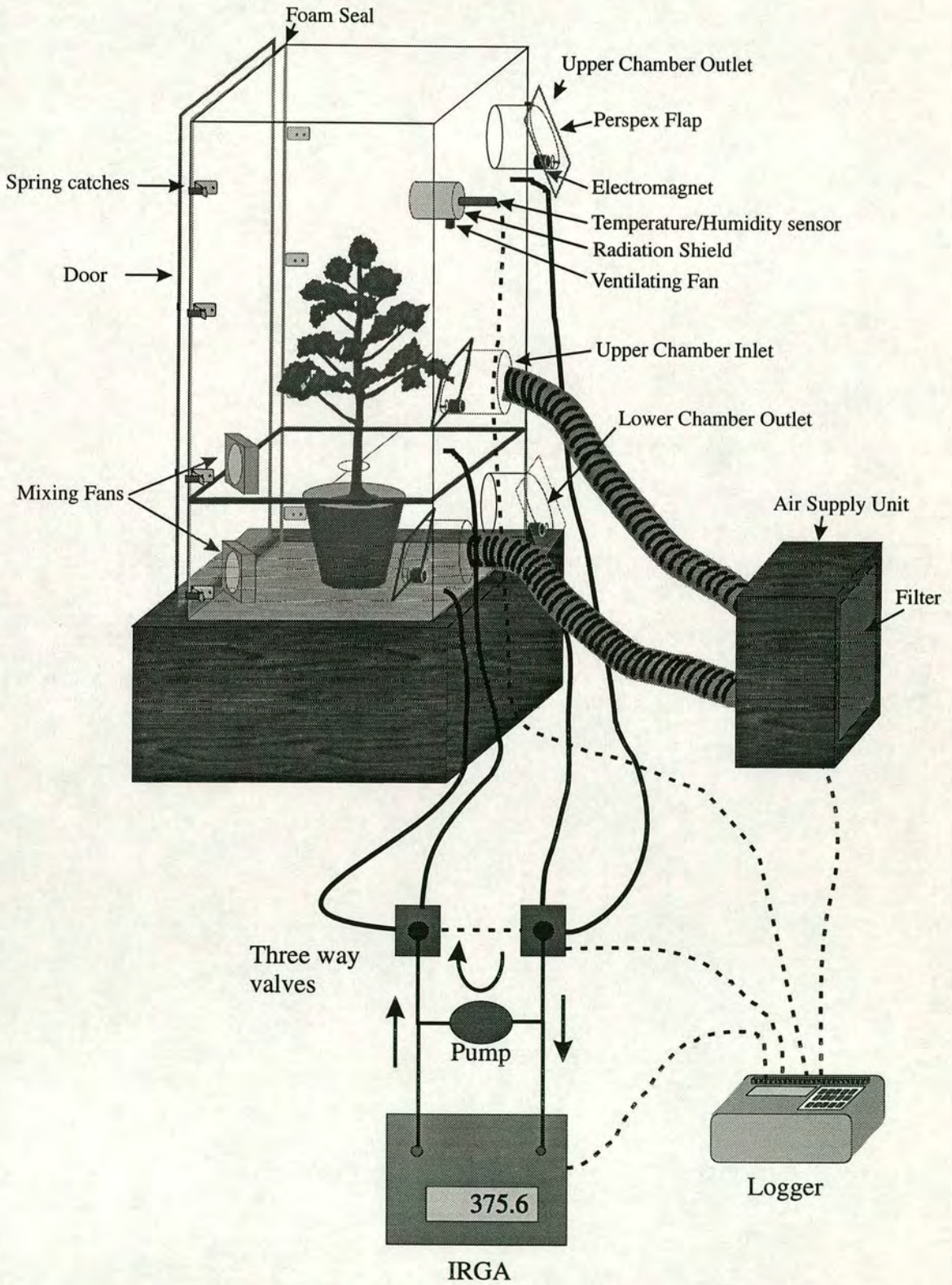
The aim was to be able to measure CO₂ fluxes from the above-ground and below-ground parts of trees independently during a 24 hour period at any CO₂ concentration while maintaining light and temperature as close as possible to the normal growth conditions. The approach adopted was a split chamber, separating shoot from root, which was normally ventilated but which could be closed airtight to make measurements of CO₂ flux using the transient method.

5.9.1 Design of the chamber

The chamber consisted of a rectangular box (108 cm tall, 42 cm wide and 48 cm deep) made from 10 mm thick acrylic sheet, welded together with solvent (Figure 5.5). One side was removable to facilitate access and when closed was held in place against a foam rubber sealing strip by eight spring clips. An acrylic sheet divided the chamber into upper and lower compartments, the lower 24 cm tall and upper 82 cm tall. The divider was in two halves, one fixed into the chamber and the other removable to allow the tree to be installed. A 7 cm circular hole between the two halves allowed the stem of the tree to pass from the lower to the upper compartment. Once a tree was in place the removable section of the divider was sealed in place with wide plastic self adhesive tape and an airtight seal made between the compartments by sticking a band of 'Blu Tac' around the tree stem just above the 'soil' surface, taping a sheet of polythene to it and the free edge of the polythene to the compartment divider.

The upper and lower compartments were ventilated by a fan blower (52BTXL, Airflow Developments Ltd., High Wycombe, UK) mounted in a wooden housing attached to the glasshouse wall. Fresh, cool air was drawn from outside the glasshouse through a filter and then passed through 5 cm diameter, flexible ducting to the compartment inlets. The inlets and outlets of the compartments were fitted with acrylic flaps hinged at the top which swung open permitting unhindered airflow while the fan was running. During a measurement cycle the flaps were held tightly closed against a foam seal by an electromagnet mounted on the chamber and armature mounted on the flap.

Whole tree CO₂ flux measurement system.



Air sampling tubes (6 mm DECABON 1300, Eaton Corporation, Samuel Moore operations, Ohio, USA) ran a distance of 4 m from the compartments to the measurement system in a nearby shed.

5.9.2 Environmental monitoring

Air temperature and humidity in the upper compartment were measured with a humidity/temperature probe (HMP35A, Vaisala (UK) Ltd., Cambridge, UK) mounted in a force-ventilated radiation shield. Needle temperature was measured with three fine-wire (0.13 mm) thermocouple junctions placed in contact with needles at different positions in the crown. A PAR sensor (Macam Photometrics Ltd., Livingston, UK) mounted on top of the chamber measured incident PPFD, while a platinum resistance thermometer pushed into the centre of the pot was used to measure 'soil' temperature. All of the sensors were monitored by a datalogger (21x, Campbell Scientific (UK) Ltd., Shephed, UK).

5.9.3 Flux measurement system

CO₂ fluxes in the compartments were determined by automatically closing and sealing a compartment then measuring the change of CO₂ concentration over time. Knowledge of the volume of the closed system enabled the calculation of the flux rate of each plant part s⁻¹. This could then be calculated on a mass or leaf area basis once the plant had been harvested (see 5.10.4).

To minimise response times and ensure adequate mixing, a pump circulated air at a high flow rate of 4 dm³ min⁻¹ through a loop of tubing from the compartment to the shed and back. Two three-way solenoid valves switched the sampling loop between the upper and lower chambers (see Figure 7.1). An infra-red gas analyser (IRGA)(Mk 225, Analytical Development Company Ltd., Hoddesdon, UK) subsampled from the loop at 300 cm³ min⁻¹ using its own internal pump. A mixing fan in each compartment ensured that the air was well stirred and that the foliage was well coupled to the compartment airmass.

Fluxes were measured twice per hour in both upper and lower compartments, at 0 and 30 minutes past the hour for the upper compartment and at 15 and 45 past each hour for the lower compartment.

A measurement cycle consisted of :

Time (mins)	Action
0	Turn off ventilation fan allowing flaps to drop closed.
0	Energise electromagnets of desired compartment to pull flaps shut.
0	Switch solenoid valves to desired compartment.
0	Turn on circulating pump to bring compartment air close to IRGA.
0.2	Turn ventilation fan on to continue ventilation of other compartment.
1	Start logging IRGA.
6	Stop logging IRGA
6	De-energise electromagnets to re-open compartment.

The logger recorded CO₂ concentration, leaf, soil and air temperature, PPFD and air humidity every 20 seconds during the 5 minute measurement cycle. The logger was also programmed to control the solenoid valves, pump, electromagnets and ventilation fan. While in open mode the CO₂ concentration within the chamber was manipulated by feeding pure CO₂ into the fan housing. The flow of CO₂ was controlled by a mass flow controller (FC260, Tylan General Corp., Torrance, CA) driven by the logger using a simple proportional algorithm. This gave adequate control of the concentration which was held either at 350 or 700 $\mu\text{mol mol}^{-1}$ during these measurements.

The IRGA was calibrated every day against one of two calibration cylinders either at 358 or 700 $\mu\text{mol mol}^{-1}$ depending on the current exposure concentration. The calibration cylinders were filled and calibrated against a set of gas mixing pumps (Wösthoff OHG, Bochum, Germany) at the beginning of the season.

5.10 Flux calculations and corrections

5.10.1 Leak correction

It is extremely difficult to built an absolutely leak tight system, especially when working with large concentration differences across chamber seals. However, provided the leak is small and proportional to the concentration gradient (*i.e.* a diffusive leak rather than a mass flow leak), it is possible to characterise it and compensate for it in measurements. The leak rate was determined frequently throughout the season by breathing into the empty chamber to raise the CO₂ concentration to around 700 $\mu\text{mol mol}^{-1}$ and then sealing the chamber and monitoring the rate of change of CO₂ concentration. The leak rate (L) could then be calculated as

$$L = \frac{\frac{\partial c}{\partial t}}{(C_c - C_a)} \quad (\text{s}^{-1}), \quad (5.1)$$

where $\frac{\partial c}{\partial t}$ is the rate of change of CO₂ concentration ($\mu\text{mol mol}^{-1} \text{s}^{-1}$) and C_c and C_a the CO₂ concentrations ($\mu\text{mol mol}^{-1}$) inside and outside the chamber respectively.

The measured rate of change of CO₂ concentration $\frac{\partial c_m}{\partial t}$ is then corrected for the leak as follows

$$\frac{\partial c}{\partial t} = \frac{\partial c_m}{\partial t} - L(C_c - C_a). \quad (5.2)$$

L was measured frequently for both upper and lower compartments and changed slightly throughout the season as minor abrasion and dirt altered the chamber seals. Typical values for L were between 0 and 0.003 s^{-1} ; values larger than this instigated a search for the cause, *e.g.* an insect trapped on a flap seal. As shown by equation 5.2, L had an effect when there was a concentration gradient across the seals and so was primarily a problem when measurements were made at $700 \mu\text{mol mol}^{-1}$.

5.10.2 H₂O flux corrections

Theoretically, by measuring the rate of change of humidity and temperature in the chamber it should be possible to calculate the transpiration rate and from that, plus the leaf temperature and knowledge of the boundary layer conductance to calculate the stomatal conductance. However, there are serious problems with using the transient technique to measure fluxes of water vapour, caused by absorption and adsorption/desorption of water from surfaces. Water vapour adsorbs to all materials to varying degrees. It adsorbs to surfaces in layers, the inner layers are often bound to the surface with great tenacity and may require quite high temperatures to be removed, while the outer layers exchange readily with air. It is therefore not surprising to find that the extent of water vapour sorption depends upon temperature and humidity, and is more of a problem at low temperatures. If a material is at equilibrium with moist air and the humidity is quickly decreased, the material surface will act as a source and water vapour will diffuse into the air until a new equilibrium is established: the opposite occurs if air humidity increases.. This exchange of water with chamber surfaces makes determining transpiration by measuring the rate of change of water content of the air mass inaccurate.

Commercial closed systems such as the LI-COR 1600 and 6200 avoid the problem of water sorption by attempting to maintain chamber humidity constant using the null balance method. Transpiration is calculated from the flow of moist air passing

through a desiccant required to hold the humidity constant, *i.e.* if absolute humidity is constant then the transpiration is equal to the water trapped by the desiccant. In most cases it is not possible to hold the humidity completely constant and the humidity may gradually rise (or fall) so that an empirical correction factor (called K_{abs} by LI-COR) is applied to this small component of the flux to account for the sorption properties of the chamber (see Appendix E). In null balance systems K_{abs} is only applied to the small transient component of the total flux and so errors are relatively small. However, in a fully transient system, such as this, the errors can be significant and a degree of caution must be exercised when interpreting the results.

One solution would have been to convert the system to a null balance system, however, this idea was rejected, because it would have required an accurately measured and actively controlled flow through a desiccant tube of up to $20 \text{ dm}^3 \text{ min}^{-1}$, consuming large amounts of desiccant and requiring time to perfect a control algorithm capable of maintaining a constant chamber humidity under changing environmental conditions.

5.10.3 Determination of K_{abs} for the chamber

The sorption characteristics of a chamber largely depend on the materials used in construction. LI-COR uses transparent teflon tape and 'Propafilm C' (ICI, UK) in their chambers, as these have been found to have good properties with respect to water vapour sorption, CO_2 exchange and radiation transmission. The chamber used in this experiment was constructed from acrylic, a material that LI-COR recommends against because of its inferior water vapour exchange characteristics. However, as acrylic is cheap, easily available and easily worked and since the main function of the chamber was to measure CO_2 fluxes and not water fluxes, problems with water vapour were not a major consideration in the design. But, since humidity was being measured as an environmental variable anyway, and there was the possibility to use the data for the calculation of transpiration and stomatal conductance, it was desirable to have some idea of the potential errors in the measurement of $\delta e/\delta t$ and therefore K_{abs} was measured for the upper compartment of the chamber.

A mass flow controller and 500 cm^3 desiccant tube containing magnesium perchlorate were added in series with the circulating pump. Then the chamber humidity and temperature were recorded as a known flow rate of air passed through the desiccant. K_{abs} was then calculated as in Appendix E. This procedure was repeated a number of times and gave values for K_{abs} in the range 1.23 to 1.6, indicating that any measurement of $\delta e/\delta t$ may be underestimated by between 20 and

40 % and so it was inadvisable to use the humidity data for calculating accurate absolute transpiration rates or stomatal conductances. However, it may still be valid to make broad comparisons between treatments as differences in transpiration rates should still be detectable even if not accurately quantifiable.

5.10.4 Calculation of CO₂ and H₂O fluxes.

CO₂ concentrations and relative humidity were recorded every 20 seconds during each 5 minute measurement cycle giving 15 data points with which to calculate $\delta c/\delta t$ and $\delta e/\delta t$. The raw data from the logger was imported into SAS (SAS institute Inc., Cary, NC, USA) and a program used to split the data into individual measurement cycles and calculate the fluxes of CO₂ and H₂O.

The equations used were as follows:

Saturation vapour pressure $e_s(T)$ at temperature T °C was calculated using the equation from Buck (1981):

$$e_s(T) = 0.6137553 \cdot \exp\left(\frac{T \cdot \left(18.564 - \frac{T}{254.4}\right)}{(T + 255.57)}\right) \text{ (kPa)} \quad (5.3)$$

Vapour pressure of the air e_a

$$e_a = e_s(T_a) \cdot \frac{H}{100} \text{ (kPa)} \quad (5.4)$$

Mole fraction w_a

$$w_a = \frac{e_a}{P} \text{ (mol mol}^{-1}\text{)} \quad (5.5)$$

where P is the atmospheric pressure in kPa (in this case 101.3 kPa was assumed) H is the relative humidity as a percentage.

Regression analysis (SAS PROC REG) was used to determine both $\delta c/\delta t$ and $\delta w_a/\delta t$ for each 5 minute measurement period. The mean values for air temperature (T_a), soil temperature (T_s), leaf temperature (T_l), compartment CO₂ concentration (C_c) and PPFD during the 5 minute interval were also calculated.

Transpiration (E) was calculated as follows

$$E = \frac{\partial w_a}{\partial t} \cdot \frac{PV}{R(T_a + 273)} \cdot 1000 \text{ (mmol s}^{-1}\text{)} \quad (5.6)$$

where V is the volume of the compartment plus tubes and analyser (158 dm³ for upper and 42 dm³ for the lower) and R is the universal gas constant.

Ambient CO₂ concentrations (C_a) recorded by the glasshouse CO₂ control system were merged with the flux measurement data in order to calculate the concentration gradient across the chamber seals. Corrections were applied to the measured $\delta c_m / \delta t$ using the most recently measured value of L (the leak rate) for each of the upper and lower compartments calculated by equation 5.2 .

The CO₂ flux (F) was then determined by

$$F = \frac{\partial c}{\partial t} \cdot \frac{PV}{R(T_a + 273)} \text{ (}\mu\text{mol s}^{-1}\text{)} \quad (5.7)$$

CHAPTER 6

Growth and Allocation

6.1 Introduction

A central question is: do CO₂-enriched plants merely grow faster and therefore become larger or does the nature of plant growth itself change (Farrar & Williams, 1991)? Assuming a plant maintains a constant C:N ratio, a reasonable assumption if we ignore non-structural compounds, then growth requires a constant balance between carbon and nutrient uptake. Carbon uptake depends on the amount of leaf and the photosynthetic rate per unit leaf mass, while nutrient uptake depends on the surface area of root and its specific uptake. By increasing the specific uptake of either the foliage or the root system the balance will be disturbed and either the root to shoot ratio or the specific uptake of the other component will need to adjust to bring the plant back into balance.

This simple model of resource allocation can be formalised as follows:

The relative growth rate of the plant can be written in terms of both carbon and nitrogen,

$$R_{GC} = \frac{F_s}{C} \frac{\partial S_C}{\partial t} - \frac{F_s}{C} \frac{\partial L_s}{\partial t} - \frac{(1-F_s)}{C} \frac{\partial L_r}{\partial t} \quad (\text{g plant g}^{-1} \text{ plant day}^{-1})$$

and
$$R_{GN} = \frac{F_r}{N} \frac{\partial S_N}{\partial t} \quad (\text{g plant g}^{-1} \text{ plant day}^{-1}).$$

W_s and W_r = mass of shoot and root, respectively (g),

F_s = shoot fraction $\frac{W_s}{W_s+W_r}$,

F_r = root fraction $\frac{W_r}{W_s+W_r}$ or $(1-F_s)$, and F_r/F_s = root mass / shoot mass ratio,

C = carbon concentration of the plant (g carbon g⁻¹ plant),

N = nitrogen concentration of the plant (g nitrogen g⁻¹ plant),

- S_C = specific uptake of carbon by the shoot (g carbon g^{-1} shoot),
 S_N = specific uptake of nitrogen by the root (g nitrogen g^{-1} root),
 L_s = specific loss of carbon from the shoot (g carbon g^{-1} shoot),
 L_r = specific loss of carbon from the root (g carbon g^{-1} shoot),
 t = time (day),

(Nitrogen is used here to represent a balanced uptake of all required nutrients.)

The relative growth rate and root and shoot fractions are then determined by the intersection of the two growth functions shown graphically in Figure 6.1. From this we can deduce a number of things, a) an increase in the efficiency of the shoot (S_C) will lead to an increase in R_G and a shift in allocation towards the root, b) an increase in the efficiency of the root will lead to an increase in R_G and a shift in allocation to the shoot, c) an increase root and shoot efficiency may leave allocation unchanged but will increase R_G , d) an increase in C:N ratio of the plant will correlate with a shift of allocation to shoot and the effect on R_G will depend on the values of C and N .

An increase in the specific rate of loss of carbon, *i.e.* the specific respiration rate of the shoot or root, will lead to a drop in R_G and an increase in the shoot fraction (Figure 6.1b).

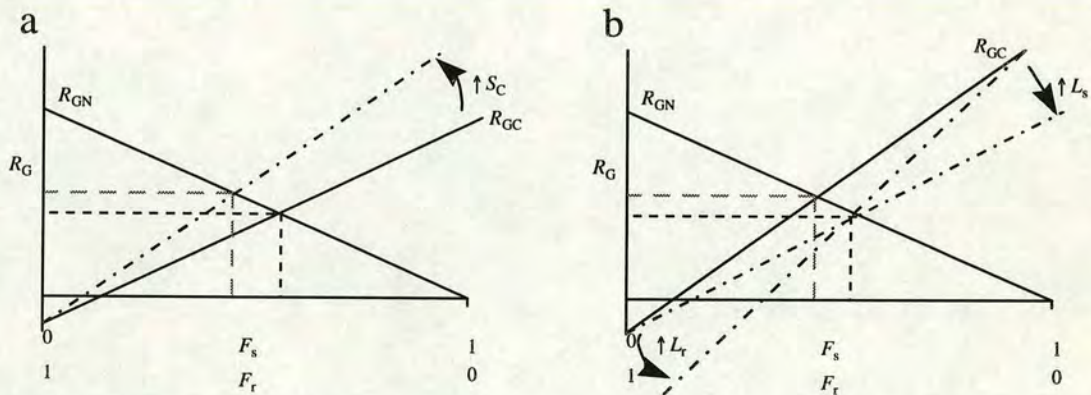


Figure 6.1 Diagram showing the relationship between relative growth rate (R_G) and allocation. The two solid lines are the functions relating R_G to carbon and nitrogen uptake. The point of intersection determines the root and shoot fractions (F_r , F_s) and the R_G . The dotted broken line in (a) shows the effect of increasing the specific carbon uptake of the shoot, S_C , and shows that the shoot fraction, F_s , decreases and R_G increases. The dotted broken lines in (b) show the effect of increasing L_s or L_r . In both cases R_G falls and F_s increases.

So in order to maximise growth, optimisation theory suggests that a plant should allocate resources between the foliage and roots, and the optimal balance between

size of the shoot and root will depend on the efficiency of root or shoot at its task. Carbon assimilation strongly depends on the amount of light absorbed and a plant will attempt to distribute its foliage in such a way as to maximise light absorbed. Likewise, nutrient uptake requires a well distributed network of fine roots actively exploiting the rooting volume. In the case of the shoot where light and CO_2 are the two main requirements for carbon assimilation, the plant may need to gain height to outgrow neighbours and so maximise light absorbed per unit leaf area and thus maximise S_C .

Plants growing in elevated $[\text{CO}_2]$ tend to have higher rates of photosynthesis than plants in ambient $[\text{CO}_2]$ even after any acclimation has occurred (see review by Luxmoore *et al.*, 1993). Therefore, to balance photosynthate production with nutrient uptake it has been suggested that plants growing in elevated $[\text{CO}_2]$ will allocate more carbon to the root system to increase root mass (e.g. Bazzaz, 1990; Rogers *et al.*, 1992), to increase mycorrhizal mass and to fuel a higher metabolic rate, thereby enhancing nutrient uptake both by the roots themselves and by mycorrhizas, but also by soil microbes via root exudates. The implications are that for trees growing in elevated $[\text{CO}_2]$ to grow more quickly they need a more rapid uptake of nutrients, to balance the increased uptake of carbon. This can be achieved in several ways: (a) by increasing the absorbing surface either by increasing the volume of soil being explored or by increasing the fine-root density within the same volume, *i.e.* by increasing F_r , (b) by increasing the specific uptake of the root system, including mycorrhizas and soil microbes, *i.e.* by increasing S_N , or (c) by increasing the rate of exploration of the rooting volume by increasing the rate of fine-root turnover so maintaining the same size of living root system but increasing fine-root production and mortality in tandem. This last method minimises the cost of maintaining a large root system while still permitting exploration of the rooting volume, and thus it also increases S_N ; however, the increase in efficiency of the live root system must be offset by the cost of producing new roots. The method adopted by the plant will depend on soil type and the particular nutrient that is most limiting; e.g. phosphate does not move through the soil, and roots must, therefore, grow to 'look' for it. There may also be genetic constraints limiting the method a tree can use to increase nutrient uptake. The degree to which each of the methods above is utilised will influence mineralisation rates, CO_2 efflux from the soil and the organic matter content of the soil.

This simple model of allocation would suggest that, given easy access to nutrients, allocation will move in favour of foliage development, while increased

photosynthetic efficiency of leaves, resulting from elevated atmospheric CO₂ concentrations, would lead to allocation towards roots. However, there are other constraints to be considered. Both fine-roots and leaves require structural support from coarse-roots and branches, respectively, which are also needed to facilitate transport of photosynthate and nutrients. Furthermore, roots serve to anchor the plant to the ground and so no matter how easily nutrients are available there must be some minimum root system. There may also be hydraulic constraints determining the balance between root, shoot and stem. Increased leaf area will increase transpiration and if the root system is insufficient to collect the water or the stem does not have the vessels to transport it then the leaves will become water stressed. Episodic events such as drought and storms may have played a role in the evolutionary development of the species; this will be especially true of long-lived species where individuals are likely to experience such events at least once whilst immature and must be able to survive in order to reach reproductive age. Furthermore, optimisation in order to maximise growth may only be true while the plant is immature, since once it reaches reproductive age the goal of optimisation will include reproductive capacity.

This chapter presents the growth and allocation data from seedling trees growing at two nutrient supply rates and two CO₂ concentrations, while Chapters 7 and 8 deal with changes to the efficiency of photosynthesis and nutrient acquisition.

6.2 Height and diameter increase over time

As described in Chapter 5, the experiment consisted of trees growing in either potting compost (referred to from here on as soil) or in sand at two CO₂ concentrations ambient, **A**, or 700 $\mu\text{mol mol}^{-1}$, **E**, and with two nutrient supply rates, high, **H**, and low, **L**. The main interest was in the effects and interaction of [CO₂] and nutrient supply on growth and allocation, with a secondary interest in the influence of the growing medium.

Sitka spruce trees have 'determinate growth', *i.e.* the number of needles on each shoot is determined by the number of primordia pre-formed in the bud during the previous summer. When the bud flushes in spring cell division and expansion cause the shoot and needles to extend, spreading the foliage to catch light (Baxter & Cannell, 1977). Shoot extension is partly determined by environmental conditions at the time of expansion, especially temperature and light (Ford *et al.*, 1987). Cells within the shoot tend to be the same length and thus it is the number of cells that determines the final length of the shoot rather than differences in cell expansion (Baxter & Cannell, 1977). The new bud forms while the shoot is extending (Cannell

& Willett, 1975). This method of growth is rather restrictive as the number of needles is fixed when the bud is formed and increasing shoot length simply spaces the needles further apart. However, young spruce trees can also produce a second flush known as 'lammas' growth whereby the apical and some dormant lateral buds flush and continue growing until September or October, thus allowing the young tree to maximise its growth potential during favourable conditions.

6.2.1 Increase in tree height

The height of the trees was measured from the soil surface to the tip of the apical bud approximately every two weeks from bud burst (4 April) until height growth stopped (~4 September, day 247) and also whenever trees were harvested (Figure 6.2). As some trees were harvested during the measurement period the number of replicates decreased from the initial 15 to 5 by the 1st of December.

Trees in the **H** treatment had strong lammas growth beginning around day 200 but very few of the **L** trees produced lammas growth. Differences in height between nutrient treatments started to occur around day 140 in the sand-grown trees but slightly later, day 160, in the soil grown trees. In the case of the soil trees the height differences were a result of the lammas growth, but in the sand trees the differences started to develop before the lammas flush and may be a result of changes to shoot expansion. The buds had been formed during the previous summer and so the number of needle primordia would be expected to be the same for sand and soil and **H** and **L** treatments within **A** and **E** treatments (which the seedlings had been exposed to in their first year). Therefore any differences in the extension of the first flush in response to nutrient or growth medium implies a change to the inter-needle expansion of the shoot. Normally this depends on the temperature and water potential of the shoot during expansion, but nutrient availability also affected expansion in the sand-grown trees. The nutrient effect seen in the sand-grown trees, but not in the soil-grown trees, can be attributed to the fact that all of the original soil was washed from the roots of the sand trees when they were re-potted at the beginning of the experiment, whereas the soil trees kept their original soil ball which probably contained some residual nutrients.

Comparisons of the final leader extension were made on data from day 247, 4/9/95 (Figure 6.3) rather than on the final harvest data, as height growth had stopped at that time and the number of replicates was nine rather than five permitting a more powerful statistical analysis.

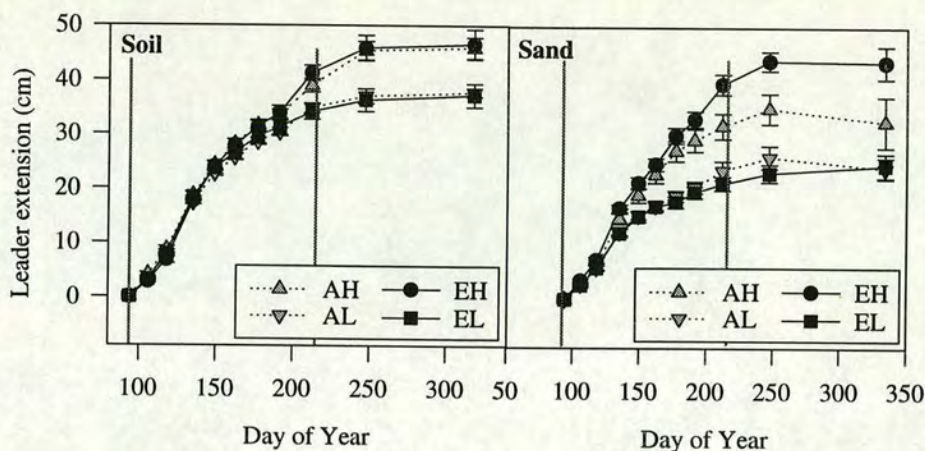


Figure 6.2 Leader extension for trees grown in soil and sand culture at two [CO₂] and two nutrient supply rates. Means ± 1 SEM *n* = 5-15. Vertical line indicate the period during which nutrients were applied.

There were significant differences between trees grown in the two mediums and also differences in response to the CO₂ treatment depending on the growth medium. Trees grown at the **H** nutrient supply rate always outgrew those with the **L** supply rate (Figure 6.3). When grown in sand, height growth was enhanced by elevated CO₂ at the **H** nutrient supply rate but, if anything, diminished in the **L** nutrient treatment, *i.e.* there was a significant nutrient x [CO₂] interaction ($P < 0.02$). The soil-grown trees showed a slightly different pattern in that **H** trees were significantly taller than **L** trees ($P < 0.0001$) but [CO₂] had no effect, and there was no [CO₂] x nutrient interaction.

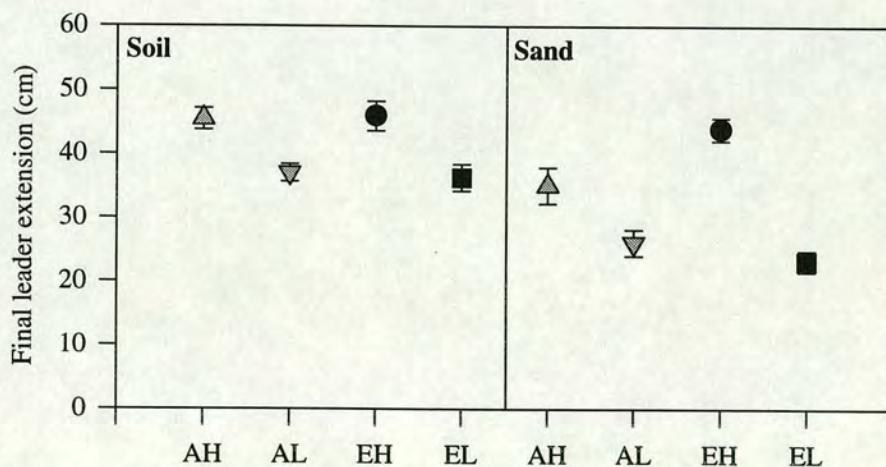


Figure 6.3 Final leader extensions at 4/9/95 for trees grown in soil and sand at two [CO₂] and two nutrient supply rates. Mean ± 1 SEM, *n* = 9.

Growth in sand compared to soil reduced the height of all but the **EH** trees, possibly as a consequence of the limited nutrient and water holding capacity of the sand compared to the soil; however, this doesn't explain why the **EH** trees were not affected.

6.2.2 Increase in diameter

Stem basal diameters were measured on four occasions through the season using a digital calliper. The diameter was taken to be the mean of two orthogonal measurements made at the base of the stem and the diameter increment was calculated as the current diameter minus the initial diameter measured on the 4th April (day 94). Diameters were also measured when trees were harvested.

Diameters increased throughout the season, slowing down after day 250. Diameter increment was increased by both elevated $[CO_2]$ and high nutrient supply, and this was especially apparent in the soil-grown trees (Figure 6.4). The **EL** trees growing in sand started to show a CO_2 effect later than the **EL** trees growing in soil, but they stopped growing around day 250 and the CO_2 effect had almost disappeared by day 335. The final point on the graphs is derived from harvest data where the number of replicates was five, partly explaining the increase in variation.

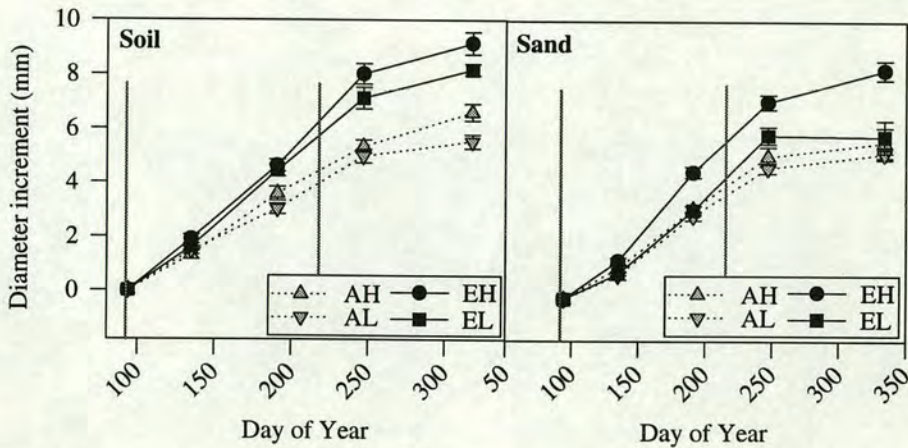


Figure 6.4 Increase in stem diameter at soil surface over the season for trees grown in soil or sand at two $[CO_2]$ and two nutrient supply rates. Means \pm 1 SEM, $n = 5-15$.

As with the height growth, analysis of variance of the final diameter increments showed differences between growth medium, nutrient and $[CO_2]$. Diameter growth in the soil-grown trees was significantly increased by both nutrient ($P < 0.008$) and $[CO_2]$ ($P < 0.002$), the largest response being to $[CO_2]$. A similar response occurred in the sand-grown trees, apart from the **EL** trees; as they had stopped growing earlier, there was a significant $[CO_2]$ x nutrient interaction.

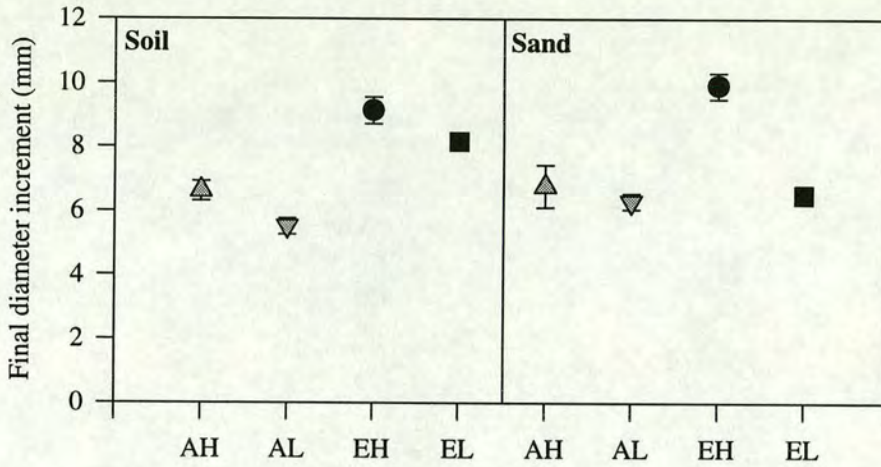


Figure 6.5 Final diameter increment measured on 15/11/95 soil, $n = 9$ and 1/12/95 sand $n = 5$. Means \pm 1 SEM.

6.3 Harvest data

6.3.1 Method

An initial harvest of 10 trees from each of the two original CO₂ treatments was made in April to obtain baseline data. Then a further five harvests were made through the season to obtain data on the mass of the tree parts as the season progressed. Three harvests of the sand-grown and two of the soil-grown trees were made (see Table 6.1).

Table 6.1 Dates of harvests and numbers of trees harvested.

Harvest	Date	Day of year	Growth medium	Number harvested per treatment (CO ₂ & N)
1	3/4/95	93	Pre-experiment	20
2	6/7/95	187	Sand	4
3	14/8/95	226	Soil	6
4	28/9/95	271	Sand	6
5	15/11/95	319	Soil	9
6	1/12/95	335	Sand	5

At each harvest the tree height and basal diameter were measured, then the tree was dissected into lammas, first flush and one year old (C+1) shoots. At harvests 2, 3 and 4 it was easy to distinguish lammas growth from the earlier first flush and so the lammas growth was separated from the first flush growth and numbers of shoots and dry mass determined separately. However, by harvests 5 and 6 the obvious difference

between the first and second flushes had disappeared and so material from both flushes was combined as ‘current’ growth.

The root system was washed and then the roots and shoots oven dried at 70 °C for 48 hours. The needles were separated from the stems and the root system separated into stump and fine roots (< 2mm) and then dry mass was measured for each tree part.

6.3.2 Number of shoots

At the beginning of the experiment the trees were one year old, having been exposed to the CO₂ treatment from seed; thus one might expect a [CO₂] effect on the number of C+1 shoots. However, one would hope not to find any initial nutrient treatment differences in the number of C+1 shoots, as this would indicate poor randomisation. Indeed, there was a small, but not significant, CO₂ effect with more shoots in **E** than in **A** (Figure 6.6, C+1).

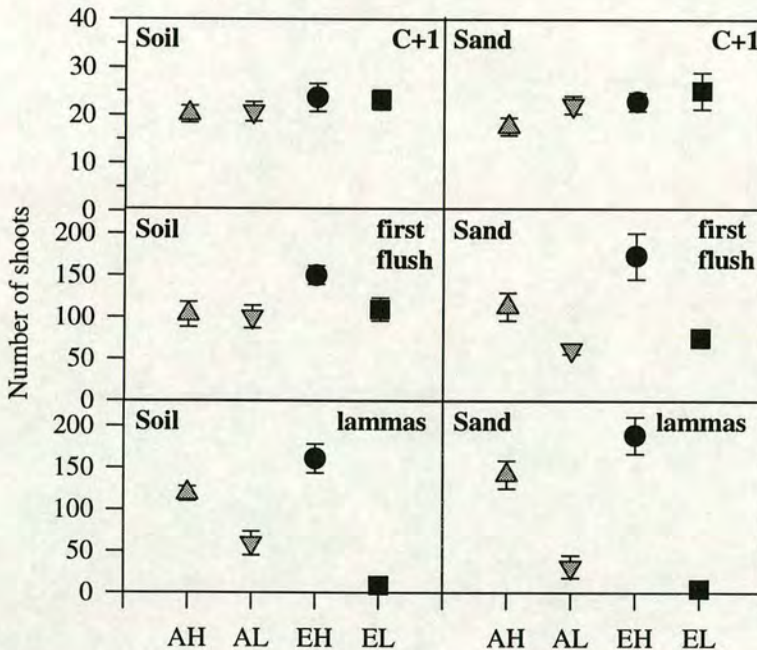


Figure 6.6 Number of C+1, first flush and lammas shoots at harvests 3 and 4, soil and sand, respectively. Means ± 1 SEM, n = 6.

The roots were actively growing at the beginning of the experiment when the nutrient treatment was first applied and so by the time the first flush occurred there could have been some differences in plant nutrient status which may have influenced the numbers of buds that burst in the first flush. There was no significant effect of [CO₂] or nutrient supply on the numbers of shoots in the first flush of soil-grown trees. However, both [CO₂] (*P* < 0.02) and nutrient supply (*P* < 0.001) increased the number shoots in the first flush of sand-grown (Figure 6.6 first flush). The nutrient

effect seen in the sand-grown trees, but not in the soil-grown trees, can be attributed to the fact that all of the original soil was washed from the roots of the sand trees when they were re-potted at the beginning of the experiment, whereas the soil trees kept their original soil ball which probably contained some residual nutrients.

The effect of nutrient supply and [CO₂] on the number of lammas shoots was the same for trees grown in both soil and sand (Figure 6.6 lammas). There was a significant increase in the number of lammas shoots in the **H** treatment ($P < 0.0001$) and a significant nutrient x [CO₂] interaction ($P < 0.02$), with [CO₂] increasing the number of shoots on trees with **H** nutrition but decreasing the number on trees with **L** nutrition. **EL** trees hardly produced any lammas growth while **EH** produced some 200 shoots per tree.

Another way to determine if either of the treatments affected the number of active growing points (shoots) is to look at the ratio of the number of lammas shoots to number of first flush shoots (Figure 6.7). A ratio of 1 indicates that on average all apical buds flushed during the lammas flush, while a value < 1 indicates some buds did not re-flush and > 1 indicates that some previously dormant buds also flushed, increasing the overall number of active meristems.

The growing medium had no effect on the fraction of shoots which re-flushed but there were significant effects caused by both nutrient supply ($P < 0.0001$) and [CO₂] ($P < 0.04$). The fraction of shoots which re-flushed was increased by **H**, and as both **AH** and **EH** had ratios >1 additional dormant buds must have flushed. Secondary flushing was restricted by **L** nutrient supply with only 50% of **AL** but almost no **EL** buds re-flushing. At **H** nutrient supply elevated [CO₂] caused a slight decrease in the numbers of buds re-flushing but in **L** nutrient trees elevated [CO₂] almost completely obviated re-flushing.

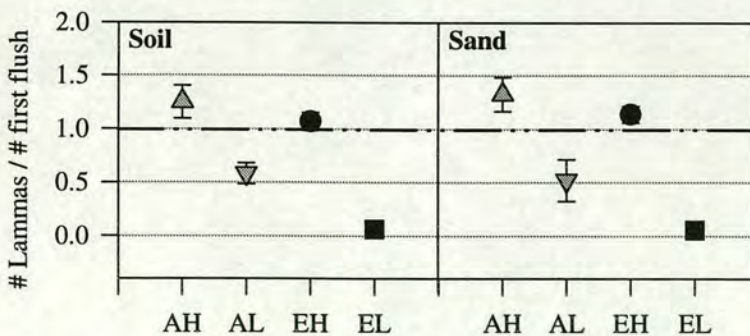


Figure 6.7 The number of lammas shoots / number of first flush shoots at harvests 3 and 4 for soil and sand, respectively. Means ± 1 SEM, $n = 5-9$. Values < 1 indicate that some shoots stopped growing while values > 1 indicate flushing of previously dormant buds.

Figure 6.8 shows the number of current year shoots at the final harvests for the two growth mediums. The analysis of variance showed that for trees grown in soil the effect of $[\text{CO}_2]$ was not significant but the effect of nutrient supply was ($P < 0.003$). Whereas for trees grown in sand $[\text{CO}_2]$ almost had a significant effect ($P < 0.08$) and nutrient supply had a significant effect ($P < 0.0002$) on the number of shoots. The number of shoots was always increased in trees with **H** nutrient supply through the stimulation of lamas growth. Growth in elevated $[\text{CO}_2]$ in sand also increased shoot production.

The difference between the nutrient treatments was much larger in trees grown in sand than in soil; in sand **H** had approximately 2.4 times as many shoots as **L** while in soil the increase was only 1.5 times. This was caused by fewer shoots on sand-grown trees with **L** nutrient supply and more shoots on trees with **H** nutrient supply than on the soil-grown trees.

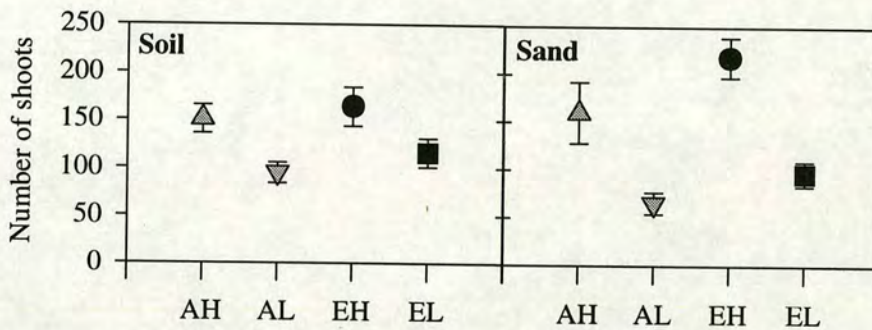


Figure 6.8 Number of shoots at the final harvest. 15/11 and 1/12 for soil and sand respectively. Means \pm 1 SEM, $n = 5-9$.

To summarise, both $[\text{CO}_2]$ and nutrient supply stimulated bud burst in the first flush and high nutrient supply stimulated a second flush in which additional, previously dormant buds burst, especially on the **A** trees. Lammas growth occurred on all shoots in the **AH** and **EH** treatment, 50 % of shoots in the **AL** treatment but on almost no shoots of the **EL** treatment.

6.3.3 Dry mass of trees

Trees increased in dry mass throughout the season and **E** trees were still increasing between mid-September and November. The **H** nutrient trees showed a rapid increase in mass between day 187 and 271 whereas the **L** trees continued growing at a steady pace up to day 271 (Figure 6.9), this corresponds with the pattern of lammas growth.

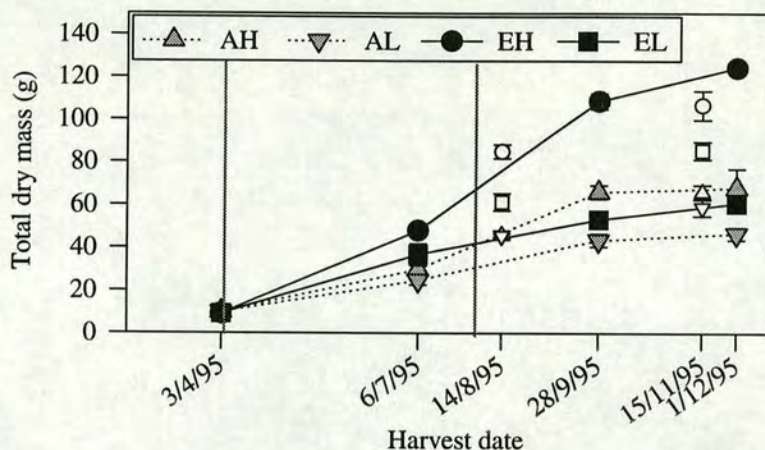


Figure 6.9 Total dry mass of trees at the six harvest dates. Sand-grown trees are filled symbols joined by lines while soil-grown trees are empty symbols overlaid. Means \pm 1 SEM, $n = 4-9$. The vertical lines indicate the period during which nutrients were applied.

An analysis of variance of the final harvest data showed that both $[CO_2]$ ($P < 0.001$) and nutrient treatments ($P < 0.01$) had significant effects on the final mass of both soil-grown and sand-grown trees and that there was a significant $[CO_2]$ by nutrient interaction ($P < 0.003$) in the sand-grown trees (Figure 6.10). The **EL** trees growing in sand failed to grow as well as those in soil, but the **EH** trees growing in sand did better than those in soil, so it seems that the growth medium influenced the response to CO_2 .

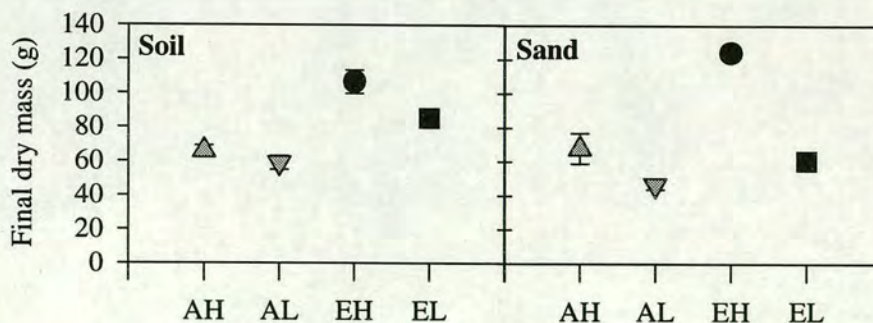


Figure 6.10 Total dry mass at final harvest 15/11 and 1/12 for soil and sand respectively. Means \pm 1 SEM, $n = 4-9$.

The relative growth rate of the trees (R_G) can be obtained from the slope of the relationship between $\ln(\text{dry mass})$ and time (Figure 6.11) and calculated as

$$R_G = \frac{\ln(W_2) - \ln(W_1)}{t_2 - t_1}$$

where W_1 and W_2 are the dry masses of the tree at times t_1 and t_2 , respectively.

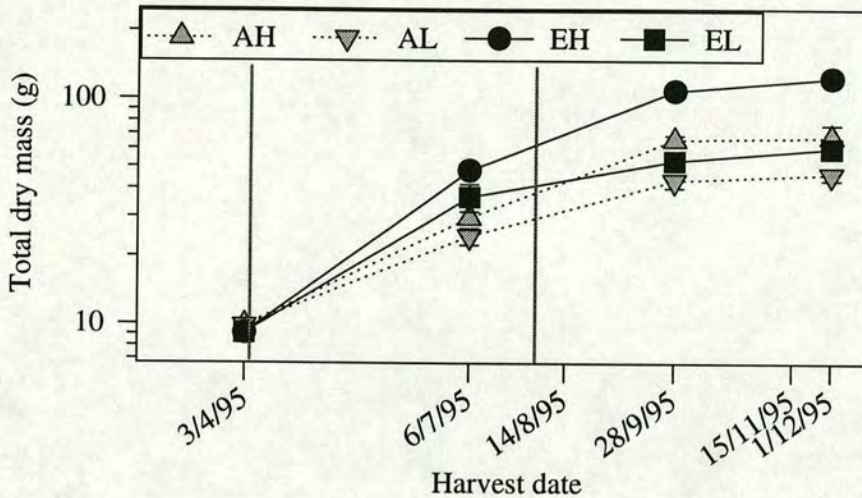


Figure 6.11 Total dry mass on a logarithmic scale for sand-grown trees at each harvest date. Means ± 1 SEM, $n = 4-9$.

Relative growth rates declined over the season in all treatments. Between April and July R_G was increased by 50% in elevated $[\text{CO}_2]$ and 20% by high nutrient supply rates (Table 6.2). Between July and September R_G of **H** trees were higher than those of **L** trees and $[\text{CO}_2]$ had less influence at **H** nutrient supply. Between September and December $[\text{CO}_2]$ again influenced R_G more than nutrient supply.

Table 6.2 Relative growth rates ($\text{mg g}^{-1} \text{day}^{-1}$) between each of the harvest dates for the sand-grown trees.

Treatment	3/4/95-6/7/95 93-187	6/7/95-28/9/95 187-271	28/9/95-1/12/95 271-335
AH	12	9.5	0.4
AL	10	6.8	1.1
EH	18	9.7	2.1
EL	15	4.6	2.1

6.4 Allocation patterns.

By the final harvests trees grown with **H** nutrient supply were roughly the same size in both sand and soil, apart from slightly larger roots in the sand grown trees (Figure 6.12). Trees grown at **L** nutrient supply rate in sand were significantly smaller than those grown in soil. Differences in the mass of above-ground and below-ground parts between treatments was more pronounced in sand grown trees.

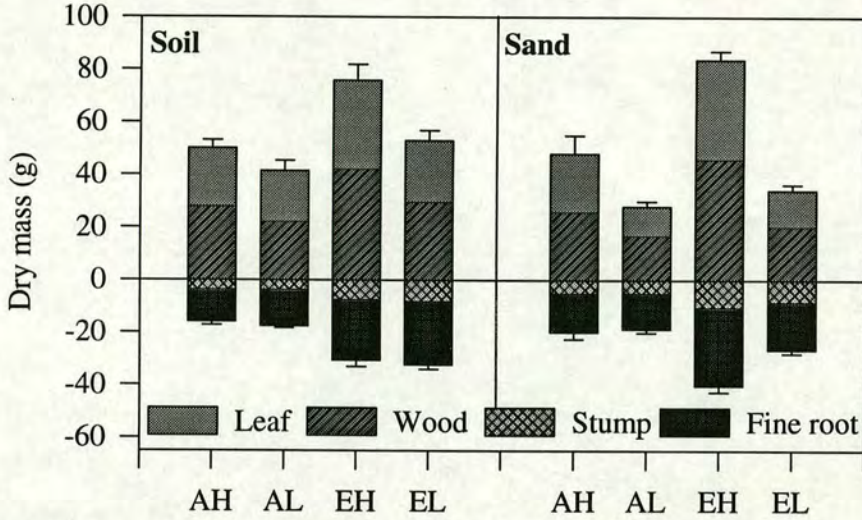


Figure 6.12 Dry mass of trees at final harvest showing amounts of leaf, wood, stump and fine root. Means \pm 1 SEM, $n = 5-9$.

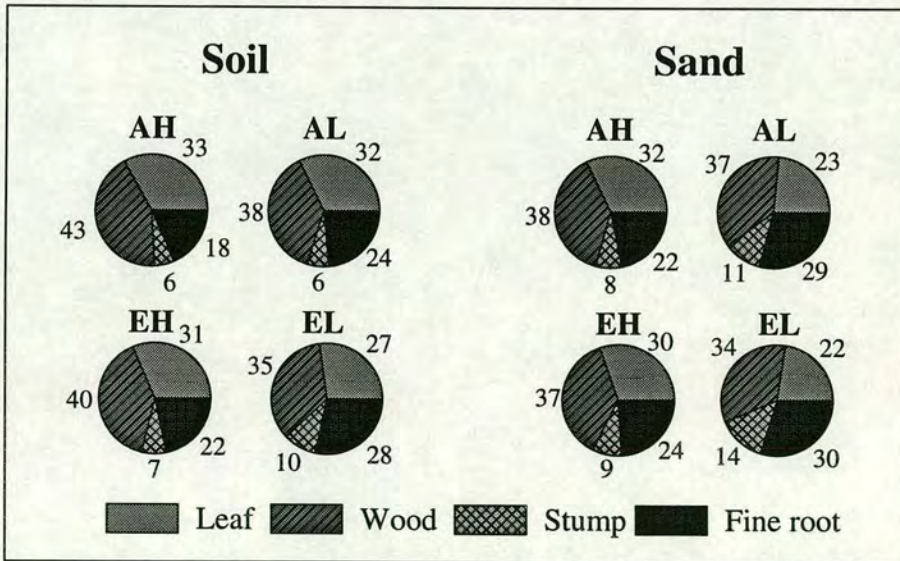


Figure 6.13 Pie charts showing percentage of dry mass in each of the four plant components. From trees at the final harvests For soil $n = 9$ and for sand $n = 5$.

Figure 6.13 shows the same data as percentages of the total dry mass giving an indication of the allocation of mass between the components of the trees. Comparing horizontally between **H** and **L** highlights an increase in the proportion of root in trees grown with **L** nutrient supply. While vertical comparisons between **E** and **A** also show a slight increase in the proportion of root. These results are discussed in more detail further on.

6.4.1 Leaf mass fraction

Trees grown with high nutrient supply rates had a larger fraction of dry mass allocated to leaves than those grown at low supply rate, and those grown at elevated CO_2 had slightly less mass allocated to leaves than those grown in ambient CO_2 (Figure 6.14). The analysis of variance of the leaf mass fraction (dry mass of needles / total dry mass of tree) at the final harvest showed a significant effect of nutrient supply which was stronger and more significant in the sand-grown trees ($P < 0.0001$) than in those grown in soil ($P < 0.01$). The $[\text{CO}_2]$ effect was not significant in either sand or soil trees.

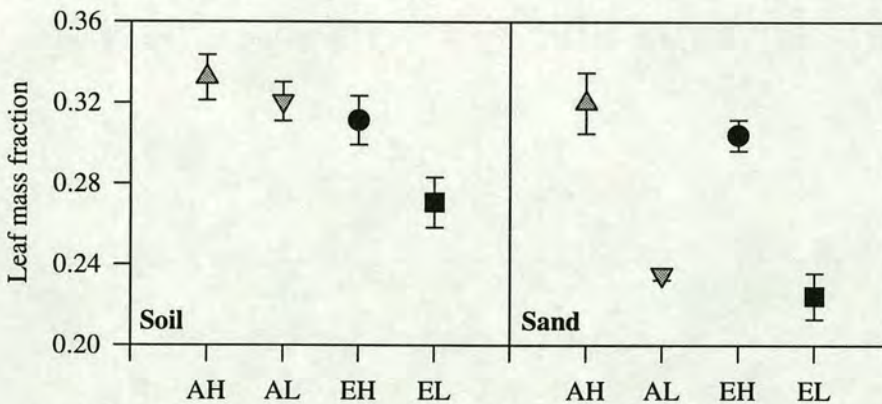


Figure 6.14 Leaf mass fraction (leaf dry mass / total dry mass) at the final harvest for trees grown in soil or sand. Means \pm 1 SEM, $n = 5-9$.

6.4.2 Root mass fraction

At the initial baseline harvest **E** trees had slightly larger root mass fractions (dry mass of root / total dry mass of tree) than **A** trees ($P < 0.1$). From this initial position, root fractions of **H** trees declined slightly then rose towards the final harvest, while those of **L** trees rose throughout the experiment, especially in the sand-grown trees.

An analysis of variance of the root fractions at the final harvests showed significant effects of the growth medium ($P < 0.0001$), $[\text{CO}_2]$ ($P < 0.04$) and nutrient supply (P

< 0.0001). There was an increase in the amount of root growth relative to shoot growth in response to sand, L nutrient supply and E [CO₂] (Figure 6.16). These results are consistent with the idea that when nutrients are limiting relative to assimilates, roots grow more than shoots until there is a balance in the supply of the two substrates for growth.

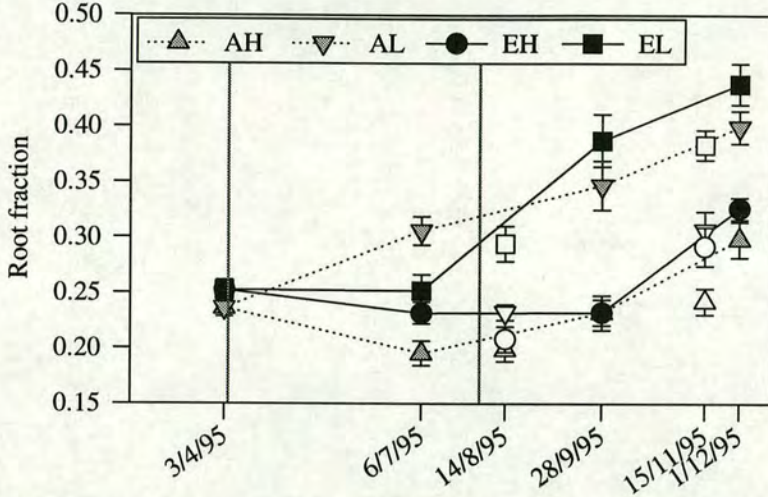


Figure 6.15 Root mass fraction (root dry mass/ total dry mass) at the six harvests. Sand-grown treatments are filled symbols joined by lines while soil grown are empty symbols overlaid. Means \pm 1 SEM, $n = 4-9$. The vertical lines indicate the period during which nutrients were applied.

The higher root fractions in trees grown in sand relative to those grown in soil could be the result of poorer nutrient holding capacity of the sand, poorer water holding capacity, pH or physical properties causing abrasion of root tips.

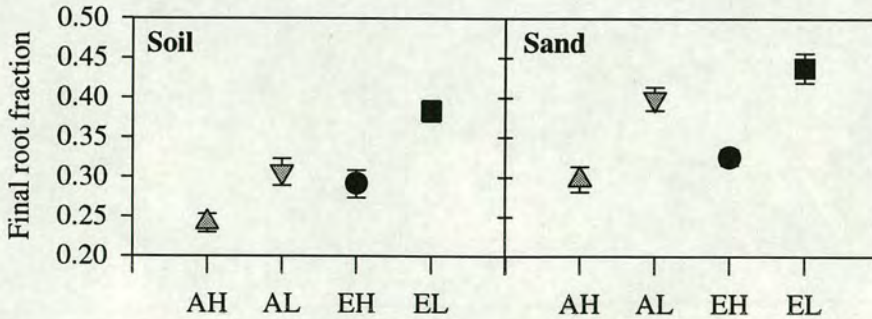


Figure 6.16 Root mass fraction at the final harvest dates 15/11 and 1/12 for soil and sand, respectively. Means \pm 1 SEM, $n = 5-9$.

6.4.3 Functional and structural mass

The proportion of the total tree mass that was ‘functional’ (needle and fine root) as opposed to structural (wood, coarse root and stump) was very consistent across both growth mediums, and nutrient and CO₂ treatments (Table 6.3). Nutrient treatment had a slight influence but it’s effect depended on the growth medium. In soil **H** nutrient decreased the proportion of ‘functional’ mass while in sand it increased it.

Table 6.3 The proportion of the mass of the tree that is functional for trees in the final harvest, *i.e.* (needle mass + fine root mass) / total tree mass. Means ± 1 SEM, *n* = 5 - 9.

	AH	AL	EH	EL
Soil	0.52 ± 0.012	0.56 ± 0.008	0.53 ± 0.11	0.56 ± 0.016
Sand	0.54 ± 0.014	0.52 ± 0.019	0.54 ± 0.010	0.52 ± 0.012

The way in which the ‘functional’ mass was partitioned between leaves and fine roots shows a clear nutrient (*P* < 0.0002) and slight CO₂ effect (ns) and some differences between the soil and sand medium (Figure 6.17). **H** trees allocated more to needle than root while **E** trees allocated slightly more to fine roots. There was a tendency for sand-grown trees to allocate more of the functional mass to fine roots than those grown in soil. This is probably a result of differences in the nutrient holding capacity of the two media, but may also be because soil-grown trees retained their original soil ball while sand-grown trees had their roots washed clean when they were re-potted. The effect of [CO₂] on allocation was stronger and that of nutrient treatment weaker in soil-grown trees than in sand-grown trees. This is again probably a result of differences in the nutrient availability of the two media.

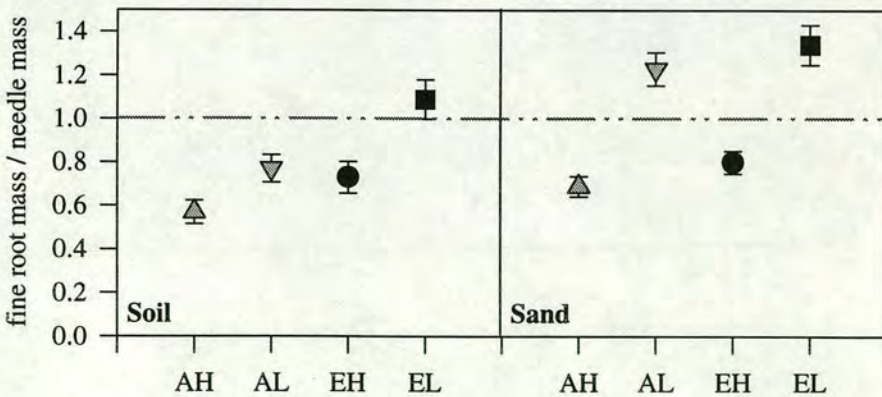


Figure 6.17 The ratio of fine root mass to needle mass at the final harvest. Means ± 1 SEM, *n* = 5-9.

6.5 Bud set

From the beginning of September until the final harvests, bud set of the leader of each tree was scored (Figure 6.18). The bud was considered to have set when a clear bud had formed as opposed to the tuft of tightly packed needles present in the still active meristem. Trees in the **EL** treatment did not have lammass growth and the buds set earliest. There was a nutrient effect with trees with **L** nutrient supply setting bud earlier than trees with **H** nutrient supply but even by 1st December not all of the **H** buds had set. Budset in the elevated [CO_2] treatment occurred slightly earlier especially in the **L** nutrient trees.

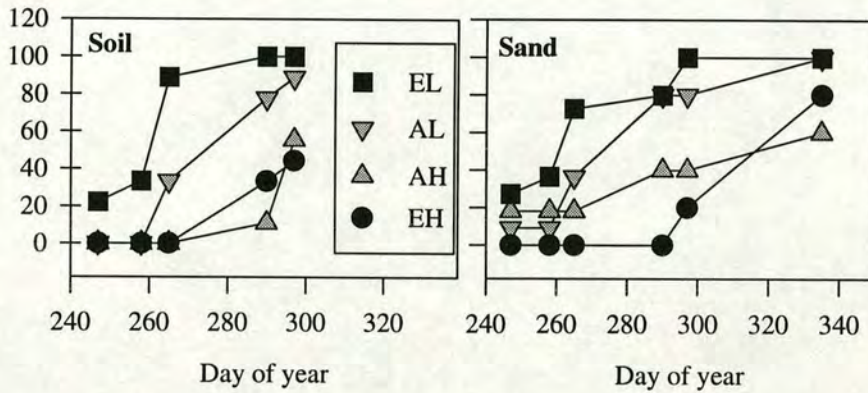


Figure 6.18 The percentage of trees with terminal buds set towards the end of the growing season.

6.6 Discussion

6.6.1 Allocation

The results of this experiment support the optimisation theory with respect to relative growth rates, R_G , and to changes in the root fraction, F_r , as the supplies of both carbon and nutrients were manipulated. At high nutrient supply rates the efficiency of the roots (*i.e.* the specific uptake of nutrient, S_N) was probably increased which led to a decrease in the root fraction, F_r , while in elevated [CO_2] the efficiency of shoots was enhanced (see Chapter 7) which induced an increase in F_r . The final values of F_r were dependant on the relative sizes of these competing effects and are shown in Figure 6.16. Townend (1993) found no change in the root/shoot ratio in Sitka spruce seedlings grown at elevated CO_2 but did find a reduction in the needle to wood ratio and this would translate into an increase in the root mass to needle mass ratio, as was found in this study (Figure 6.17). Murray *et al.* (1996) found a 35%

increase in the root/shoot ratio in the first year of a three year experiment on Sitka spruce seedlings but they found that by the third year this CO₂ effect had diminished to 10%.

Increase in the efficiency of either the roots, S_N , or the shoots, S_C , will result in a change in F_r but will also cause an increase in the overall growth rate of the tree. This is seen in Table 6.2 where relative growth rates increase from **AL** to **AH** to **EL** to **EH**, at least during the early part of the season. An increase in photosynthetic efficiency will lead to an increase in growth efficiency (*i.e.* stem wood production per unit leaf area) and this implies a potential increase in carbon sequestration by forests (subject to critical assumptions about forest canopy development in a CO₂ enriched atmosphere (see Norby *et al.*, 1995)).

An interesting question arises as to what might happen if growth itself were constrained either by genetic limitations to development or some other factor. This seems to happen in trees with determinate growth which cannot produce a second flush and also in conditions where the root system is prevented from expanding. Arp (1991) suggested that the reduction in photosynthetic capacity over time, observed in many elevated [CO₂] experiments, may be related to restriction in the size of available sinks for carbohydrates, caused by restricted rooting volume. I would suggest that it is not the sink limitation *per se* but the imbalance between carbon and nutrient acquisition that leads to a build up of carbohydrates and a consequent feedback inhibition of photosynthesis *i.e.* providing the roots can uptake nutrients at an adequate rate to permit the shoot to grow the fact that the roots are prevented from growing by limited rooting volume should not result in a build up of carbohydrates. Of course eventually the size of the constrained root system will be too small to acquire nutrients at an adequate rate to balance the photosynthate produced by an ever increasing shoot and then down-regulation of photosynthesis will occur. McConnaughay *et al.* (1993) investigated the effects of pot size, pot shape and nutrient availability on the growth response of two herbaceous species to elevated CO₂ and concluded that all three variables influenced plant growth.

This raises further questions about the controls on root/shoot ratios. If nutrients are supplied to the roots at optimum rates and concentrations, using a system such as that devised by Ingestad and Lund (1986), the root system would not need to 'search' for nutrients and the amount of fine roots would be expected to be the minimum required to balance the uptake of nutrients with the fixation of carbon by the shoot, thus defining the minimum root fraction. Increasing the photosynthetic efficiency of the shoot by raising the atmospheric [CO₂] should then lead to an increase in F_r .

Pettersson *et al.* (1993) used such a system to investigate the effects of $[\text{CO}_2]$ on small birch and found that $[\text{CO}_2]$ did not affect F_r , but F_r was higher at lower N-supply. However, their experiment was not designed to answer this specific question and further carefully designed experiments using this approach are required to test this hypothesis.

If growth of either the root or the shoot is constrained such that an imbalance between carbon and nutrient uptake would arise then the plant could respond by reducing the efficiency of the non-limited organ thus permitting further growth of the non-limited component. Alternatively, growth could be directed into structural rather than functional tissue in which case one would expect to see an increase in wood and coarse root production. In this experiment the proportion of structural tissue was very consistent at between 44 and 48 % of total tree mass (Table 6.3). However, this experiment was not a good test of the hypothesis as large pot size was chosen to avoid any physical constraint on root growth and the trees produced considerable free growth of shoots.

6.6.2 Growth

The height growth of the trees was strongly influenced by nutrient availability while increases in diameter were influenced more by elevated CO_2 concentrations (see Figure 6.3 & Figure 6.5). Both elevated CO_2 and high nutrient supply rates stimulated bud flushing in the first flush but by the second flush **EL** trees hardly produced any lammas growth. This was probably partly a result of the trees adjusting to the new growth conditions. Prior to the initial bud burst all trees had an adequate nutrient status (see Chapter 7). However, once growth began the **L** trees and especially the **EL** trees depleted their reserves such that by the second flush **EL** trees could not maintain the growth rate and failed to produce any lammas growth.

Stimulation of shoot growth at high nutrient supply rates was very strong with the result that **EH** and **AH** trees had very many more active shoots than **EL** and **AL** trees. This increase in the number of active shoots was proportional to tree height but disproportional with respect to tree mass, with **AH** trees having many more shoots per unit tree mass than **EH** trees. This is in part a result of increased non-structural carbohydrate storage in **E** shoots (see Chapter 7) but this does not account for all of the difference.

The number of needles on a shoot is determined in August when the primordia are initiated during bud development. It would have been interesting to see how the trees differed in the following spring, and if the number of new shoots generated in the

current year and the size of the buds laid down in the current year reduced the differences between treatments in the amounts of free growth produced during the following summer. This might indicate that the results observed in the current year were a consequence of the tree adjusting to the growing conditions.

Buds set earlier in trees grown at low nutrient supply rates and also slightly earlier in trees grown at elevated CO₂ concentration. Similar results were found by Murray *et al.* (1994) where trees grown at elevated CO₂ set bud 22 days earlier. They proposed that this shortening of the growth period might reduce growth, however, since trees grown in elevated [CO₂] tended to have higher growth rates and since most growth has slowed considerably by the end of the season it is unlikely to have any significant effect. The risk of frost damage to trees growing at high nutrient supply rates would be more of a problem but since nutrients tend to be limiting in natural systems this is not a serious concern.

6.6.3 Difference between soil and sand

Trees grown in both soil and sand showed the same basic response to [CO₂] and nutrient supply but there were some differences in the extent of the response. Trees grown in sand tended to show a stronger response to the nutrient treatment especially when grown at elevated [CO₂]. This is especially true of the total dry mass at the final harvest where **AH** trees were slightly heavier in sand trees and **AL** were slightly lighter in sand trees while at elevated [CO₂] the effect was exaggerated with **EH** heavier and **EL** much lighter in sand trees than soil trees.

The differences observed early in the experiment were probably a result of nutrients in the soil ball transplanted along with the soil-grown trees which resulted in soil trees having access to more nutrients than sand trees, this would have a larger impact on the **L** trees. The nutrients carried over in the soil ball were probably depleted fairly rapidly but the resultant effect on the trees may have persisted.

Differences in the physical and chemical properties of the two mediums probably also influenced the responses to the treatments. Water holding properties, movement of water, penetrative and abrasive properties, pH buffering and cation exchange capacity would all have been different and could potentially have influenced the trees response to [CO₂] and nutrient supply. The root fractions at the final harvests were higher in sand-grown trees than soil-grown trees of the same treatment in every case (Figure 6.16). This indicates possible differences in the ability of the roots to acquire nutrients, where sand-grown trees require more root per unit tree mass to obtain nutrients because their roots are less efficient *i.e.* S_N is lower.

6.7 Conclusions

Changes in the fraction of dry mass allocated to the root system and relative growth rates were consistent with the trees allocating resources to optimise growth. The fraction of tree mass that was functional (needle and fine root) was consistent across all treatments, at about 50%, while the needle/fine root ratio varied in response to nutrient supply and CO₂ concentration.

The ability of young spruce trees to produce lammas growth permitted them to respond to increased nutrient availability and increased CO₂ concentrations by extending existing shoots and, in the case of high nutrient trees, by producing more shoots.

Relative growth rates declined during the year but by the end of the year elevated CO₂ was still stimulating relative growth rates.

Trees grown in soil responded in a similar way to those grown in sand culture. The differences that were observed were attributed to differences in the amounts of nutrient carried over when the trees were transplanted and differences in the physical and chemical properties of the two mediums.

CHAPTER 7

Leaf Photosynthesis, Carbohydrate and Nutrient Content

7.1 Introduction

Plants require a balance of nutrients and photosynthates in order to grow and maintain a healthy physiological state. By measuring concentrations of key nutrients, soluble carbohydrates and starch in leaves and roots of plants growing in different sets of conditions, in conjunction with measuring photosynthesis, growth and allocation, we can gain insight into the mechanisms that allow plants to adapt to a range of environmental conditions. Once we understand how plants function we will be in a better position to predict how they will respond to climate change.

Many of the responses observed in plants grown in elevated CO₂ concentrations such as down-regulation of photosynthesis, increase in starch content and changes in root/shoot ratio can be attributed to limited nutrient supply (Pettersson *et al.*, 1993) or limited sink strength induced by restricted rooting volume (Arp, 1991; McConnaughay *et al.*, 1993). Increased carbohydrate concentrations in leaves have been attributed to inadequate sink activity (see review by Stitt, 1991), inadequate phloem transport (Körner *et al.*, 1995) and potassium deficiency (Nitsos & Evans, 1969). Large, unusually shaped starch grains have been postulated to cause damage, either through contortion of the chloroplast grana or through actual disruption of chloroplasts (Cave *et al.*, 1981, Wulff & Strain, 1981). In some cases RuBP regeneration can be limited by the availability of inorganic phosphate in the chloroplasts, caused when the utilisation of trios-phosphate for the production of sucrose and starch fails to keep pace with the production of trios-phosphates in the Calvin cycle (Herold, 1980; Sharkey, 1985; Harley & Sharkey, 1991; Harley *et al.*, 1992).

Growth in elevated [CO₂] may lead to changes in the optimal balance of nutrients. Conroy *et al.* (1990) concluded that higher foliar phosphorus concentrations were required to realise the maximum growth potential of pines in elevated CO₂.

Thus in order to interpret the results obtained from elevated CO₂ studies it is vital that we measure carbohydrate and nutrient concentrations. Failure to do so may lead to erroneous interpretation of the underlying mechanisms and consequently to substantial errors in predictions about how trees and forests will respond to climate change.

This chapter firstly covers the carbohydrate and nutrient concentrations of needles and fine roots at each of the six harvest dates. It then describes the measurement of shoot photosynthesis in response to changing CO₂ concentration, relating it to the nutrient and chlorophyll concentrations of those shoots. It concludes by discussing the interactions between nutrients, carbohydrates and photosynthesis.

7.2 Plant material

7.2.1 Sampling strategy for nutrient and carbohydrates

When trees were harvested they were separated into current year and older shoots, and fine and coarse roots. Sub-samples of the current needles and fine roots from each of the six harvests were analysed for starch, soluble carbohydrates and macro-nutrient concentrations. Table 6.1 in Chapter 6 gives the dates and numbers of trees at each harvest.

To investigate diurnal changes of starch and soluble carbohydrates approximately 50 current needles were taken from the upper third of the crown from sand grown trees at different times of day on 28th June and the 21st September. The primary aim was to determine the degree to which starch and soluble carbohydrate concentrations changed between early morning, when one would expect them to be at their lowest, and mid-afternoon when they should be at their highest. The secondary aim was to determine the way concentrations changed throughout the day, and this required sampling every few hours. However, to sample at five times during the day and obtain a minimum of three replicates for each of the four treatments would have required too many samples and so it was decided to sample one treatment five times throughout the day, to give an idea of the daily trend, and the other treatments only when the carbohydrate concentrations were expected to be at the extremes. On 28th June samples were taken at 1:00, 5:00, 10:00, 15:00 and 20:00 for the **AH** treatment and at 5:00 and 15:00 for the **AL**, **EH**, and **EL** treatments. Three replicates per treatment were taken at each time. This sampling strategy was modified for the 21st September sampling when six replicates were taken for each treatment at 5:00 and 16:00.

7.2.2 Material preparation

Ideally plant tissue to be analysed for carbohydrate content should be freeze dried since oven drying can, under some circumstances, lead to losses of carbohydrate caused by respiration and volatilisation (Chiariello *et al.*, 1989). To minimise any losses, a forced draft oven at 65-70 °C should be used as this is sufficient to stop enzymatic activity, whereas higher temperatures cause carbohydrates and proteins to complex into lignin like materials (Chapin & Van Cleve, 1989).

As our freeze drier was out of service for most of this experiment, plant material was oven dried at 70 °C for 48 hours then sub-samples were taken and finely ground in a ball mill. This material was stored in sealed polythene bags in desiccators until used for each of the analyses. To test that the oven drying had not caused losses of starch or soluble carbohydrates, some fresh duplicate samples were frozen and kept at -20 °C until the freeze drier was repaired, then freeze dried and analysed in the same way as the oven-dried samples.

7.3 Starch

7.3.1 Method

Starch content was determined colorimetrically using the iodine method described by Allen (1989) (see Chapter 3, 3.6.2 for details).

7.3.2 Starch content at harvests

At the initial harvest the starch content in needles of the **A** trees was unexpectedly slightly higher than that of **E** trees but this rapidly reversed so that **E** needles had higher concentrations than **A** needles within the same nutrient treatment (Figure 7.1). After being given nutrients, the needles of the **H** trees developed lower starch contents than those of the **L** trees. Foliar starch concentrations fell through the year in all but the **EL** treatment where there was an initial rise. Trees grown in 'soil' showed the same pattern but had lower starch concentrations than trees grown in sand in August.

Needles from the first harvest were almost one-year-old while those from subsequent harvests were from the new growth, and thus there was a discontinuity in the age of needles between the first and subsequent harvests which may explain part of the sudden drop in starch content.

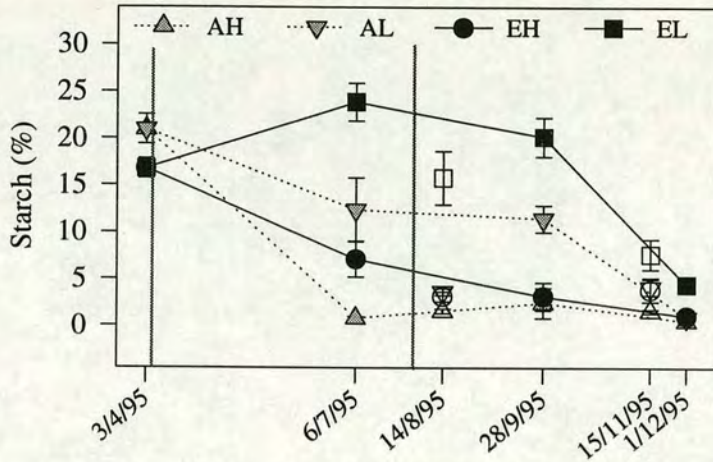


Figure 7.1 Starch content as a percentage of the dry mass in current needles at each of the harvests. Filled symbols are sand-grown trees while empty symbols are 'soil'-grown. Means ± 1 SEM, $n = 4-6$. The 3/4/95 point is for 1994 cohort needles while the remaining points are for 1995 cohort needles. Vertical lines indicate the period during which nutrients were applied.

Starch concentrations in the roots of **A** trees were initially higher than those in the **E** roots but, as in the case of the needles, this quickly switched. Furthermore, as in the needles **L** trees had higher starch concentrations in the roots than **H** trees. At the final harvests of both sand and 'soil'-grown trees root starch concentrations had risen, and thus is consistent with starch storage in the roots over winter. Starch concentrations in roots of trees grown in 'soil' showed a similar pattern but were slightly lower than in sand-grown trees in August but were higher by November.

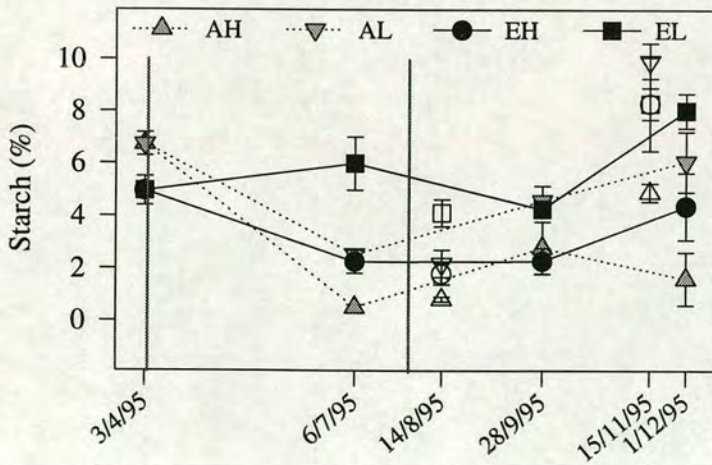


Figure 7.2 Starch content as a percentage of the dry mass in roots at each of the harvests. Filled symbols are sand-grown trees while empty symbols are 'soil' grown. Means ± 1 SEM, $n = 4-6$. The 3/4/95 point is for 1994 cohort needles while the remaining points are for 1995 cohort needles. Vertical lines indicate the period during which nutrients were applied.

7.3.3 Diurnal changes in starch content of needles.

Starch concentrations in current needles did not vary significantly throughout the day, as seen in Figure 7.3. The AH treatment was sampled at a higher frequency than the other treatments in order to observe any diurnal pattern, but unfortunately it contained almost no starch at any time of the day. The other treatments were sampled at times when it was thought that the concentrations would be at their extremes but they showed no differences with time. This lack of diurnal change of starch concentration was verified later in the season (Figure 7.4).

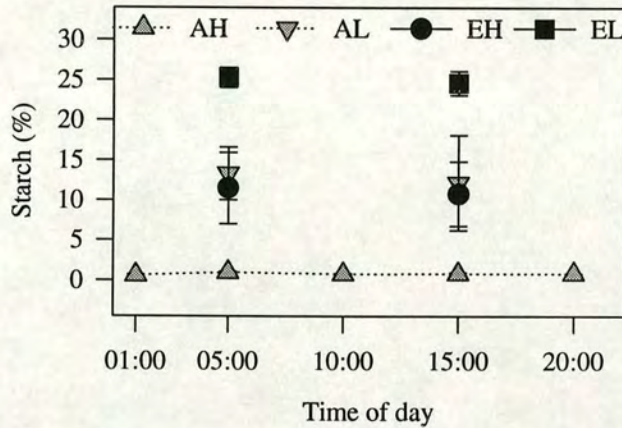


Figure 7.3 Starch content as a percentage of dry mass for current-year needles of sand-grown trees through the course of 1/7/95. Means \pm 1 SEM, $n = 3$.

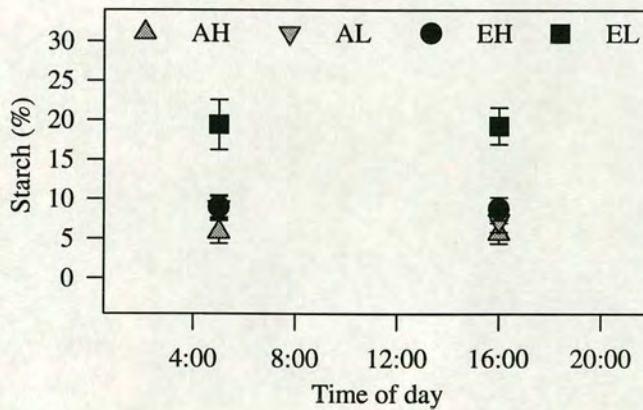


Figure 7.4 Starch content of current needles of sand-grown trees at 5 am and 4 pm on 21st September. Means \pm 1 SEM, $n = 6$.

The lack of diurnal change in starch content is not particularly surprising as conifers store starch in the needles to supply resources for new growth in the spring. One might expect a gradual increase in starch content over the season possibly with a

small diurnal oscillation as excess photosynthate is temporarily stored in needles during daylight then exported to active meristems at night.

7.4 Soluble carbohydrates.

7.4.1 Method.

Water soluble carbohydrate concentration of needles were measured by anion-exchange chromatography with pulsed amperometric detection (see Chapter 3, 3.6.3 for details).

7.4.2 Soluble carbohydrates at harvests.

Expressing soluble carbohydrate concentrations on a starch-free, dry mass basis allows us to see changes in soluble carbohydrate independent of changes in starch. The soluble carbohydrate concentration in the current needles rose throughout the experiment in all treatments up until the end of September when it fell in **A**, continued to rise in **EL** and remained constant in **EH** (Figure 7.5). At ambient [CO₂] trees in the **L** nutrient treatment had higher soluble carbohydrate concentrations than trees in the **H** nutrient treatment, while in elevated [CO₂] the nutrient treatment did not affect soluble carbohydrate concentrations. Trees grown in sand and 'soil' had very similar concentrations.

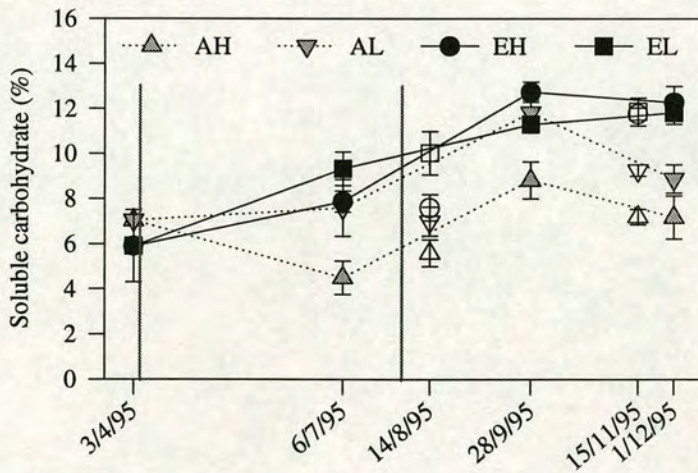


Figure 7.5 Soluble carbohydrates as a percentage of the starch-free dry mass in current needles at each of the harvests. Filled symbols are sand-grown trees while empty symbols are 'soil' grown. Means \pm 1 SEM, $n = 4-6$. The 3/4/95 point is for 1994 cohort needles while the remaining points are for 1995 cohort needles. Vertical lines indicate the period during which nutrients were applied.

Soluble carbohydrate concentrations in the roots fell over the course of the experiment for all but the **EH** treatment and by the end of the experiment all treatments apart from **EH** had very similar concentrations.

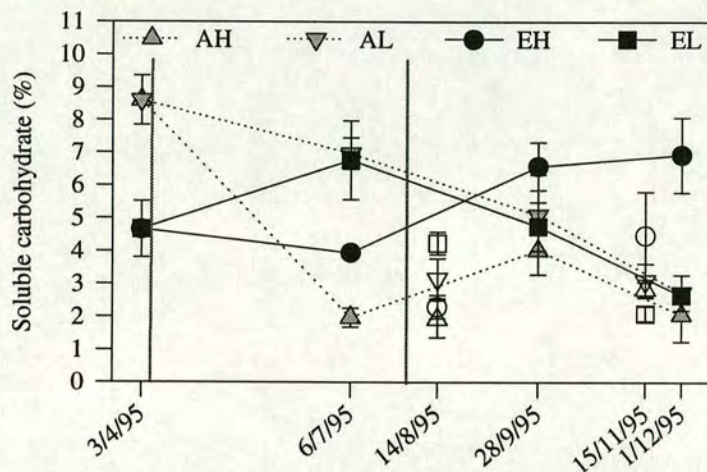


Figure 7.6 Soluble carbohydrates as a percentage of the starch-free dry mass in roots at each of the harvests. Filled symbols are sand-grown trees while empty symbols are ‘soil’ grown. Means \pm 1 SEM, $n = 4-6$. The 3/4/95 point is for 1994 cohort needles while the remaining points are for 1995 cohort needles. Vertical lines indicate the period during which nutrients were applied.

7.4.3 Diurnal variation in soluble carbohydrate concentrations in needles.

Unlike the starch there was a diurnal change in the concentrations of soluble carbohydrates in the current needles (Figure 7.7). As would be expected, concentrations were lowest in the early morning before photosynthesis began and rose to a maximum by mid-afternoon. Both the minimum concentration and amplitude of the change were biggest in the trees grown in elevated CO_2 where concentrations doubled from 6% to 12%.

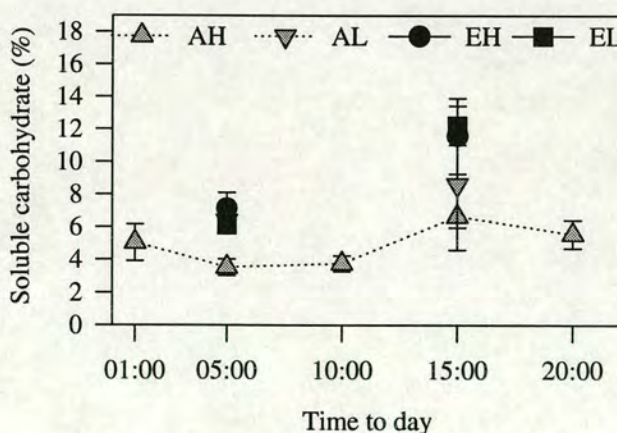


Figure 7.7 Soluble carbohydrates in current needles of sand-grown trees as a percentage of starch-free dry mass measured throughout 1/7/95. Mean \pm 1 SEM, $n = 3$.

Nutrient treatment had no effect in July when **EH** and **EL** had similar and higher concentrations than **AH** and **AL**, but by September **EH** needles had higher concentrations than **EL** while **AH** and **AL** had similar concentrations. Concentrations were higher in September than July and the amplitude of the diurnal change was less (Figure 7.8), possibly indicating saturation.

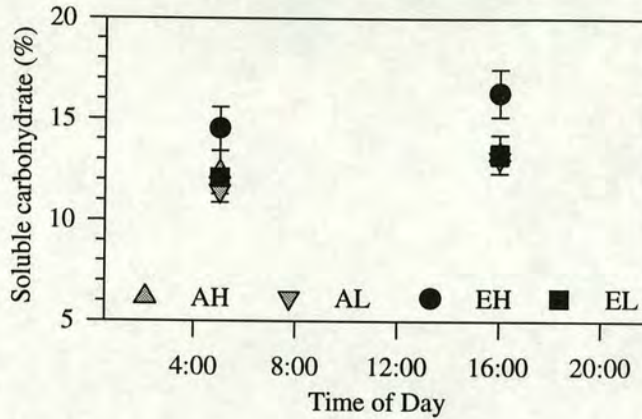


Figure 7.8 Soluble carbohydrate content of current needles of sand-grown trees as a percentage of starch-free dry mass at 5 am and 4 pm on 21st September. Mean \pm 1 SEM, $n = 6$.

7.5 Total non-structural carbohydrates

7.5.1 At harvests

Summing the starch and soluble carbohydrates gives the total non-structural carbohydrate (TNC) content of the tissue. TNC in the current needles was dominated by starch at the beginning of the year but by the end of the year the starch concentration had fallen and soluble carbohydrates accounted for 60 to 70% of the TNC. The needles analysed at the first harvest were 11 months old (current needles just prior to bud burst) and had high levels of starch. Subsequent harvests were of the new needle cohort and so the initial drop in TNC, in all but the **EL** treatment, is partly attributable to the change in needle cohort but is probably also a result of consumption of storage reserves for new growth.

TNC in the roots (Figure 7.10) was composed equally of starch and soluble carbohydrates. There was no clear seasonal change in the TNC content of the roots. At the start of the experiment **A** roots had more than **E** roots but this situation rapidly reversed. The general trend was that both **E** and **L** led to higher concentrations of TNC although the relative differences varied throughout the year. Trees grown in 'soil' showed the same pattern as those grown in sand.

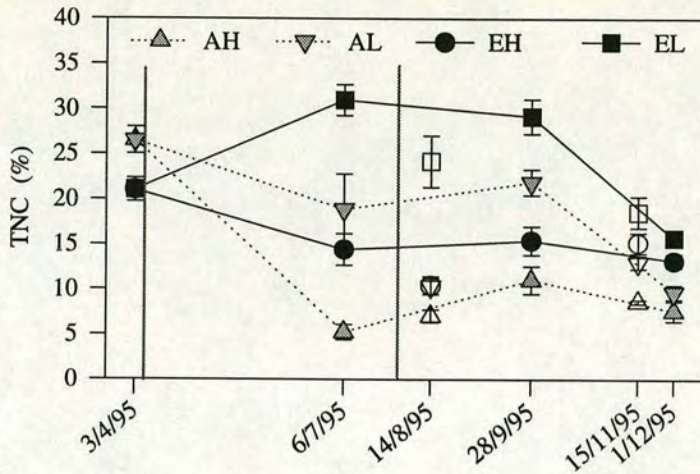


Figure 7.9 Total non-structural carbohydrates as a percentage of dry mass for current year needles at each of the harvest dates. Filled symbols are sand-grown trees while empty symbols are 'soil' grown. Means \pm 1 SEM, $n = 4-6$. The 3/4/95 point is for 1994 cohort needles while the remaining points are for 1995 cohort needles. Vertical lines indicate the period during which nutrients were applied.

TNC in roots of **E** trees rose at the end of the season as a result of increasing starch despite falling soluble carbohydrate concentrations. The large rise in soluble carbohydrates in **EH** at the end of the year led to **EH** having the highest TNC.

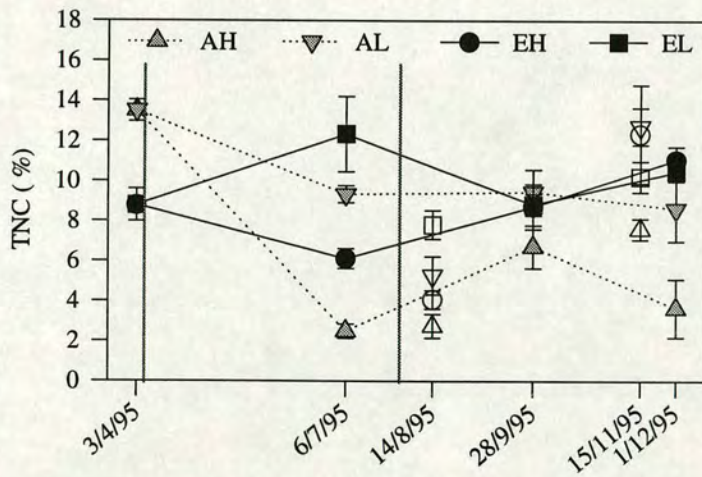


Figure 7.10 Total non-structural carbohydrates as a percentage of dry mass for roots at each of the harvest dates. Filled symbols are sand-grown trees while empty symbols are 'soil'-grown. Means \pm 1 SEM, $n = 4-6$. The 3/4/95 point is for 1994 cohort needles while the remaining points are for 1995 cohort needles. Vertical lines indicate the period during which nutrients were applied.

7.6 Nutrient concentrations

7.6.1 Method

Finely ground sub-samples of the oven-dried, current-year needles and roots were analysed. N, P, K, Ca and Mg were determined using the methods described by Allen (1989) with some modifications. One sample from each tree at each harvest was analysed, so the number of replicates per treatment ranged from four to six depending on the harvest date. Results are presented on a non-structural-carbohydrate-free dry mass basis, *i.e.* the dry mass of the tissue after subtraction of starch and soluble carbohydrates (see Chapter 3, 3.6.4 for more details of the assay).

7.6.2 Results

The nitrogen concentration of current needles was very similar for both **A** and **E** at the start of the experiment (Figure 7.11). It should be noted that the first harvest was just prior to bud burst and so current needles were 11 months old, but, at the second and subsequent harvests the new year's growth was being analysed.

An alternative way of presenting the nutrient concentrations is to show them relative to the nitrogen concentration which can give some indication of nutrient imbalances (Figure 7.12). The horizontal broken line on the graphs shows the concentration of each nutrient relative to nitrogen in the feed solution (Appendix C).

Both the initial drop in nutrient concentrations (Figure 7.11), and the drop in concentrations relative to nitrogen (Figure 7.12) may be a response to a change in the composition of the nutrient solution between that supplied during their first year and that during this experiment. The observed changes are consistent with plants changing from a solution low in nitrogen to one higher in nitrogen relative to other nutrients.

The most outstanding result is that the concentrations of calcium and magnesium were very high in both needles and roots and that the ratio of these elements compared to nitrogen was far higher in the plant than in the feed solution. The most probable cause of this discrepancy is high concentrations of Ca and Mg in the mains water supply, 10.6 and 1.85 mg dm³ respectively. Thus depending on the time of year, one dm⁻³ of water supplied between 1.8 - 9 times the weekly requirement of Ca and 0.23 - 1.2 times that for Mg for the **H** treatment and 10 times those amounts for the **L** treatment. So effectively the plants had free access to these two elements, and this explains why there are no differences in the concentration of these nutrients between treatments (Figure 7.11).

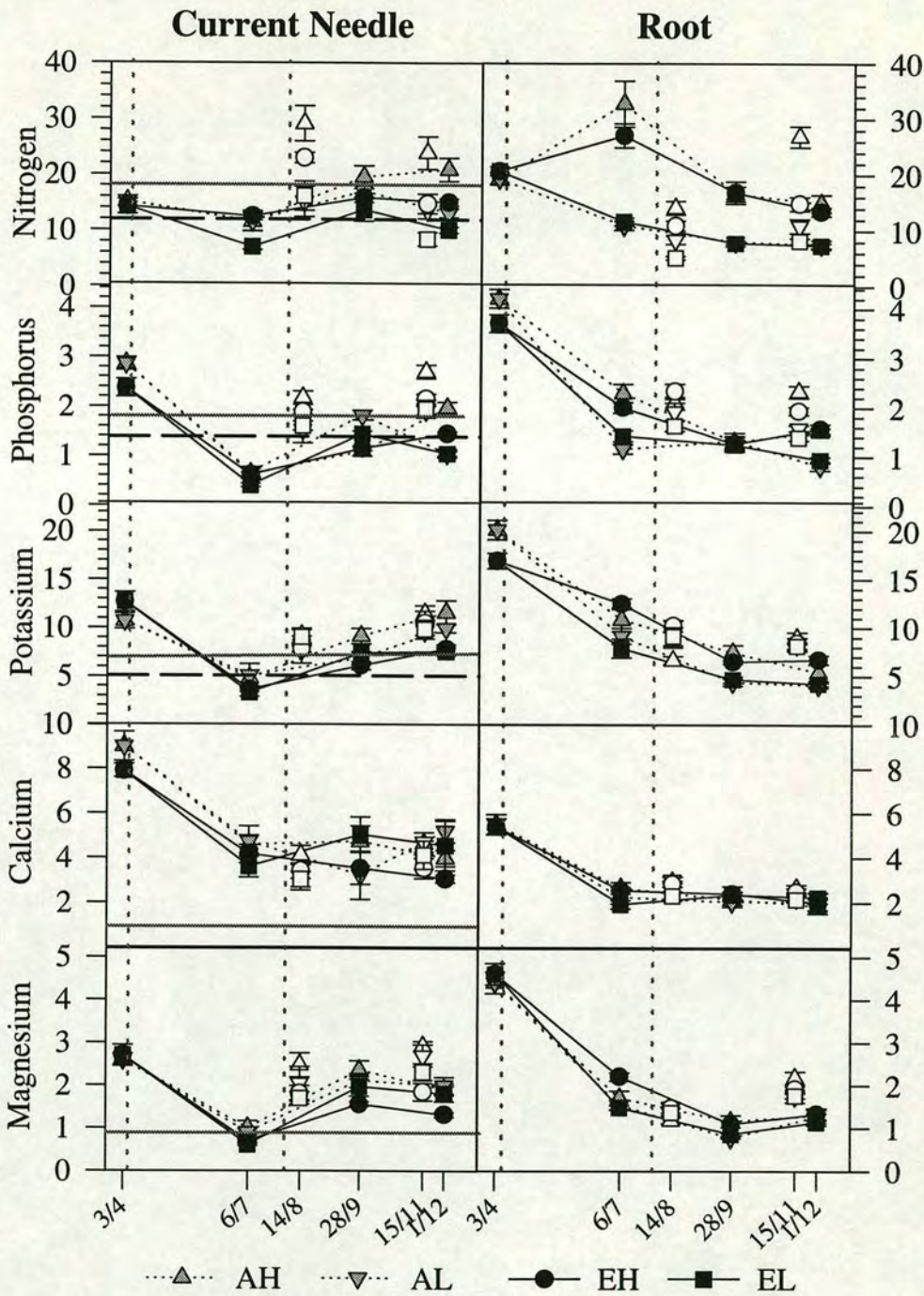


Figure 7.11 Nutrient concentration (mg g^{-1}) of carbohydrate-free, dry mass for current needles and roots at each of the harvest dates. The filled symbols are sand-grown trees and the open symbols are 'soil'-grown trees. Means \pm SEM $n = 4-6$. The horizontal broken lines on the foliar graphs indicate the level below which the tree is thought to be deficient (Binns *et al.*, 1980). The horizontal grey lines indicate optimal concentrations for Norway spruce (Linder, 1995). The broken vertical lines indicate the period during which nutrients were applied.

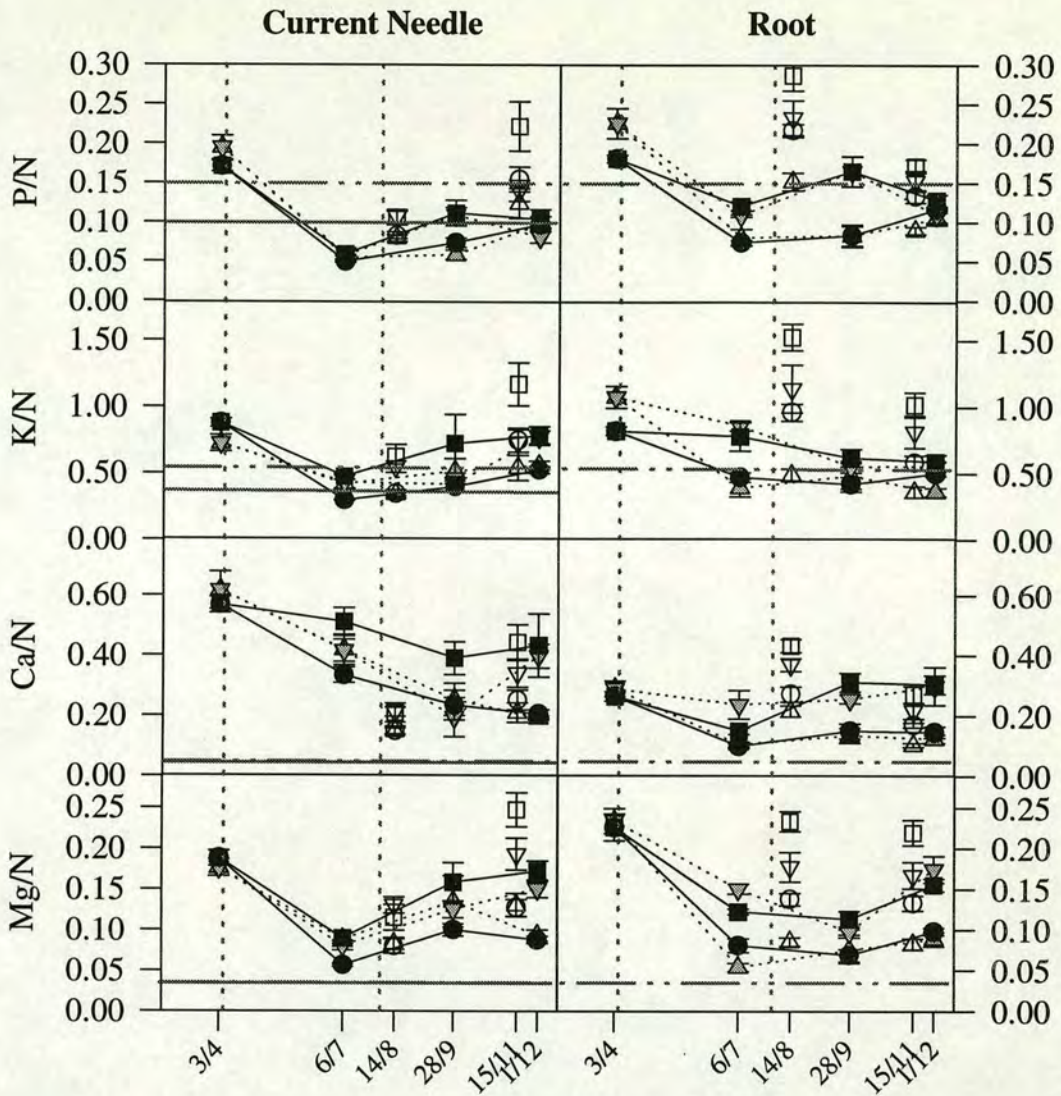


Figure 7.12 Nutrient concentrations in current needles and roots at each harvest date expressed as a fraction of the nitrogen content (g g^{-1}). The horizontal broken lines indicate the mass proportion of each nutrient relative to nitrogen in the nutrient solution used to feed the trees. The filled symbols are sand-grown trees and the open symbols are 'soil'-grown trees. Means ± 1 SEM, $n = 4-6$. The horizontal grey lines indicate optimal ratios for Norway spruce (Linder, 1995). The broken vertical lines indicate the period during which nutrients were applied.

An interesting observation is that calcium concentrations in needles were higher in the **L** than the **H** nutrient treatment while root concentrations were the same for all treatments. Calcium commonly accumulates in leaves because it is carried in the transpiration stream and then left behind when the water evaporates and, unlike other nutrients, it is not re-translocated in the phloem but tends to be precipitated as calcium oxalate crystals in the cell walls of the mesophyll, particularly the phloem and in the outer wall of the epidermis (Marschner, 1995). Thus one might expect

calcium concentrations in leaves to follow cumulative transpiration and this was indeed the case: transpiration was highest in **AL** followed by **AH**, **EL** and finally **EH** (see Chapter 8, 8.3.1).

7.6.3 Nitrogen content of the trees

The nutrient solution was applied for the first 115 days of growth, from 8th April to 31st July, in line with the expected period of growth. Once application stopped any further growth would utilise the unused nutrient pool remaining in the pot or reserves in the trees, possibly leading to a reduction in the tissue concentrations. But since the nitrogen concentration of tissues may also change with ontogeny, changes in concentration do not necessarily reflect nutrient limitation. I calculated the nitrogen content of the needles and roots at each harvest by multiplying the dry mass by the nitrogen concentration: these were then added together to give the nitrogen content of the trees. The nitrogen concentration of the wood was not known so wood nitrogen content is missing from the values presented. Wood mass accounted for approximately 40% of total dry mass (see Chapter 6, Figure 6.13) but the nitrogen concentration was probably lower than that of the needles and roots (Murray, personal communication).

In all treatments the nitrogen content of the trees increased throughout the experiment but the rate of increase declined after the end of September (Figure 7.13). **H** trees had much higher contents than **L** and **E** trees slightly higher than **A**.

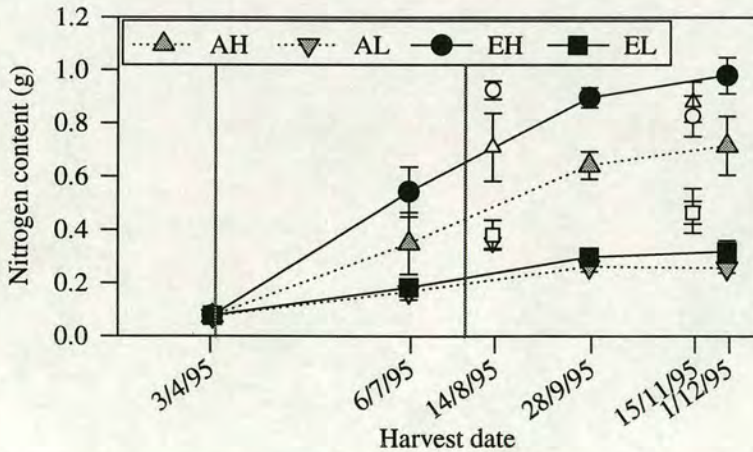


Figure 7.13 Nitrogen content of the seedlings (needle + root) over time. The filled symbols are sand-grown trees and the open symbols are 'soil' grown trees. Means \pm 1 SEM, $n = 4-6$. Vertical lines indicate the period during which nutrient was applied.

7.6.4 Discussion

Uptake of nutrients by the root at low soil nutrient concentrations has been designated 'mechanism I' of ion absorption and has been analysed by means of Michaelis-Menten kinetics based upon the carrier concept (Ingestad, 1982). The uptake and concentration of nutrients in the root depends on both the concentration in the roots and the soil solution and also on the growth rate of the tree. As the concentration in the roots rises so the flux into the roots tends to fall (Marschner, 1995). In experiments where nutrient solution has been continually brought to the root, thus preventing localised depletion, maximum growth rates can occur at very low nutrient concentrations. However, in soil where nutrients can be locally depleted growth may be affected, even when the mean concentration in the soil solution is relatively high. Furthermore, high external concentrations can lead to 'luxury' uptake, such that nutrients are absorbed in excess to current requirements and stored as internal reserves to supply future demand should uptake become limited. Internal cycling of nutrients from the root to the shoot and back to the root occurs, depending on the current demand for nutrients by the various sinks within the plant. Thus the concentration of nutrients in plant tissues depends on a number of interacting processes and environmental variables and the interpretation of tissue concentrations is difficult without reference to soil nutrient concentrations and growth rates.

Concentrations of N, P and K were highest in **AH** and lowest in **EL** needles, while **AL** and **EH** were intermediate. Concentrations in the roots followed a similar pattern but there was a much stronger effect of nutrient supply with **H** roots having higher concentrations than **L** roots. These results suggest that high nutrient supply rate may be inducing 'luxury' uptake and storage of nutrient within the roots. While increase in photosynthesis, as a result of growth in elevated $[CO_2]$ combined with increased nutrient availability, is stimulating growth which, in turn, is reducing nutrient concentrations in the needles.

Nitrogen concentrations in **H** roots were particularly high in July and may reflect luxury uptake. Once the nutrient application was stopped nitrogen concentration in the roots of **H** trees began to decline but the concentrations in the needles remained fairly stable. The decline in root concentrations may indicate mobilisation of nitrogen reserves within the root to supply growth of both roots and shoots. There may also be an effect of ontogeny since root growth tends to increase in September as shoot growth declines. A discussion about nitrogen and its influence on photosynthesis follows in section 7.9.3.

Foliar potassium concentrations were higher in **A** than in **E** trees and were almost independent of nutrient supply rate. Potassium is the most abundant cation in the cytoplasm and K^+ , and its accompanying anions, make a major contribution to the osmotic potential of cells, and tissues. Soluble carbohydrates also influence the osmotic potential of cells and so the clear, inverse relationship between potassium (Figure 7.11) and soluble carbohydrate concentrations (Figure 7.5) is unsurprising. Potassium is highly mobile within the plant and it is possible that potassium concentrations were adjusted in response to increases in soluble carbohydrates to maintain a suitable osmotic potential in cell vacuoles. Furthermore, potassium is involved with the function of many enzymes including starch synthase and plants deficient in potassium tend to accumulate soluble carbohydrates and exhibit reductions in starch content (Nitsos & Evans, 1969). Potassium is also involved in phloem loading, deficiency leading to reductions in sucrose export rates from leaves (Marschner, 1995). However, potassium concentrations were well above those deemed deficient for Sitka spruce (Binns *et al.*, 1980) and there was no evidence of deficiency in any of the treatments. Further investigation is required to determine if potassium supply rates play a role in the response of plants to growth at elevated $[CO_2]$.

7.7 Organic material in the sand

To close the carbon balance for the trees growing in sand culture, it was necessary to measure any changes in the organic content of the growth medium. Organic matter could enter the growth medium initially as dead roots, root hairs and root exudates which may then become converted to microbial/fungal biomass or oxidised and lost as CO_2 . The CO_2 exchange of the tree and root/sand was measured (see Chapter 8) as was the increase in root biomass (Chapter 6) and changes in the soil organic matter content determined. Firstly, to determine the amounts of organic matter, the loss on ignition was determined for samples of the sand in which the trees had been growing. Then soluble carbohydrates were measured using the very sensitive HPLC system described in section 7.4.1.

7.7.1 Loss on ignition

Method

During the final harvest of the sand-grown trees a sample of sand was taken from each of the five pots per treatment for analysis of organic content. After all of the roots had been removed by passing the sand through a 4 mm sieve, the sand was

homogenised and total 'fresh' mass measured. A sub-sample was taken and stored at $-20\text{ }^{\circ}\text{C}$ until the analysis. One sample of 500 g of the sand from each of the five replicates per treatment was placed in an oven at $80\text{ }^{\circ}\text{C}$ for 24 hours then re-weighed and the water content determined. Then 100 g of each of the oven-dried sand samples was placed in a muffle furnace at $400\text{ }^{\circ}\text{C}$ overnight, cooled and re-weighed to give loss on ignition. Four 100 g samples of clean, unused sand were also used to give the baseline amount of organic matter present in the sand prior to use.

Results

The loss on ignition of the sand samples was very low: the clean, unused sand lost 0.04 to 0.06 % of it's mass, while the samples from the pots lost 0.15 to 0.2 % after taking into account the baseline loss. This percentage loss was multiplied by the mass of sand in each pot to give the loss per pot. Analysis of variance showed no significant differences attributable to $[\text{CO}_2]$ or nutrient treatment. Loss on ignition is equivalent to the amount of organic matter in the sand and was independent of the size of the root system. Root systems of **EH** trees were more than twice the size of **AL** trees and yet the organic matter per pot was the same.

Expressing the loss on ignition in terms of the amount of root extracted from each pot gives an indication of any differences between treatments in the production of organic matter per unit root mass (Figure 7.14). Both $[\text{CO}_2]$ ($P < 0.005$) and nutrient treatments ($P < 0.01$) significantly influenced the amount of organic matter in the sand per unit mass of root: **L** and **A** both increased the amount. By the end of the experiment between 22 and 38 % of the organic matter in the rhizosphere was outwith the living root system.

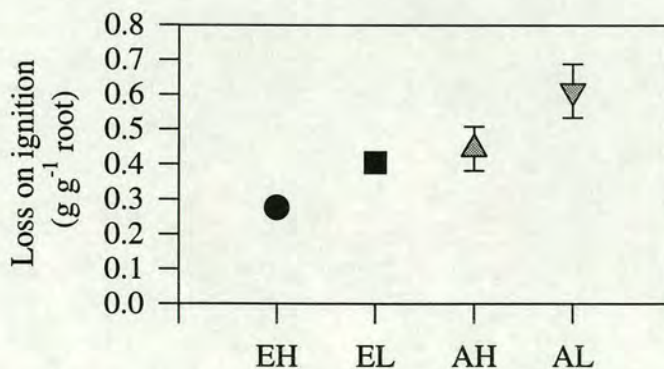


Figure 7.14 Loss on ignition from the sand after roots were removed at harvest 6 relative to the dry mass of root removed from the pot. Means \pm 1 SEM, $n = 5$.

7.7.2 Soluble carbohydrate in sand

Method

Fifty grams of the 'fresh' sand from each of the five samples per treatment, stored in the $-20\text{ }^{\circ}\text{C}$ freezer (see 7.7.1), was placed in a 50 cm^3 beaker to which 20 cm^3 of double-distilled water was added. The mixture was stirred four times during the subsequent 30 minute extraction period. The solution was transferred to a centrifuge tube and centrifuged at 4000 rpm for 20 minutes then the supernatant was filtered ($20\text{ }\mu\text{m}$) and run through the HPLC without dilution. The concentration of soluble sugars was calculated per gram of dry sand using the fresh/dry relationship obtained previously (see 7.7.1). Four replicate samples of fresh, unused sand were also analysed to detect any background amounts of soluble carbohydrates in the sand.

Results

There was no detectable soluble carbohydrate in the clean, unused samples of sand but there were measurable amounts in the samples in which trees had been grown. The majority of the soluble carbohydrate was glucose (39-53 %) followed by fructose (17-26 %) then inositol (2-10 %) and finally four unknown compounds made up the remaining (12-20 %). Figure 7.15 shows the concentration of total soluble carbohydrates per unit mass of sand for each of the four treatments, showing a clear effect of $[\text{CO}_2]$, with **E** having approximately three times as much soluble carbohydrate per unit mass of dry sand as the **A** treatment ($P < 0.002$). Nutrient supply had no influence on the amounts of soluble carbohydrates found in the sand.

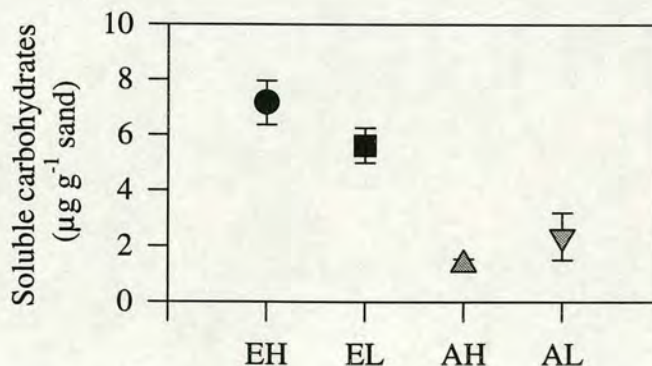


Figure 7.15 Soluble carbohydrate content in the sand at the end of the year. Means \pm 1 SEM, $n = 5$.

Each tree was growing in approximately 5 kg of sand so the total amounts of soluble carbohydrate per pot were of the order 40 mg, compared to the root mass of 20-40 g.

Figure 7.16 shows the amount of soluble carbohydrate found in the sand expressed per unit mass of root extracted from the sand. Trees grown in elevated $[\text{CO}_2]$ had twice as much soluble carbohydrate (0.8 mg g^{-1}) per unit root mass as those grown in ambient $[\text{CO}_2]$ (0.4 mg g^{-1}) ($P < 0.02$). There was also an indication that **L** trees had more than **H** trees but this was not statistically significant ($P < 0.14$).

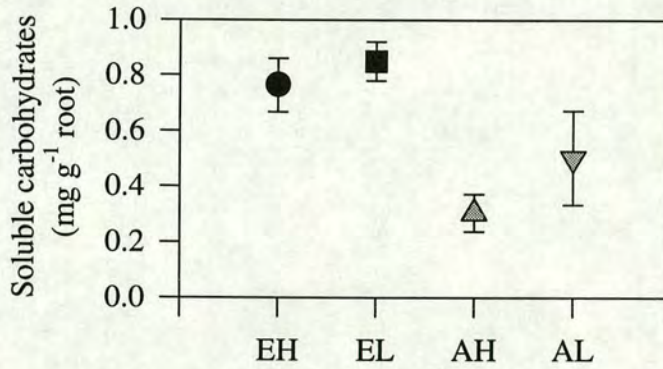


Figure 7.16 Soluble carbohydrate content in the sand per unit dry mass of root. Means \pm 1 SEM, $n = 5$.

Dividing the amount of soluble carbohydrate found in the sand by the loss on ignition gives an estimate of the concentration of soluble carbohydrate in the organic matter in the sand (0.02-0.08%), which is two orders of magnitude less than that found in roots (2-8 %). The concentration of soluble carbohydrate in the sand organic matter was significantly higher ($P < 0.005$) in the **E** pots than in the **A** pots by a factor of three (Figure 7.17). Nutrient treatment did not have a significant effect on the concentration of soluble carbohydrates.

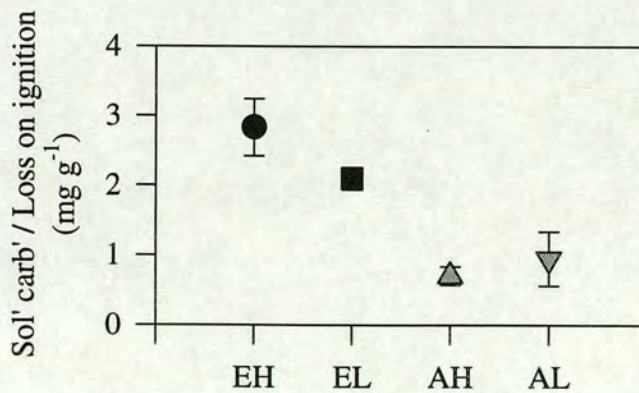


Figure 7.17 Soluble carbohydrate relative to loss on ignition in sand. Means \pm 1 SEM, $n = 5$.

7.7.3 Discussion

The organic matter found in the sand at the end of the experiment would have been composed of mucilage, sloughed off dead cells, microbes, amino acids, carbohydrates and fungal hyphae. Similar amounts were found in the pots of all treatments regardless of the differences in root sizes (Figure 6.4) so when expressed per unit root mass there were significant differences between treatments such that **A** and **L** trees produced more soil organic matter per unit root than **E** and **H** trees.

One explanation, is that **A** and **L** trees had a faster rate of root turnover, *i.e.* higher rates of root initiation and mortality, thus maintaining a relatively small live root system at any point in time while still exploring the rooting volume. Whereas, **E** trees could afford to maintain a larger root system (both in terms of cost of production and maintenance) and so roots could be kept alive for longer. By contrast, **H** trees did not need as large or active a root system since nutrients were more readily available (see Chapter 6 for a more detailed discussion on allocation).

The soluble carbohydrate concentration in the 'soil' organic matter was much higher in the **E** trees than the **A** trees. This may be the result of increased root exudation by trees which have a lot of carbohydrate available to utilise for nutrient acquisition. There was evidence of mycorrhizas present in the sand-grown trees, indicated by typically shaped root tips and hyphal networks on the surface of the sand. Although mycorrhizal infection was not quantified, its presence does lend credibility to the hypothesis that the **E** trees were supplying soluble carbohydrates to mycorrhizas to enhance nutrient acquisition.

Even though the concentration of soluble carbohydrates in 'soil' organic matter was higher in **E** than **A** pots, concentrations in both were much lower than in living roots. Low soluble carbohydrate content of rhizosphere organic matter may indicate that it was partially decomposed dead matter (cellulose, lignin, fungal chitin etc.), where easily digested soluble compounds had been metabolised by the soil microbes.

7.8 A/C_i responses of individual shoots

7.8.1 Methodology

A portable gas photosynthesis system (CIRAS, PP systems, Hitchin, UK) with a conifer cuvette was used to measure assimilation (A) in relation to intercellular space $[CO_2]$ (C_i) on shoots of six trees from each treatment during the period 16-31 August 1995. At first, measurements were made in the glasshouse, but variable PPFD and temperature introduced too much variation and so the trees were taken into the laboratory to obtain more stable temperature and saturating PPFD. A mercury vapour lamp (Wotan HQI-R 250W/NDC, Wotan Lamps Ltd., UK) mounted above the cuvette supplied $1200 \mu\text{mol m}^{-2} \text{s}^{-1}$ at the shoot. An air conditioning system was used to keep the room temperature at about 18°C .

Shoots used for A/C_i responses were prepared at least two days before the first measurement was made. One current-year-shoot from each of the 24 trees was selected and needles removed to permit a good chamber seal. The length, width and thickness of 15 of the needles that were removed were measured and the projected area per needle calculated as the length \times width. The needles were then oven dried at 70°C for 48 hours and weighed and the specific leaf area calculated. The number of needles remaining on each shoot were counted permitting the calculation of the total project needle area within the cuvette.

Trees were taken into the laboratory at least eight hours prior to measuring them so that they could adjust to the change in conditions. The CIRAS is designed to be able to make unattended measurements of A/C_i response curves and can be pre-programmed to step through a series of CO_2 concentrations. The CO_2 concentration of air entering the cuvette was started at $1700 \mu\text{mol mol}^{-1}$ and left for 30 minutes to allow the shoot to adjust to the conditions within the cuvette. The CO_2 concentration was then dropped to $0 \mu\text{mol mol}^{-1}$ in 10 steps each one being held for about 5 minutes until a steady state was obtained.

7.8.2 Analysis of A/C_i response functions

There was considerable variation in the A/C_i responses between shoots and in many cases, because the stomata were partially closed, the C_i did not exceed $500 \mu\text{mol mol}^{-1}$ despite a C_a of $1800 \mu\text{mol mol}^{-1}$ (Figure 7.18). Given the limited amount of data at high values of C_i , it was decided that it would be inappropriate to attempt a complex analysis such as fitting the full Farquhar *et al.* (1980) model to the data.

However, the carboxylation limited section of the model was used to extract parameters from the data with $C_i < 300 \mu\text{mol mol}^{-1}$.

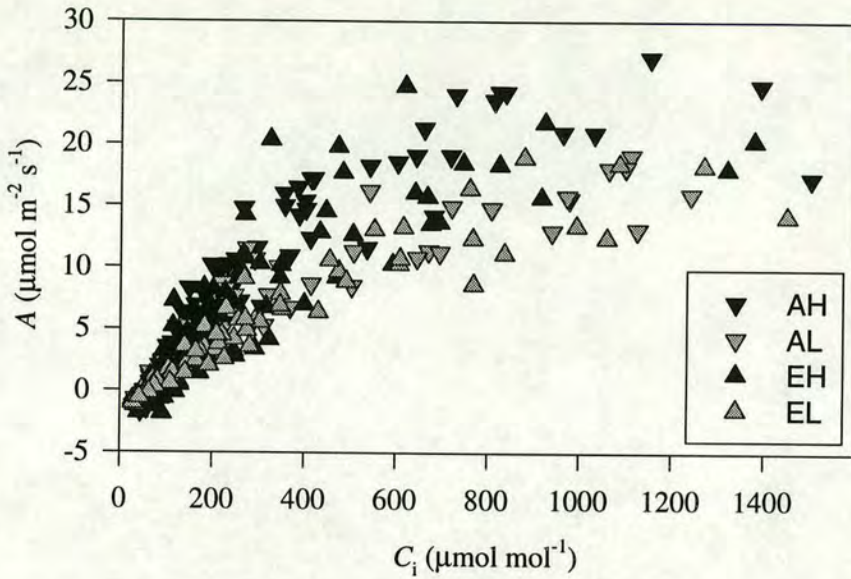


Figure 7.18 Assimilation v Internal CO_2 concentration (A/C_i) measured on current year shoots under saturating light. Six replicates per treatment.

The initial slope of the A/C_i has sometimes been called the carboxylation efficiency. Farquhar *et al.* (1980) suggested that at low C_i assimilation follows the kinetics of RuBP carboxylase-oxygenase (Rubisco) and is determined by the RuBP saturated rate of the enzyme. Under these conditions CO_2 assimilation (A) may be expressed as:

$$A = V_{\text{cmax}} \frac{(C_i - \Gamma^*)}{(C_i + k_c(1 + O/k_o))} - R_d \quad (1)$$

where V_{cmax} is the maximum rate of carboxylation and k_c and k_o are Michaelis constants for carboxylation and oxygenation, respectively, and were corrected for temperature following Farquhar *et al.* (1980). R_d is the rate of CO_2 evolution in the light resulting from processes other than photorespiration. O is the oxygen concentration, taken as $0.21 \text{ mol mol}^{-1}$. Γ^* is the CO_2 compensation concentration in the absence of mitochondrial respiration.

V_{cmax} and R_d were obtained for each individual A/C_i response using non-linear regression (Proc NLIN, SAS institute Inc., Cary, NC).

V_{cmax} varied with nutrient treatment ($P < 0.05$) and slightly but not significantly with CO_2 treatment. The **H** treatment had larger V_{cmax} than **L**, and **AH** larger than **EH** (Figure 7.19A). This reduction in carboxylation efficiency in shoots grown with a

low nutrient supply has frequently been observed (Wong, 1979; von Caemmerer & Farquhar, 1981) and has also been seen in plants grown in elevated CO_2 , where it is an indication of down-regulation of photosynthesis. This reduction in V_{cmax} may be a result of reduction in total Rubisco content or reduction in the activity of Rubisco (see review by Bowes, 1991).

R_d was higher in **H** trees than **L** trees ($P > 0.001$) but there was no significant CO_2 treatment effect (Figure 7.19B). This higher mitochondrial respiration in needles of **H** trees thus is related to the leaf N content, as will be shown later (also see Chapter 8 for discussion of respiration).

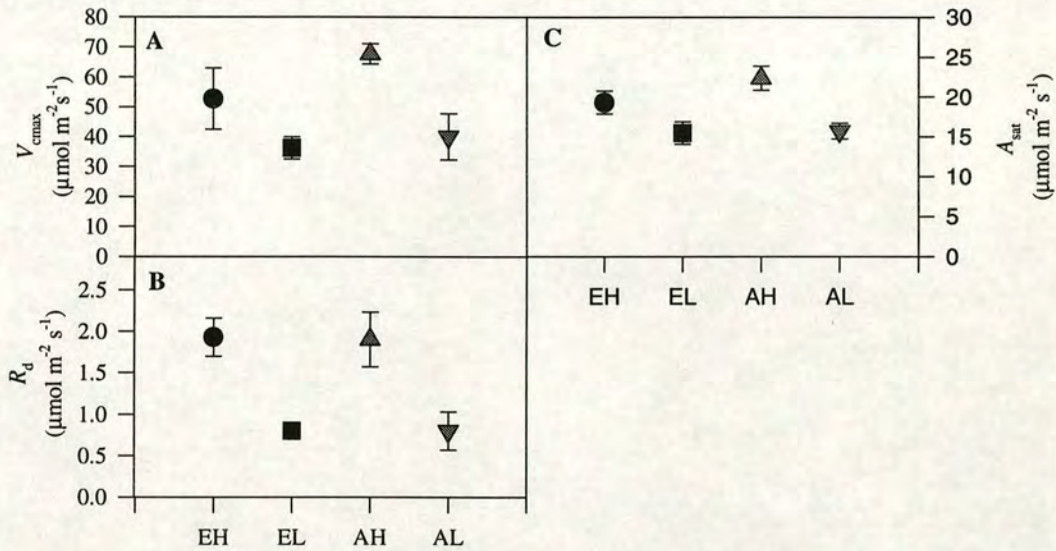


Figure 7.19 (A) V_{cmax} and (B) R_d extracted from A/C_i response curves ($C_i < 300$). (C) Saturated photosynthetic rate (A_{sat}), the mean value of A for $C_i > 500$. $n = 4-6$, means ± 1 SEM.

The saturated photosynthetic rate A_{sat} was taken as the mean value of assimilation when C_i was greater than $500 \mu\text{mol mol}^{-1}$ (Figure 7.19C). **H** had higher A_{sat} than **L** ($P < 0.001$) but the CO_2 treatments were not significantly different. At high C_i assimilation becomes limited both by RuBP regeneration, which is largely dependant on light reactions and electron transport and possibly by P_i limitation, as an imbalance between triose phosphate production in the Calvin cycle and utilisation, in sucrose and starch formation, leads to a feedback inhibition (Sharkey, 1985; Harley & Sharkey, 1991; Harley *et al.*, 1992). This is discussed in more detail later.

7.8.3 Nutrient analysis of A/C_i shoots

After the A/C_i response had been measured the needles were removed dried and analysed for nutrients. Figure 7.20 shows the nutrient concentrations per unit leaf area while Table 1 shows the results of the statistical analysis. There was significantly more nitrogen in the **H** needles than the **L** needles but $[CO_2]$ did not affect the nitrogen content per unit leaf area. **E** needles had significantly higher concentrations of calcium than **A** needles but the concentrations were the same for needles from both nutrient supply rates. The other nutrients showed an interaction between nutrient supply rate and $[CO_2]$ in all cases **AH** had higher concentrations than **AL** but **EH** and **EL** had similar concentrations.

Table 1 Statistical significance for nutrients from the shoots used in the A/C_i measurements. n.s indicates $P > 0.1$.

	N	P	Ca	Mg	K
$[CO_2]$	n.s	n.s	0.093	n.s	n.s
Nutrient	0.0001	0.0124	n.s	0.0001	0.0099
$[CO_2]$ *Nut	n.s	0.0163	n.s	0.0595	0.0165

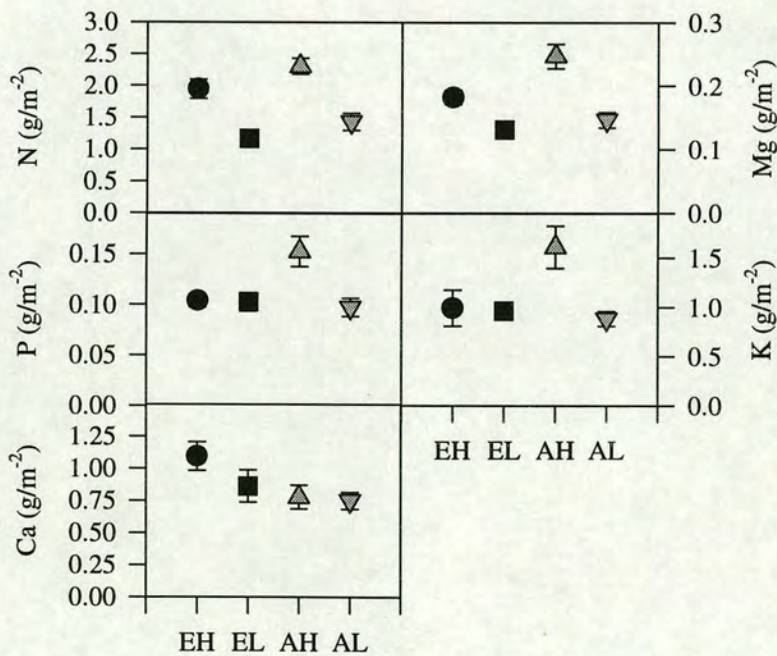


Figure 7.20 Nutrient content of the needles from the shoots used to measure A/C_i responses. Means \pm 1 SEM, $n = 6$.

7.8.4 Chlorophyll content of A/C_i shoots.

Chlorophyll *a*, chlorophyll *b* and total chlorophyll were determined on fresh needles according to the method described by Porra *et al.* (1989) (see Chapter 3, 3.6.1).

Five needles from the same shoot were used to determine length, width, thickness and dry mass. Projected area was calculated as the width (at mid point) x length. Chlorophyll concentration was then calculated on an area basis.

H had more chlorophyll *a* and *b* than **L** ($P < 0.001$) but **E** and **A** were not significantly different. The **AH** needles had 25% more chlorophyll than the **AL** while the **EH** had 66% more than the **EL**. There were no significant differences in the chlorophyll *a/b* ratio (Figure 7.21).

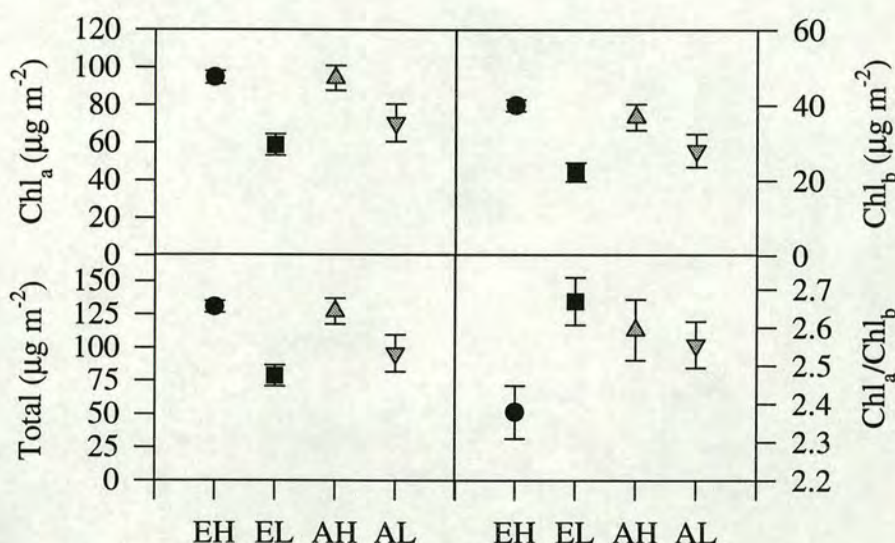


Figure 7.21 Chlorophyll content of needles used in A/C_i response measurements. Showing Chlorophyll *a* and *b*, total and *a/b* ratio. Means \pm 1 SEM, $n = 6$.

The chlorophyll concentration increased linearly with the nitrogen concentration such that chlorophyll was a constant proportion of total leaf nitrogen (Figure 7.22). There were no significant differences in the chlorophyll per unit total nitrogen (Table 2). This linear relationship between total leaf nitrogen and chlorophyll has commonly been seen when variation is caused by leaf age and nitrogen supply for plants grown in high PPFD (Evans, 1989).

Table 2 Total chlorophyll concentration per g of total nitrogen in needles used in A/C_i measurements; means \pm 1 SEM, $n = 6$.

	EH	EL	AH	AL
Chl / N ($\mu\text{g g}^{-1}$)	68.8 ± 4.6	69.1 ± 6.3	55.2 ± 3.0	65.9 ± 5.5

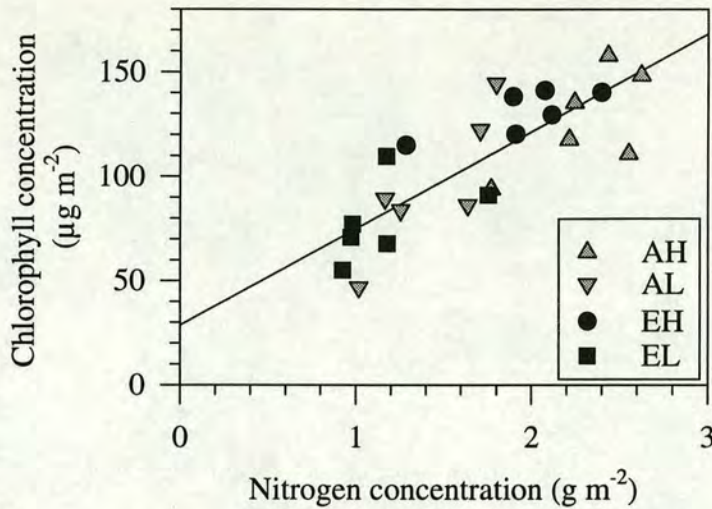


Figure 7.22 Chlorophyll concentration v nitrogen concentration for shoots used in A/C_i measurements. The regression is $\text{chl} = 28.6 + 46.4[\text{N}]$, $r^2 = 0.66$.

7.9 Discussion

7.9.1 Plant carbohydrates

In contrast to deciduous trees, conifers accumulate starch in mature needles in early spring (Little, 1970). At the onset of bud break, carbohydrates stored in these needles are mobilised and exported to the newly developing needles and meristems, which constitute a strong sink (Ericsson, 1978). Starch concentrations in needles during this experiment were consistent with these processes. Prior to bud burst one-year-old needles contained 15 - 20% starch followed by lower concentrations in developing needles. In Autumn starch concentrations in needles fell while those in roots rose, indicating probable translocation of carbohydrate to roots for the winter (Ford & Deans, 1977). Had the experiment continued through the winter and following spring needle starch concentrations almost certainly would have risen again as spruce growing in oceanic climates can have a positive carbon balance during all months of the year (Hagem, 1947,1962; Neilson *et al.*, 1972). In a study by Bradbury & Malcolm, (1978) during the period September to May, the largest increase in plant mass occurred during October, March and April but smaller increases occurred throughout the winter months.

Growth in elevated CO_2 usually leads to an increased rate of photosynthesis and an accumulation of carbohydrate which can lead to high concentrations of starch and soluble carbohydrates in leaves (Cave *et al.*, 1981; Madsen, 1969; Wulff & Strain,

1981). A plant can respond to the increased availability of carbohydrate in several different (and not mutually exclusive) ways:

- (a) Unused storage capacity could be utilised, both within the leaves and elsewhere in the plant.
- (b) New sinks could be initiated and the growth of existing sinks accelerated to utilise the extra photosynthate. The extent to which sink metabolism responds to increased availability of carbohydrate depends partly on genetic factors (e.g. determinate versus indeterminate growth) and partly on environmental variables (e.g. nitrogen availability, Stitt, 1991). When sink strengths are high, demand for photosynthate reduces starch pools, even in plants grown in elevated [CO₂]. Conversely, starch accumulation increases when sink demand is low (Clough *et al.*, 1981).
- (c) The rate of photosynthesis could be decreased by reduction in the amounts and activities of photosynthetic enzymes.

The extent to which these mechanisms may have played a role during this experiment are discussed below.

(a) Starch concentrations in roots were higher in **E** trees and **L** trees, both of which also had larger root:shoot ratios (see Chapter 6) giving a large storage pool in the root system.

(b) **H** trees had more meristems and grew faster than **L** trees (see Chapter 6) and so demand for photosynthate was high and foliar starch concentrations were low.

(c) Foliar starch concentrations were strongly influenced by nutrient supply rate and also by CO₂ concentration, with larger amounts of starch in **E** and **L** treatments, whereas soluble carbohydrate concentration was more strongly influenced by nutrient supply rate than CO₂ concentration. It is possible that in elevated CO₂ the soluble carbohydrate pools were saturated and no further response to nutrient was possible (see Figure 7.5). Maximum photosynthetic rates were significantly lower in **L** trees compared to **H** and only slightly lower in **E** trees compared to **A** despite high starch concentrations. The likely explanations for these responses are discussed below; firstly the effects of carbohydrate accumulation and secondly the effects of nutrients on photosynthetic performance.

7.9.2 Effect of carbohydrates on photosynthesis

Sucrose is synthesised in the cytosol from triose-phosphates, which are exported from the chloroplast via the phosphate translocator in exchange for P_i (Stitt *et al.*, 1987)(see Figure 7.23). It has been proposed that when sucrose synthesis is inhibited, there is an accumulation of phosphorylated metabolites in the cytosol and less P_i is recycled to the chloroplast leading to an inhibition of photosynthesis (Herold, 1980; Sharkey, 1985; Harley & Sharkey, 1991; Harley *et al.*, 1992). Sucrose synthesis is regulated by a balance between two opposing processes: one which increases the rate

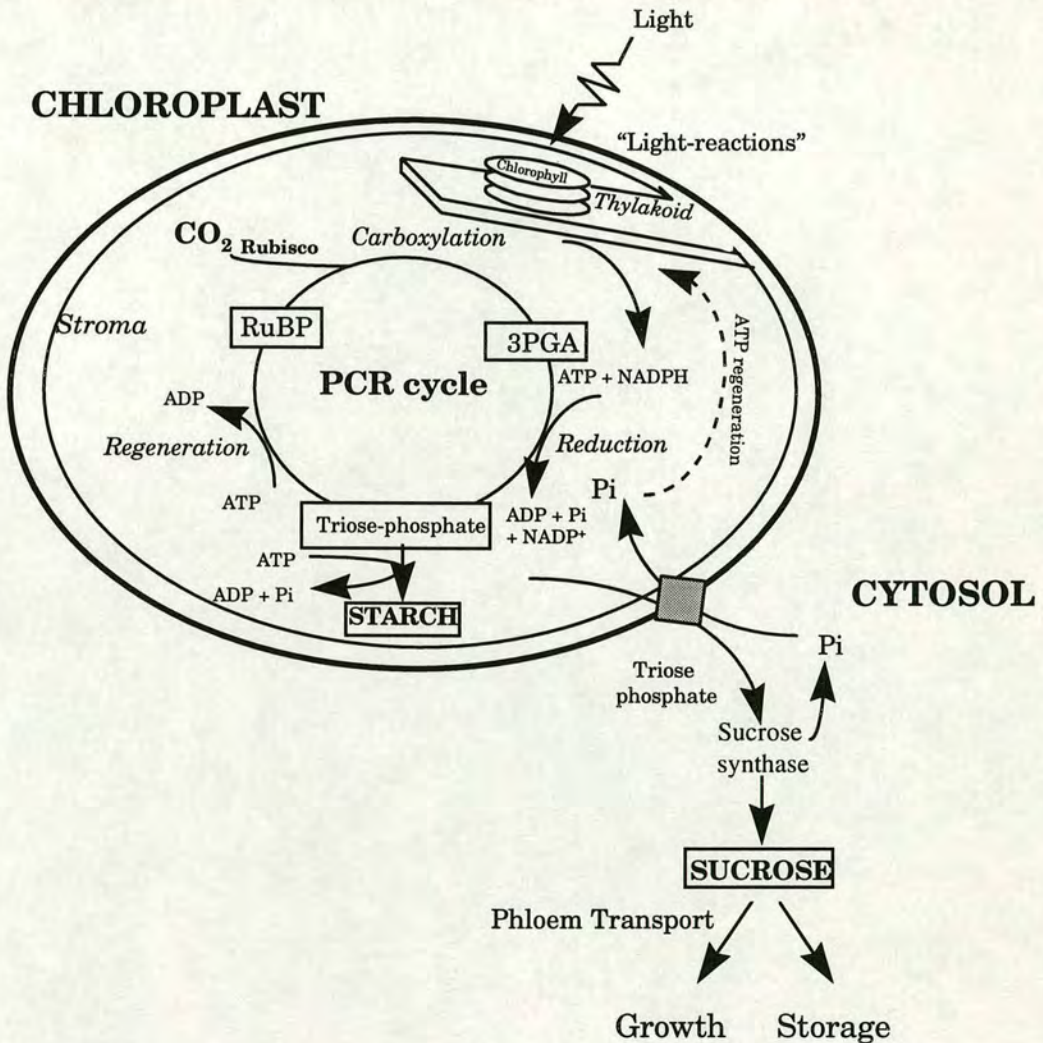


Figure 7.23 Diagram of a chloroplast showing the pathways of carbohydrates and P_i thought to be involved in feedback inhibition of photosynthesis (reprinted from Rey, 1997).

of sucrose synthesis in response to rising rates of photosynthesis and another which inhibits sucrose synthesis when sucrose accumulates in the leaf (Stitt, 1991). The interaction between these processes is crucial in determining whether an

accumulation of sucrose leads to an inhibition of photosynthesis, or whether it leads to a change of partitioning (*i.e.* more starch and less sucrose production), but is overridden before photosynthesis becomes inhibited. Starch synthesis may be stimulated by feedback regulation of sucrose synthesis when a reduction in P_i concentration in the cytosol leads to less trios-phosphate moving out of the chloroplast and consequently more being directed into the production of starch within the chloroplast. An increase in starch synthesis maintains stroma P_i cycling and allows photosynthesis to continue; however, if starch synthesis also becomes limited then photosynthesis will be inhibited. There is increasing evidence that limitations imposed on assimilation of CO_2 caused by trios-phosphate utilisation may be a common occurrence under conditions of high C_i and high irradiance (Harley *et al.*, 1992).

Needles in this experiment did not accumulate very high starch concentrations even when grown in elevated $[CO_2]$, except in the **EL** treatment where concentrations in new needles initially rose to 25%. In fact from July onwards starch concentrations declined while soluble carbohydrate concentrations increased, such that total non-structural carbohydrates remained fairly constant. The lack of diurnal variation in starch concentration suggests that photosynthates were leaving the chloroplasts as they were produced. This hypothesis is consistent with the diurnal changes in foliar soluble carbohydrate concentrations which varied considerably throughout the day, from 3% to 6% in **H** and from 6% to 12% in **L** trees (Figure 7.7). Spruce trees commonly store starch in their needles and concentrations of 25% are not unusual so it would seem unlikely that they have evolved in such a way that this would limit their ability to assimilate carbon. Large, unusually shaped starch grains have been postulated to cause damage, either through contortion of the chloroplast grana or through actual disruption of chloroplasts (Cave *et al.*, 1981; Wulff & Strain, 1981) but I suggest that unless starch concentrations are very high they will not influence assimilation rates, at least in trees that store starch in their leaves. The large diurnal variation in soluble carbohydrates especially seen in trees growing in elevated CO_2 suggests an imbalance between sucrose production and utilisation/translocation. Körner *et al.* (1995) suggested that increases in leaf carbohydrate concentrations in elevated $[CO_2]$ may be caused by the inability of phloem loading to keep pace with carbohydrate production. They found that plants using symplastic phloem loading (trees) tended to accumulate higher concentrations than those using apoplastic loading (herbaceous species).

I have used a very simple model, in which export of soluble carbohydrate from needles is proportional to concentration within the needles, to test if the observed increase in soluble carbohydrates in **E** trees can be attributed solely to increased photosynthetic rates (see Appendix F). Assuming soluble carbohydrates do not build up from one day to the next, production and export over 24 hours are equal and the higher photosynthetic rates in **E** trees (see Chapter 8) must have been balanced by higher rates of export. The fact that the minimum diurnal concentration was higher in **E** than **A** indicates either that the rate of export was inadequate to bring the concentration down overnight, before photosynthesis in the morning started to increase it again, or that the needles had adjusted the 'operating point', *i.e.* the foliar concentration of soluble carbohydrates required to maintain osmotic potential and physiological processes. Results from the model suggest that the increased minimum diurnal concentration and larger diurnal amplitude observed in trees grown and measured in elevated [CO₂] can be explained by an increase in photosynthetic rate without any modification to the translocation system or the 'operating point'. Thus, phloem loading and sink limitations are not needed to explain the observed trends in foliar soluble carbohydrate concentrations, but this does not mean that they did not contribute.

If translocation rate is related to foliar concentration then the decrease in starch and increase in soluble carbohydrate concentrations as the season progressed may have been related to source driven increase in export of carbohydrates from the needles.

The lack of diurnal variation in starch concentration and large variation in soluble carbohydrates suggests that starch is used for long term storage in needles while soluble carbohydrates are used for short term storage and translocation. However, once storage pools are full, and if sinks for the carbohydrate produced are not available, or if transport cannot keep pace with carbohydrate production, there may be feedback inhibition of photosynthesis.

7.9.3 Effects of nitrogen on photosynthesis.

From the steady state model of photosynthesis (Farquhar *et al.*, 1980), the A/C_i response consists of two phases, an initial linear response where the carboxylation efficiency (*i.e.* the amount of active Rubisco) determines the slope $\delta A/\delta C_i$, followed by an inflection to a slower rise where A is limited by the rate of regeneration of RubP, which depends on the rate of electron transport, a function of PPF, and on the availability of P_i (Figure 7.24). Although the regeneration of RuBP requires the other enzymes of the Calvin cycle, they represent only a small fraction of the protein

involved, because of the dominance of the thylakoid proteins. Thus photosynthesis at low C_i correlates with the amount and activity of Rubisco, while at high C_i it correlates with the chloroplast/thylakoid protein complexes and hence with the thylakoid nitrogen content (Evans, 1989).

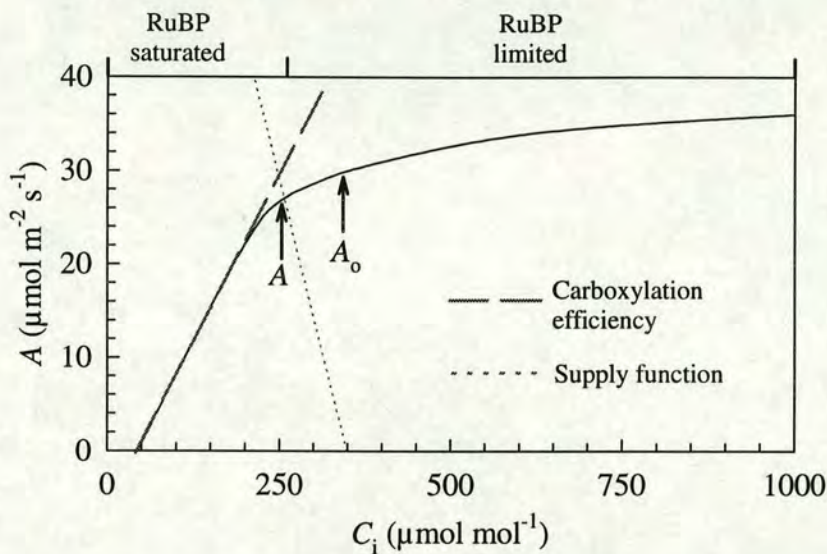


Figure 7.24 Generalised response of A to C_i , indicating the points used in the calculation of stomatal limitation. Where A indicates the photosynthetic rate with C_a of $350 \mu\text{mol mol}^{-1}$ and A_o the rate with a C_i of $350 \mu\text{mol mol}^{-1}$ (adapted from Long *et al.*, 1993)

It has been suggested that plants are able to optimise the allocation of resources, particularly nitrogen, in order to preserve a balance between carboxylation (*i.e.* Rubisco) and light-harvesting and electron transport (*i.e.* chlorophyll/thylakoid proteins). In support of this Wullschleger (1993) found in a retrospective study of A/C_i response curves of 109 species a strong correlation between maximum carboxylation rate and maximum rate of electron transport. As $[\text{CO}_2]$ increases so the carboxylation/oxygenation of Rubisco moves in favour of carboxylation leading to an increase in the efficiency of Rubisco. If the optimisation theory is correct, this should lead to re-partitioning of nitrogen from Rubisco to other processes such as light harvesting and electron transport. Acclimation to growth at elevated $[\text{CO}_2]$ has been commonly, but not invariably, shown to involve a decrease in Rubisco activity (see review by Bowes 1991). However a decrease in activity does not necessarily relate to a decrease in Rubisco protein content. The activation state of Rubisco depends on a complex mechanism involving Mg^{2+} , CO_2 and Rubisco activase (see review by Bowes 1991). Rubisco accounts for 10-30% of total leaf nitrogen and to a first approximation, thylakoid nitrogen is proportional to the chlorophyll content ($50 \text{ mol thylakoid N mol}^{-1} \text{ Chl}$) (Evans, 1989).

The decrease in the maximum carboxylation rate, V_{cmax} (Figure 7.19A), and the decrease in the maximum rate of assimilation at saturating PPFD and high C_i , A_{sat} (Figure 7.19C) are evidence for strong down-regulation of photosynthesis in response to nutrient treatment but only weak down-regulation in response to CO_2 treatment.

As would be expected, both V_{cmax} and A_{sat} correlate strongly with leaf nitrogen concentration as shown in Figure 7.25 and Figure 7.26, respectively, but in both cases the relationship is independent of growth $[\text{CO}_2]$. Harley *et al.* (1992) found similar results on cotton but in their case they did find a slight decrease in V_{cmax} / leaf nitrogen, which could be interpreted as a decrease in Rubisco activity/ leaf nitrogen in leaves grown in elevated $[\text{CO}_2]$. The fact that all treatments fall on the same line, which passes close to the origin indicates that the V_{cmax} /leaf nitrogen ratio is the same, regardless of growth $[\text{CO}_2]$ or nutrient supply. This suggests that observed acclimation of photosynthesis to nutrient and $[\text{CO}_2]$ can be explained by changes in leaf nitrogen concentration, associated with changes in Rubisco amount.

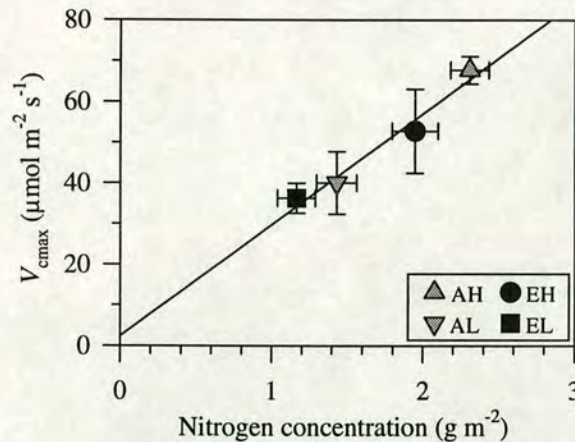


Figure 7.25 Relationship between the initial slope of the A/C_i function and nitrogen concentration of needles for shoots used in A/C_i measurements. Mean \pm 1 SEM, $n = 6$. The dashed line is the regression $V_{\text{cmax}} = 2.3 + 27.3[\text{N}]$, $r^2 = 0.96$.

The relationship between the saturated rate of photosynthesis, A_{sat} , and leaf nitrogen concentration (Figure 7.26A) and that between A_{sat} and chlorophyll concentration (Figure 7.26B) agree with the hypothesis that A_{sat} is limited by RuBP regeneration which is dependent on light harvesting and electron transport and thus on the thylakoid chlorophyll-protein amounts. As with V_{cmax} , all treatments fell on the same line, but in this case the line has a positive intercept. Thus an increase in leaf nitrogen concentration led to a proportionally large increase in V_{cmax} but a smaller proportional increase in chlorophyll e.g. an increase from 1% to 2% N led to a 100% increase in V_{cmax} (from Figure 7.25) but only a 71% increase in chlorophyll

concentration (from Figure 7.22). Therefore an increase in leaf nitrogen concentration led to a proportional increase in Rubisco activity but a disproportionately lower increase in chlorophyll and probably thylakoid proteins. Assuming a constant fraction of Rubisco is active this indicates a change in nitrogen partitioning whereby an increase in leaf nitrogen concentration leads to a decrease in the nitrogen invested in light harvesting and electron transport relative to that invested in carboxylation. Furthermore, it appears that neither growth $[CO_2]$ nor nutrient supply rate directly altered the partitioning of nitrogen and any changes were a result of changes in nitrogen concentration. These results are consistent with the idea that adding carbon *via* elevated $[CO_2]$ causes the trees to become nutrient deficient so that they exhibit some of the same responses as trees grown in ambient air with a low rate of nutrient supply.

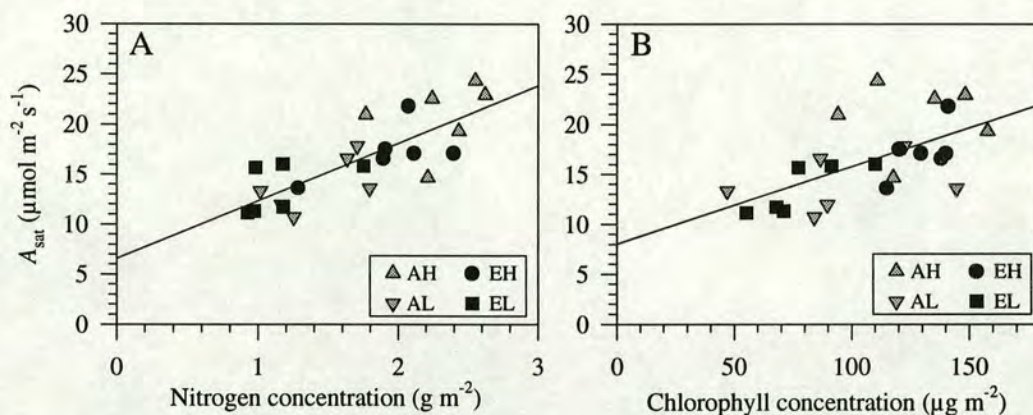


Figure 7.26 Maximum rate of CO_2 assimilation A_{sat} against leaf nitrogen concentration (A) (regression $A_{sat} = 6.6 + 5.7[N]$, $r^2 = 0.62$) and against leaf chlorophyll concentration (B) (regression $A_{sat} = 8.0 + 0.078[Chl]$, $r^2 = 0.37$) for needles used in A/Ci measurements.

Day respiration, R_{day} , also showed a strong response to nutrient treatment and plotting R_{day} against leaf nitrogen again shows an interesting relationship (Figure 7.27). R_{day} increased with increasing leaf nitrogen concentration but **E** trees had less leaf nitrogen than **A** at the same R_{day} , and, therefore, would have a higher R_{day} at the same nitrogen concentration. The response of dark respiration to elevated CO_2 is currently in debate with both increases and decreases being observed (see Chapter 8 for a more detailed discussion). However, in this case R_{day} is obtained at saturating light and therefore may not relate closely to respiration measured in the dark (Villar *et al.*, 1995). **E** needles had higher starch and soluble carbohydrate concentrations than **A** needles and the increased rates of respiration per unit nitrogen may reflect higher costs in phloem loading. Azcon-Bieto and Osmond (1983) found a stimulation

of plant respiration by the non-structural carbohydrate status in illuminated wheat leaves.

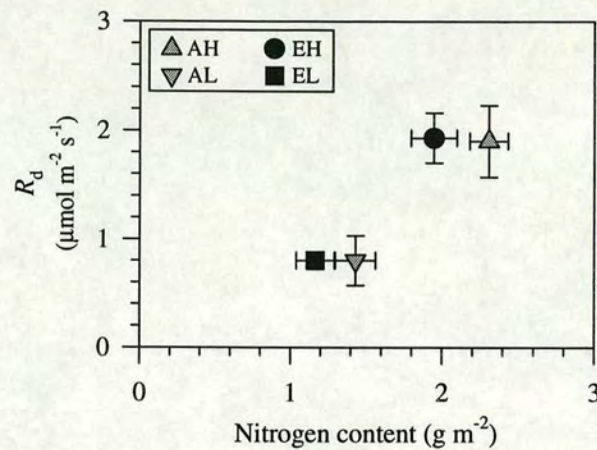


Figure 7.27 The relationship between R_d and leaf nitrogen concentration. R_d was obtained by non-linear regression from A/C_i response curves. Mean \pm 1 SEM, $n = 6$.

In summary: the down-regulation of photosynthesis observed in response to growth in elevated CO_2 concentrations and low nutrient supply rate can be explained by the reduction in the leaf nitrogen concentrations. Partitioning of nitrogen between Rubisco and light harvesting and electron transport processes depended on leaf nitrogen concentration: increasing nitrogen concentration decreased the proportion of nitrogen allocated to light harvesting relative to carboxylation. Elevated CO_2 did not appear to effect this partitioning directly, but only indirectly as a result of reducing leaf nitrogen concentrations which decreased carboxylation relative to light harvesting.

7.10 Conclusions

The starch concentration was higher in trees grown in elevated CO₂ and trees grown at low nutrient supply rates. Starch concentrations were high at the beginning of the year then fell as reserves were used for growth. This, plus the lack of diurnal variation in foliar starch concentrations indicates that starch is used as a long term storage pool and not for short term buffering of photosynthetic production.

Foliar soluble carbohydrate concentrations were higher in elevated CO₂ trees and only showed a response to nutrient supply rate in ambient trees, where they were higher in the low nutrient treatment. This suggests that if carbohydrate production exceeds nutrient supply then carbohydrate concentrations can build up but storage pools may become saturated especially at elevated CO₂ concentrations.

Foliar soluble carbohydrate concentrations showed a large diurnal variation in amplitude, which was largest in the elevated CO₂ trees. The diurnal variations in soluble carbohydrate concentrations and differences in size of those concentrations between treatments suggest that soluble carbohydrates are used as temporary storage to buffer the effects of photosynthesis and translocation. The higher concentrations in needles of trees grown at elevated CO₂ can be attributed to the increased photosynthetic rates found in those needles and do not necessarily indicate sink or transport limitation.

No evidence was found for a reduction in photosynthesis in response to foliar carbohydrate concentrations. The effect of elevated CO₂ and nutrient supply on photosynthesis can be explained by changes in leaf nitrogen concentrations.

Partitioning of nitrogen between carboxylation (Rubisco) and RuBP regeneration (thylakoid/chlorophyll-protein) was not directly affected by CO₂ concentration but was influenced by leaf nitrogen concentrations such that proportionately more nitrogen was allocated to carboxylation than to RuBP regeneration as leaf nitrogen concentration increased.

There was more organic matter in the sand per unit root mass in ambient and low nutrient than in elevated and high nutrient treatments. This may have been a result of changes in fine root turnover and the costs of maintaining a large root system.

There were higher concentrations of soluble carbohydrates found in the sand of trees grown in elevated CO₂, which may be a result of increased root exudation from trees which have an excess of photosynthate.

CHAPTER 8

CO₂ and H₂O Fluxes From Seedling Trees

8.1 Measurements of CO₂ and H₂O exchange of whole trees

This chapter describes the measurement and analyses CO₂ fluxes measured using the whole tree chamber described in Chapter 5. A carbon budget is derived from measured CO₂ fluxes, estimates of tree growth and changes in soil organic matter.

8.1.1 Measurement protocol

The aim was to determine diurnal fluxes of CO₂ into and out of the tree and, since photosynthesis and respiration vary with time of day, it was necessary to measure each tree for at least 24 hours. Furthermore, to determine if acclimation to CO₂ had occurred it was necessary to measure trees at both the growth concentration and the reciprocal concentration, therefore trees were placed in the chamber for 48 hours. The first 24 hours were at the growth CO₂ concentration *e.g.* **A**, and the second at the reciprocal concentration *e.g.* **E**.

Whole tree CO₂ fluxes were measured during the period from June to September 1995. Trees were selected for measurement from each of the treatments in such a way that the selected trees were evenly distributed amongst the open top chambers and those due for harvest had been measured prior to the harvest dates. Six of each of ambient [CO₂]-low nutrient (**AL**), ambient [CO₂]-high nutrient (**AH**), elevated [CO₂]-low nutrient (**EL**) and elevated [CO₂]-high nutrient (**EH**) trees growing in sand culture were measured in this system.

8.1.2 Determination of leaf area and plant mass

Trees were harvested up to two months after they were measured in the chamber and so the mass of each tree component (needle, wood, root) at the time of the flux measurement was obtained by back-calculating from the final harvest using the

growth rate, determined from the harvests, for trees in that particular treatment. The projected needle area was calculated from needle dry mass using the specific leaf area determined from six sub-samples of current year needles obtained for each treatment in August (see Chapter 7, 7.8.1).

The following points are relevant with respect to interpreting the CO₂ exchange data; **H** trees were larger than **L** trees and **E** trees larger than **A** trees (Figure 8.1). There were differences in the root to shoot ratio with **L** trees having a relatively larger root system than **H** trees and **E** larger than **A** (Table 1). Furthermore, the specific leaf area was higher in the **A** than the **E** treatment and also higher in the **H** than the **L** treatment. Chapter 6 describes the harvest data in more detail.

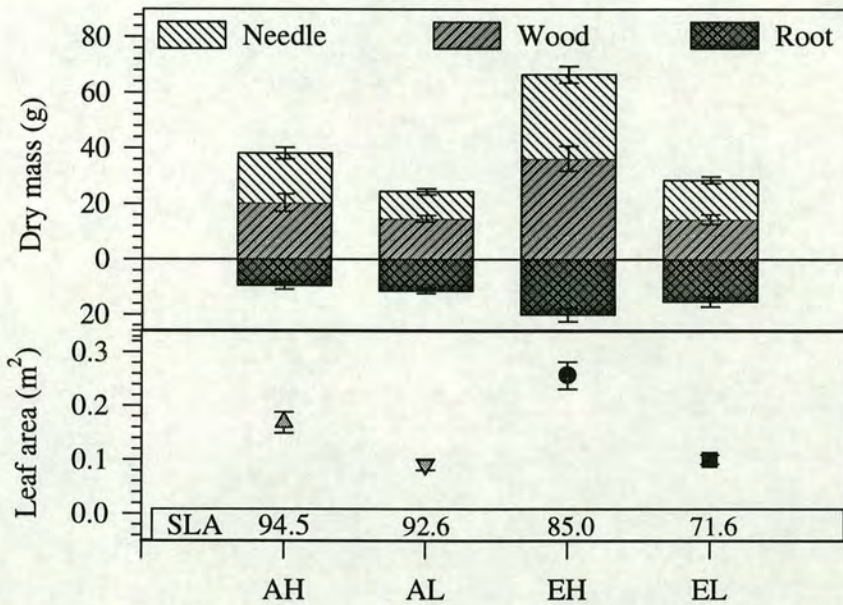


Figure 8.1 Mean dry mass of tree parts (upper) and leaf area (lower) back-calculated to the time of gas exchange measurements for the four treatments. Means \pm 1 SEM, $n = 6$. The specific leaf area ($\text{cm}^2 \text{g}^{-1}$) determined from a sub-sample of needles is also shown.

Table 1 Root fraction at the time of gas exchange measurements. Mean \pm 1 SEM, $n = 6$.

	AH	AL	EH	EL
Root fraction	0.20 ± 0.016	0.32 ± 0.024	0.23 ± 0.007	0.35 ± 0.034

8.1.3 Environmental conditions

June to September 1995 was a particularly hot, sunny summer. Figure 8.2 shows the air temperature, pot temperature, vapour pressure deficit (VPD) and photosynthetically active photon flux density (PPFD) within the measurement chamber during the measurements. Air and pot temperatures are shown for both daytime (PPFD > 10 $\mu\text{mol m}^{-2} \text{s}^{-1}$) and night-time (PPFD < 10 $\mu\text{mol m}^{-2} \text{s}^{-1}$) while VPD and PPFD are shown for daytime only. The missing data between days 180 and 205 was a period when tests on the chamber were being made.

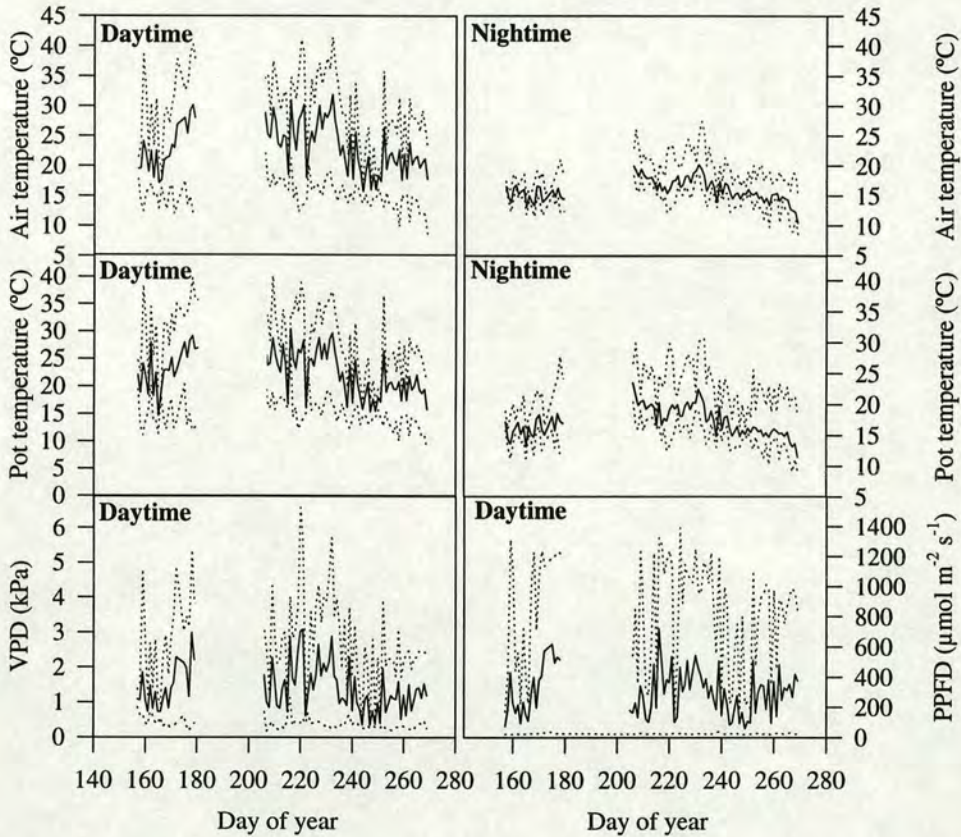


Figure 8.2 Environmental conditions within the measurement chamber during the measurement period. Daytime was defined as PPFD > 10 $\mu\text{mol m}^{-2} \text{s}^{-1}$. Lines indicate maximum, mean and minimum values.

Mean daytime air temperature ranged from 20-30 °C but under extreme conditions of high ambient temperature and strong sunshine temperatures within the chamber reached almost 40 °C. The conditions under which the measurements were made were similar to those in which the trees were growing (Figure 5.3) and so the trees should have been acclimatised to them. Attempts to reduce the high daytime temperatures included adding an extra fan to direct cool air from outside the

glasshouse onto the outside of the chamber and shading the lower compartment to reduce the radiation-load on the black pot.

Pot temperatures were measured close to the center of the pot with a PRT probe and, despite the mass of sand and water within the pots (5 - 6 kg) and shading from direct radiation loading, they still fluctuated quite widely throughout the day.

Mean daytime vapour pressure deficits ranged from 0.5 to 3 kPa, with extreme values exceeding 5 kPa. The distribution was highly skewed with median 0.89 kPa and upper 75% quartile 1.7 kPa and 90% of the daytime VPD was less than 2.7.

Maximum PPFD within the chamber exceeded 1000 $\mu\text{mol m}^{-2} \text{s}^{-1}$ on most days but rarely attained higher values because of transmission losses through the acrylic roof of the glasshouse and chamber walls.

8.1.4 Typical data

The following figures show data collected for an ambient CO₂, low nutrition tree (AL) over a four day period in June 1995. The CO₂ concentration was switched between 350 $\mu\text{mol mol}^{-1}$ and 700 $\mu\text{mol mol}^{-1}$ and then back to 350 $\mu\text{mol mol}^{-1}$ during the period to investigate both the plant and the system behaviour. Maximum PPFD varied from day to day (Figure 8.3A) and rarely exceeded 1000 $\mu\text{mol m}^{-2} \text{s}^{-1}$. Diurnal variation of the air and pot temperatures was considerable (Figure 8.3B), partly because of the natural diurnal change in ambient temperature but also because of the radiation load on the chamber and 'greenhouse' effect within the glasshouse and chamber.

The vapour pressure deficit rose in response to increasing air temperature (Figure 8.3C) and during this period sometimes exceeded 2.5 kPa and so may well have influenced stomatal conductance. Furthermore, falling water potentials in the early afternoon may have led to stomatal closure.

Uptake of CO₂ by the above-ground part of the tree closely followed changes in the PPFD and also increased when the tree was measured at 700 $\mu\text{mol mol}^{-1}$. The well-matched response of changing PPFD and CO₂ fluxes demonstrates the adequately fast response time of the system. A graph of flux v PPFD (Figure 8.4) clearly shows the response of the above-ground part of the tree to PPFD and the increased assimilation rate when the tree was measured at 700 $\mu\text{mol mol}^{-1}$ CO₂ concentration.

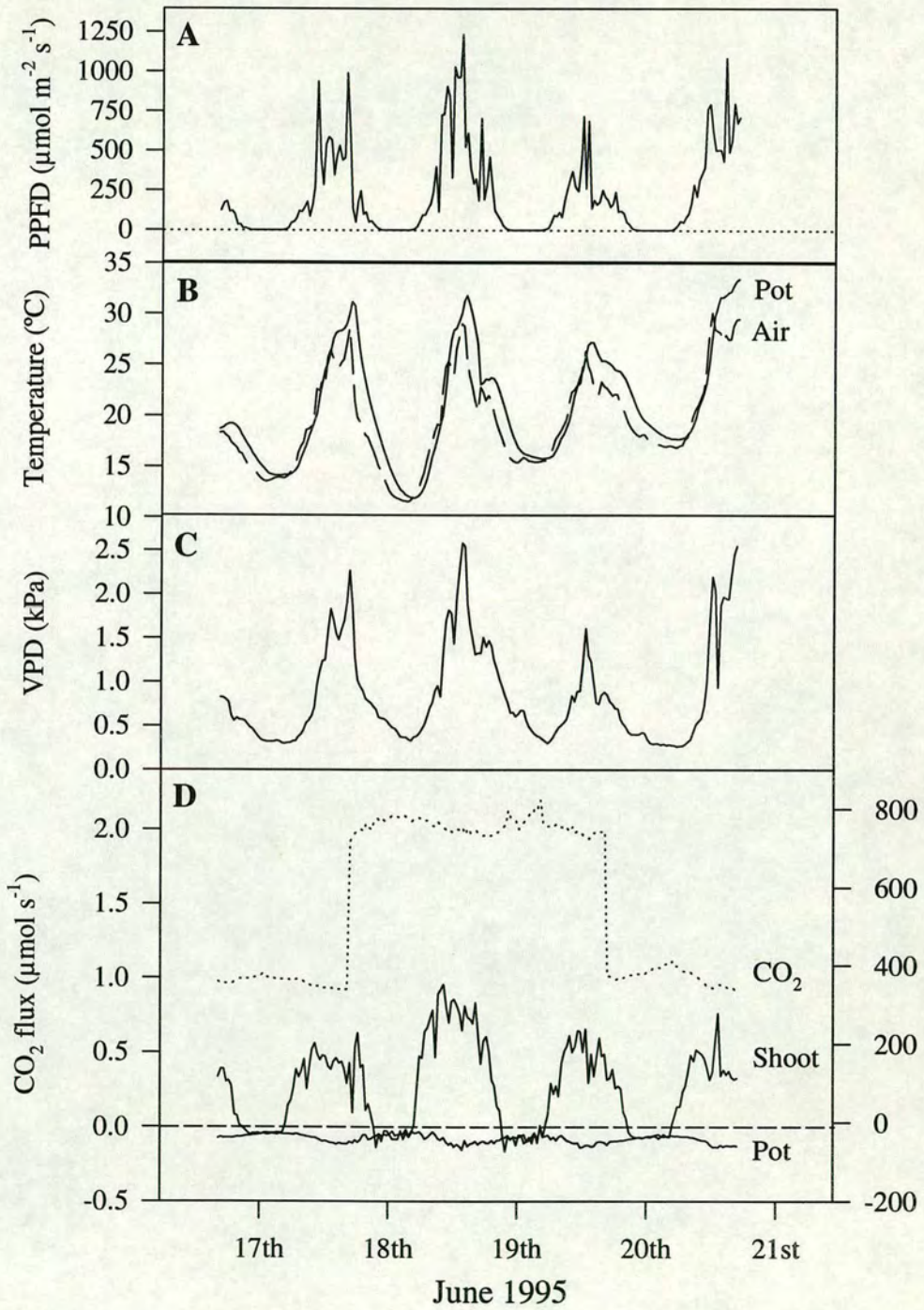


Figure 8.3 Measurements on a AL tree over four days (17-20 June) showing A. PPFD, B. air and pot temperature, C. vapour pressure deficit and D. CO₂ fluxes for above and below ground and CO₂ concentration at which measurements were made.

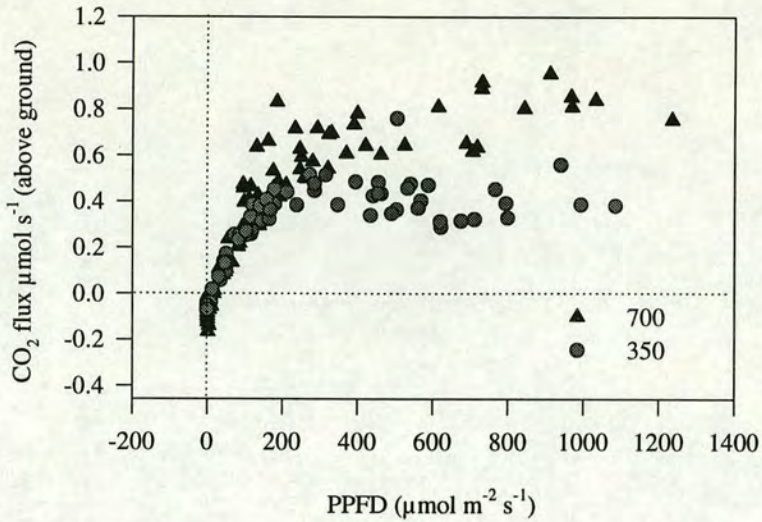


Figure 8.4 The relationship between above-ground CO₂ flux and PPFD for an AL tree over the four day period 17-20 June 1995 measured at both 350 and 700 $\mu\text{mol mol}^{-1}$ [CO₂]. Measurement conditions were the same as in Figure 8.3.

CO₂ fluxes from the pot decreased through the night and increased during the day to peak in late afternoon (Figure 8.3D). This was largely in response to temperature as shown by Figure 8.5 where there is a very clear relationship between the CO₂ efflux from the pot and the temperature of the pot, with a Q₁₀ of around 2. The measurements are noticeably more noisy when measured at 700 $\mu\text{mol mol}^{-1}$ but the mean values and trend are the same at both concentrations.

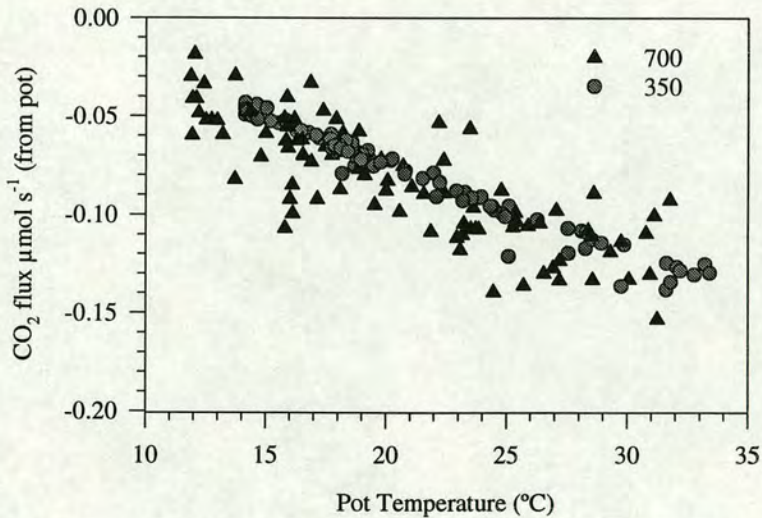


Figure 8.5 CO₂ flux v temperature for the pot (sand + root) for an AL tree over the four day period 17-20 June 1995. Measurement conditions as in Figure 8.3.

Transpiration rates were lower when the tree was measured at 700 $\mu\text{mol mol}^{-1}$ CO₂ (Figure 8.6). This in combination with increased assimilation rates would lead to a large increase in the instantaneous water use efficiency, however as mentioned in

Chapter 5, 5.9.3 there is an unknown underestimate in the size of the transpiration rate and caution has to be exercised when interpreting the results.

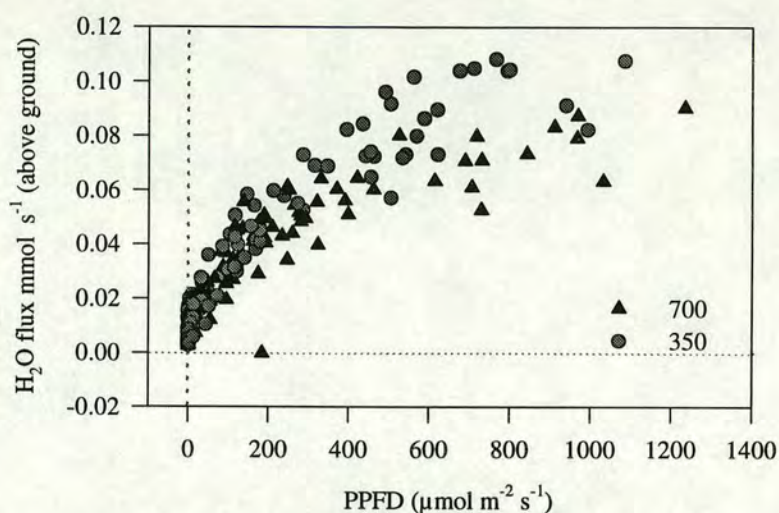


Figure 8.6 The relationship between transpiration and PPFD for an AL tree over the four day period 17-20 June 1995. Measurement conditions as in Figure 8.3.

8.2 CO₂ budget of trees

The preceding data show the competence of the system for measuring the fluxes of CO₂ from the above and below-ground portions of potted trees. By integrating the 24 hourly fluxes, a 24-hourly CO₂ budget can be derived.

Flux rates for above-ground and below-ground compartments were integrated over the daylight (PPFD > 10 μmol m⁻² s⁻¹) and night-time periods to give the total CO₂ exchange, then CO₂ budgets were constructed for each tree at both its growth and reciprocal CO₂ concentration. The budget comprises the net-uptake of CO₂ by the above-ground parts during daylight hours minus the losses from the above-ground parts during the night-time and losses from the roots and rhizosphere over the 24 hour period.

8.2.1 Basis for comparisons

Trees grown in elevated [CO₂] or with high rates of nutrient supply tend to grow faster and so at a given point in time tend to be bigger than their 'ambient grown' counterparts. It is possible these treatments increase the rate of development of a tree which follows the same developmental path as a tree growing under ambient conditions. However, it is more likely that trees grown in elevated [CO₂] or with increased nutrient availability follow a different developmental pathway. This raises

the question of which basis should be used to compare trees. Should trees be compared at the same;

- a) chronological age, t days from planting,
- b) the same size, or
- c) the same physiological age, *i.e.* just after leaf flush or flowering.

There are problems and benefits to using each of these bases and the most suitable will largely depend on the question being asked. For example, if we are interested in biomass development and how quickly a forest will reach canopy closure or a harvestable size then comparing trees at the same chronological age makes sense. However, as trees grow larger allocation between roots and shoots tends to change and so if we are interested in the influence of the treatment variables on root to shoot ratio then maybe we should compare trees of the same size. It is also possible that trees will mature at different rates, and as trees at different stages of maturity may have different physiology, *e.g.* allocating resources to reproduction rather than to growth, comparison of allocation patterns may be misinterpreted when trees are compared at the same chronological age or the same size.

During this experiment the measurements of whole tree fluxes were made over a period of three months and trees ranged in both chronological age and size. It is not possible to know the extent to which trees differed in physiological age but as they were only two years old and measurements were made during middle of the growing season it is assumed that the trees were of similar physiological age.

A further consideration with respect to comparing fluxes of CO₂ or water is that big trees will usually have bigger fluxes through simple scaling. Thus, elevated CO₂ may result in a larger tree that uses more water and fixes more carbon per day but is morphologically and physiologically identical to its smaller ambient counterpart. If we want to know if the underlying physiological processes have changed then we need to look at the specific fluxes *i.e.* the flux divided by the plant mass or area. For this reason the daily integrals of CO₂ gains and losses from the different plant parts have been expressed per unit mass of the individual plant part, thus enabling comparisons of specific flux rates between treatments. However, component fluxes have been expressed on the whole-tree mass basis when calculating the whole tree budget. This method has the added advantage of minimising within treatment variation resulting from variations in tree size which should aid detection of any treatment differences in carbon allocation.

8.2.2 Data analysis

Results were analysed by analysis of variance using a split plot design, the chambers representing the main plots and the nutrient treatment the sub-plots (Proc GLM, SAS Institute Inc., Cary, NC). Harley's F_{\max} test was used to test that group variances were similar.

8.2.3 CO₂ gain

CO₂ fixed by the trees during daylight hours expressed on both a leaf area (Figure 8.7) and a dry mass of needle (Figure 8.8) basis show a very similar pattern. The CO₂ treatment effect was significant ($P < 0.03$) when measured at 700 $\mu\text{mol mol}^{-1}$ and expressed on and area basis but not significant when measured at 350 $\mu\text{mol mol}^{-1}$. When expressed on a mass basis (Figure 8.8) there was a significant effect of CO₂ treatment at both measurement [CO₂] ($P < 0.008$). The nutrient effect was not statistically significant. When measured at 700 $\mu\text{mol mol}^{-1}$ compared to 350 $\mu\text{mol mol}^{-1}$ [CO₂] the amount of CO₂ fixed was almost double for all treatments. A trees fixed about 1.5 times as much CO₂ per unit leaf area as E trees when measured at the same [CO₂] and E trees fixed only slightly more CO₂ per unit area than A trees when measured at their respective growth [CO₂]. The relationship is slightly different when viewed on a dry mass of needle basis because of the differences in specific leaf area. However, the general pattern was the same and appears to indicate almost complete down-regulation of photosynthesis to CO₂ that was independent of the nutrient supply rate.

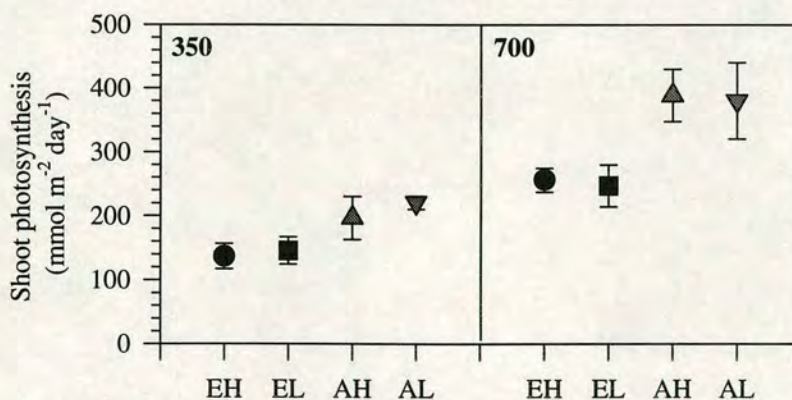


Figure 8.7 Net CO₂ fixed by the trees per m² projected needle area during daylight hours (PPFD > 10 $\mu\text{mol m}^{-2} \text{s}^{-1}$). Measured at 350 and 700 $\mu\text{mol mol}^{-1}$ [CO₂]. Means \pm 1 SEM, $n = 6$.

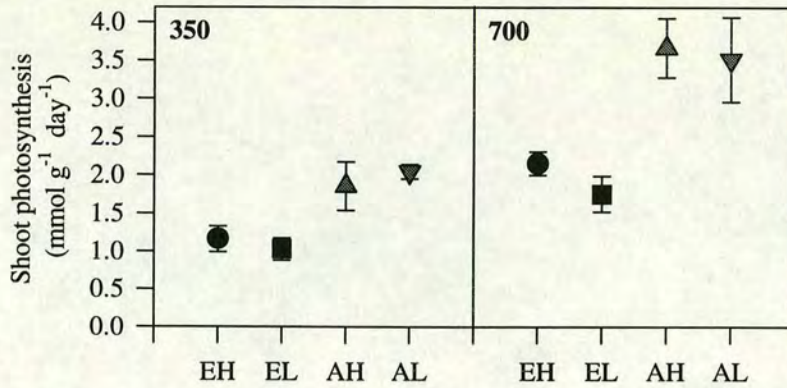


Figure 8.8 Net CO₂ fixed by the trees per g dry mass of needle during daylight hours (PPFD > 10 μmol m⁻² s⁻¹) measured at 350 and 700 μmol mol⁻¹ [CO₂]. Means ± 1 SEM, *n* = 6.

8.2.4 CO₂ loss

There were no statistically significant differences between treatments in the night-time losses of CO₂ on a dry mass of shoot basis by the above-ground parts of the trees (Figure 8.9). Variance was large partly as a result of variations in temperature between measurements but also as a result of the lack of precision of the system, which leads to relatively large random errors when fluxes are very low. However, setting aside lack of statistical significance, there does appear to be a slight trend towards lower respiration rates when measured at 700 μmol mol⁻¹ [CO₂] compared to 350 μmol mol⁻¹ [CO₂] in all but the EL trees and A trees seem more sensitive to the [CO₂] at which they were measured.

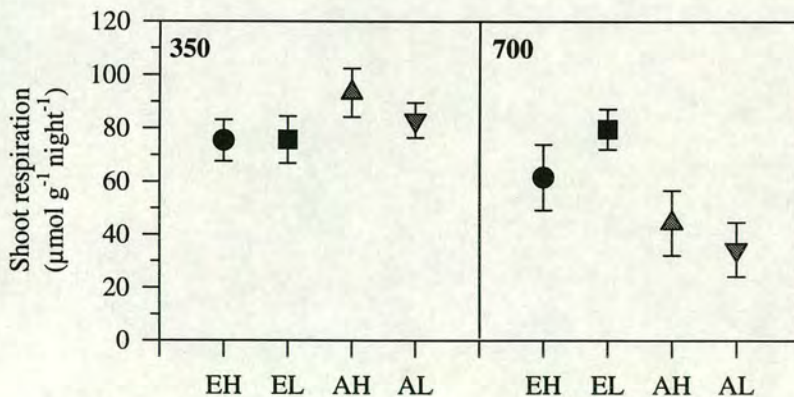


Figure 8.9 CO₂ lost from the above ground parts per g shoot dry mass during night-time (PPFD < 10 μmol m⁻² s⁻¹). Measured at 350 and 700 μmol mol⁻¹ [CO₂]. Means ± 1 SEM, *n* = 6.

The amount of CO₂ lost from the root zone per unit root mass (Figure 8.10) was slightly higher in the high nutrient treatments especially in the A trees but this

difference was not statistically significant. There was no statistically significant difference between efflux rates measured at 350 compared to 700 $\mu\text{mol mol}^{-1}$.

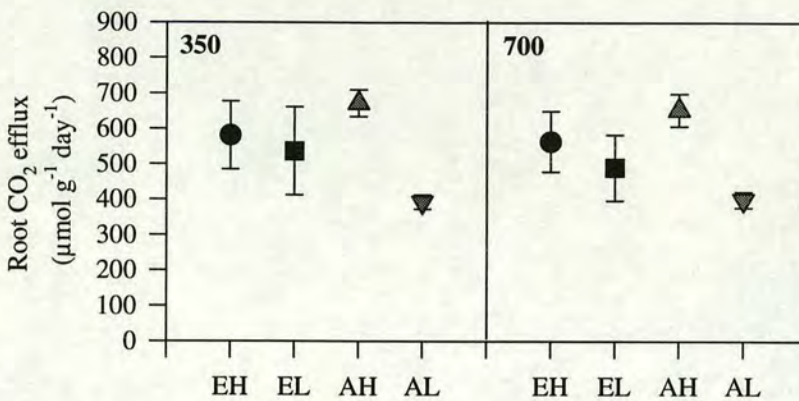


Figure 8.10 CO₂ lost from the below ground parts (root + medium) per g root dry mass during 24 hours. Measured at 350 and 700 $\mu\text{mol mol}^{-1}$ [CO₂]. Means \pm 1 SEM, $n = 6$.

8.2.5 CO₂ Budgets

The 24-hourly CO₂ budgets for each of the treatments measured at both 350 and 700 $\mu\text{mol mol}^{-1}$ [CO₂] are shown in Figure 8.11 and Table 2. Note that these values are now expressed per unit tree dry mass rather than the specific component dry mass basis used above. The trees were growing rapidly during the experiment and so it is unsurprising that the amount of CO₂ fixed was large relative to the daily losses (Figure 8.11 upper) giving rise to a moderately large specific net CO₂ gain (Figure 8.11 lower). When measured at the same [CO₂] the specific net carbon gain of **A** trees was more than twice that of **E** trees ($P < 0.002$) primarily because of lower photosynthesis in **E** trees (Figure 8.11 lower), since respiration rates were not significantly influenced by measurement [CO₂] and were relatively small compared to photosynthesis. Furthermore, because of the almost complete down-regulation of photosynthesis in **E** trees, **A** and **E** trees retained approximately the same amount of CO₂ per unit plant mass when measured at their growth concentrations.

There was a nutrient effect on specific net CO₂ gain, trees in the **H** nutrient treatment retaining more CO₂ than those in the **L** nutrient treatment. The difference between **H** and **L** was not significant when measured at 350 but was when measured at 700 $\mu\text{mol mol}^{-1}$ [CO₂] ($P < 0.02$). Thus, comparing trees measured at their growth [CO₂] shows that the specific net CO₂ gain was affected by nutrient supply but not by growth in elevated [CO₂].

Care must be exercised when interpreting results obtained when trees were measured at the reciprocal [CO₂] since they may not have been in steady state and changes in the storage pools (starch and soluble carbohydrates) may influence the carbon balance, leading to overestimates of CO₂ retained in the **E** trees measured at 350 and underestimates in the **A** trees measured at 700 μmol mol⁻¹.

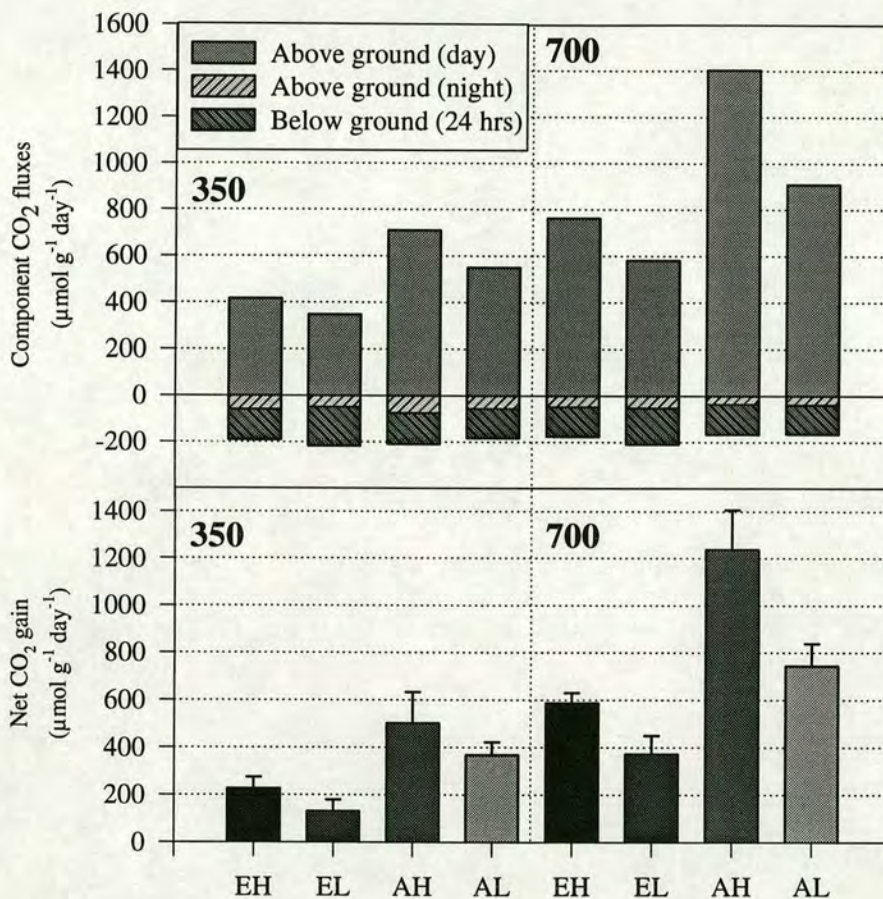


Figure 8.11 Daily CO₂ budgets on a tree dry mass basis measured at 350 and 700 μmol mol⁻¹ [CO₂] (upper) and the net CO₂ gain per day (lower). Means ± 1 SEM, *n* = 6.

A more complete carbon budget can be derived by combining estimates of tree growth and changes in soil organic matter content with the measured CO₂ fluxes. For clarity all values in the budget are in mol C per g of tree mass per day which are equivalent to mol CO₂ per g of tree mass per day.

The carbon balance can be formalised as follows:

$$G + \Delta S_c + L_u = F + L_s + L_r$$

where *G* is the relative growth rate determined from harvest data,
 ΔS_c is the estimated increase in C in the sand,
 L_u is the residual, the loss of C unaccounted for,

F is the net C fixed by the shoot during daylight,
 L_s is the loss from the shoot at night, and
 L_r is the loss from the root over 24 hours.

Estimates of the relative growth rate for each treatment during the measurement period were obtained from the harvest data (Chapter 6, Table 6.2). These were converted from a dry mass increment per unit dry mass to a molar CO₂ exchange per unit dry mass by dividing by 24 (assuming 50% of dry mass is carbon, Matthews, 1993), to give a value of 'measured' growth (G).

Using information about the organic matter content of the sand per unit mass of root (Chapter 7, Figure 7.14) and assuming that the ratio of organic matter:root mass and the root:shoot ratio were constant during the experiment then, the change in soil carbon per unit plant dry mass (ΔS_c , mol g⁻¹ day⁻¹) during a measurement can be estimated as:

$$\Delta S_c = \frac{W_{\text{root}} \cdot L_{\text{ign}} \cdot R_G}{W_{\text{plant}} \cdot 24}$$

where W_{root} = dry mass of root during measurement. (g)
 L_{ign} = specific loss on ignition (g g⁻¹ root dry mass)
 R_G = Relative growth rate (g g⁻¹ day⁻¹).
 W_{plant} = dry mass of plant at time of measurement (g).
 24 = 12 g mol⁻¹ / 0.5 g carbon g⁻¹ dry mass.

The greyed columns in Table 2 show the components of the budget as a percentage of the CO₂ fixed during the daylight hours (F). The fraction of CO₂ retained by each treatment ($G + \Delta S_c + L_u$) was much higher when measured at 700 than at 350 $\mu\text{mol mol}^{-1}$ [CO₂]. **AH** trees measured at 700 $\mu\text{mol mol}^{-1}$ retained the largest fraction of CO₂ (88%) while **EL** trees measured at 350 $\mu\text{mol mol}^{-1}$ the lowest (38%). These are the two extremes and, as they were measured at their reciprocal [CO₂], they are likely to have experienced changes in their carbon storage pools.

Comparison of trees measured at their growth [CO₂] shows that on average roughly 70% of CO₂ fixed is retained by the tree and pot. **AH** and **AL** trees retained 70.4 and 67.0%, respectively, while **EH** and **EL** trees retained 77.0 and 64.1%, respectively, indicating a possible interaction between CO₂ and nutrient supply. The main cause of these differences in the fraction of carbon retained appears to be the amount respired by the root system. **L** trees lost a larger fraction of fixed CO₂ through the root system than **H** trees and elevated CO₂ seems to have enhanced this difference, **EL** trees losing 26.9% while **EH** trees lost 16.8%. Thus **L** trees lost a greater fraction of CO₂

from their root systems despite the fact that **EL** trees had similar and **AL** trees lower specific root respiration rates (Figure 8.10) than their **H** counterparts, this can be explained by the increased root fraction found in **L** trees compared to **H** trees (Table 1). The same is true for the observed differences in response to growth [CO₂].

To aid interpretation of the results the carbon balance can be represented as follows:

Net daily shoot exchange - loss from root = net gain + error

$$(F + L_s) + L_r = (G + \Delta S_c) + L_u$$

which can be re-written as

$$F_s \cdot a_s - F_r \cdot a_r = \text{net gain} + L_u$$

where F_s is the shoot fraction,

F_r is the root fraction,

a_s is the specific activity of the shoot (mol g⁻¹ day⁻¹) and

a_r is the specific activity of the root (mol g⁻¹ day⁻¹).

F_s , a_s , F_r and a_r can be qualitatively represented as functions (f_1 to f_4) of the first order treatment effects, N = nutrient supply rate and CO₂ = growth [CO₂], based on the results seen in the preceding sections.

$$F_s = f_1(N), \text{ where } f_1(\mathbf{H}) > f_1(\mathbf{L}).$$

$$a_s = f_2(\text{CO}_2), \text{ where } f_2(\mathbf{E}) > f_2(\mathbf{A}).$$

$$F_r = f_3(N), \text{ where } f_3(\mathbf{L}) > f_3(\mathbf{H}).$$

$$a_r = f_4(N), \text{ where } f_4(\mathbf{H}) > f_4(\mathbf{L}).$$

It follows that $(F + L_s) = f_1(N) \cdot f_2(\text{CO}_2)$

$$\text{and } L_r = f_3(N) \cdot f_4(N)$$

and therefore that the net uptake of C by the shoot increases with both nutrient supply and [CO₂] through increases in shoot fraction and increases in specific photosynthetic rates. However, the loss from the root system depends on two opposing functions of nutrient supply. On the one hand the root fraction decreases with increasing nutrient supply, but on the other hand, specific root respiration increases with increasing nutrient supply.

Table 2 The daily C budget for small trees measured between July and September 1995. The units are $\mu\text{mol C per g tree dry mass}$. Each value is the mean of six replicates and the numbers in parenthesis are the SEM. The greyed columns show values as a percentage of net C fixed by the shoot during daylight hours.

Measured at	350						700									
	EH		EL		AH		AL		EH		EL		AH		AL	
Treatment	$\mu\text{mol g}^{-1} \text{day}^{-1}$	%	$\mu\text{mol g}^{-1} \text{day}^{-1}$	%	$\mu\text{mol g}^{-1} \text{day}^{-1}$	%	$\mu\text{mol g}^{-1} \text{day}^{-1}$	%	$\mu\text{mol g}^{-1} \text{day}^{-1}$	%	$\mu\text{mol g}^{-1} \text{day}^{-1}$	%	$\mu\text{mol g}^{-1} \text{day}^{-1}$	%	$\mu\text{mol g}^{-1} \text{day}^{-1}$	%
C Fixed (F)	417 (66)	100	348 (66)	100	711 (133)	100	551 (42)	100	763 (65)	100	582 (90)	100	1404 (181)	100	910 (100)	100
Respired by shoot (L_s)	58 (6.4)	13.9	50 (6.3)	14.2	75 (7.1)	10.5	56 (15)	10.2	48 (9.8)	6.2	52 (6.1)	9.0	36 (10)	2.5	38 (15)	4.2
Respired by root (L_r)	132 (20)	31.7	167 (21)	48.0	136 (14)	19.1	126 (10)	22.8	129 (18)	16.8	156 (17)	26.9	131 (13)	9.3	127 (8.3)	14.0
Net gain ($G+\Delta S_c+L_u$)	227 (48)	54.4	132 (47)	37.8	501 (129)	70.4	369 (54)	67.0	587 (44)	77.0	373 (78)	64.1	1238 (170)	88.2	745 (94)	81.8
'Measured' growth (G)	-	-	-	-	396 (37)	55.7	283 (58)	51.4	404 (29)	52.9	192 (75)	32.9	-	-	-	-
ΔS_c	-	-	-	-	35	4.9	55	10.0	40	5.2	27	4.6	-	-	-	-
Residual (L_u)	-	-	-	-	70	9.8	31	5.6	143	18.9	154	26.6	-	-	-	-

Subtracting the estimates of 'measured' growth and increase in 'soil' carbon from the net gain derived from measured CO₂ fluxes gives the residual CO₂ flux (L_u), which is the component of the specific flux of CO₂ unaccounted for by growth. Values of L_u were much higher in **E** trees than **A** trees but there was no effect of nutrient treatment. In **E** trees between 19 to 27 % of CO₂ fixed by the shoot remained unaccounted for. Discussion of these results follows later.

8.3 Water loss from trees

8.3.1 Transpiration

Transpiration rates were integrated and divided by the leaf area to give 24 hourly rates per m² (Figure 8.12). Transpiration rates were not affected by the measurement CO₂ concentrations but there were treatment differences. **E** trees had lower rates than **A** trees, and **H** trees lower rates than **L** trees, but these differences were not statistically significant. Such responses would be ecologically important as they suggest that trees growing in a high [CO₂] environment would loose less water and this response would be increased at high nutrition. However before making such an interpretation one must consider some of the other variables.

There was twice as much leaf area in **H** as in **L** trees (see Figure 8.1) and **E** trees also had more leaf area than **A** trees. This may explain part of the difference found in transpiration rates per unit leaf area. Large trees have more mutual shading and larger canopy aerodynamic resistances which may lead to lower available energy per unit leaf area, a drop in leaf temperature and a smaller leaf to air vapour pressure gradient so reducing the transpiration per unit leaf area.

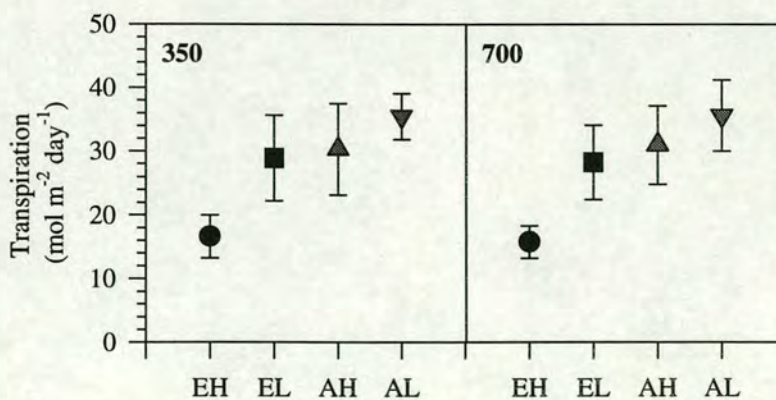


Figure 8.12 Integrated transpiration per unit projected needle area over 24 hours for trees measured at both 350 and 700 μmol mol⁻¹ [CO₂]. Means ± 1 SEM, $n = 6$.

Another possibility is that big trees will lose more water given the same specific transpiration rate which may lead to local depletion of water around roots and lower water potentials at the leaf inducing stomatal closure. However, as leaf water potentials were not measured in this experiment it is not possible to test this hypothesis.

The lack of sensitivity of transpiration to measurement [CO₂] is surprising as one might have expected stomata to close in response to increased [CO₂] (Eamus, 1991). It is possible that the mixing fan was not adequately coupling the foliage to the chamber air and so the degree of stomatal control over transpiration was limited (Jarvis & McNaughton, 1986). Further implications of this are discussed later.

8.3.2 Water use efficiency

Water use efficiency (WUE) was calculated as the net CO₂ fixed / water lost by the above-ground part of trees over 24 hours. WUE was always much higher when the tree was measured at 700 μmol mol⁻¹ [CO₂] (Figure 8.13) solely as a result of the increase in the amount of CO₂ fixed, since water loss was not influenced by the measurement [CO₂].

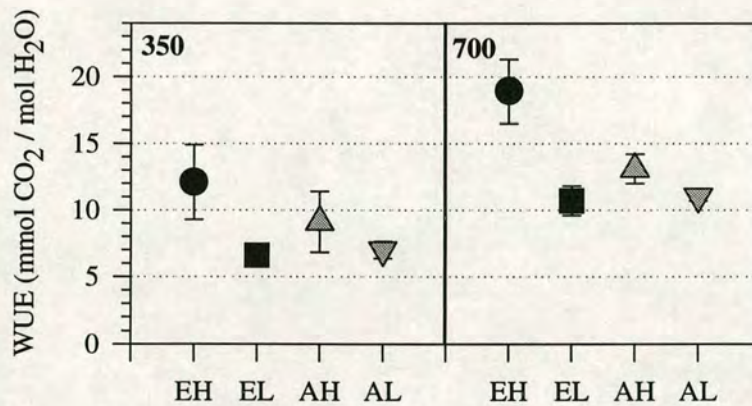


Figure 8.13 Water use efficiency calculated as net CO₂ fixed / water lost by the shoot. Shown for trees measured at both [CO₂]. Means ± 1 SEM, *n* = 6.

Comparison of trees measured at their growth concentrations shows that **EL**, **AH** and **AL** all had similar WUE while that of **EH** was twice as large. Both **E** (*P* < 0.01) and **H** (*P* < 0.012) significantly increased WUE, with larger increases in WUE in response to nutrient in trees grown and measured at 700 μmol mol⁻¹ [CO₂].

H trees lost less water and fixed more CO₂ than **L** trees at both growth [CO₂] this gave rise to the relatively high WUE in **H** trees. **EH** trees had a markedly higher

WUE than the other treatments especially when compared at 700 $\mu\text{mol mol}^{-1}$ [CO₂] as a result of the relatively low transpiration rates (see Figure 8.12).

It must be emphasised that the transpiration may have been underestimated by 20-40% (see Chapter 5, 5.9.2) and the correct values for WUE may be somewhat smaller. However, the relative differences between treatments will probably remain the same.

8.4 Discussion

8.4.1 Differential response between tree and shoot

The net daytime uptake of CO₂ by the aboveground parts of the trees per unit leaf area showed strong down-regulation in response to growth [CO₂] but no response to nutrient supply (Figure 8.7). This appears to be in contradiction to the measurements of the A/C_i response functions where nutrient supply significantly affected both carboxylation efficiency and A_{sat} , but growth [CO₂] did not have a statistically significant effect on either (see Chapter 7, Figure 7.19). At first it seemed impossible to reconcile these disparate responses to the treatment variables, however recognition of the problem as one of scaling from shoot to tree leads to the following explanation.

From the transpiration data measured at the tree scale (Figure 8.12) it can be seen that **H** trees lost less water per unit leaf area than **L** trees and **E** trees less than **A**. If we assume that there were no systematic differences between treatments in VPD, the main variable driving transpiration, then **H** trees must have had lower conductances from leaf to bulk air than **L** (and **E** trees lower conductances than **A** trees). These conductances include the stomatal conductance and the boundary layer conductances of both leaf and canopy. Low conductances may have led to a 'conductance limitation' of photosynthesis, as **H** trees would be forced to operate at lower C_i than **L** trees and this could account for the observed differences in the response to treatment at the two scales.

This effect is demonstrated graphically in Figure 8.14 where the idealised A/C_i responses at the shoot scale show a strong nutrient treatment effect and weak [CO₂] treatment effect. When measured at 700 $\mu\text{mol mol}^{-1}$ [CO₂] (Figure 8.14A) it is possible to obtain the observed relationship between treatments seen at the tree scale (as seen in Figure 8.7) if there is a larger conductance limitation in **H** trees, as indicated by the less steep line between the C_a (700) and the A/C_i function (Farquhar & Sharkey, 1982). The same is true when simulating the predicted effect at the

growth concentrations (Figure 8.14B) where it can be seen that the large nutrient and small [CO₂] response seen at the scale of the shoot is transposed into a small nutrient and large [CO₂] effect at the scale of the tree as a result of larger conductance limitation in **H** trees.

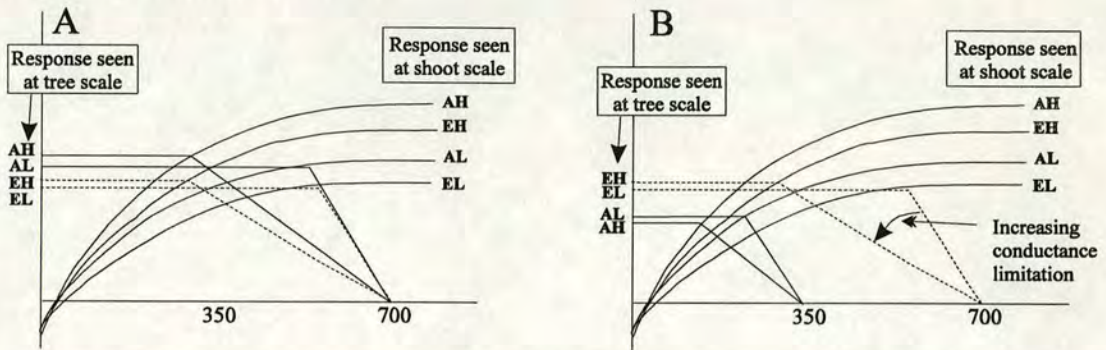


Figure 8.14 Idealised A/C_i response curves showing how the strong nutrient treatment effect on the response curve at the shoot scale can translate to a CO₂ treatment effect at the tree scale if conductance limitation varies with nutrient treatment. **A.** represents all trees measured at 700 $\mu\text{mol mol}^{-1}$ while **B.** represents trees measured at their growth CO₂ concentrations.

This hypothesis is consistent with the observed transpiration rates, measured A/C_i responses and integrated daytime net CO₂ uptake of the above ground portion of the tree. So it would seem probable that the **H** trees had lower conductances between leaf and bulk air and this resulted in a limitation of photosynthesis when measured in the whole tree chamber. This decreased conductance could be as a result of stomatal closure and/or decreased boundary layer conductances of both shoot and tree related to the much larger leaf area and denser canopy of **H** trees via mechanisms explained in section 8.3.

Some other possible explanations are; i) that **H** trees carried twice as much leaf area as **L** trees which was clumped onto many more shoots (see Chapter 6) and so probably had more self shading of shoots. Thus the average light incident per unit leaf area would have been less and consequently assimilation per unit leaf area would be lower in **H** trees than **L** trees on a whole tree basis. ii) A/C_i were measured on current shoots and the proportion of total leaf area represented by current shoot varied strongly with nutrient treatment. **H** trees had much more current shoot than **L** trees and if current shoots had a different response to CO₂ or nutrient treatment than older shoots then that might have influenced the whole tree response more in the **L** trees where a higher proportion of total leaf area was in the older age class. iii) A/C_i response functions were measured at saturating PPFD on shoots whereas whole tree measurements were made at a range of PPFD throughout the day. Differences in the

shape of the A/C_i response between treatments at various PPFDs may have contributed to the lack of nutrient effect seen in the daily net CO₂ uptake of the trees.

8.4.2 Respiration

A reduction in respiration by plants as atmospheric carbon dioxide concentration increases would increase their strength as a sink for carbon. In mature forests, photosynthesis is approximately balanced by respiration. Therefore a decrease in respiration as atmospheric CO₂ concentrations increase could be just as important as an increase in photosynthesis for the ability of forests to sequester carbon.

The effect of elevated CO₂ concentration on respiration rates is currently a contentious issue as increases, decreases and no responses have all been observed. The issue can be broken into two parts; the long term effect of growth at elevated [CO₂] on respiration rates and the instantaneous effect of [CO₂] on respiration rates.

Plant respiration is commonly represented by the growth and maintenance model which states that part of the respiration is associated with maintaining the existing biomass and part with the synthesis of new tissue. Maintenance respiration is associated with protein turnover and maintaining ion gradients across membranes and is temperature dependant, while growth respiration depends on the type of compounds being produced some being more energetically expensive than others (Penning de Vries *et al.*, 1974).

Growth in elevated [CO₂] has been shown to lead to changes in tissue composition with a reduction in protein and nitrogen content (Wullschleger *et al.*, 1992; Rouhier *et al.*, 1994; Murray *et al.*, 1996). Since protein turnover is a substantial component of maintenance respiration, there is often a positive correlation between tissue nitrogen content and maintenance respiration (Bunce, 1994). Also, since proteins are relatively expensive to synthesise, the coefficient of growth respiration might be less in elevated [CO₂]. Thus one might expect to see a reduction in respiration rates in trees grown in elevated CO₂, especially under nutrient limiting conditions. In this study there does seem to be a small effect of nutrient supply rate on the below-ground CO₂ efflux, with higher effluxes in the **H** treatment (Figure 8.10). The **H** tree roots had higher nitrogen concentrations (see Chapter 7, 7.6.2) and so the higher respiration rate is consistent with both higher maintenance and growth respiration rates related to protein turnover and the high cost of protein synthesis, respectively. Growth in elevated [CO₂] did not affect CO₂ efflux from the pot per unit root dry mass but did appear to reduce the effect of nutrient treatment.

Some researchers have found a direct, instantaneous, reversible response of respiration rates to [CO₂] but that is not universal. In a study of soybean, tomato and amaranth grown at two [CO₂] the rate of respiration measured at 700 μmol mol⁻¹ [CO₂] ranged from 0.99 to 0.65 times that measured at 350 μmol mol⁻¹, with plants grown at 350 μmol mol⁻¹ CO₂ showing a larger response to measurement [CO₂] than those grown at 700 μmol mol⁻¹ [CO₂] (Bunce, 1990). El Kohen *et al.* (1991) also found a rapidly reversible reduction in respiration rates in *Castanea sativa* shoots, with lower rates measured at 700 μmol mol⁻¹ than at 350 μmol mol⁻¹ [CO₂]. Several mechanisms for a short-term response of respiration to [CO₂] have been proposed including enhanced dark CO₂ fixation by a carboxylase, such as phosphoenolpyruvate carboxylase, causing decreased net CO₂ emission in the dark (Amthor, 1995a), alterations of intercellular pH, diversion of electron transport to the alternative (cyanide-resistant) pathway (Amthor, 1991) and inhibition of respiratory enzymes by very high carbon dioxide concentrations (Qi *et al.*, 1994).

This experiment did not find clear evidence to support a direct short term response of respiration rates to [CO₂]. However, above-ground respiration rates were slightly lower when measured at 700 μmol mol⁻¹ [CO₂], while below-ground respiration was insensitive to the [CO₂] at which it was measured. This is consistent with the theory of stimulation of dark CO₂ fixation which would result in a response in photosynthetic tissues but not in non-photosynthetic tissues.

Qi *et al.* (1994) found that root respiration rates of Douglas-fir seedlings decreased exponentially between [CO₂] of 130 and 7015 μmol mol⁻¹, equivalent to a decrease of 4 to 5 nmol CO₂ g⁻¹ dry mass of root s⁻¹ for every doubling of [CO₂]. They attributed this to decreased electron transport down the alternative pathway, a mechanism which has been implicated in the suppression of respiration by wheat roots (Gifford *et al.*, 1985). However, as soil [CO₂] are commonly in the range of 1-3% it would be surprising if a relatively small change of 0.035 % would have any detectable effect on soil CO₂ efflux.

8.4.3 CO₂ budget

Generally growth in elevated [CO₂] has been associated with increased photosynthetic rates per unit leaf area, even when down-regulation occurs (Luxmoore *et al.*, 1993). There is also usually an increase in growth rate, but in many cases the increase in photosynthesis is much larger than that in growth leading to the conclusion that a proportion of the carbon must be going somewhere other than into increasing the biomass of the plant.

In this experiment the proportion of CO₂ fixed by the tree during daylight which was not accounted for in the measured losses of CO₂ and carbon going into growth and soil (L_u), was 6 to 10 % in the trees grown and measured at 350 $\mu\text{mol mol}^{-1}$ while it was 19 to 27 % in trees grown and measured at 700 $\mu\text{mol mol}^{-1}$. Trees grown in elevated CO₂ fixed more carbon per unit plant mass, lost a similar amount, grew more and had a larger amount unaccounted for than trees grown in ambient [CO₂].

L_u can be sub-divided into the unmeasured flux of carbon and, as it is the residual in the 24-hourly carbon balance, an error term. The unmeasured flux of carbon accounts for any non-CO₂ fluxes of carbon out of the system, such as hydrocarbon emissions, and leaching of soluble compounds, such as carbohydrates and amino acids from the pot. However, leaching was minimised by watering frequently and sparingly to avoid any throughflow. The error term includes errors in measurements and any day-to-day fluctuations in carbon storage pools within the tree caused by variations in the weather as well as variations in the timing of growth and root activity since while the estimate of growth, G , was based on data from harvests 10 weeks apart, which would smooth out day-to-day variations, the components of the carbon exchange obtained from CO₂ fluxes (F , L_s & L_r) were measured over 24 hours and so would be subject to day-to-day variations in conditions. Such “errors” would increase variation rather than give rise to a systematic bias between treatments.

The relative sizes of the components of the carbon balance indicate that photosynthesis, followed by the estimate of growth and root efflux, are the most important while shoot respiration and changes in soil carbon are comparatively small. Thus, L_u will be most sensitive to errors in F , G and L_r , while errors in L_s and ΔS_c would need to be relatively big to have a significant effect.

The carbon content of organic compounds varies considerably; lignin (66.7%), cellulose (44.4%) and carbohydrates (40%) and so part of the difference in L_u between **A** and **E** trees may be attributable to changes in the chemical composition of the trees and soil organic matter. I have assumed that 50% of the dry mass of both tree and 'soil organic' matter is carbon in both **A** and **E** treatments. From a review of 14 sources, the carbon content of spruce trees ranged from 47.2% to 52.7% with a mean of 49.8% (Matthews, 1993). The **E** trees produced more non-structural carbohydrates (see Chapter 7) which have a relatively low carbon content and this would decrease the overall carbon content, which in turn would lead to a lower calculated value for G and consequently, a higher value for L_u in **E** trees. However, increasing the TNC from 0% to 20% would result in the overall carbon content changing from 50% to 48%, this is an extreme since roots and main stem do not

contain such high TNC concentrations. The organic matter found in the sand was probably composed of partially decomposed roots and some living soil organisms and was probably depleted in easily decomposed compounds, such as carbohydrates, and relatively rich in compounds such as lignin, thus the carbon content was probably between 50 and 60%. Using a value of 60% instead of 50% would increase the calculated value of ΔS_c by 20%, leading to a reduction in L_u of between 3% (EL) and 35% (AL). Thus, changes in the chemical composition of the trees and soil organic matter may account for some of the error in the carbon balance.

A further explanation could be that E trees lost more carbon through volatile hydrocarbons (e.g. monoterpenes and isoprene). Boissard *et al.* (1997) found that volatile hydrocarbon emissions accounted for 0.1% of carbon fixed by photosynthesis in Sitka spruce, while Sharkey *et al.* (1991) found that for short periods hydrocarbon emissions from oak leaves could account for up to 20% of the carbon being fixed by photosynthesis but this was thought to be a result of flushing out of pools of volatile hydrocarbons and not a result of sustained production.

Research is currently underway to investigate the effect of [CO₂] on hydrocarbon emissions from Sitka spruce and preliminary results suggest that trees grown in elevated CO₂ do indeed emit more hydrocarbons (P. Scholefield, personal communication). However the amounts are relatively small with emissions during daylight accounting for about 3% of carbon fixed by photosynthesis over the same period.

8.4.4 Does growth at elevated CO₂ lead to an increase in the flow of carbon through the atmosphere-plant-soil system?

The question is; does growth at elevated [CO₂] lead to an increase in the flow of carbon from atmosphere to plant to soil where the carbon could remain for long periods in persistent compounds or could be oxidised and returned to the atmosphere? This question is important for two reasons; firstly, a build-up of persistent, non-degradable carbon compounds in the soil would represent a sink for carbon which could ameliorate the anthropogenic increase in atmospheric CO₂ concentrations. Secondly, part of the flow of carbon from the atmosphere to the soil via the plant is in the form of high-energy carbon compounds and so corresponds to a flow of energy which could be utilised to increase rates of nutrient mineralisation. Thus, a change in the flux of carbon through plants may be ecologically very important.

In this experiment the flux of carbon through the plant can be estimated from the efflux of CO₂ from the pot (L_r) plus any changes in the carbon content of the sand (ΔS_c), this was 171, 181, 169 and 183 $\mu\text{mol C g}^{-1} \text{ tree day}^{-1}$ for **AH**, **AL**, **EH** and **EL** trees, respectively (see Table 2). So growth in elevated [CO₂] did not affect the flux of carbon through the trees, but the flux was slightly larger in trees grown at low nutrient supply rates. This may reflect the extra energetic cost involved in obtaining nutrients when they are in short supply in the rhizosphere. Dividing the flux of carbon through the tree by the growth rate (G) gives the flux through the tree per unit growth and was 0.43, 0.64, 0.42 and 0.95 for **AH**, **AL**, **EH** and **EL**, respectively. Again **AH** and **EH** have similar values indicating that for each mol of C that goes into growth 0.43 mols flows from the atmosphere to the soil. The value was larger for trees grown at low nutrient supply especially in elevated [CO₂]. The high value for the **EL** trees is a result of the low growth rate and may be misleading if the trees were not in steady state. Elevated [CO₂] combined with stored reserves of nutrients may have caused an initially high growth rate in **EL** trees which led to a rapid decline in nutrient status and subsequent low growth rates, as the trees gradually adjusted to the growth conditions.

The flux of carbon from the tree to the soil as a percentage of the CO₂ fixed by the shoot ($((L_r + \Delta S_c) / (F - L_s)) * 100$) was similar in **AH** and **EH** trees 27 and 24 %, respectively, and slightly higher in **AL** and **EL** trees 37 and 34 %, respectively. These results suggest that **L** trees lose a greater proportion of the CO₂ fixed by the above-ground parts through the root system than **H** trees. This is a result of less CO₂ being fixed by the shoot while similar amounts were lost by the root. Although **H** trees had higher root respiration rates than **L** trees per unit root mass they had smaller root fractions (Table 1). More interestingly **E** trees lost a slightly lower proportion of carbon fixed by the shoot than **A** trees at both levels of nutrition despite having slightly larger root fractions (Table 1).

8.5 Conclusions

Whole tree photosynthetic rates showed strong down-regulation with respect to growth CO₂ concentration but there were no significant differences between trees grown at different nutrient supply rates. This differs from the results found in measurements at the level of the shoot where nutrient treatment had a strong influence while growth CO₂ concentration did not, these differences can be attributed to differences in stomatal and boundary layer conductances.

Respiration rates of the above-ground parts of trees were slightly lower when measured at 700 μmol mol⁻¹ [CO₂] however, below-ground respiration rates were insensitive to the concentration at which they were measured. Specific root respiration rates were higher in trees grown at high nutrient supply rates. The proportion of carbon fixed by the shoot that was subsequently lost by the root system was higher in trees grown at low nutrient supply rates, as a result of the larger root to shoot ratio.

The daily net CO₂ gain per unit plant mass, which is related to the relative growth rate, was higher in trees grown at high nutrient supply rates and did not vary significantly with the CO₂ concentration at which the trees were grown.

Water use efficiency was higher in trees grown and measured in elevated CO₂ both as a result of reduced transpiration rates and increased photosynthetic rates. However the reduced transpiration rates did not seem to be in response to measurement [CO₂] but may have been as a result of changes in stomatal and boundary layer conductances as a result of changes in overall leaf area, canopy structure, mutual shading and an acclimation of stomatal response.

CHAPTER 9

Synthesis and Conclusions

This chapter brings together the results from the branch bag and seedling experiments and interprets the observed differences in responses with respect to tissue age and functional differences between branches and seedlings. It also presents the main conclusions drawn from the experiments and suggests avenues for future research.

9.1 Summary of results

Table 9.1 shows a summary of the main effects of growth in elevated [CO₂] on seedlings and mature branches. It allows a quick overall impression of the main effects but neglects interactions. The following sections discuss the results in more detail.

Table 9.1 Summary of main effects of growth in elevated [CO₂] on seedlings in two nutrient treatments high supply, **H** and low supply, **L** and on two age-classes of needles on mature branches. ++ large increase, + increase, • no change, - decrease, -- large decrease, ? not measured, N/A not applicable. Symbols in bold indicate the result was statistically significant ($P < 0.05$) at least at some time during the experiment.

Process or state variable	Seedlings		Mature branches	
	H	L	current	C+1
Starch concentration	+	++	•	•
Soluble carbohydrate concentration	++	+	•	+
Nitrogen concentration	-	-	•	•
Chlorophyll concentration	•	•	•	•
Down-regulation of photosynthesis	+	•	•	+
Stomatal conductance at growth [CO ₂]	?	?	-	-
Stomatal density	?	?	?	•
Growth of branch or seedling	++	+	•	
Root fraction	+	+	N/A	N/A
Leaf area ratio	--	--	N/A	N/A
Wood mass / needle mass	•	•	•	•
Number of shoots	+	+	•	•

9.2 Growth

The growth of mature branches in branch bags was not affected by elevated $[\text{CO}_2]$ (cf. Dufrene *et al.*, 1993; Teskey, 1995) but there was growth enhancement in seedling trees. Townend (1995) and Murray *et al.* (1996) also found increased growth and increase in dry mass in Sitka spruce seedlings in response to elevated $[\text{CO}_2]$.

I attribute the different responses of branches and seedlings to the fact that where an individual branch was exposed to elevated $[\text{CO}_2]$ the extra assimilate produced was exported to the tree in response to sink demand elsewhere in the tree. Estimates of the carbon balance of the branches supports this fact. Furthermore, the extra CO_2 fixed by a single branch in elevated $[\text{CO}_2]$ would have been small relative to the CO_2 fixed by the rest of the canopy and so unlikely to influence the carbon balance of the tree.

Once a branch is more than one or two years old it no longer imports carbon from the tree but supplies its own requirements for maintenance and growth, while exporting excess assimilate to the tree for the growth of roots, growth of new branches at the top of the canopy and for maintenance of the stem and roots. The allocation of assimilates between a branch's own meristems and those elsewhere in the tree depends on the relative strengths of those sinks.

Teskey (1995) used a similar branch bag technique on *Pinus taeda* and found growth enhancement in response to elevated $[\text{CO}_2]$. *Pinus taeda* produces a second flush of leaf growth and it was this second flush or 'free growth' which responded to elevated $[\text{CO}_2]$. Moreover, his branches were high up, in a fairly open canopy, and so received high irradiance that may have stimulated shoot development which could then make use of the extra assimilate available in the elevated $[\text{CO}_2]$ branches.

Although mature spruce branches do not produce 'free growth' they may still have the potential for a growth response by producing more buds, bigger shoots or more wood production in the second and third years of exposure, but they did not show any of these responses. During the course of this experiment the experimental branches were becoming progressively lower in the canopy and by 1994 were in deep shade. I suggest that the low PPFD and lower red : far-red light ratio reduced meristematic activity within the branches irrespective of assimilate production; and I have shown that increased carbohydrate production within a branch does not influence meristematic activity. Although much of the extra assimilate produced by branches in elevated $[\text{CO}_2]$ was exported to the tree, potentially this assimilate could be used

within a branch to maintain a positive carbon balance lower in the canopy and so increase the depth of the live crown and leaf area index of the stand. Unfortunately, this experiment was not continued long enough for the branches to reach the critical point in carbon balance where this hypothesis could be tested.

In the case of the seedling trees where the whole crown was exposed to elevated $[\text{CO}_2]$ a doubling of CO_2 fixed per unit leaf area represents a doubling of CO_2 fixed by the crown, clearly increasing the potential for growth. The ability of seedling spruce trees to produce 'free growth' enabled them to respond to elevated $[\text{CO}_2]$ by extending existing shoots but also, when grown with high nutrient supply, by initiating new shoots midway through the season. The seedlings were grown under moderately bright light and new growth occurred at all points within the crown. Seedlings grown with a high nutrient supply showed a larger growth response to elevated $[\text{CO}_2]$ than those grown with a low nutrient supply.

9.3 Allocation

In the branch bag experiment the only possibility for altered allocation in response to growth in elevated $[\text{CO}_2]$ was a change in the wood mass relative to needle mass, however this did not occur. In seedlings, the allocation amongst needles, stem, fine and coarse roots was influenced both by nutrient supply and to a lesser extent by $[\text{CO}_2]$. The root fraction increased in response to low nutrient supply and to a lesser extent to growth in elevated $[\text{CO}_2]$.

These results are in agreement with the functional balance model in which assimilates are allocated between new shoot or root growth depending on whether assimilate production or nutrient uptake is limiting.

It has been suggested that woody plants have a larger potential to respond to elevated $[\text{CO}_2]$ than herbaceous species because, when growth of physiologically active tissues is limited, *e.g.* by nutrient availability, woody plants can allocate excess assimilate to the development of wood and hence obviate the need to reduce photosynthetic rate. In both branch bag and seedling experiments the proportion of wood to 'functional' tissue was not influenced by growth in elevated $[\text{CO}_2]$. However, neither the branch bag or the seedling experiment can indicate for certain whether or not mature trees will produce more wood in elevated $[\text{CO}_2]$, since the seedlings have different morphology than mature trees and the branches in the branch bags were not sink limited. Therefore, the possibility remains that a mature tree in a

closed canopy growing in elevated $[\text{CO}_2]$ may produce more wood, thus increasing carbon sequestration in the medium term.

9.4 Needle carbohydrates

There were differences in the seasonal pattern of starch storage between mature branches and seedlings. The needles on mature branches only contained starch during the early summer and this quickly disappeared as the demand for carbohydrates in new shoots developed. Whereas needles on seedlings contained starch throughout the year, with larger amounts in needles of the seedlings grown at low nutrient supply and in elevated $[\text{CO}_2]$. However, there was a gradual decline in foliar starch concentrations over the course of the experiment and this suggests that growth was supplied partly by stored starch and partly by photosynthate production. When growth was limited by low nutrient supply, photosynthate production met most of the demand, especially in elevated $[\text{CO}_2]$, and consequently starch concentration decreased slowly. Whereas in the high nutrient supply treatment growth potential was sufficient to utilise all photosynthate produced and also to utilise the starch reserves regardless of the growth $[\text{CO}_2]$.

The lack of diurnal variation in the starch concentration indicates that it was a long-term and not a short-term storage pool. The needles on mature branches had slightly higher concentrations of soluble carbohydrates than the needles on seedlings. However, variables other than the age of the tree may be responsible for these differences, e.g. the position of the branch in the canopy. A further possibility is that starch storage is under genetic control since in natural conditions seedlings tend to establish in forest gaps where they are likely to experience competition for light with fast growing herbaceous species. In the late winter and early spring before the herbs have grown, spruce seedlings can photosynthesise and re-fill their starch reserves so that they would be in a better position to compete with the herbaceous species when they grow in the late spring and summer. Once the spruce have outgrown the understorey they would no longer need this starch storage strategy.

9.5 Photosynthesis

Current needles of mature branches did not show any down-regulation of photosynthesis but one-year old needles did show down-regulation, after they had been growing in elevated $[\text{CO}_2]$ for one year. This down-regulation was coincident with an increase in foliar soluble carbohydrate concentrations but there were no

differences in starch or nutrient concentrations. By contrast the down-regulation (reduction in V_{cmax} and A_{sat}) observed in current needles of seedlings was correlated with a reduction in the nitrogen concentration of the needles, which fell in response to low nutrient supply and to a lesser extent elevated $[\text{CO}_2]$.

It seems probable that two independent mechanisms were involved in the down-regulation of photosynthesis; in the C+1 needles on mature branches a build up of soluble carbohydrates, possibly caused by a reduction in the transport capacity of the needle phloem, led to feedback inhibition, whilst in the seedlings down-regulation was a result of a reduction in foliar nitrogen concentration, possibly as a result of the re-partitioning of nitrogen from proteins involved in photosynthesis to other more limiting processes elsewhere in the plant, e.g. nutrient acquisition. The stimulus for the re-partitioning of nitrogen in the seedling trees was probably the higher starch and soluble carbohydrate concentrations seen in needles of the trees grown in elevated $[\text{CO}_2]$ and with low nutrient supply.

There was no evidence for re-partitioning of nitrogen within leaves between Rubisco and light harvesting and electron transport proteins.

Thus it seems probable that some down-regulation of photosynthesis is likely to occur in Sitka spruce growing in elevated $[\text{CO}_2]$ regardless of age or nutrient availability. Furthermore, trees growing with a high rate of supply of nutrients may down-regulate more than those grown with a low rate of supply of nutrients, because they have higher photosynthetic capacity and foliar nitrogen concentrations, and therefore a larger potential for down-regulation in absolute terms.

9.6 Stomatal conductance and transpiration

Stomatal density of needles on mature branches was unaffected by growth in elevated $[\text{CO}_2]$ and short-term measurements of stomatal conductance showed a decrease with increasing $[\text{CO}_2]$, but stomatal conductance did not show acclimation to growth in elevated $[\text{CO}_2]$. This suggests that stomatal conductance will probably be slightly lower in needles growing in elevated $[\text{CO}_2]$. However, the effect this has on transpiration rate of individual plants and canopies will depend on how well the foliage is coupled to the atmosphere. It is often supposed that increase in leaf area may compensate for reduction in stomatal conductance leading to little change in transpiration rate. However, this interpretation is oversimplistic.

At the individual tree scale

Based on the results of the seedling experiment, elevated $[\text{CO}_2]$ increases the rates of growth and of leaf area development, especially at high nutrient supply. Consequently, after a set period of time seedlings in elevated $[\text{CO}_2]$ have grown bigger than those in ambient and the transpiration rate *per plant* is influenced both by the reduced stomatal conductance and the increased total leaf area. Provided there is adequate water available in the rooting zone the extra transpiration requirement, as a result of increased plant size, would have little effect, since the tree has simply got larger more quickly but may have followed the same developmental pathway, *i.e.* with respect to allometric relations, physiology and morphology, therefore all that has occurred is that the development period has been compressed.

A more meaningful comparison is between trees grown in ambient and elevated $[\text{CO}_2]$ when at the same size. As stomatal conductance tends to be lower at elevated $[\text{CO}_2]$, it seems probable that whole tree transpiration rate will be lower when comparing two similarly sized trees. More importantly the trees grown in elevated $[\text{CO}_2]$ tend to have lower leaf area ratio and larger root fraction than the trees grown in ambient CO_2 and this may allow them to access a larger rooting volume per unit leaf area and hence gain access to more water during drought. Comparison of trees grown at different growth rates at the same size, as measured by dry mass, height or stem volume, has complications in so far as the crown structure will almost certainly be different and this has implications for radiation distribution within the crown, aerodynamic resistance and hydraulic conductivity all of which influence transpiration rates, either directly or through changes to stomatal conductance.

At the stand scale

In a typical clear-cut and re-plant forestry situation, an increase in the growth rate of seedlings is likely to reduce the time it takes to reach canopy closure. Once canopy closure is attained the transpiration and interception losses of a stand depends on LAI and stomatal conductance and so if canopy closure is attained sooner less water will flow out of the catchment.

Where Sitka spruce is growing in natural ecosystems in a quasi-steady state, such as the Olympic peninsula in Washington state, seedling trees grow in canopy gaps. An increase in growth rate of such seedlings, or indeed of the stand as a whole, is unlikely to alter the water use of the stand, but changes in canopy structure and stomatal conductance might.

However, on a regional scale the degree to which stomata have control over evapotranspiration in a future high [CO₂] atmosphere may be limited, since reduced transpiration rates will lead to drier air which will tend to increase transpiration rate until a new equilibrium is attained which may not be very different from the *status quo*.

9.7 Advantages and limitations of Branch Bags

The use of branch bags to study the effects of elevated [CO₂] on branches has both advantages and limitations. It has highlighted potential direct effects at the needle scale *in the absence of sink limitation*; namely an increase in soluble carbohydrate concentration and down-regulation of photosynthesis in one-year-old needles where none occurred in current needles. Since more than 60% of the needles on a mature spruce are older-than one year this is an important result. However, the degree to which down-regulation would have occurred had the whole tree been exposed to elevated [CO₂] is uncertain.

As with all studies involving artificial conditions, care must be taken when interpreting results. The small increase in temperature in the branch bags induced earlier bud burst which may have concealed a potential effect of [CO₂] on bud burst. This could also be true for growth enhancement, but I think it unlikely.

9.8 Flux of carbon through the plant to the soil

From measurements of the carbon budget of seedling trees grown at two rates of nutrient supply and two [CO₂], it appears that growth in elevated [CO₂] does not increase the flux of carbon through the plant to the soil but growth at low nutrient supply does. This is primarily because of the relatively larger root system found in low nutrient trees and highlights the extra cost involved in acquiring nutrients when they are in short supply. However, caution is required when extrapolating the results from the experiment with seedlings because they were grown in sand culture and, although there was evidence of mycorrhizas present, the system would still have had different characteristics to a 'living' soil system.

9.9 Future Research

There is a clear implication from the comparisons between branches and seedlings that many of the evident effects of elevated CO₂ on the growth and physiology of young trees result from the lack of adequate sinks for the extra assimilate produced in elevated CO₂. However PPF, light quality and maturity of tissue must also be taken into account.

Arising from these experiments and the literature the following improved and new hypotheses can be formulated and tested.

- *When meristematic activity in a bagged branch is high, for example at the top of the canopy, branches exposed to elevated [CO₂] will utilise the extra assimilate produced for extra growth within the branch, i.e. local sinks will take precedence over remote sinks.* Branch bags could be placed at different positions down through the canopy to explore source sink relations at the scale of the branch.
- *Branches growing in elevated [CO₂] are able to maintain a positive carbon balance lower in the canopy and so increase the LAI of the canopy.* To test this, branch bags could be placed either over branches naturally occurring in shade or shaded bags could be used. This approach would also give another angle in the investigation of the relationship between the distribution of photosynthetic rate, nitrogen and absorbed light within canopies, i.e. the “acclimation hypothesis”.
- *If local sinks take precedence over remote sinks then cones on branches exposed to elevated [CO₂] should benefit, with increases in production of seeds, seed size and viability.* To test this, branch bags could be placed over branches with cones to investigate how growth in elevated [CO₂] affects cone production and interaction between the sink demand of cones and photosynthesis of neighbouring shoots (see Dick *et al.*, 1990).
- *To investigate branch autonomy and carbon flow in trees branch bags could be used inside whole tree chambers to look at reciprocal effects i.e. a tree growing in elevated [CO₂] with a branch exposed to ambient [CO₂].*
- *High flux rates of assimilates from a needle lead to a reduction in the ability to transport assimilates, possibly as a result of higher phloem mortality.* Experiments using ambient and elevated CO₂, high and low PPF could be used to test this hypothesis. More generally, secondary development of needle phloem

and what determines the amount of live phloem at any time requires more research.

Further areas where there is an obvious gap in current knowledge and a need for more research:

- Stomatal action in general, but also with in response to $[\text{CO}_2]$, is still poorly understood. For example, why are stomatal conductance and photosynthetic rate well correlated in some species and not others?
- Below-ground processes such as fine root turnover, soil fauna and mycorrhiza and their interaction with trees are still poorly understood, especially with regard to growth in elevated $[\text{CO}_2]$.

Appendix A

Calculations used with LCA-3 measurements.

The ADC LCA-3 operates as an open system. Air is drawn into the unit and passes through a set of conditioning tubes where CO₂ can be scrubbed and water vapour can be added or removed. The air flow is then split; part passes directly to the gas analyser cell and gives the reference [CO₂] while the other stream passes through a mass flow sensor and then to the hand held cuvette. Air entering the cuvette passes over a humidity sensor giving the inlet relative humidity. A fan constantly stirs the air within the cuvette to reduce the boundary layer and ensure the air leaving the cuvette is representative of that surrounding the shoot. A thermistor records the air temperature within the cuvette and a fine thermistor is placed in contact with the leaf to monitor leaf temperature. A second humidity sensor monitors the relative humidity of air leaving the cuvette and passing back to the main unit where the [CO₂] concentration is measured. The following equations are used to calculate the transpiration, photosynthetic rate, stomatal conductance and internal CO₂ concentration.

$$e_s(T_a) = \left(\frac{6.13755 \cdot T_a \left(18.564 - \frac{T_a}{254.4} \right)}{T_a + 255.57} \right) \cdot 10^{-3} \quad \text{bar}$$

$$e_{in} = \frac{H_{in} \cdot e_s(T_a)}{100} \quad \text{and} \quad e_{out} = \frac{H_{out} \cdot e_s(T_a)}{100} \quad \text{bar}$$

$$w = \frac{v_{20}}{1000} \cdot \frac{1}{22.4} \cdot \frac{273}{293} \cdot \frac{1}{1.1013} \cdot \frac{10000}{a} \quad \text{mol m}^{-2} \text{ s}^{-1}$$

$$E = \frac{e_{out} - e_{in}}{P - e_{out}} \cdot w \quad \text{mol m}^{-2} \text{ s}^{-1}$$

$$g_s = \frac{1}{\left(\frac{e_s(T_1) - e_{out}}{e_{out} - e_{in}} \cdot \frac{P - e_{out}}{P} \cdot \frac{1}{w} \right) - r_b} \quad \text{mol H}_2\text{O m}^{-2} \text{ s}^{-1}$$

$$g_c = \frac{1}{\frac{1.6}{g_s} + 1.37 \cdot r_b} \quad \text{mol CO}_2 \text{ m}^{-2} \text{ s}^{-1}$$

Then assimilation rate and internal [CO₂] were calculated,

$$A = C_{\text{in}} - \left(C_{\text{out}} \cdot \frac{P - e_{\text{in}}}{P - e_{\text{out}}} \right) \cdot w \quad \mu\text{mol m}^{-2} \text{ s}^{-1}$$

$$C_i = \frac{\left[g_c - \frac{E}{2} \right] \cdot C_{\text{out}} - A}{g_c + \frac{E}{2}} \quad \mu\text{mol mol}^{-1}$$

where

T_a = air temperature within the cuvette,

T_1 = temperature of needles measured with surface contact thermistor,

$e_s(T)$ = saturation vapour pressure at T °C (mb) (Buck 1981),

$e_{\text{in}}, e_{\text{out}}$ = water vapour pressure of air entering and leaving the cuvette (mb),

$H_{\text{in}}, H_{\text{out}}$ = relative humidity of air entering and leaving the cuvette,

w = molar flow rate of air through the cuvette per unit leaf area ($\text{mol m}^{-2} \text{ s}^{-1}$),

v_{20} = volume flow entering the cuvette corrected to 20 °C and 1 bar,

E = transpiration rate ($\text{mol m}^{-2} \text{ s}^{-1}$),

g_s = stomatal conductance of needles for water vapour ($\text{mol m}^{-2} \text{ s}^{-1}$),

g_c = shoot conductance for CO_2 ($\text{mol m}^{-2} \text{ s}^{-1}$),

P = atmospheric pressure (mb),

a = projected leaf area of needles on shoot (m^2),

$C_{\text{in}}, C_{\text{out}}$ = CO_2 concentration of air entering and leaving the cuvette ($\mu\text{mol mol}^{-1}$),

A = assimilation rate ($\mu\text{mol m}^{-2} \text{ s}^{-1}$),

C_i = internal CO_2 concentration within the needles ($\mu\text{mol mol}^{-1}$),

r_b = boundary layer resistance of shoot for water vapour ($\text{m}^2 \text{ s mol}^{-1}$ see below).

The boundary layer resistance of a spruce shoot within the cuvette was determined following the procedure of Parkinson (1984) which yielded values between 0.2 and 0.4 $\text{m}^2 \text{ s mol}^{-1}$. Variation of r_b between 0.2 and 0.4 varies stomatal conductance by $\pm 2\%$ and C_i by $\pm 0.2\%$ and so using a constant value of 0.3 $\text{m}^2 \text{ s mol}^{-1}$ for all shoots was deemed acceptable.

Appendix B

Design of light-source for ADC PLC (C) cuvette.

The requirements for a light source were an even distribution of light in the plane of the shoot, minimal heating and portability. The light source consisted of a fan-ventilated housing containing four precisely positioned tungsten halogen bulbs, which could be either 10 W or 20 W depending on the required illumination and available power supply. The housing was attached to a "Perspex"TM plate which replaced the standard PLC heat shield and thus also required the removal of the PPF sensor (see Figure 4B.1). I used a miniature PPF sensor from PP systems and a home made amplifier which plugged into a 2.5 mm three-way socket mounted on a modified cuvette. The socket was connected to the cuvette circuitry such that power was supplied to the external amplifier and the (0-1 V) return signal was fed to the LCA-3 bypassing the standard PPF sensor circuitry.

A number of design features helped to dissipate heat from the lamps: a) the shroud was made from aluminium to maximise heat transfer, b) an infrared blocking filter stopped radiated heat from reaching the shoot, and c) three fans maintained a supply of cooling air over the cuvette and the bulb assembly.

The bulbs and fans were all 12 V and the total power requirement was 40-80 W, depending on the bulbs used. The inside of the housing was painted brilliant matt white to aid uniform distribution of light while the lower half of the cuvette was covered with reflective foil to maximise the amount of light absorbed by the shoot. The PPF in the plane of the shoot within the cuvette was up to $1200 \mu\text{mol m}^{-2} \text{s}^{-1}$ with 20 W bulbs or $800 \mu\text{mol m}^{-2} \text{s}^{-1}$ with 10 W bulbs. A slot in the housing below the "Perspex" plate allowed the insertion of neutral density filters permitting the measurement of light response functions.

The increase in air temperature within the cuvette was $< 5 \text{ }^\circ\text{C}$ using the 20 W bulbs and $< 3 \text{ }^\circ\text{C}$ using the 10 W bulbs.

The optimal positions of the bulbs in relation to the cuvette were calculated using a 3D model by Keith Parkinson (PP systems) personal communication.

List of parts and suppliers

Four bulbs (10 W or 20 W) M42 class M halogen projection lamps and G4 holders.
International lamps Ltd. Harlow, Essex. CM19 5FG. FAX 01279 442222.

NIR blocking filter, BD 10024103.
Balzers Ltd., Bradburne Drive, Tilbrook, Milton Keynes, MK7 8AZ.
Fax 01908 377776.

Fans: two 40 x 40 mm (stock no. 582 956) and
one 60 x 60 mm (stock no. 582 962)
R.S. Components Ltd, Corby, Northants, NN17 9RS. Tel 01536 201234.

PAR1 miniature PPF sensor.
PP systems, 24/26 Brook Street, Hitchin, Hertfordshire, SG5 4LA.
Fax 0162 731807.

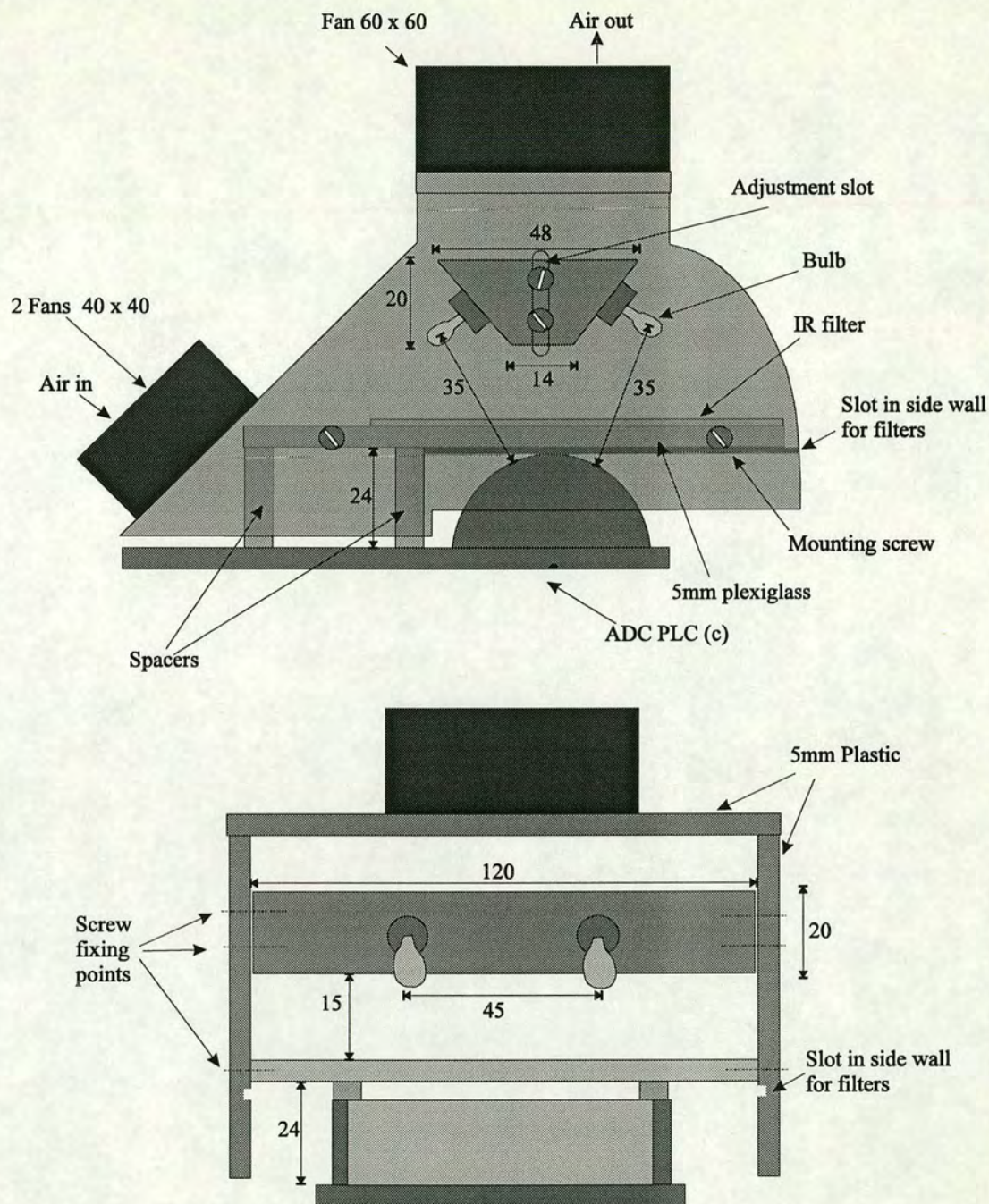


Figure 4B.1 Light source for the ADC PLC(C) cuvette. All dimensions in mm.

Appendix C

Nutrient Solution.

Two stock solutions were made up at the beginning of the season and mixed and diluted just prior to application (Ingestad & Kähr, 1985).

<u>Solution B</u>	<u>g dm⁻³</u>
NH ₄ NO ₃	140.2
KNO ₃	37.2
KH ₂ PO ₄	41.3
K ₂ SO ₄	14.0

<u>Solution C</u>	<u>g dm⁻³</u>	(weights in parentheses are when water of crystallisation is present)
Conc. HNO ₃	1.6 ml	
Ca(NO ₃) ₂	14.3	(20.6)
Mg(NO ₃) ₂	26.0	(44.9)
MnSO ₄	0.55	(0.81)
H ₃ BO ₃	0.57	
CuCl ₂	0.032	(0.043)
ZnSO ₄	0.036	(0.064)
Na ₂ MoO ₄	0.007	(0.008)
Fe ₂ (SO ₄) ₃	2.5	

2 dm³ of solution B were made up. Salts were added in the order shown and each dissolved before the addition of the next.

1 dm³ of solution C was made following the same procedure.

NB. Fe₂(SO₄)₃ must be added last and it takes some time for the solution to clear.

Solutions B and C were mixed in the ratio 1.7 B : 1 C giving a proportional composition of 100 N, 55 K, 15 P, 3 Ca, and 4 Mg and N concentration of 37g dm⁻³

25 dm³ of application strength (i.e. 0.05 g N dm⁻³) solution requires 21.3 cm³ of B and 12.5 cm³ of C added to 25 dm³ of distilled water.

Appendix D

Calculation of nutrient addition rates.

To maintain nutrient concentrations in the plant during the exponential growth period of growth, exponentially increasing amounts of nutrients must be made available per unit of time (Ingestad, 1982). The relative growth rate (R_G) is:

$$R_G = \frac{\ln W_2 - \ln W_1}{t_2 - t_1}, \quad (1)$$

where W_1 and W_2 are the plant mass on days t_1 and t_2 , respectively. If W_1 and W_2 are expressed in grams, R_G is expressed in $\text{g} \cdot \text{g}^{-1} \cdot \text{d}^{-1}$. Common expressions are $\text{g} (100 \text{ g})^{-1} \text{d}^{-1}$ or $\% \text{d}^{-1}$. Plant mass on day t_2 can be calculated from:

$$W_2 = W_1 \cdot \exp[R_G(t_2 - t_1)]. \quad (2)$$

The increase in mass over the time period t_1 to t_2 is expressed by:

$$(W_2 - W_1) = W_1[\exp\{R_G(t_2 - t_1)\} - 1]. \quad (3)$$

The nutrient amount required to be taken up during the time period t_1 to t_2 (U , g) to maintain an unchanged internal nutrient percentage concentration ($N_i\%$ of weight) is :

$$U = \frac{N_i}{100} \cdot (W_2 - W_1). \quad (4)$$

From equations (3) and (4) we derive the relationship between uptake rate and relative growth rate:

$$U = \frac{N_i}{100} \cdot W_1[\exp\{R_G(t_2 - t_1)\} - 1]. \quad (5)$$

To satisfy this required uptake rate the addition rate of the nutrient (A_N , $\mu\text{mol d}^{-1}$) must increase in an exponential manner with a relative addition rate (R_A) which is equal to the relative growth rate (R_G). From equations (2) and (5) the required addition rate on day t is:

$$A_N = \frac{N_i}{100} \cdot W_1[\exp(R_A t)][\exp(R_A) - 1]. \quad (6)$$

In this experiment the chosen R_G was $2\% \text{d}^{-1}$ (see Chapter 5, 5.6.1). As nutrients were added every six days the R_G and thus also R_A was 12% per period.

The target nitrogen concentration (N_i) was 2.3%, chosen as the optimum based on results found by Ingestad (1979).

The initial dry mass of the plants (W_1) determined at the first harvest was approximately 10 g.

Using equation 6 the following nutrient applications were calculated.

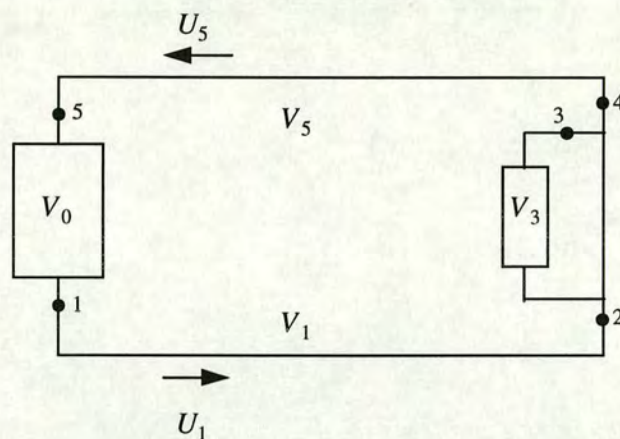
Date	Day	Nitrogen (mg)	Date	Day	Nitrogen (mg)
08/04/95	1	33	07/06/95	61	110
14/04/95	7	37	13/06/95	67	124
20/04/95	13	42	19/06/95	73	140
26/04/95	19	47	25/06/95	79	157
02/05/95	25	53	01/07/95	85	177
08/05/95	31	60	07/07/95	91	200
14/05/95	37	68	13/07/95	97	225
20/05/95	43	77	19/07/95	103	254
26/05/95	49	86	25/07/95	109	287
01/06/95	55	97	31/07/95	115	323

The table gives the amount of nitrogen to add on each date and from this and the known nitrogen concentration of the stock solution the amount of solution to add to each pot was calculated.

Appendix E

Corrections to H₂O fluxes.

The following equations are derived from LI-6200 Technical Reference, LI-COR Ltd., Lincoln, Nebraska, USA.



Schematic of a closed system.

Definition of variables.

E	(mol m ⁻² s ⁻¹)	Transpiration rate of a plant in the chamber.
l	(m ²)	Leaf area in the chamber.
v_0	(m ³)	Chamber volume.
v_1	(m ³)	Volume from chamber to desiccant.
v_3	(m ³)	Desiccant volume.
v_5	(m ³)	Volume from desiccant to chamber.
u_1	(mol s ⁻¹)	Flow rate leaving the chamber.
u_2	(mol s ⁻¹)	Flow rate entering the chamber.
w_n		Mole fraction of water vapor at location n ($n=1,3,5$).
ρ	(mol m ⁻³)	Density of air.

The mass balance of water in the system is given by

$$lE = (u_1 w_1 - u_5 w_5) + v_0 \cdot \rho \cdot \frac{\partial w_1}{\partial t} K_{\text{abs}} \quad (\text{E-1})$$

where the first term accounts for water absorbed by the desiccant and the second term the water involved in changes in air humidity, which in a null balance system should be close to zero. The factor K_{abs} is included to account for non-steady state conditions where $\delta w / \delta t$ is not zero and adsorption/desorption of water by internal surfaces would lead to an error in the calculation of the mass balance of water.

K_{abs} is determined empirically by observing the rate of change of humidity in an empty chamber as a known amount of air passes through the desiccant.

$$K_{\text{abs}} = \frac{F_d \cdot e \cdot (T_a + 273) \cdot R \cdot 1000}{P \cdot V \cdot \frac{\delta e}{\delta t}}, \text{ (dimensionless) (E-2)}$$

where F_d is the flow of air through the desiccant ($\mu\text{mol s}^{-1}$),

e is water vapour pressure of air (kPa),

T_a is the air temperature ($^{\circ}\text{C}$),

R is the universal gas constant $8.314 \text{ J mol}^{-1} \text{ K}^{-1}$,

P is atmospheric pressure (kPa),

V is the volume of the system (cm^3),

$\frac{\delta e}{\delta t}$ is the rate of change of e (kPa s^{-1}).

With no desorption of water from the chamber surfaces the humidity should fall in accordance with the amount of water absorbed by the desiccant and K_{abs} will be 1. However, if water is desorbing from surfaces a discrepancy between the rate of change of humidity predicted from flow through the desiccant and actual humidity measured by the humidity sensor in the chamber will arise and K_{abs} will become larger than one. LI-COR suggests acceptable values for K_{abs} are in the range 1.0-1.3 and values outside this range indicate a problem with the system; such as dirty walls, exhausted desiccant or chamber not at equilibrium with the environment. Furthermore, K_{abs} is not constant but changes with temperature and surface contamination of the chamber walls and also the humidity of the air and so needs to be determined frequently and when conditions change.

Appendix F

A simple model describing soluble carbohydrate production and export from spruce needles.

Assuming a steady state system in which photosynthate production and export are the same from one day to the next and that all assimilate produced during 24 hours is exported within 24 hours, the model can be used to determine soluble carbohydrate concentrations and fluxes at any time during the day.

$P =$ If $5:00 < t < 20:00$ then

$$\sin((5-t)*(\pi/(20-5))*k_{in})$$

else 0.

$$E = (C_f * k_{out})$$

$$C_{f(t+1)} = C_{f(t)} + P - E$$

where

$t =$ time (hours).

$P =$ soluble carbohydrate production represented as a half rectified sine wave with sunrise at 5:00 and sunset at 20:00.

$E =$ export rate which is proportional to the concentration.

$C_{f(t)} =$ foliar soluble carbohydrate concentration at time (t).

$k_{out} =$ export coefficient.

$k_{in} =$ production coefficient.

The model was implemented as a Microsoft Excel 5.0 spreadsheet. The pattern of soluble carbohydrate concentration seen in the data can be modelled using the following parameters.

	Ambient	Elevated
k_{in}	0.23	0.43
k_{out}	0.019	0.019

The output is shown in figures F.1 & F.2. Figure F.1 shows the concentrations throughout the day overlaid with the actual values measured on the 1st July for the **AH** and **EL** treatments (as seen in Chapter 7, Figure 7.7). Figure F.2 shows the rates of production and export. The model shows that the observed diurnal response, where **E** has a higher minimum value and larger amplitude, can be explained by **E** having higher photosynthetic rates but the same translocation coefficient, *i.e.* translocation is proportional to the foliar concentration and the same constant of proportionality is used for **E** and **A**.

The fit to the **AH** treatment is not perfect partly because the model finds a steady state solution which assumes carbohydrate production is the same every day. However, the data suggest that carbohydrate production on the previous day was larger, since the initial concentration at 01:00 was as high as the final concentration at 20:00 and under steady state conditions this is not possible, as translocation would have reduced the concentration during the intervening 5 hours.

This simple model does not take into account feedback inhibition of photosynthesis or export limitation imposed by phloem loading and reduced sink strengths, but it does show that these mechanisms do not need to be invoked to explain the observed response to treatment.

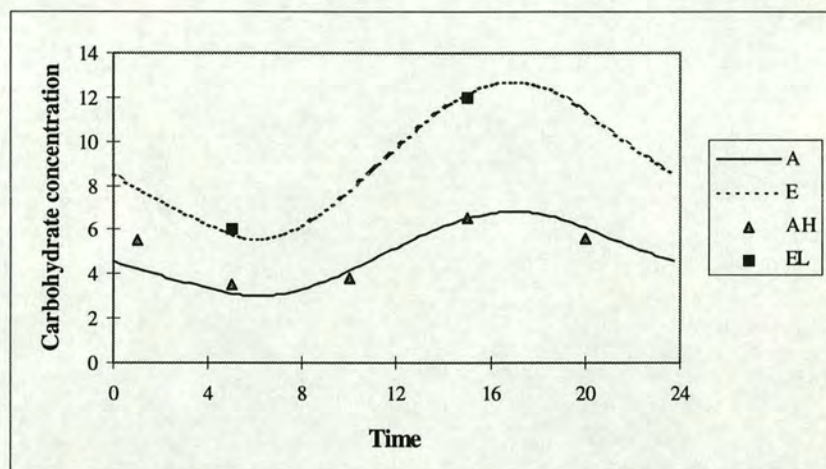


Figure F.1 Modelled soluble carbohydrate concentration in ambient and elevated CO_2 needles over the course of 24 hours. The symbols show the measured data for the **AH** and **EL** treatments on 1st July 1995.

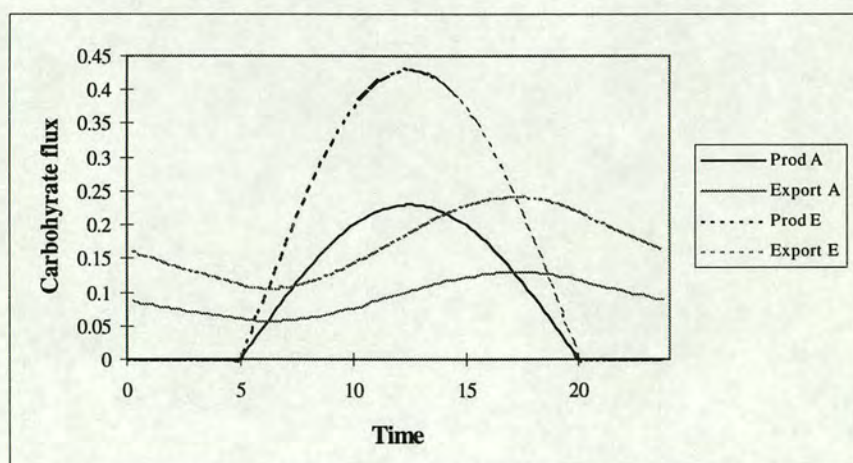


Figure F.2 Modelled production and export rates of soluble carbohydrates in needles over the course of 24 hours. P1, P2 ambient and elevated CO_2 production, E1 & E2 ambient and elevated CO_2 export respectively.

References

- Allen, S.E., 1989. *Chemical Analysis of Ecological Materials*. 2nd Edition. Blackwell Scientific Publications. Oxford. 368 p.
- Allen, S.J., Brenner, A & Grace, J. 1994. A low cost psychrometer for field measurements of atmospheric humidity. *Plant, Cell and Environment* **17**, 219-225.
- Amthor, J.S. 1991. Respiration in a future, higher-CO₂ world. *Plant, Cell and Environment* **14**, 13-20.
- Amthor, J.S. 1995a. Terrestrial higher-plant response to increasing atmospheric [CO₂] in relation to the global carbon cycle. *Global Change Biology* **1**, 243-274.
- Amthor, J.S. 1995b. Plant respiratory responses to elevated CO₂ partial pressure. In: *Advances in Carbon Dioxide Effects Research* (eds. L.H. Allen Jr, M.B. Kirkham, D.M. Olszyk, C. Whitman), American Society of Agronomy, Madison, WI.
- Amthor, J.S., Koch, G.W. & Bloom, A.J. 1992. CO₂ inhibits respiration in leaves of *Rumex crispus* L. *Plant Physiology* **98**, 757-760.
- Arp, W.J. 1991. Effects of source-sink relations on photosynthetic acclimation to elevated CO₂. *Plant, Cell and Environment* **14**, 869-876.
- Azcon-Bieto, J & Osmond, C.B. 1983. Relationship between photosynthesis and respiration: the effect of carbohydrate status on the rate of CO₂ production by respiration in darkened and illuminated wheat leaves. *Plant Physiology* **71**, 574-581.
- Ball, J.T., Woodrow, I.E. & Berry, J.A. 1987. A model predicting stomatal conductance and its contribution to the control of photosynthesis under different environmental conditions. *Progress in Photosynthesis Research* (ed. I. Biggins), pp. 221-224, Martinus Nijhoff Publishers, Netherlands.
- Barnola, J.M., Raynaud, D., Korotkevich, V.S. & Lorius, C. 1987. Vostok ice core provides 160,000 year record of atmospheric CO₂. *Nature* **329**, 408-414.
- Barton, C.V.M., Lee, H.S.J. & Jarvis, P.G. 1993. A branch bag and CO₂ control system for long-term CO₂ enrichment of mature Sitka spruce (*Picea sitchensis* (Bong.) Carr.). *Plant, Cell and Environment* **16**, 1139-1148.

- Baxter, S.M. & Cannell, M.G.R. 1977. Branch development on leaders of *Picea sitchensis*. *Canadian Journal of Forest Research* **8**, 121-128.
- Bazzaz, F.A. 1990. The response of natural ecosystems to the rising global CO₂ levels. *Annual Review of Ecology and Systematics* **21**, 167-196.
- Bazzaz, F.A. & Miao, S.L. 1993. Successional status, seed size, and responses of tree seedlings to CO₂, light, and nutrients. *Ecology* **74**, 104-112.
- Binns, W.O., Mayhead, G.J & MacKenzie, J.M. 1980. Nutrient deficiencies of conifers in British forests - An illustrated guide. Forestry Commission Leaflet 76. HMSO. UK.
- Bloom, A.J., Chaplin, F.S. III & Mooney, H.A. 1985. Resource limitation in plants-an economic analogy. *Annual Review of Ecological Systems* **16**, 363-392.
- Boissard, C., Hewitt, N.C., Street, R.A., Duckham, S.C., Cao, X.L., Milne, R., Fowler, D., Beverland I.J. & Moncrieff, J.B. 1997. Quantitative determination of non-methane hydrocarbon fluxes from a Sitka spruce (*Picea sitchensis*) plantation at the branch and canopy scales. *Journal of Geophysical Research* (In press).
- Bonte, J. & Mathy, P. 1988 *CEC Research Project on Open-top Chambers: Results on Agricultural Plants*. C.E.C Publications, Brussels.
- Bowes, G. 1991. Growth at elevated CO₂: photosynthetic responses mediated through Rubisco. *Plant, Cell and Environment* **14**, 795-806.
- Boyle, J.R. & Voigt, G.K. 1973. Biological weathering of silicate minerals. Implications for tree nutrition and soil genesis. *Plant and Soil* **38**, 191-201.
- Boyle, J.R., Voigt, G.K. & Sawhney, B.L. 1974. Chemical weathering of biotite by organic acids. *Soil Science* **117**, 42-45.
- Bradbury, I.K. & Malcolm, D.C. 1978. Dry matter accumulation by *Picea sitchensis* seedlings during winter. *Canadian Journal of Forest Research* **8**, 207-213.
- Buck, A.L. 1981. New equations for computing vapour pressure. *Journal of Applied Meteorology* **20**, 1527-1532.
- Bunce, J.A. 1990. Short- and long-term inhibition of respiratory carbon dioxide efflux by elevated carbon dioxide. *Annals of Botany* **65**, 637-642.
- Bunce, J.A. 1992. Stomatal conductance, photosynthesis and respiration of temperate deciduous tree seedlings grown outdoors at an elevated concentration of carbon dioxide. *Plant, Cell and Environment* **15**, 541-549.
- Bunce, J.A. 1994. Responses of respiration to increasing atmospheric carbon dioxide concentrations. *Physiologia Plantarum* **90**, 427-430.

- Cannell, M.G.R. 1987. Photosynthesis, foliage development and productivity of Sitka spruce. Proceedings of the Royal Society of Edinburgh, 93B, pp. 61-73.
- Cannell, M.G.R. & Willett, S.C. 1975. Rates and times at which needles are initiated in buds on differing provenances of *Pinus contorta* and *Picea sitchensis* in Scotland. *Canadian Journal of Forest Research* **5**, 367-380.
- Cave, G, Tolley, L.C. & Strain, B.R. 1981. Effect of carbon dioxide enrichment on chlorophyll content, starch content and starch grain structure in *Trifolium subterraneum* leaves. *Physiologia Plantarum* **51**, 171-174.
- Ceulemans, R. & Mousseau, M. 1994. Tansley Review No. 71. Effects of elevated atmospheric CO₂ on woody plants. *New Phytologist* **127**, 425-446.
- Chandler, J.W. & Dale, J.E. 1990. Needle growth in Sitka spruce (*Picea sitchensis*): effects of nutrient deficiency and needle position within shoots. *Tree Physiology* **6**, 41-56.
- Chapin, F.S & Van Cleve, K. 1989. Approaches to studying nutrient uptake, use and loss in plants. In: *Plant Physiological Ecology*, pp. 185-208. Chapman and Hall, London.
- Chiariello, N.R., Mooney, H.A & Williams, K. 1989. Growth, carbon allocation and cost of plant tissues. In: *Plant Physiological Ecology* (eds. R.W. Pearcy, J. Ehleringer, H.A. Mooney & P.W. Rundel), pp. 327-366. Chapman and Hall, London.
- Clement, C.R., Hopper, M.J., Jones, L.H.P. & Leafe, E.L. 1978. The uptake of nitrate by *Lolium perenne* from flowing nutrient solution. II. Effect of light, defoliation and relationship to CO₂ flux. *Journal of Experimental Botany* **29**, 1173-1183.
- Clough, J.M., Peet, M.M. & Kramer, P.J. 1981. Effects of high atmospheric CO₂ and sink size on rates of photosynthesis of a soybean cultivar. *Plant Physiology* **67**, 1007-1010.
- Coleman, J.S., McConnaughay, K.D.M. & Bazzaz, F.A. 1993. Elevated CO₂ and plant nitrogen-use: is reduced tissue nitrogen concentration size-dependent? *Oecologia* **93**, 195-200.
- Conroy, J.P., Milham, P.J., Mazur, M. & Barlow, E.W.R. 1990. Growth, dry weight partitioning and wood properties of *Pinus radiata* D. Don. after two years of CO₂ enrichment. *Plant, Cell and Environment* **13**, 329-337.
- Cregg, B.M., Teskey, R.O. & Dougherty, P.M. 1993. Effect of shade stress on growth, morphology, and carbon dynamics of Loblolly-pine branches. *Trees - Structure and Function* **7**, 208-213.

- Cure, J.D. & Acock, B. 1989. Crop responses to carbon dioxide doubling: a literature survey. *Agricultural and Forest Meteorology* **38**, 127-145.
- DeLucia, E.H., Sasek, T.W. & Strain, B.R. 1985. Photosynthetic inhibition after long-term exposure to elevated levels of atmospheric carbon dioxide. *Photosynthesis Research* **7**, 175-184.
- Dick, J.McP., Jarvis, P.G. & Barton, C.V.M. 1990. Influence of male and female cones on assimilate production of *Pinus contorta* trees within a forest stand. *Tree Physiology* **7**, 49-63.
- Dufrene, E, Pontailler, J-Y & Saugier, B. 1993. A branch bag technique for simultaneous CO₂ enrichment and assimilation measurements on beech (*Fagus sylvatica* L.). *Plant, Cell and Environment* **16**, 1131-1138.
- Drake, B. 1992. The impact of rising CO₂ on ecosystem production. *Water, Air and Soil Pollution* **64**, 25-44.
- Eamus, D. 1991. The interaction of rising CO₂ and temperature with water use efficiency. *Plant, Cell and Environment* **14**, 861-867.
- Eamus, D. & Jarvis, P.G. 1989. The direct effects of increase in the global atmospheric CO₂ concentration on natural and commercial temperate forests. *Advances in Ecological Research* **19**, 1-55.
- Eamus, D., Berryman, C.A. & Duff, G.A. 1993. Assimilation, stomatal conductance, specific leaf area and chlorophyll responses to elevated CO₂ of *Maranthes corymbosa*, a tropical monsoon rain forest species. *Australian Journal of Plant Physiology* **20**, 741-755.
- El Kohen, A., Pontailler, J.Y. & Mousseau, M. 1991. Effect of doubling of atmospheric CO₂ concentrations on dark respiration in aerial parts of young chestnut trees (*Castanea sativa* Mill.). *C.R. Academic Science Series III* **312**, 477-481.
- Ellsworth, D.S., Oren, R., Huang, C., Phillips, N., & Hendrey, G.R. 1995. Leaf and canopy responses to elevated CO₂ in a pine forest under free-air CO₂ enrichment. *Oecologia* **104**, 139-146.
- Ericsson, A. 1978. Seasonal changes in the translocation of ¹⁴C from different age-classes of needles on 21-year-old Scots pine trees (*Pinus silvestris*). *Physiologia Plantarum* **43**, 351-358.
- Evans, J.R. 1989. Photosynthesis and nitrogen relationships in leaves of C₃ plants. *Oecologia* **78**, 9-19.
- Ewers, F.W. 1982. Secondary growth in needle leaves of *Pinus longaeva* (Bristlecone Pine) and other conifers: quantitative data. *American Journal of Botany* **69**, 1552-1559.

- Farquhar, G.D. & Sharkey, T.D. 1982. Stomatal conductance and photosynthesis. *Annual Review of Plant Physiology* **33**, 317-345.
- Farquhar, G.D., von Caemmerer, S. & Berry, J.A. 1980. A biochemical model of photosynthetic CO₂ assimilation in leaves of C₃ species. *Planta* **149**, 78-90.
- Farrar, J.F. & Williams, M.L. 1991. The effects of increased atmospheric carbon dioxide and temperature on carbon partitioning, source-sink relations and respiration. *Plant, Cell and Environment* **14**, 819-830.
- Flower-Ellis, J.G.K. 1993. Dry-matter allocation in Norway spruce branches: a demographic approach. *Studia Forestalia Suecica* **191**, 51-73.
- Ford, E.D. & Deans, J.D. 1977. Growth of a Sitka spruce plantation: spatial distribution and seasonal fluctuations of lengths, weights and carbohydrate concentrations of fine roots. *Plant and Soil* **47**, 463-485.
- Ford, E.D., Milne, R. & Deans, J.D. 1987. Shoot extension in *Picea sitchensis* II. Analysis of weather influences on daily growth rate. *Annals of Botany* **60**, 543-552.
- Gifford, R.M., Lambers, H. & Morison, J.I.L. 1985. Respiration of crop species under CO₂ enrichment. *Physiologia Plantarum* **63**, 351-356.
- Hagem, O. 1947. The dry matter increase of coniferous seedlings in winter. *Meddelelse, Vestlandets Forstlige Forsøksstation* **26**, 1-276.
- Hagem, O. 1962. Additional observations on the dry matter increase of coniferous seedlings in winter. Investigations in an oceanic climate. *Meddelelse, Vestlandets Forstlige Forsøksstation* **37**, 249-347.
- Harley, P.C. & Sharkey, T.D. 1991. An improved model of C₃ photosynthesis at high CO₂: reversed O₂ sensitivity explained by lack of glycerate re-entry into the chloroplast. *Photosynthesis Research* **27**, 169-178.
- Harley, P.C., Thomas, R.B., Reynolds, J.F. & Strain, B.R. 1992. Modelling photosynthesis of cotton grown in elevated CO₂. *Plant, Cell and Environment* **15**, 271-282.
- Heaton, T.H.E and Crossley, A. 1995. Carbon-isotope variations in a plantation of Sitka spruce, and the effect of acid mist. *Oecologia* **103**, 109-117.
- Herold, A. 1980. Regulation of photosynthesis by sink activity-the missing link. *New Phytologist* **86**, 131-144.
- Houpis, J.L.J. & Surano, K.A. 1988. Standardisation of branch exposure chambers: basic performance specifications, test procedures, and field implementation. In: *The response of trees to air pollution: The role of branch studies*. (eds. W.E. Winner & L.B. Phelps), pp. 75-87. EPA, USDA, Boulder, CO.

- Houpis, J.L.J, Costella, M.P. & Cowles, S. 1991. A branch exposure chamber for fumigating Ponderosa pine to atmospheric pollution. *Journal of Environmental Quality* **20**, 467-474.
- Idso, K.E. & Idso, S.B. 1994. Plant responses to atmospheric CO₂ enrichment in the face of environmental constraints: a review of the past 10 years' research. *Agricultural and Forest Meteorology* **69**, 153-203.
- Idso, K.E., Kimball, B.A. & Allen, S.G. 1991. Net photosynthesis of sour orange trees maintained in atmospheres of ambient and elevated CO₂ concentration. *Agriculture and forest meteorology* **54**, 95-101.
- Ingestad, T. 1979. Mineral nutrient requirements of *Pinus silvestris* and *Picea abies* seedlings. *Physiologia Plantarum* **45**, 373-380.
- Ingestad, T. 1982. Relative addition rate and external concentration: driving variables used in plant nutrition research. *Plant, Cell and Environment* **5**, 443-453
- Ingestad, T. & Kähr, M. 1985. Nutrition and growth of coniferous seedlings at varied relative nitrogen addition rate. *Physiologia Plantarum* **65**, 109-116.
- Ingestad, T & Lund, A.-B. 1986. Theory and techniques for steady state mineral nutrition and growth of plants. *Scandinavian Journal of Forest Research* **1**, 439-453.
- Jarvis, P.G. 1976. The interpretation of the variations in leaf water potential and stomatal conductance found in canopies in the field. *Philosophical Transactions of the Royal Society of London Series B- Biological Sciences* **273**, 593-610.
- Jarvis, P.G. 1989. Atmospheric carbon dioxide and forests. *Philosophical Transactions of the Royal Society of London. Series B. Biological Sciences* **324**, 369-392.
- Jarvis, P.G. & McNaughton, K.G. 1986. Stomatal control of transpiration: scaling up from leaf to region. *Advances in Ecological Research* **15**, 1-49.
- Jones, P.D., Wigley, M.L. & Briffa, K.R. 1994. Global and hemispheric temperature anomalies - land and marine instrumental records. In: *Trends '93, A Compendium of Data on Global Change* (eds. T.A. Boden, D.P. Kaiser, R.J. Stepanski & F.W. Stoss), pp. 603-608. Carbon Dioxide Information Analysis Center, Oak Ridge National Laboratory, Oak Ridge, TN.

- Keeling, C.D., Bacastow, R.B., Carter, A.F., Piper, S.C., Whorf, T.P., Heimann, M., Mook, W.G. & Roeloffzen, H. 1989. A 3-dimensional model of atmospheric CO₂ transport based on observed winds: I. Analysis of observational data. In *Aspects of Climate Variability in the Pacific and the Western Americas*. (ed. D.H. Peterson) pp. 165-235. *Geophysical Monographs* **55**.
- Keeling, C.D. Whorf, T.P., Wahlen, M. & van der Plicht, J. 1995. Interannual extremes in the rate of rise of atmospheric carbon dioxide since 1980. *Nature* **375**, 666-670.
- Körner, C.H., Pelaez-Riedl, S. & van Bel, A.J.E. 1995. CO₂ responsiveness of plants: a possible link to phloem loading. *Plant, Cell and Environment* **18**, 595-600.
- Kramer, P.J. 1981. Carbon dioxide concentration, photosynthesis and dry matter production. *Bioscience* **31**, 29-33.
- Krueger, K.W. & Ruth, R.H. 1969. Comparative photosynthesis of red alder, Douglas-fir, Sitka spruce, and western hemlock seedlings. *Canadian Journal of Botany* **47**, 519-527.
- Leuning, R. 1990. Modelling stomatal behaviour and photosynthesis of *Eucalyptus grandis*. *Australian Journal of Plant Physiology* **17**, 159-175.
- Leuning, R. 1995. A critical appraisal of a combined stomatal-photosynthesis model for C₃ plants. *Plant, Cell and Environment* **18**, 339-355.
- Leverenz, J.W. 1987. Chlorophyll content and the light response curve of shade-adapted conifer needles. *Physiologia Plantarum* **71**, 20-29.
- Leverenz, J.W. & Jarvis, P.G. 1980. Photosynthesis in Sitka spruce (*Picea sitchensis* (Bong.) Carr.) IX. The relative contribution made by needles at various positions on the shoot. *Journal of Applied Ecology* **17**, 59-68.
- Leverenz, J., Deans, J.D., Ford, E.D., Jarvis, P.G., Milne, R. & Whitehead, D. 1982. Systematic spatial variation of stomatal conductance in a Sitka spruce plantation. *Journal of Applied Ecology* **19**, 835-851.
- Lewin, K.F., Hendrey, G.R., Nagy, J. & LaMorte, R. 1994. Design and application of a free-air carbon dioxide enrichment facility. *Agricultural and Forest Meteorology* **70**, 15-29.
- Linder, S. 1995. Foliar analysis for detecting and correcting nutrient imbalances in Norway spruce. *Ecological Bulletins* **44**, 178-190.

- Linder, S. & McDonald, A.J.S. 1994. Plant nutrition and the interpretation of growth response to elevated concentrations of atmospheric carbon dioxide. In: *Design and Execution of Experiments on CO₂ Enrichment* (eds. E.D. Schulze and H.A. Mooney). Ecosystems Research Report 6, CEC, pp 73-82, Brussels-Luxembourg.
- Linder, S. & Rook, D.A. 1984. Effects of mineral nutrition on carbon dioxide exchange and partitioning of carbon in trees. In: *Nutrition of Plantation Forests*. (eds. G.D. Bowen & E.K.S. Nambiar), pp. 211-236. Academic Press, London.
- Little, C.H.A. 1970. Derivation of the springtime starch increase in balsam fir (*Abies balsamea*). *Canadian Journal of Botany* **48**, 1995-1999.
- Liu, S & Teskey, R.O. 1995. Responses of foliar gas exchange to long-term elevated CO₂ concentrations in mature loblolly pine trees. *Tree Physiology* **15**, 351-359.
- Long, S.P., Baker, N.R. & Raines, C.A. 1993. Analysing the responses of photosynthetic CO₂ assimilation to long-term elevation of atmospheric CO₂ concentration. *Vegetatio* **104/105**, 33-45.
- Ludlow, M.M. & Jarvis, P.G. 1971. Photosynthesis in Sitka spruce (*Picea sitchensis* (Bong.) Carr.). I. General characteristics. *Journal of Applied Ecology* **8**, 925-953.
- Luxmoore, R.J., Wullschleger, S.D. & Hanson, P.J. 1993. Forest responses to CO₂ enrichment and climate warming. *Water, Air and Soil Pollution* **70**, 309-323.
- Madsen, E. 1969. Effect of CO₂-concentration on accumulation of starch and sugar in tomato leaves. *Physiologia Plantarum* **21**, 168-175.
- Marschner, H. 1995. *Mineral Nutrition of Higher Plants*. Academic Press, London.
- Matthews, G. 1993. The carbon content of trees. *Technical Paper 4*, Forestry Commission, Edinburgh, pp. 1-21. ISBN 0 85538 317 8.
- McConnaughay, K.D.M., Berntson, G.M. & Bazzaz, F.A. 1993. Limitations to CO₂-induced growth enhancement in pot studies. *Oecologia* **94**, 550-557.
- Molla, M.A.Z., Chowdhary, A.A. & Islam, A.H. 1984. Microbial mineralization of organic phosphate in soil. *Plant and Soil* **78**, 393-399.
- Morison, J.I.L. 1987. Intercellular CO₂ concentration and stomatal response to CO₂. In: *Stomatal Function* (eds. E. Zeigler, G.D. Farquhar & I.R. Cowan), pp. 229-251. Stanford University Press, Stanford CA.

- Morison, J.I.L. & Jarvis, P.G. 1983. Direct and indirect effects of light on stomata. I. In Scots pine and Sitka spruce. *Plant, Cell and Environment* **6**, 95-101.
- Mousseau, M. & Saugier, B. 1992. The direct effects of increased CO₂ on gas exchange and growth of forest tree species. *Journal of Experimental Botany* **43**, 1121-1130.
- Murray, M.B., Smith, I.R., Leith, I.D., Fowler, D., Lee, H.S.J., Friend, A.D. & Jarvis, P.G. 1994. Effects of elevated CO₂, nutrition and climatic warming on bud phenology in Sitka spruce (*Picea sitchensis*) and their impact on the risk of frost damage. *Tree Physiology* **14**, 691-706.
- Murray, M.B., Leith, I.D. & Jarvis, P.G. 1996. The effect of long term CO₂ enrichment on the growth, biomass partitioning and mineral nutrition of Sitka spruce (*Picea sitchensis* (Bong.) Carr.). *Trees* **10**, 393-402.
- Neftel, A., Moor, E., Oeschger, H. & Stauffer, B. 1985. Evidence from polar ice-cores for the increase in atmospheric CO₂ in the past two centuries. *Nature* **315**, 45-47.
- Neilson, R.E., Ludlow, M.M. & Jarvis, P.G. 1972. Photosynthesis in Sitka spruce (*Picea sitchensis* (Bong.) Carr.). II. Response to temperature. *Journal of Applied Ecology* **9**, 721-745.
- Niinemets, Š & Kull, O. 1995. Effects of light availability and tree size on the architecture of assimilative surface in the canopy of *Picea abies*: variation in needle morphology. *Tree Physiology* **15**, 307-315.
- Nitsos, R.E. & Evans, H.J. 1969. Effects of univalent cations on the activity of particulate starch synthesase. *Plant Physiology* **44**, 1260-1266.
- Norby, R.J. & O'Neill, E.G. 1989. Growth dynamics and water use of seedlings of *Quercus alba* L. in CO₂-enriched atmospheres. *New Phytologist* **111**, 491-500.
- Norby, R.J. & O'Neill, E.G. 1991. Leaf area compensation and nutrient interactions in CO₂-enriched seedlings of yellow poplar (*Liriodendron tulipifera* L.). *New Phytologist* **117**, 515-528.
- Norby, R.J., Pastor, J. & Melillo, J.M. 1986. Carbon-nitrogen interactions in CO₂-enriched white oak: physiological and long-term perspectives. *Tree Physiology* **2**, 233-241.
- Norby, R.J., Gunderson, C.A., Wullschleger, S.D., O'Neill, E.G. & McCracken, M.K. 1992. Productivity and compensatory responses of yellow-poplar trees in elevated CO₂. *Nature* **357**, 322-324.
- Norby, R.J., Wullschleger, S.D., Gunderson, C.A. & Nietch, C.T. 1995. Increased growth efficiency of *Quercus alba* trees in a CO₂-enriched atmosphere. *New Phytologist* **131**, 91-97.

- Norman, J.M. & Jarvis, P.G. 1974. Photosynthesis in Sitka spruce (*Picea sitchensis* (Bong.) Carr.) Measurement of canopy structure and interception of radiation. *Journal of Applied Ecology* **11**, 375-398.
- Parkinson, K.J. 1984. A simple method for determining the boundary layer resistance in leaf cuvettes. *Plant, Cell and Environment* **8**, 223-226.
- Penning de Vries, F.W.T., Brunsting, A.H.M. & van Laar, H.H. 1974. Products, requirements and efficiency of biosynthesis. A quantitative approach. *Journal of Theoretical Biology* **45**, 339-77.
- Pettersson, R., McDonald, A.J.S. & Stadenberg, I. 1993. Response of small birch plants (*Betula pendula* Roth.) to elevated CO₂ and nitrogen supply. *Plant, Cell and Environment* **16**, 1115-1121.
- Pitman, M. 1977. Ion transport into the xylem. *Annual Review of Plant Physiology* **28**, 71-88.
- Porra, R.J., Thompson, W.A. & Kriedemann, P.E. 1989. Determination of accurate extinction coefficients and simultaneous equations for assaying chlorophylls a and b extracted with four different solvents: verification of the concentration of chlorophyll standards by: atomic absorption spectroscopy. *Biochimica et Biophysica Acta* **975**, 384-394.
- Prioul, J.L. & Chartier, P. 1977. Partitioning of transfer and carboxylation components of intracellular resistance to photosynthetic CO₂ fixation: a critical analysis of methods used. *Annals of Botany* **41**, 789-800.
- Qi, J., Marshall, J.D. & Mattson, K.G. 1994. High soil carbon dioxide concentrations inhibit root respiration of Douglas fir. *New Phytologist* **128**, 435-442.
- Ragg, J.M. & Fitty, D.W. 1967. *Soils of the country around Haddington and Eyemouth*. Memoirs of the soil survey of Great Britain. Scotland. Macaulay Institute for Soil Research. HMSO. Edinburgh, pp. 340.
- Reichle, D.E., Dinger, B.E., Edwards, N.T., Harris, W.F. & Sollins, P. 1973. Carbon flow and storage in a forest ecosystem. In: *Carbon and the Biosphere*. (eds. G.M. Woodwell & E.V. Pecan), pp. 345-365. USA: US Atomic Energy Commission,.
- Rey, A. 1997. Response of young birch trees to increasing atmospheric carbon dioxide concentrations. PhD Thesis, University of Barcelona.
- Rogers, H.H., Peterson, C.M., McCrimmon, J.N. & Cure, J.D. 1992. Response of plant roots to elevated atmospheric carbon dioxide. *Plant, Cell and Environment* **15**, 749-752.
- Rook, D.A. 1992. Super Sitka for the 90's. Forestry Commission Bulletin, 103, HMSO, London.

- Ross, G.J.S. 1981. The use of non-linear regression methods in crop modelling. In: *Mathematics and Plant Physiology* (eds. D.A. Rose & D.A. Charles-Edwards), pp. 269-282. Academic Press. New York.
- Rouhier, H., Billes, G., El Koen, A., Mousseau, M. & Bottner, P. 1994. Effect of elevated CO₂ on carbon and nitrogen distribution within a tree (*Castanea sativa* Mill.) - soil system. *Plant and Soil* **162**, 281-292.
- Rufty, Jr, T.W., MacKown, C.T. & Volk, R.J. 1989. Effects of altered carbohydrate availability on whole-plant assimilation of ¹⁵NO₃⁻. *Plant Physiology* **89**, 457-463.
- Sage, R.F. 1994. Acclimation of photosynthesis to increasing atmospheric CO₂: the gas exchange perspective. *Photosynthesis Research* **39**, 351-368.
- Sage, R.F., Sharkey, T.D. & Seeman, J.R. 1988. The in-vivo response of ribulose-1,5-bisphosphate carboxylase activation state and the pool sizes of photosynthetic metabolites to elevated CO₂ in *Phaseolus vulgaris* L. *Planta* **174**, 407-416.
- Sasek, T.W., DeLucia, E.H. & Strain, B.R. 1985. Reversibility of photosynthetic inhibition in cotton after long-term exposure to elevated CO₂ concentrations. *Plant Physiology* **78**, 619-622.
- Sharkey, T.D. 1985. Photosynthesis in intact leaves of C₃ plants: physics, physiology and rate limitations. *The Botanical Review* **51**, 53-105.
- Sharkey, T.D., Berry, J.A. & Sage, R.F. 1988. Regulation of photosynthetic electron transport rates as determined by: room temperature chlorophyll a fluorescence in *Phaseolus vulgaris* L. *Planta* **176**, 415-424.
- Sharkey, T.D., Loreto, F & Delwiche, C.F. 1991. The biochemistry of isoprene emission from leaves during photosynthesis. In: *Trace Gas Emissions by Plants* (eds. T.D. Sharkey, E.A. Holland & H.A. Mooney), Academic Press, San Diego, pp. 153-184.
- Shinozaki, K., Yoda, K., Hozumi, K. & Kira, T. 1964a. A quantitative analysis of plant form - the pipe model theory. 1. Basic analysis. *Japanese Journal of Ecology* **14**, 97-105.
- Shinozaki, K., Yoda, K., Hozumi, K. & Kira, T. 1964b. A quantitative analysis of plant form - the pipe model theory. 2. Further evidence of the theory and its application in forest ecology. *Japanese Journal of Ecology* **14**, 133-139.
- Sprugel, D.G., Hinckley, T.M. & Schnap, W. 1991. The theory and practice of branch autonomy. *Annual Review of Ecological System* **22**, 309-34.
- Stitt, M. 1991. Rising CO₂ levels and their potential significance for carbon flow in photosynthetic cells. *Plant, Cell and Environment* **14**, 741-762.

- Stitt, M. 1993. Enhanced CO₂, photosynthesis and growth; what should we measure to gain a better understanding of the plants response? In: *Design and Execution of Experiments on CO₂ Enrichment* (eds. E.D. Schulze & H.A. Mooney). Ecosystems Research Report 6, pp. 3-28, EEC, Brussels-Luxembourg.
- Stitt, M., Huber, S.C. & Kerr, P. 1987. Control of photosynthetic sucrose formation. In: *Biochemistry of Plants*. Vol. 10 (eds. M.D. Hatch & N.K. Boardman), pp. 328-409. Academic Press, New York.
- Szawiawski, R.K. & Wierzbicki, B. 1978. Net photosynthetic rate of some coniferous species at diffuse high irradiance. *Photosynthetica* **12**, 412-417.
- Tans, P.P., Fung, I.Y. & Takahashi, T. 1990. Observational constraints on the global atmospheric CO₂ budget. *Science* **247**, 1431-1438.
- Teskey, R.O. 1995. A field study of the effects of elevated CO₂ on carbon assimilation, stomatal conductance and leaf and branch growth of *Pinus taeda* trees. *Plant, Cell and Environment* **18**, 565-573.
- Teskey, R.O., Dougherty, P.M. and Wiselogle, A.E. 1991. Design and performance of branch chambers suitable for long-term ozone fumigation of foliage in large trees. *Journal of Environmental Quality* **20**, 591-595.
- Thomas, R.B. & Strain, B.R. 1991. Root restriction as a factor in photosynthetic acclimation of cotton seedlings grown in elevated carbon dioxide. *Plant Physiology* **96**, 627-634.
- Thomas, R.B., Lewis, J.D. & Strain, B.R. 1994. Effects of leaf nutrient status on photosynthetic capacity in loblolly pine (*Pinus taeda* L.) seedlings grown in elevated atmospheric CO₂. *Tree Physiology* **14**, 947-960.
- Tissue, D.T. & Oechel, W.C. 1987. Responses of *Eriophorum vaginatum* to elevated CO₂ and temperature in the Alaskan tussock tundra. *Ecology* **68**, 401-410.
- Tissue, D.T., Thomas, R.B. & Strain, B.R. 1993. Long-term effects of elevated CO₂ and nutrients on photosynthesis and rubisco in loblolly pine seedlings. *Plant, Cell and Environment* **16**, 859-865.
- Townend, J. 1993. Effects of elevated carbon dioxide and drought on the growth and physiology of clonal Sitka spruce plants (*Picea sitchensis* (Bong.) Carr.) *Tree Physiology* **13**, 389-399.
- Townend, J. 1995. Effects of elevated CO₂, water and nutrients on *Picea sitchensis* (Bong.) Carr. seedlings. *New Phytologist*, **130:2**, 193-206
- Villar, R., Held, A.A. & Merino, J. 1995. Dark leaf respiration of an evergreen and deciduous plant species. *Plant Physiology* **107**, 421-427.

- von Caemmerer, S. & Farquhar, G.D. 1981. Some relationships between the biochemistry of photosynthesis and gas exchange of leaves. *Planta* **153**, 376-387.
- Wang, Y.P. & Jarvis, P.G. 1990. Influence of crown structural-properties on PAR absorption, photosynthesis, and transpiration in Sitka spruce - application of a model (MAESTRO). *Tree Physiology* **7**, 297-316.
- Waring, R.H. & Schlesinger, W.H. 1985. Forest Ecosystems: Concepts and Management. Academic Press Inc., Orlando, FL, pp. 340.
- Watson, R.T., Rodhe, H., Oeschger, H. & Siegenthaler, U. 1990. Greenhouse gases and aerosols. In: *Climate Change, The IPCC Scientific Assessment* (eds. J.T. Houghton, G.J. Jenkins & J.J. Ephraums) pp. 1-40. Cambridge University Press, Cambridge.
- Wong, S.C. 1979. Elevated atmospheric partial pressure of CO₂ and plant growth. I. Interactions of nitrogen nutrition and photosynthetic capacity in C₃ and C₄ plants. *Oecologia* **44**, 68-74.
- Woodwell, G.M., Whittaker, R.H., Reiners, W.A., Likens, G.E., Delwiche, C.C. & Botkin, D.B. 1978. The biota and the world carbon budget. *Science* **199**, 141-146.
- Wulff, R.D. & Strain, B.R. 1981. Effects of CO₂ enrichment on growth and photosynthesis in *Desmodium paniculatum*. *Canadian Journal of Botany* **60**, 1084-1091.
- Wullschleger, S.D. 1993. Biochemical limitations to carbon assimilation in C(3) plants - a retrospective analysis of the A/C_i curves from 109 species. *Journal of Experimental Botany* **44**, 907-920.
- Wullschleger, S.D., Norby, R.J. & Gunderson, C.A. 1992. Growth and maintenance respiration in leaves of *Liriodendron tulipifera* L. exposed to long-term carbon dioxide enrichment in the field. *New Phytologist* **121**, 515-523.